

Sunday	Monday	Tuesday	Wednesday	Thursday	Friday
24	25	26	27	28	29
7:30 - 8:30	Continental Breakfast at Telluride Conference Center				
	Opening remarks 8:15				
8:30 - 9:05	E. Cornell	N. Mavalvala	F. Merkt	C. Koch	T. Rosenband
9:05 - 9:40	P. Bouyer	G. Tino	D. Neumark	Y. Takahashi	J. Ye
9:40 - 10:15	I. Bloch	T. Hänsch	D. Meschede	P. Hannaford	Closing remarks
10:15 - 10:45	Coffee	Coffee	Coffee	Coffee	Coffee Box Lunch & Departure
10:45 - 11:20	G. Gabrielse	M. Romalis	M Ritsch-Marté	H.P. Buechler	
11:20 - 11:55	N. Fortson	W. Ubachs	V. Balykin	W. Vassen	
12:00 - 2:00	Lunch	Lunch	Box lunch & Excursions	Lunch	
2:00 - 2:35	C. Roos	E. Giacobino		A. Browaeys	
2:35 - 3:10	S. Haroche	E. Polzik		E. Hinds	
3:10 - 3:40	Coffee	Coffee		Coffee	
3:40 - 4:15	T. Ruchon	D. Jin		P. Maunz	
4:15 - 4:50	P. de Natale	R. Ballagh		H.J. Kimble	
Arrival Registration & Informal Reception 4:00 to 10:00					
	Poster Session I 7:00 ---	Poster Session II 7:00 ---	Town Talk R. Blatt & MountainFilm PINHEAD - TSRC-ICOLS 6:00 – 7:30	Banquet/Picnic 7:00 ---	

**KOSTERLITZ-THOULESS CROSS-OVER OBSERVED IN A
BOSE GAS IN A 2-D OPTICAL LATTICE**

V. SCHWEIKARD, S. TUNG, E.A. CORNELL

JILA, Campus Box 440, Boulder, CO 80309-0440

The energy cost for the formation of a vortex in a 2-D lattice is proportional to the intersite tunneling energy J . At a temperature $T > J$, energy cost in forming a free vortex is more than balanced by the entropy gain, and it becomes thermodynamically favorable for free vortices to proliferate. With both J and T as experimentally controlled parameters, we observe the surface density of vortices in a condensate and determine an empirical value of J/T for which this so-called Kosterlitz-Thouless cross-over occurs.

Ultracold Bose Gases in 1D Disorder

P. BOUYER, L. SANCHEZ-PALENCIA, D. CLÉMENT, P. LUGAN and A. ASPECT

*Laboratoire Charles Fabry de l'Institut d'Optique,
CNRS and Univ. Paris-Sud, Campus Polytechnique,
RD 128, F-91127 Palaiseau cedex, France
*E-mail: philippe.bouyer@institutoptique.fr
www.atomoptique.fr*

M. LEWENSTEIN

*ICREA and ICFO-Institut de Ciències Fotòniques,
Parc Mediterrani de la Tecnologia,
E-08860 Castelldefels (Barcelona), Spain*

G. SCHLYAPNIKOV

*Laboratoire de Physique Théorique et Modèles Statistiques,
Univ. Paris-Sud, F-91405 Orsay cedex, France
Van der Waals-Zeeman Institute, Univ. Amsterdam,
Valckenierstraat 65/67, 1018 XE Amsterdam, The Netherlands*

We study an interacting ultracold Bose gas in the presence of 1D disorder. We show that the expansion of an initially confined interacting 1D Bose-Einstein condensate can exhibit Anderson localization in a weak random potential with correlation length σ_R . For speckle potentials the Fourier transform of the correlation function vanishes for momenta $k > 2\sigma_R$ so that the Lyapunov exponent vanishes in the Born approximation for $k > 1/\sigma_R$. Then, for the initial healing length of the condensate $\xi_{in} > \sigma_R$ the localization is exponential, and for $\xi_{in} > \sigma_R$ it changes to algebraic. We also present the case of a non-expanding gas with repulsive interatomic interactions varying from zero to the Thomas-Fermi regime. We show that for weak interactions the Bose gas populates a finite number of localized single-particle Lifshits states, while for strong interactions a delocalized disordered Bose-Einstein condensate is formed. We discuss the schematic quantum-state diagram and derive the equations of state for various regimes.

Keywords: Bose-Einstein Condensate, Anderson localization, 1D Disorder

TOWARDS QUANTUM MAGNETISM WITH ULTRACOLD ATOMS IN OPTICAL LATTICES*

IMMANUEL BLOCH

*Institut für Physik, Johannes Gutenberg-Universität Mainz
Staudingerweg 7, 55099 Mainz, Germany*

Tunneling of material particles through a classically impenetrable barrier constitutes one of the hallmark effects of quantum physics. When interactions between the particles compete with their mobility through a tunnel junction, intriguing novel dynamical behavior can arise where particles do not tunnel independently. In single-electron or Bloch transistors, for example, the tunneling of an electron or Cooper pair can be enabled or suppressed by the presence of a second charge carrier due to Coulomb blockade. Using optical superlattices, we have been able to record the time-resolved dynamics of single atoms and interacting atom pairs across a tunnel junction. In the regime of dominating interactions between the particles, we observe that particles can only undergo tunneling in a second order hopping process as a stable pair¹, known as co-tunneling in mesoscopic physics.

By employing a spin-mixture of atoms in such superlattices², we also directly record super-exchange mediated spin-spin interactions between atoms on neighboring lattice sites³⁻⁵. Although no direct long-range interaction is present between the atoms, second order hopping processes mediate an effective spin-spin interaction between the particles on adjacent lattice sites in the form of an isotropic Heisenberg type exchange term. We show how the super-exchange interactions can be controlled in the experiment and allow e.g. changing from ferromagnetic to antiferromagnetic interactions between the particles. Super-exchange interactions lie at the heart of quantum magnetism in strongly correlated electronic media¹ and can be useful for the generation of large robust entangled multi-particle states in experiments, for which novel schemes will be outlined. Furthermore, I will present results on how quantum noise correlations can be used to efficiently detect several strongly correlated quantum phases in optical lattices⁶⁻⁸.

* This work is supported by DFG, EU, and AFOSR.

NEW MEASUREMENT OF THE ELECTRON MAGNETIC MOMENT AND THE FINE STRUCTURE CONSTANT

GERALD GABRIELSE

*Physics Department, Harvard University, 17 Oxford Street
Cambridge, MA, 02138, United States*

Remarkably, the famous UW measurement of the electron magnetic moment¹ has stood since 1987. With QED theory, this measurement has determined the accepted value of the fine structure constant. Here we report a new Harvard measurement of these fundamental constants.² The new measurement has an uncertainty that is about six times smaller, and it shifts the values by 1.7 standard deviations. The more accurate value of the electron magnetic moment, together with QED theory, determines the fine structure constant³ about 10 times more accurately than any rival method. One electron suspended in a Penning trap is used for the new measurement, like in the old measurement. What is different is that the lowest quantum levels of the spin and cyclotron motion are resolved⁴, and the cyclotron as well as spin frequencies are determined using quantum jump spectroscopy. In addition, a 0.1 K Penning trap that is also a cylindrical microwave cavity⁵ is used to control the radiation field, to suppress spontaneous emission by more than a factor of 100, to control cavity shifts, and to eliminate the blackbody photons that otherwise stimulate excitations from the cyclotron ground state. Finally, great signal-to-noise for one-quantum transitions is obtained using electronic feedback to realize the first one-particle self-excited oscillator.⁶ The new methods may also allow a million times improved measurement of the 500 times smaller antiproton magnetic moment. A popular account⁷ and numerous secondary accounts are available.⁸⁻¹²

¹ R.S. Van Dyck, Jr., P.B. Schwinberg and H.G. Dehmelt, *Phys. Rev. Lett.* **59**, 26 (1987).

² B. Odom, D. Hanneke, B. D'Urso and G. Gabrielse, *Phys. Rev. Lett.* **97**, 030801 (2006).

³ G. Gabrielse, D. Hanneke, T. Kinoshita, M. Nio, B. Odom, *Phys. Rev. Lett.* **97**, 030802 (2006).

⁴ S. Piel and G. Gabrielse, *Phys. Rev. Lett.* **83**, 1287 (1999).

⁵ G. Gabrielse and F.C. MacKintosh, *Int. J. Mass Spec.* **57**, 1 (1984).

⁶ B. D'Urso, R. Van Handel, B. Odom, D. Hanneke, and G. Gabrielse, *Phys. Rev. Lett.* **94**, 113002 (2005).

⁷ G. Gabrielse, *Physics World*. (March 2007).

⁸ D. Kleppner, *Scienc* **313**, 448-499 (2006).

⁹ A. Czarnecki, *Nature*. **442**, 516-517 (2006).

¹⁰ B. Schwarzschild, *Physics Today*. 15-17 (August 2006).

¹¹ G. Gabrielse and D. Hanneke, *Cern Courier*. (October 2006).

¹² M. Inman, *New Scientist*. **2568**, 40-43 (2006)

T-VIOLATION AND THE SEARCH FOR A PERMANENT ELECTRIC DIPOLE MOMENT OF THE MERCURY ATOM

E. N. FORTSON*

*Department of Physics, University of Washington,
Seattle, WA 98195, USA*

**E-mail: fortson@phys.washington.edu*

There has been exciting progress in recent years in the search for a permanent electric dipole moment (EDM) of an atom, a molecule, or the neutron. An EDM along the axis of spin can exist only if time reversal symmetry (T) is violated. Although such a dipole has not yet been detected, mainstream theories of possible new physics, such as Supersymmetry, predict the existence of EDMs within reach of modern experiments. After a brief survey of current and planned EDM searches worldwide, I will describe the newest version of our own EDM experiment with mercury atoms, and discuss the implications of recent results for the existence of new T-violating (and hence CP-violating) interactions.

To search for an EDM, we measure the ^{199}Hg nuclear spin precession frequency in a vapor of spin polarized mercury atoms. A magnetic field produces Larmor precession, and a strong electric field modifies the precession frequency in proportion to the size of the EDM. We spin polarize the ^{199}Hg nuclei by optical pumping on the 253.7 nm absorption line in mercury. To drive this transition several milliwatts of stable, tunable UV radiation are obtained by quadrupling the output of an infrared diode laser. This laser system has operated continuously for several years with only occasional maintenance.

In the current version of the experiment we perform measurements simultaneously in a linear stack of four vapor cells. The two inner cells have oppositely directed electric fields, and the outer two have no electric field applied to them. Common-mode magnetic field noise cancels out if we observe the frequency difference between the two electric field cells, while noise in the magnetic field gradient and various systematic effects can be

cancelled by taking linear combinations of the frequencies in all four cells.

The previous version of our experiment (M. V. Romalis, W. C. Griffith, J. P. Jacobs, and E. N. Fortson, *Phys. Rev. Lett.*, 86:2505–2508, 2001), which used two cells, achieved Larmor frequency sensitivity at the nanohertz level, yielding an upper bound on the EDM of $|d(^{199}\text{Hg})| < 2.1 \times 10^{-28} \text{ ecm}$. This result, together with results of other EDM experiments, placed tight constraints on T-violation in Supersymmetry. The new version of our experiment currently improves on the previous sensitivity by a factor of 5. The latest results will be reported in the talk.

QUANTUM INFORMATION PROCESSING AND RAMSEY SPECTROSCOPY WITH TRAPPED IONS

C. F. ROOS, M. CHWALLA, T. MONZ, P. SCHINDLER, K. KIM, M. RIEBE, P. O. SCHMIDT, W. HÄNSEL, HÄFFNER and R. BLATT

*Institut für Experimentalphysik, Universität Innsbruck, and
Institut für Quantenoptik und Quanteninformation, Österreichische Akademie der
Wissenschaften
6020 Innsbruck, Austria*

High-resolution laser spectroscopy and quantum information processing have a great deal in common. For both applications, ions held in electromagnetic traps can be employed, the ions' quantum state being manipulated by lasers. Quantum superposition states play a key role, and information about the experiment is inferred from a quantum state measurement that projects the ions' superposition state onto one of the basis states. For this reason, it is natural to investigate whether techniques for processing quantum information might also have applications in precision spectroscopy.

In my talk, I will present generalized Ramsey experiments investigating ion-ion couplings which are important in the context of high-fidelity quantum gates. Secondly, experiments aiming at making quantum information processing more robust against environmental noise will be discussed. I will show how to apply (quantum mechanically) correlated states of two ions for precision measurements of atomic constants. These ion-trap experiments demonstrate high-precision spectroscopy in a decoherence-free subspace using a pair of calcium ions for a determination of energy level shifts and transition frequencies in the presence of phase noise. For the measurement, maximally entangled ions are advantageous for achieving a good signal to noise ratio. As the preparation of these states is more involved than single-ion superposition states, we also explore the possibility of using classically correlated ions for achieving long coherence times.

QUANTUM-NON DEMOLITION MEASUREMENT OF LIGHT: THE BIRTH, LIFE AND DEATH OF TRAPPED PHOTONS

SERGE HAROCHE

Ecole Normale Supérieure and Collège de France, Paris.

Microwave photons, trapped in a very high-Q cavity¹ over time intervals reaching half a second, are non-destructively detected by a beam of two-level Rydberg atoms which behave as microscopic clocks interacting dispersively one by one with the field. This quantum non-demolition (QND) procedure, first proposed in², is achieved with a Ramsey interferometer detecting the light shift-induced alterations of the atomic clock's rate.

Applied to fields containing single photons, the method amounts to a measurement of the photon number parity, which is in principle pinned down with a single atom. Following over time the evolution of the parity signal, we have observed for the first time the quantum jumps of light revealing directly the birth and death of individual photons in the cavity³ (see Figure).

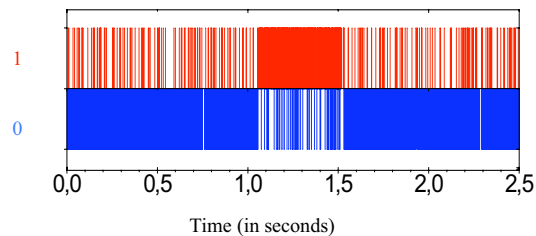


Figure: Output of Ramsey interferometer exhibiting field quantum jumps. Each atomic detection is shown as a vertical bar (1/0 in qubit notation). First, atoms are mainly found in 0 (even parity), signaling vacuum. A sudden transition from 0 to 1 (odd parity) reveals the birth of a photon around $t=1$ s. Another transition around $t=1.5$ s signals the return of cavity to vacuum. Between these jumps, a single photon has survived for about 0.5 s. Due to interferometer imperfections, a small fraction of atoms is erroneously detected in 1 in vacuum and in 0 in the one-photon state.

Counting larger photon numbers involves a multi-atom step-by-step extraction of information from the field obtained with a sequence of atoms crossing the cavity one at a time. Coherent states of radiation containing several photons progressively collapse into Fock states, as successive atoms are read out⁴. Photon number states $|n\rangle$ with n up to 7 are prepared and measured in this way. The subsequent history of these states is observed while the field

ascades down towards vacuum due to cavity damping. A statistical analysis of a large number of field trajectories recovers all the dynamical properties of light predicted by the quantum theory of radiation.

Before the field collapses into a Fock state, our progressive QND measurement prepares non-classical states of light. Superpositions of coherent states with different phases ("Schrödinger cats") as well as coherent sums of Fock states of the form $|n\rangle + |n+q\rangle$ with $q \gg 1$ are generated. The decoherence of these strange states will be investigated. Further applications of these ideal measurements to studies of fundamental properties of light trapped in one or two cavities will be briefly discussed.

1. S.Kuhr et al, *Appl.Phys.Lett.* **90**, 164101 (2007).
2. M.Brune et al, *Phys.Rev.Lett.* **65**, 976 (1990).
3. S.Gleyzes et al, *Nature*, **446**, 297 (2007).
4. C.Guerlin et al, *to be published*.

Attosecond pulse trains: shaping and applications

Thierry Ruchon*, Johan Mauritsson, Erik Gustafsson, Per Johnsson, Thomas Remetter, Marko Swoboda and Anne L'Huillier

*Department of Physics
Lund University*

P.O. Box 118, 221 00 LUND, Sweden

**E-mail: thierry.ruchon@fysik.lth.se*

www.atto.fysik.lth.se/

Focusing an intense infrared laser field in a gas medium, high order harmonics spanning from the ultraviolet to the soft X-ray region are generated. It provides the bandwidth required for getting attosecond pulses. However, the different frequency components in the harmonic spectrum are not naturally synchronized and the bursts obtained are usually not short.

In this communication, we will first report on progress in controlling the chirp of the harmonics over a broad spectrum using metallic filters. Previous experiments allowed us to observe 170 as pulses centered at 30 eV using harmonics generated in a static argon cell along with Al filters.¹ We have extended this technique to harmonics generated in a neon cell flowed by a kHz pulsed valve, which were filtered with aluminium, silicium or zirconium foils. We obtained pulse durations down to 130 as, centered at 80 eV.² Second, we will report on the use of phase matching to achieve a better synchronisation of the harmonics emission itself. In particular the roles of the length of the media and of the ionization rate on the temporal structure of the attosecond pulses will be highlighted.

Attosecond pulses have been used to study photoionization by XUV radiation in presence of a strong IR field. When using long IR pulses for the generation (35 fs), attosecond pulse trains with two pulses per cycle are obtained, and consecutive electron wave packets get different momentum shifts from the IR field. Recently, adding a small portion of doubled frequency light to the generation IR field, we have shaped attosecond pulse trains in order to get only one burst per laser period.³ Now, photoionization takes place in the same IR field for all bursts in the train, thus increasing the counting statistics compared to a single event. Recent results and movies recorded with this "stroboscope" will be presented.

Keywords: Attosecond technology; Atomic physics; Ultrafast pump-probe experiments

References

1. R. López-Martens, K. Varjú, P. Johnsson, J. Mauritsson, Y. Mairesse, P. Salières, M. B. Gaarde, K. J. Schafer, A. Persson, S. Svanberg, C.-G. Wahlström and A. L'Huillier, *Phys. Rev. Lett.* **94**, p. 033001 (2005).
2. E. Gustafsson, T. Ruchon, M. Swoboda, R. L. Martens, P. Balcou and A. L'huillier, *Optics Letters* **32**, 1353 (2007).
3. J. Mauritsson, P. Johnsson, E. Gustafsson, A. L'Huillier, K. J. Schafer and M. B. Gaarde, *Phys. Rev. Lett.* **97**, p. 013001 (2006).

Frequency-comb-assisted mid-infrared spectroscopy

P. DE NATALE*, D. MAZZOTTI, G. GIUSFREDI, S. BARTALINI and P. CANCIO

*CNR-Istituto Nazionale di Ottica Applicata and LENS, Via N. Carrara 1,
Sesto Fiorentino, I-50019 Italy*

**E-mail: paolo.denatale@inoa.it
www.inoa.it*

P. MADDALONI, P. MALARA and G. GAGLIARDI ,

*CNR-Istituto Nazionale di Ottica Applicata and LENS, Comprensorio 'A.Olivetti',
Via Campi Flegrei 34,
Pozzuoli, I-80078 Italy*

I. GALLI and S. BORRI

*LENS and Dipartimento di Fisica, Università di Firenze, Via N. Carrara 1,
Sesto Fiorentino, I-50019 Italy*

A new class of spectrometers, including one or more sources of coherent radiation referenced to an optical frequency-comb synthesizer, is already available and still progressing at a very fast pace.¹⁻³ The peculiar features of these spectrometers make them well suited for a wide range of applications, and their suitability for very high resolution and trace-gas spectroscopy has been carefully studied. These IR sources have unique capabilities in terms of achievable precision for absolute frequency measurements, very high sensitivity for trace-gas detection as well as compactness and ruggedness when a fiber-based set-up is chosen. To date, the best results for spectroscopic applications have been demonstrated using, as sources of IR radiation, difference-frequency-generation (DFG) set-ups^{1,4-6} or, more recently, a quantum cascade laser.² For DFG, we obtained an IR power up to several milliwatts, narrow spectral linewidth and a wide tunability in the $2.8 \div 4.5 \mu\text{m}$ spectral range, by mixing widely tunable lasers, often fiber-amplified, in periodically-poled LiNbO₃ crystals. This allows to access a large number of fundamental, thus very strongly absorbing, rovibrational transitions of many stable and transient molecular species. We used enhancement Fabry-Perot cavities with a finesse in excess of 24 000 to

further increase detection sensitivity. Application of such spectrometers to sensitive, precise and quantitative spectroscopy of selected test molecules will be shown.

References

1. D. Mazzotti, P. Cancio, A. Castrillo, I. Galli, G. Giusfredi and P. De Natale, *J. Opt. A* **8**, S490 (2006).
2. S. Bartalini, P. Cancio, G. Giusfredi, D. Mazzotti, P. De Natale, S. Borri, I. Galli, T. Leveque, and L. Gianfrani, *Opt. Lett.* **32**, 988 (2007).
3. P. Maddaloni, G. Gagliardi, P. Malara, and P. De Natale, *New Journal of Physics* **8**, 262 (2006).
4. P. Malara, P. Maddaloni, G. Gagliardi, and P. De Natale, *Optics Express* **14**, 1304-1313 (2006).
5. P. Maddaloni, P. Malara, G. Gagliardi, and P. De Natale, *Applied Physics B* **85**, 219-222 (2006).
6. P. Maddaloni, G. Gagliardi, P. Malara, and P. De Natale, *J. Opt. Soc. Am. B* **23**, 1938-1945 (2006).

GRAVITATIONAL WAVE INTERFEROMETERS AND THE SEARCH FOR THE ELUSIVE WAVES^{*}

NERGIS MAVALVALA[†]

*LIGO Laboratory, Massachusetts Institute of Technology, NW17-161
Cambridge, MA 02139, USA*

LIGO SCIENTIFIC COLLABORATION

<http://ligo.org>

As the Laser Interferometer Gravitational-wave Observatory (LIGO) and its international counterparts are carrying out the most sensitive astrophysical searches to date, we enter an exciting new era of gravitational wave astronomy. A report on the present status and recent results from the currently operational LIGO interferometers will be followed by a discussion of planned enhancements and the path to higher sensitivity next-generation detectors.

^{*} This work is supported by the National Science Foundation cooperative agreement nos. PHY-0107417 and PHY-0457264.

[†] Email: Nergis@ligo.mit.edu

PRECISION GRAVITY TESTS BY ATOM INTERFEROMETRY

G. M. TINO

*Dipartimento di Fisica and LENS Laboratory - Università di Firenze
Istituto Nazionale di Fisica Nucleare, Sezione di Firenze
via Sansone 1, Polo Scientifico
I-50019 Sesto Fiorentino (Firenze), Italy
E-mail: guglielmo.tino@fi.infn.it
<http://www.lens.unifi.it/tino/>*

Experiments we are performing using atom interferometry to determine the gravitational constant G [1] and test the Newtonian gravitational law at micro-metric distances [2] will be presented. Other experiments in progress, planned or being considered using atom interferometers in ground laboratories and in space [3] will be also discussed.

References

1. A. Bertoldi *et al.*, *Eur. Phys. J. D* **40**, 271 (2006).
2. G. Ferrari *et al.*, *Phys. Rev. Lett.* **97**, 060402 (2006).
3. G. M. Tino *et al.*, *Nuclear Physics B (Proc. Suppl.)* **166**, 159 (2007).

NO ABSTRACT SUBMITTED

T.W. HÄNSCH

Atomic magnetometers and their applications

M.V. Romalis

*Physics Department, Princeton University,
Princeton, NJ 08544, USA*

**E-mail: romalis@princeton.edu*

I will review recent progress in the development of atomic magnetometers and their applications¹. Atomic magnetometers typically use optical measurements of the Zeeman resonance in a dense vapor of alkali-metal atoms. Their fundamental sensitivity is limited by atomic collisions and by controlling the effects of these collisions one can measure magnetic fields in the atto-Tesla range, surpassing the sensitivity of even low-temperature SQUID magnetometers. Technical sources of noise, such as magnetic noise generated by magnetic shields, can also be suppressed, using, for example, a ferrite magnetic shield. Recently several new applications of atomic magnetometers have been demonstrated, including detection of brain magnetic fields, NMR, and nuclear quadrupole resonance. The fundamental sensitivity limits of atomic magnetometers still have not been reached and I will discuss paths for their further improvements and new applications.

References

1. D. Budker and M. Romalis, *Nature Phys.* **3**, 227 (2007).

ON A VARIATION OF THE PROTON-ELECTRON MASS RATIO

WIM UBACHS

Laser Centre Vrije Universiteit Amsterdam, The Netherlands

Recently indication on a possible variation of the proton-to-electron mass ratio m_p/m_e was found from a comparison between laboratory H_2 spectroscopic data and the same lines in quasar spectra. These methods and the progress thereafter will be discussed.

Recently the finding of an indication for a *decrease* of the proton-to-electron mass ratio $\mu = m_p/m_e$ by 0.002% in the past 12 billion years was reported [1]. We will discuss the methods that led to that result and put it in perspective. Laser spectroscopy on molecular hydrogen, using a narrow-band and tunable extreme ultraviolet laser system at the Laser Centre Vrije Universiteit Amsterdam, results in transition wavelengths of spectral lines in the B-X Lyman and C-X Werner band systems at an accuracy of $(4 - 10) \times 10^{-8}$, depending on the wavelength region. This corresponds to an absolute accuracy of 0.000004 - 0.000010 nm. A database of 233 accurately calibrated H_2 lines is produced for future reference and comparison with astronomical observations. Recent observations of the same spectroscopic features in cold hydrogen clouds at redshifts $z=2.5947325$ and $z=3.0248970$ in the line of sight of two quasar light sources (Q 0405-443 and Q 0347-383) resulted in 76 reliably determined transition wavelengths of H_2 lines at accuracies in the range 2×10^{-7} to 10^{-6} . Those observations were performed with the Ultraviolet and Visible Echelle Spectrograph at the Very Large Telescope of the European Southern Observatory at Paranal, Chile. A third ingredient in the analysis is the calculation of an improved set of sensitivity coefficients K_i , a parameter associated with each spectral line, representing the dependence of the transition wavelength on a possible variation of the proton-to-electron mass ratio. Details of the methods are reported in Ref. [2].

A statistical analysis of the data yields an indication for a variation of the proton-to-electron mass ratio of $\Delta\mu/\mu = (2.45 \pm 0.59) \times 10^{-5}$ for a weighted fit and $\Delta\mu/\mu = (1.98 \pm 0.58) \times 10^{-5}$ for an unweighted fit. This result has a statistical significance of 3.5σ . Mass-variations as discussed relate to *inertial* or kinematic masses, rather than gravitational masses. The observed decrease in μ

corresponds to a rate of change of $d\ln \mu/dt = -2 \times 10^{-15}$ per year, if a linear variation with time is assumed.

Ongoing and future activities concerning laboratory experiments on the H_2 spectrum as well as planned astronomical observations that should lead to improvements on a constraint on μ -variation will be discussed.

Acknowledgments

The author wishes to acknowledge the XUV-laser team at LCVU for their contributions: R. Buning, K. S. E. Eikema, S. Hannemann, U. Hollenstein, T. I. Ivanov, C. A. de Lange, J. Philip, Th. Pielage, E. Reinhold, E.J. Salumbides, J. P. Sprengers, and M. O. Vieitez.

References

1. E. Reinhold, R. Buning, U. Hollenstein, A. Ivanchik, P. Petitjean, W. Ubachs, *Phys. Rev. Lett.* **96**, 151101 (2006).
2. W. Ubachs, R. Buning, K. S. E. Eikema, E. Reinhold, *J. Mol. Spectr.* **241**, 155 (2007).

QUANTUM STATE GENERATION AND STORAGE WITH ATOMIC MEDIA

E. GIACOBINO, J. CVIKLINSKI, J. ORTALO, V. JOSSE, A. DANTAN, M. PINARD,
A. BRAMATI

*Laboratoire Kastler Brossel, Université Paris 6, ENS, CNRS, 4 Place Jussieu,
F 75252 Paris Cedex 05 France*

Cold atomic ensembles and atomic vapors have a good potential for both generation and storage of non classical states of light. Generation of non classical states of light is possible through the high non-linearity of atomic samples excited close to a resonance line. Quadrature squeezing, polarization squeezing and entanglement have been demonstrated. Quantum state storage is made possible by the presence of long lived angular momenta in the ground state. Cold atoms are thus a promising resource in quantum information.

Atomic ensembles are known to be good media to generate squeezed states of light. More recently their potential for the generation of other kinds of quantum states such as entangled states and for the storage of quantum states has been evidenced.

After producing large quadrature squeezing using cold cesium atoms interacting with circularly polarized light in an optical cavity, further properties of cold atom media have been demonstrated. We have shown that if linearly polarized light interacts with cold atoms in a cavity, the output light is made of two squeezed modes, the mean field mode and the orthogonal vacuum mode. Cold atoms thus generate polarization squeezing [1]. Let us note that atomic vapors have been shown recently to produce large intensity squeezing [2].

Moreover, entanglement can also be directly generated by the atomic system. Entanglement, one of the basic properties of quantum mechanics, can be obtained for continuous variables by mixing two squeezed fields on a beam splitter. Here, since the two squeezed modes propagate along the same beam, entanglement is easily obtained by an appropriate choice of polarizations [1].

The rich properties of cold atoms also allow exploring other kinds of quantum features. Indeed an ensemble of atoms can record a quantum electromagnetic signal, a single photon, or quantum fluctuations of a classical beam in a quantum state of its ground level. The quantum register can then be

read using a classical beam, allowing recovering the quantum signal. Atomic ensembles have been widely studied as potential quantum memories [3]. Indeed, the long-lived collective spin of an atomic ensemble with two ground state sublevels appears as a good candidate for the storage and manipulation of quantum information conveyed by light. Various schemes have already been studied base on 3-level systems interacting with two light fields. However, the experimental realisation of the storage of quantum states, together with the read out, with fidelity higher than the classical one is still missing.

We have studied a set of N three-level atoms in a Λ configuration which interacts on each transition with one mode of the electromagnetic field in an optical cavity, either in the EIT or the Raman configuration. We consider a simple situation in which the control field, close to resonance with one transition, with some detuning, is a strong, classical one, and the second field close to resonance with the other transition with the same detuning, is a quantum field with a zero mean value.

Taking into account all the noise sources, including the atomic noise generated by spontaneous emission and optical pumping, it can be shown that the two quadratures of the quantum field can be mapped onto the two transverse components of the ground state atomic spin with an efficiency close to 100%[4]. After a write time which is on the order of the characteristic interaction time between atoms and fields, the control and signal fields can be switched off. The quantum variables are stored in the ground state. For the read-out, the control field is turned on again. The quantum variables can be retrieved in the outgoing field with a very good efficiency again, with an appropriate choice of the detection temporal profile [5].

References

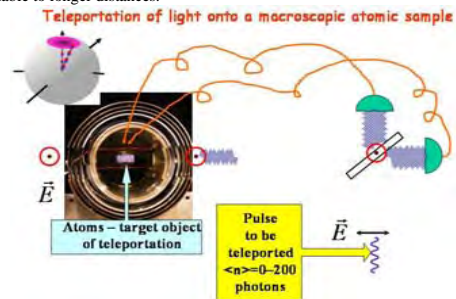
- 1 V. Josse *et al*, *Phys. Rev. Lett.* **91**, 103601 (2003); V. Josse *et al*, *Phys. Rev. Lett.* **92**, 123601 (2004)
- 2 C.F. McCormick, A. M. Marino V. Boyer, P.D. Lett., *quant-ph/0703173*
- 3 M.D Lukin, *Rev. Mod. Phys.* **75**, 457 (2003) ; L.M. Duan, J.I. Cirac, P. Zoller and E.S. Polzik, *Phys. Rev. Lett.* **85**, 5643 (2000)
- 4 A. Dantan and M. Pinard, *Phys. Rev.* **A69**, 043810 (2004); Dantan, A. Bramati, M. Pinard, E. Giacobino, *Laser Physics* **15**, 170 (2005)
- 5 A. Dantan *et al*, *Phys. Rev. A* **032338** (2006)

Quantum teleportation between light and matter

Eugene Polzik
Niels Bohr Institute, Copenhagen University

Spectroscopy which is sensitive to the quantum fluctuations of both light and matter becomes a powerful tool in quantum state engineering and control. A qualitatively new feature of such spectroscopy is that the atomic object and the light become entangled. As the first example we will discuss the recent application to quantum information – the teleportation between light and atoms.

Quantum teleportation is a way to transfer an unknown quantum state between two objects. It is performed using a quantum (entangling) channel and a classical communication channel. Teleportation is an important ingredient in distributed quantum networks, and can also serve as an elementary operation in quantum computers [1]. The teleportation between objects of a different nature—light and matter, which respectively represent ‘flying’ and ‘stationary’ media has been recently demonstrated for the first time [2]. A quantum state of a few-photon pulse is teleported onto a macroscopic object (an atomic ensemble containing 10^{12} caesium atoms). The fidelity up to 64% higher than any classical communication can possibly achieve has been demonstrated. An important factor for the implementation of quantum networks is the teleportation distance between transmitter and receiver; this is 0.5 metres in the present experiment and should be scalable to longer distances.



The Figure shows a paraffin coated glass cell filled with a gas of Cs atoms in a magnetic field corresponding to the Zeeman frequency of 322 kHz. A strong “entangling” pulse E polarized orthogonally to the plane of the Figure propagates through the atoms from left to right. As a result of the interaction, sidebands of this pulse at 322 kHz are scattered into the polarization in the plane of the Figure. These entangled with atoms sidebands are mixed on the 50/50 beamsplitter with a weak pulse with the frequency of the upper sideband - the object of teleportation. Bell measurements (quantum limited polarization homodyning spectroscopy) of two quadratures of light are then performed by detectors. The outputs of the detectors are the 322 kHz components of the photocurrent integrated over the pulse duration. Finally classical feedback conditioned on the outputs is applied to atoms. Atomic collective spin is rotated by the feedback signal thus completing the teleportation protocol.

The teleportation is demonstrated for weak coherent states with the mean photon number 0 - 300. This teleportation protocol is suitable also for a light qubit. Fidelity of the teleportation can theoretically reach 100% if a squeezed state of the strong pulse is used.

The second example of quantum limited spectroscopy which we will briefly discuss is a recently proposed method for quantum non-demolition detection of various spin states of strongly interacting ultracold gasses and magnetic ordering [3]. By performing an off-resonant polarization spectroscopy on a spinor condensate or a lattice it is possible to unambiguously distinguish between various quantum phases, such as polar, ferromagnetic, dimer, etc.

1. Deterministic atom-light quantum interface. J. Sherson, B. Julsgaard, and E.S. Polzik. *Advances of Atomic Molecular and Optical Physics*, Vol. 54, November 2006, Academic Press.
2. Quantum teleportation between light and matter. J. F. Sherson, H. Krauter, R. K. Olsson, B. Julsgaard, K. Hammerer, I. Cirac, and E. S. Polzik, *Nature*, **443**, 557- 560, (2006.)
3. Quantum polarization spectroscopy of ultracold spinor gases. K. Eckert, L. Zawitkowski, A. Sanpera, M. Lewenstein, and E.S. Polzik. *Phys. Rev. Lett.* **98**, 100404 (2007).

AN ATOMIC FERMI GAS NEAR A P-WAVE FESHBACH RESONANCE

2

DEBORAH JIN[†]

*NIST and JILA, University of Colorado, Boulder, 440 UCB
Boulder, CO 80309-0440, USA*

Atomic scattering resonances, called Feshbach resonances, have been used to create molecular Bose-Einstein condensates and Fermi superfluids. Past work has focused on s-wave, or non-rotating, pairs created from two fermionic atoms. I will report on investigations of pair creation in an ultracold Fermi gas of potassium-40 atoms near a p-wave Feshbach resonance.

[†] Work partially supported by grant 2-4570.5 of the Swiss National Science Foundation.

BRAGG SCATTERING OF CORRELATED ATOMS FROM A DEGENERATE FERMION GAS

R. J. BALLAGH, K. J. CHALLIS, and C. W. GARDINER

*Jack Dodd centre for Photonics and Ultra-Cold atoms
Physics Department, University of Otago,
Dunedin, New Zealand*

** E-mail: ballagh@physics.otago.ac.nz*

www.physics.otago.ac.nz/pr/research/ultra-cold-atoms

Superfluidity in fermion systems arises due to correlated (Cooper paired) particles on the Fermi surface. Techniques for probing this correlation have primarily concentrated on the energy gap associated with the pairing. Here we show that Bragg scattering with laser fields provides a coherent probe mechanism which can reveal a unique signature of the pairing correlation. We solve the time-dependent Bogoliubov de Gennes equations in three dimensions to present a quantitative analysis of the scattering. A Bragg field of the form $A \cos(\mathbf{q} \cdot \mathbf{r} - \omega t)$ applied to a gas in an equilibrium BCS state produces the expected momentum transfer of $\hbar \mathbf{q}$ to some of the atoms. The key result however is that an additional spherical shell appears in atomic momentum space, centered on $\hbar \mathbf{q}/2$, as shown in the left hand frame of the figure.

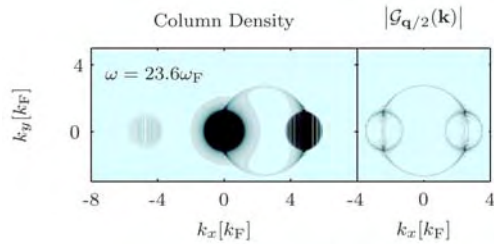


Fig. 1. Column density and pair correlation function for Bragg scattered atoms. Units k_F and ω_F are Fermi wavevector and frequency; $\mathbf{q} = 4.8k_F \hat{k}_x$ and $A = 1.8\hbar\omega_F$.

The correlation function plotted in the right hand frame of the figure, $\mathcal{G}_{\mathbf{q}/2}(\mathbf{k}, t) = \langle \hat{\phi}_{\uparrow}(\mathbf{q}/2 + \mathbf{k}, t) \hat{\phi}_{\uparrow}(\mathbf{q}/2 - \mathbf{k}, t) \rangle$ (where $\hat{\phi}_{\uparrow}$ is the spin-up momentum space field operator) demonstrates that the atoms scattered into the spherical shell are pair correlated. The atomic collisional interaction is critical to this phenomenon, and we find that the usual contact potential approximation is inappropriate. We investigate the parameter dependence of the correlated pair scattering, and develop an analytic model that provides an interpretation of the major features and the underlying mechanisms, including the frequency threshold behaviour and the spherical geometry.

STARK AND ZEEMAN DECELERATIONS OF NEUTRAL ATOMS AND MOLECULES*

S. D. HOGAN, E. VLIEGEN, D. SPRECHER, N. VANHAECKE, B. H. MEIER AND F. MERKT[†]

*Laboratorium für Physikalische Chemie, ETH Zurich
CH 8006 Zurich, Switzerland*

The development of general methods with which to control the translational motion of atoms and molecules in the gas phase is of particular interest in high resolution spectroscopy and studies of cold reactive collisions. Several of these techniques start from cold samples formed in supersonic expansions and aim at stopping them in the laboratory frame. The techniques employed include multi-stage Stark deceleration of polar molecules [1], optical Stark deceleration [2], and Rydberg Stark deceleration [3,4]. Recently, the Zeeman equivalent of the multi-stage Stark deceleration method has also been realized experimentally [5]. Recent progress in Rydberg Stark deceleration and in multi-stage Zeeman deceleration of free radicals will be presented as briefly outlined below.

1. Stark Deceleration of Rydberg atoms and molecules

Recent progress in the development of methods by which to decelerate and manipulate the translational motion of Rydberg atoms and molecules [3,4] in the gas phase using static and time-varying inhomogeneous electric fields has led to the experimental realization of Rydberg atom optics elements including a lens [6] and a mirror [7]. These experiments exploit the very large electric dipole moments associated with Rydberg Stark states.

With the goal of achieving complete control of a cloud of Rydberg atoms or molecules in three-dimensions, we have recently designed and constructed two- and three-dimensional electrostatic traps for these particles. The design of these traps will be presented along with the results of a series of experiments in which we have trapped a cloud of atomic hydrogen Rydberg atoms in states with principal quantum numbers around $n=30$. The dynamics of the Rydberg atoms

[†] This work is supported by ETH Zurich and the Swiss National Science Foundation..

in the traps have been investigated by pulsed field ionization and imaging techniques. Trap losses by collisional and radiative processes have been observed and quantified.

2. Zeeman deceleration of free radicals

The Zeeman decelerator developed in Zurich [5] is composed of a series of co-axial solenoids through which a pulsed gas beam propagates. By applying current pulses in each solenoid to generate a pulsed magnetic field as the gas pulse enters, we can take advantage of the linear Zeeman interaction of a ground state atom or molecule with unpaired electrons to decelerate the gas pulse in a manner analogous to that employed in a multi-stage Stark decelerator [1].

The optimal magnetic field pulse sequences are determined in numerical particle trajectory simulations, and subsequently programmed and applied to the coils. They permit us to implement the concepts of phase stability as in the Stark decelerator and in charged particle accelerators [8,9].

The results of a recent series of experiments in which we have decelerated ground state atomic hydrogen with the Zeeman decelerator will be presented. In these experiments magnetic fields of 1-2 T were pulsed in each coil for tens of microseconds, with rise and fall times as short as 5 μ s. We have characterized the decelerated part of the gas pulse and studied the effects on the deceleration of zero-field time windows during which electron spin flips can occur.

References

1. H. L. Bethlem, G. Berden, and G. Meijer, *Phys. Rev. Lett.* **83**, 1558 (1999).
2. R. Fulton, A. I. Bishop, and P. F. Barker, *Phys. Rev. Lett.* **93**, 243004 (2004).
3. S.R. Procter, Y. Yamakita, F. Merkt, and T.P. Softley, *Chem. Phys. Lett.* **374**, 667 (2003).
4. E. Vliegen, H. J. Woerner, T. P. Softley and F. Merkt, *Phys. Rev. Lett.* **92**, 033005 (2004).
5. E. N. Vanhaecke, U. Meier, M. Andrist, B. H. Meier and F. Merkt, *Phys. Rev. A* **75**, 031402(R) (2007).
6. E. Vliegen, P. A. Limacher and F. Merkt, *Eur. Phys. J. D* **40**, 73E (2006).
7. E. Vliegen and F. Merkt, *Phys. Rev. Lett.* **97**, 033002 (2006).
8. V. Veksler, *J. Phys. (USSR)* **9**, 153 (1945).
9. E. M. McMillan, *Phys. Rev.* **68**, 143 (1945).

DYNAMICS OF MOLECULES AND CLUSTERS WITH FEMTOSECOND AND ATTOSECOND RESOLUTION

DANIEL M. NEUMARK

Department of Chemistry, University of California, Berkeley, CA 92720, and Chemical Sciences Division, Lawrence Berkeley National Laboratory, Berkeley, CA 94720

Time-resolved photoelectron spectroscopy measurements provide a powerful means of following complex dynamics in molecules and clusters. Experiments with femtosecond time-resolution can monitor nuclear motion in clusters in real-time, while the emerging field of attosecond science offers the potential to follow electronic dynamics. Results will be presented on the femtosecond dynamics of negatively-charged clusters in which an excess electron is bound to an aggregate of solvent molecules (water, methanol, acetonitrile). These experiments provide a vital link with the dynamics of solvated electrons in bulk liquids. We have also made significant recent progress in generating isolated attosecond pulses in the vacuum-ultraviolet and soft x-ray energy regimes; recent results and prospects for investigating attosecond dynamics in molecules and clusters will be presented.

**CONTROLLING NEUTRAL ATOMS AND PHOTONS
WITH OPTICAL CONVEYOR BELTS
AND ULTRATHIN OPTICAL FIBERS**

DIETER MESCHEDE

*Institut für Angewandte Physik der Universität Bonn,
Wegelerstr. 8 D-53115 Bonn, Germany*

We store caesium atoms in a 1D standing wave optical dipole trap with no more than one atom per site and sufficient spacing to individually control the properties of each atom. The caesium ground state hyperfine levels are used as qubit states, and all single-atom qubit operations have been realized in the past already, thereby realizing a neutral atom quantum register for a bottom-up approach towards quantum information processing with neutral atoms. With a second optical dipole trap we extract atoms from their trapping sites and insert them into other micropotentials. This allows us to regularize the spacing of stored atoms, to insert two atoms into one and the same micropotential in order to induce controlled interactions, and to insert atoms in a controlled way into high finesse optical resonators.

In a new line of research we are exploring the potential of light confined by micro-structured thin optical fibers for controlled light-matter interaction in quantum optics. We have constructed fully tunable bottle micro-resonators and we have found that we can very efficiently detect and manipulate atoms or molecules in the immediate vicinity of fibres with sub-wavelength diameters.

WIDE-FIELD CARS-MICROSCOPY

CHRISTOPH HEINRICH, ALEXANDER HOFER,
STEFAN BERNET, MONIKA RITSCH-MARTE

*Division for Biomedical Physics, Innsbruck Medical University,
Innsbruck, Austria*

**E-mail: monika.ritsch-marte@i-med.ac.at*

We have developed a non-scanning version of a Coherent anti-Stokes Raman Scattering (CARS) microscope¹. In contrast to the more common confocal implementation, where one scans tightly focussed fs- or ps-pulses over the sample, we use ns-pulses and a special excitation geometry that is designed to satisfy the phase matching condition over the whole field of view. This allows fast image acquisition, even snapshots with a *single* shot of the ns laser pulses are possible².

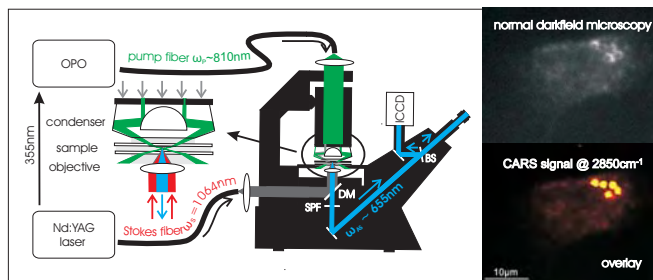


Fig. 1. Schematic setup of the wide-field CARS-microscope (left) and selective imaging of small lung surfactant vesicles (diameter 1 - 0.9 μm) inside living alveolar cells (right).

The dark-field condenser used to satisfy the phase matching condition provides a narrow *sheet of light* illumination which very effectively suppresses the non-resonant CARS background. It also improves the optical sectioning capability that is inherent to nonlinear optical imaging, by axially confining the nonlinear interaction zone.

The performance of our wide-field CARS-microscope is demonstrated on var-

ious test samples: The spatial resolution is sufficient for chemically selective imaging of (sub-)micron vesicles, containing e.g. lipids or lung surfactant, inside living cells. Moreover, the good spectral resolution of 5 cm^{-1} and the low non-resonant background allow one to visually differentiate the various types of lipid droplets in a mixed micro-emulsion directly in the unprocessed images, and to quantify the saturation of the fatty acids contained in the different vegetable oils.

Keywords: CARS microscopy, vibrational imaging, Raman spectroscopy

References

1. C. Heinrich, S. Bernet and M. Ritsch-Marte, Appl. Phys. Lett. **84**, 816 (2004).
2. C. Heinrich, S. Bernet and M. Ritsch-Marte, New J. Phys. **8**, 36 (2006).

This work was supported by the Austrian Science Fund FWF (Project P16658-N02).

ATOM NANO-OPTICS AND NANOLITHOGRAPHY

VICTOR BALYKIN

Institute of Spectroscopy, Troitsk, Moscow region, 142190 Russia

We report on a new approach in atom-nano-optics that is based on the use of one, two and three dimensional spatially on nanometer scale localized laser fields as well as the creation of nanostructures on the surface.

Atom nano-optics is part of an extensive research domain that embraces the manipulation of free atoms on the nanoscale [1, 2].

We report on a new approach in atom-nano-optics that is based on the use of one, two and three dimensional spatially on *nanometer scale* localized laser fields. *One-dimensional* field is an evanescent wave. Evanescent waves find widespread use in laser atom optics [3]. *Two-dimensional* field is produced through the diffraction of laser light on a small (in comparison to wavelength) aperture in a conductive plane [4]. In this case, a local maximum of field intensity is formed near the aperture. The magnitude of the maximum is governed mainly by the size of the aperture. The use of two parallel conductive screens with small coaxial apertures permits to create a *three-dimensional* localized laser field [1, 5]. The two plates spaced a distance smaller than the wavelength form a plane waveguide for the laser radiation coupled into it. If the electric field strength vector of the laser radiation is normal to the plane of the waveguide, the radiation can propagate through the waveguide, no matter how thin it is. The light field near the apertures is strongly modified. There is a light field intensity minimum in the direction normal to the plane of the waveguide. Such a light field configuration can be called as *photon hole*. Its characteristic size is determined by the size of the apertures a , the thickness of the waveguide d and its volume $V \ll \lambda^3$. Another nanofield can be created by using two conductive screens with coaxial apertures and spaced at distance of $d = a/2$ apart. The electric field strength vector is parallel to the waveguide plane in this configuration. The intensity distribution in the aperture region drops off rapidly outside the waveguide in the direction normal to the waveguide and has its maximum at the center of the waveguide. Such a light field configuration can be called a *photon dot*. The characteristic volume of such a photon dot is $V \ll \lambda^3$. The characteristic size of a photon dot or a photon hole is in the nanometer region. We discuss an application of the nanofields in atom optics and laser spectroscopy.

The most difficult problem in atom optics is the problem of high-resolution focusing of neutral atoms, which is promising as a nondestructive method for probing the surface at the atomic level, as well as for the creation of nanostructures on the surface. Although there are many proposals for focusing of atomic beams, this problem is experimentally unsolved. The main difficulty is

the creation of the interaction potential of the atom with the electromagnetic field that is close to an “ideal” lens for atoms.

We report on implementation of another approach [6] to the problem of focusing and construction of an image in atom optics, which is based on a well known idea of “*optical pinhole camera*”. In our experiment with *the atom pinhole camera* the atomic beam passes through a set of holes in a metal mask and thereby forms, by analogy with optics, a “glowing” object of a given geometry. The atoms pass through the holes in the mask, propagate in vacuum along rectilinear trajectories, similar to light rays, and incident on a thin film placed at a distance of L from the mask with a large number of nanoholes. Each nanohole of the film is a pinhole camera for atoms, which forms its individual image of the object on the substrate surface placed at a distance of l behind the film. In this geometry, a set of the images of the object, which are decreased by a factor of about $m = L / l = 10000$ and are formed by atoms deposited on the surface, is created on the substrate. By using an array of apertures, the total number of nanostructures produced in one process exceeds 10^7 on a 2×2 mm area of the substrate surface. The nanostructures produced have heights in the range of 1-10 nm and lateral spatial features of less than 50 nm.

References

1. V. I. Balykin, V.V. Klimov and V. S. Letokhov, *Atom Nano-Optics*, Optics & Photonics News, **16**, 33 (2005).
2. V.I. Balykin, V.V. Klimov, V.S. Letokhov, *Atom Nanooptics*, In “Handbook of Theoretical and Computational Nanotechnology”, eds., M. Rieth and W. Schommers, American Scientific Publishers (2006).
3. H. Oberst, S. Kasashima, V. Balykin, F. Shimizu, *Phys. Rev.* **A68**, 013606 (2003).
4. V. Balykin, V. Klimov, V. Letokhov, *J. Phys. II France*, **4**, 1981 (1994).
5. V. Balykin, V. Klimov, Letokhov, *JETP Lett.*, **78**, 8 (2003).
6. V. I. Balykin, P. A. Borisov, V. S. Letokhov, P. N. Melent'ev, S. N. Rudnev, A. P. Cherkun, A. P. Akimenko, P. Yu. Apel, and V. A. Skuratov, *JETP Lett.*, **84**, 466 (2006).

Ultracold & ultrafast: Making and manipulating ultracold molecules with time-dependent laser fields

C. P. Koch

Institut für Theoretische Physik, Freie Universität Berlin,

Arnimallee 14, D-14195 Berlin, Germany

E-mail: ckoch@physik.fu-berlin.de

www.physik.fu-berlin.de/~ag-koch

While ultracold matter brought quantum effects onto the macroscopic scale, ultrafast lasers made quantum dynamical phenomena observable in real-time. Bringing the two together seems natural and holds the promise of employing quantum interferences in an unprecedented way. Photoassociation provides an optimal framework for the merger since in principle it relies only on the presence of optical transitions. Combining it with coherent control where the potential energy surfaces governing the dynamics can be 'shaped', a general route toward stable ultracold molecules is obtained.

I will present theoretical predictions for coherent formation of ultracold alkali and alkaline earth dimer molecules in a two-color pump-dump scheme. The pump or photoassociation pulse transfers part of the atomic density into an electronically excited molecular state, giving rise to a non-stationary wavepacket. Subsequently, the dump or stabilization pulse catches this wavepacket, sending it back to the electronic ground state before spontaneous decay sets in. This pump-dump scheme leads to ultracold ground state molecules as well as pairs of hot atoms. The efficiency of molecule formation is determined by the shape of the excited state potentials. The probability of photoassociation is highest for excitation into the long-range $1/R^3$ excited-state potentials of homonuclear dimers. Potentials favorable to efficient stabilization exist in the heavy alkali systems due to spin-orbit coupling: Softly repulsive potential walls and resonantly coupled potentials allow for molecular binding energies of the order of 10–100 cm^{-1} . In the alkaline earth dimers, potentials with $1/R^3$ long-range behavior do not show any features favorable for stabilization. However, an additional external field can be employed to take over the role of the resonant spin-orbit coupling of the alkalis, and qualitatively change the excited state dynamics. This field-induced resonant coupling is completely controlled externally. If molecule formation is to be followed by subsequent Raman steps, the field-induced resonant coupling can be adjusted to facilitate dynamics toward the vibronic ground state.

I will conclude by discussing future perspectives of manipulating ultracold matter with ultrafast lasers.

HIGH-RESOLUTION LASER SPECTROSCOPY OF ULTRACOLD YTTERBIUM

YOSHIRO TAKAHASHI,

*Department of Physics, Graduate School of Science, Kyoto University, Oiwakecho,
Kitashirakawa, Sakyo-ku, Kyoto City, Kyoto, 606-8502, Japan*

We have performed high-resolution laser spectroscopy using ultracold ytterbium (Yb) atoms. The various quantum degenerate gases of Yb have been successfully created and the scattering lengths have been precisely determined by high-resolution two-color photo-association spectroscopy. High-resolution laser spectroscopy of ultracold Yb atoms using the ultra-narrow intercombination transitions $^1S_0\text{-}^3P_0$ and $^1S_0\text{-}^3P_2$ has been also performed.

The study of ultracold dilute gases is undoubtedly one of the most interesting research fields. In particular, a ultracold gas of ytterbium (Yb) is remarkable in that it offers many interesting possibilities. The two valence electrons result in singlet and triplet states connected by extremely narrow intercombination transitions which have received considerable attention as a frequency standard with unprecedented precision^{1,2}. The existence of rich varieties of stable isotopes of five bosons (^{168}Yb , ^{170}Yb , ^{172}Yb , ^{174}Yb , and ^{176}Yb) and two fermions (^{171}Yb and ^{173}Yb) will allow us to study various interesting quantum degenerate gases using Yb atoms.

Recently we have successfully created various quantum degenerate gases of Yb atoms by all optical means. In addition to the previously obtained Bose-Einstein condensation (BEC) of ^{174}Yb , we have obtained BEC of ^{170}Yb and ^{176}Yb . In particular, the mixture of BEC of ^{176}Yb and ^{174}Yb has been obtained by a sympathetic cooling method. The similar all optical method has been successfully applied to obtain Fermi degeneracy of 6 spin mixtures of ^{173}Yb atoms³ and ^{174}Yb - ^{173}Yb quantum degenerate mixture.

We have also performed the high-resolution two-color photo-association spectroscopy to determine the binding energies of least bound states of six isotopes of Yb. Based on these measurements and theoretical considerations, we have accurately determined the scattering lengths of all Yb isotopes as well as those of different isotope pairs. The obtained scattering lengths are consistent with the behaviors of our successfully obtained BECs of ^{174}Yb , ^{170}Yb , and ^{176}Yb ,

2

and evaporative cooling. The optical Feshbach resonance experiment has been also performed to change the scattering length⁴.

In addition, we have performed high-resolution laser spectroscopy of ultracold bosonic and fermionic Yb atoms using the ultra-narrow intercombination transitions $^1S_0\text{-}^3P_0$ and $^1S_0\text{-}^3P_2$. By performing the spectroscopy with the different trap confinement for the ground and excited states, the spectrum can reflect the energy distribution of the ultracold gas. We will also discuss the possible application of ultracold Yb atoms in an optical lattice to a scalable quantum computation by making use of the large magnetic moment for the 3P_2 state and ultra-narrow linewidth of the $^1S_0\text{-}^3P_2$ transition.

Acknowledgments

This work was done under the collaboration with T. Fukuhara, S. Sugawa, A. Yamaguchi, S. Kato, M. Kitagawa, S. Uetake, K. Enomoto, Y. Takasu, P. S. Julienne, R. Ciurylo, and P. Naidon.

References

1. M. Takamoto, F.-L. Hong, R. Higashi, and H. Katori, *Nature* **435**, 321 (2005).
2. Z. W. Barber, C. W. Hoyt, C. W. Oates, L. Hollberg, A. V. Taichenachev, and V. I. Yudin, *Phys. Rev. Lett.* **96**, 083002 (2006).
3. T. Fukuhara, Y. Takasu, M. Kumakura, and Y. Takahashi., *Phys. Rev. Lett.* **98**, 030401 (2007).
4. R. Ciurylo, E. Tiesinga, and P. S. Julienne, *Phys. Rev. A* **71**, 030701(R) (2005).

BOSE-EINSTEIN CONDENSATES ON PERMANENT MAGNET MICROSTRUCTURES ON AN ATOM CHIP

S. WHITLOCK, M. SINGH, R. ANDERSON, B.V. HALL, M. VOLK, A.I. SIDOROV AND
P. HANNAFORD

*ARC Centre of Excellence for Quantum-Atom Optics and
Centre for Atom Optics and Ultrafast Spectroscopy
Swinburne University of Technology, Melbourne, Australia 3122*

We report on recent experiments on Bose-Einstein condensates on permanent magnet microstructures mounted on an atom chip [1]. Magnetic microstructures based on permanent magnetic films can produce highly stable, reproducible potential wells with low technical noise and low heating rates and they can be produced with large trap depth and high trap frequencies without ohmic heating. Our permanent magnet microstructures are fabricated in-house using perpendicularly magnetised TbGdFeCo magneto-optical thin films.

Ultracold atoms near the transition temperature have a narrow distribution of energies and thus concentrate in local minima of the potential so that the atomic density decreases with the rise of the potential. By using rf-induced spin-flips to remove atoms where the Zeeman splitting matches the rf frequency, we have mapped small variations of the magnetic field close to an edge of a magneto-optical film and have demonstrated that ultracold atoms can be used as a sensitive surface microprobe [2]. We have also carried out experiments on a double-well potential with tunable asymmetry on the magneto-optical film to dynamically split a BEC of ^{87}Rb atoms. By controlling the barrier height and double-well asymmetry, we show that the distribution of the superfluid between the two wells responds strongly to the asymmetry and that such a double well can be a sensitive sensor of gradients of potentials [3].

We also report investigations on the use of perpendicularly magnetised thin films to construct periodic magnetic lattices for manipulating BECs and ultracold atoms on an atom chip [4]. Magnetic lattices do not involve laser beams and hence there is no decoherence due to spontaneous emission, and only atoms in low magnetic field seeking states can be trapped, allowing the possibility of performing radiofrequency evaporative cooling *in situ* in the lattice and the study of very low temperature phenomena in a lattice.

References

1. B.V. Hall, S. Whitlock, F. Scharnberg, P. Hannaford and A. Sidorov, *J. Phys. B* **39**, 27-36 (2006).
2. S. Whitlock, B.V. Hall, T. Roach, R. Anderson, M. Volk, P. Hannaford and A.I. Sidorov, *Phys. Rev. A* **75**, 043602 (2007).
3. B.V. Hall, S. Whitlock, R. Anderson, P. Hannaford and A.I. Sidorov, *Phys. Rev. Lett.* **98**, 030402 (2007).
4. S. Ghanbari, T.D. Kieu, A. Sidorov and P. Hannaford, *J. Phys. B* **39**, 847 (2006).

STRONGLY CORRELATED QUANTUM PHASES WITH COLD POLAR MOLECULES

HANS-PETER BÜCHLER

*Theoretische Physik, Universität Innsbruck, Technikerstr. 25
Innsbruck, Austria*

The quest for quantum degenerate polar molecules marks one of the latest developments in the rapidly evolving field of ultracold gases. A characteristic property of these heteronuclear molecules is a finite permanent electric dipole moment, which allows for driving an anisotropic dipole-dipole interaction between the particles using static electric fields and/or microwave fields.

This strong and tunable long-range interaction offers the opportunity for wide application in designing strongly correlated systems. We will present some examples of possible strongly correlated systems which can be obtained in polar molecules such as crystalline structures, and Hubbard models with three-body interactions. This crystalline phase has potential applications as an alternative method to optical lattice for creating lattice structures for cold atomic gases with the advantage of a natural honeycomb and triangular lattice structure and the coupling to phonons as a heat bath. Furthermore, the strong repulsion on short distances provides a reduction of inelastic collisions and consequently the long life-time makes these crystals very appealing for the usage as a quantum information storage devices.

ULTRACOLD METASTABLE HELIUM-4 and HELIUM-3 GASES

W. VASSEN*, T. JELTES, J. M. McNAMARA and W. HOGERVORST

Laser Centre Vrije Universiteit, De Boelelaan 1081,
1081 HV Amsterdam, The Netherlands

*E-mail: w.vassen@few.vu.nl
www.few.vu.nl/~wim

V. KRACHMALNICOFF, M. SCHELLEKENS, A. PERRIN, H. CHANG,
D. BOIRON, A. ASPECT and C. I. WESTBROOK

Laboratoire Charles Fabry de l'Institut d'Optique,
CNRS, Univ. Paris-sud, Campus Polytechnique RD 128,
91127 Palaiseau Cedex, France

Bose-Einstein condensation (BEC) of metastable ^4He ($^4\text{He}^*$) atoms has been observed for the first time in 2001 [1,2]. Since then research of ultracold $^4\text{He}^*$ focused on determining ultracold collisional properties such as scattering length and two-body loss rate coefficients on the one hand and photo-association of (long-range) molecules on the other hand. In 2005, for the first time, atom bunching was observed for $^4\text{He}^*$ bosonic atoms [3]. In Amsterdam we have observed BEC of $^4\text{He}^*$ in 2005 and realized condensates containing more than 10^7 atoms [4]. Adding the fermionic isotope ^3He we have realized a degenerate Fermi gas (DFG) by sympathetic cooling of $^3\text{He}^*$ by $^4\text{He}^*$ [5,6]. Being able to create ultracold samples of either $^4\text{He}^*$, $^3\text{He}^*$, or a mixture of the two, we studied, in collaboration with the group of Chris Westbrook, the analogue of the Hanbury Brown Twiss effect for $^3\text{He}^*$ fermions and observed antibunching, as shown, together with bunching observed for $^4\text{He}^*$ in the same apparatus, in Fig. 1 [7].

References

1. A. Robert, O. Sirjean, A. Browaeys, J. Poupard, S. Nowak, D. Boiron, C. I. Westbrook and A. Aspect, *Science* **292**, 461 (2001).
2. F. Pereira Dos Santos, J. Léonard, J. Wang, C. J. Barrelet, F. Perales, E. Rasel, C. S. Unnikrishnan, M. Leduc and C. Cohen-Tannoudji, *Phys. Rev.*

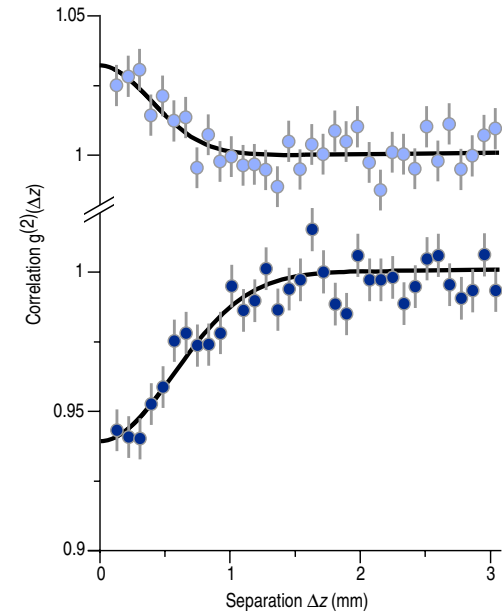


Fig. 1. Normalized probability of the joint detection of two atoms at two points in space separated by a vertical distance Δz , for $^4\text{He}^*$ (bosons) in the upper plot, and $^3\text{He}^*$ (fermions) in the lower plot (from Ref. [7]).

Lett. **86**, 3459 (2001).

3. M. Schellekens, R. Hoppeler, A. Perrin, J. Viana Gomes, D. Boiron, A. Aspect and C. I. Westbrook, *Science* **310**, 648 (2005).
4. A. S. Tychkov, T. Jeltjes, J. M. McNamara, P. J. J. Tol, N. Herschbach, W. Hogervorst and W. Vassen, *Phys. Rev. A* **73** (2006) 031603(R).
5. J. M. McNamara, T. Jeltjes, A. S. Tychkov, W. Hogervorst and W. Vassen, *Phys. Rev. Lett.* **97** (2006) 080404.
6. W. Vassen, T. Jeltjes, J. M. McNamara and A. S. Tychkov, in *Proceedings of the International school of physics "Enrico Fermi", Course CLXIV-Ultracold Fermi Gases*, eds. M. Inguscio, W. Ketterle, C. Salomon, arXiv:cond-mat/0610414 (2006).
7. T. Jeltjes, J. M. McNamara, W. Hogervorst, W. Vassen, V. Krachmalnicoff, M. Schellekens, A. Perrin, H. Chang, D. Boiron, A. Aspect and C. I. Westbrook, *Nature* **445** (2007) 402.

Single atoms in optical tweezers for quantum computing

A. Browaeys*, J. Beugnon, C. Tuchendler, H. Marion, A. Gaëtan, Y. Miroshnychenko,
Y.R.P. Sortais, A.M. Lance M.P.A. Jones, G. Messin, P. Grangier
*Laboratoire Charles Fabry de l'Institut d'Optique, CNRS, Univ. Paris-sud, Campus
Polytechnique, RD 128, 91127 Palaiseau cedex, France*
**E-mail: antoine.browaeys@institutoptique.fr*

Our group is interested in neutral atom quantum computing. With this goal in mind, we have recently shown how a single rubidium atom trapped in an optical tweezer can be used to store, manipulate and measure a qubit.¹

I will detail in this talk how we trap and observe a single atom in an optical tweezer created by focusing a far-off resonant laser down to a sub-micron waist. Our qubit is encoded on the $|0\rangle = |F = 1, M = 0\rangle$, $|1\rangle = |F = 2, M = 0\rangle$ hyperfine sublevels of a rubidium 87 atom. We initialize the qubit by optical pumping. We read the state of the qubit using a state selective measurement limited by the quantum projection noise. We perform single qubit operation by driving a two-photon Raman transition. We have measured the coherence time of our qubit by Ramsey interferometry. After applying a spin-echo sequence, we have found an irreversible dephasing time of about 40 ms.

Neutral atoms are promising candidate for the realization of a large scale quantum register. To perform a computation, an additional key feature is the ability to perform a gate between two arbitrary qubits of the register. As a first step, we have demonstrated a scheme where the qubit is transferred between tweezers with no loss of coherence and no change in the external degrees of freedom of the atom. We have then moved the atom over distances typical of the separation between atoms in an array of dipole traps, and shown that this transport does not affect the coherence of the qubit. We thus believe that this optical tweezer can be used as a “moving head” in the architecture of a neutral atom based quantum computer.

References

1. M.P.A. Jones, J. Beugnon, A. Gaëtan, J. Zhang, G. Messin, A. Browaeys, P. Grangier, Phys. Rev. A **75**, 013406(R) (2007).

**ATOM DETECTION AND PHOTON PRODUCTION IN A
SCALABLE, OPEN, OPTICAL MICROCAVITY**

E. A. HINDS, M. TRUPKE, J. GOLDWIN, B. DARQUIÉ,
G. DUTIER, S. ERIKSSON, AND J. ASHMORE

Centre for Cold Matter, Imperial College, Prince Consort Road, London SW7 2AZ, UK

A microfabricated Fabry-Perot optical resonator has been used for atom detection and photon production with less than 1 atom on average in the cavity mode. Our cavity design combines the intrinsic scalability of microfabrication processes with direct coupling of the cavity field to single-mode optical waveguides or fibers. The presence of the atom is seen through changes in both the intensity and the noise characteristics of probe light reflected from the cavity input mirror. An excitation laser passing transversely through the cavity triggers photon emission into the cavity mode and hence into the single-mode fiber. These are first steps towards building an optical microcavity network on an atom chip for applications in quantum information processing.

2

Entanglement of two single-atom quantum bits at a distance

P. Maunz*, D. L. Moehring, S. Olmschenk, K. C. Younge, D. N. Matsukevich,
L.-M. Duan, C. Monroe

*FOCUS Center and Department of Physics, University of Michigan,
Randall Lab, 450 Church Street, Ann Arbor, MI 48109-1040*

**E-mail: pmaunz@umich.edu
http://iontrap.physics.lsa.umich.edu/*

We demonstrate the entanglement of the quantum states of two $^{171}\text{Yb}^+$ ions trapped in independent vacuum chambers separated by a distance of one meter. The two ions each emit a single photon which is entangled with the quantum state of the ion. The interference and subsequent detection of these photons heralds the entanglement of the long-lived atomic quantum bits. We measure correlations of the quantum bits in two different bases and obtain an entanglement fidelity greater than 75%.

Trapped atomic ions are among the most attractive implementations of quantum bits for applications in quantum information processing, owing to their long trapping lifetimes and long coherence times. While nearby trapped ions can be entangled through their Coulomb-coupled motion, it is more natural to entangle remotely-located ions through a photonic coupling, eliminating the need to control the ion motion. When two atomic ions each become entangled with an emitted single photon, subsequent interference and detection of these photons in a Bell state can leave the trapped ion qubits in an entangled state.¹⁻³ Although this entanglement is probabilistic, the successful generation of an entangled pair is heralded by a photon coincidence detection and thus allows the preparation of entanglement with high fidelity. Moreover, such a photonic coupling can be tailored to operate quantum gates between the ions and efficiently generate extended networks of entangled qubits for long distance quantum communication or cluster states for scalable quantum computation.

In the experiment, individual $^{171}\text{Yb}^+$ ions are stored in two independent Paul traps located in vacuum chambers separated by approximately one meter. Each atom is first prepared in a known excited state with ultrafast laser pulses. From this excited state, a single spontaneously emitted

photon becomes entangled with the final state of each atom. The spatial and polarization mode of the emitted photons are selected such that the photonic qubit is encoded in two resolved frequencies and the atomic qubit is represented by two ground state hyperfine levels. When the two photons—one from each ion—are mode-matched on a beam splitter, the photons will exit from different ports of the beam splitter only if they are in a well defined antisymmetric entangled state. Hence, the coincidence detection of these two photons projects the two atoms onto a maximally entangled antisymmetric state and heralds the entanglement of the two ion qubits. The resulting entanglement is directly verified via state detection of the two trapped atom with near-perfect detection efficiency.

Acknowledgments

This work is supported by the National Security Agency and the Disruptive Technology Office under Army Research Office contract W911NF-04-1-0234, and the National Science Foundation Information Technology Research (ITR), and Physics at the Information Frontier (PIF) Programs.

References

1. C. Simon and W. T. M. Irvine, *Phys. Rev. Lett.* **91**, p. 110405 (2003).
2. L.-M. Duan, B. B. Blinov, D. L. Moehring and C. Monroe, *Quant. Inf. Comp.* **4**, 165 (2004).
3. D. L. Moehring, M. J. Madsen, K. C. Younge, R. N. Kohn, Jr., P. Maunz, L.-M. Duan, C. Monroe and B. B. Blinov, *JOSA B* **24**, 300 (January 2007).

Quantum Optics with Single Atoms and Photons

H. J. Kimble

*Norman Bridge Laboratory of Physics 12-33, California Institute of Technology,
Pasadena, CA 91125, USA; e-mail: hjkimble@caltech.edu*

Over the past several decades, experimental capabilities in Quantum Optics have progressed to achieve remarkable control over the interactions of single atoms and photons. I will describe several recent examples from the Caltech Quantum Optics Group, including a quantum interface for matter and light realized within the setting of cavity QED, and the coherent manipulation of the entangled states of two remotely located atomic ensembles.

1. Reversible state transfer between light and a single trapped atom

An important goal in quantum information science is the realization of quantum networks for the distribution and processing of quantum information,¹ including for quantum computation, communication, and metrology. In the initial proposal for the implementation of quantum networks,² atomic internal states with long coherence times serve as ‘stationary’ qubits, stored and locally manipulated at the nodes of the network. Quantum channels between different nodes are provided by optical fibers to transport photons (‘flying’ qubits). A crucial requirement for such networks is the reversible mapping of quantum states between light and matter. Cavity quantum electrodynamics provides a promising avenue for attaining this capability by using strong coupling for the interaction of single atoms and photons.³

I will describe an important advance related to the interface of light and matter, namely the demonstration of the reversible mapping of a propagating optical field to and from the hyperfine ground states of a single, trapped Cesium atom.⁴ Specifically, we map an incident coherent state with $\bar{n} = 1.1$ photons into a coherent superposition of $F = 3$ and $F = 4$ ground states with transfer efficiency $\zeta = 0.057$. We then map the stored atomic state back to a field state. The coherence of the overall process is confirmed by observations of interference between the final field state and a phase-

coherent reference field, resulting in a fringe visibility $v_a = 0.46 \pm 0.03$. We thereby provide the first verification of the fundamental primitive upon which the protocol of Cirac *et al.* is based.²

2. Functional Quantum Nodes for Entanglement Distribution over Scalable Quantum Networks

An approach of particular importance for the distribution of entanglement is the seminal paper by Duan, Lukin, Cirac, and Zoller (DLCZ) for the realization of quantum networks based upon entanglement between single photons and collective atomic excitations.⁵ DLCZ proposed to use pairs of atomic ensembles (U_i, D_i) at each quantum node i , with the sets of ensembles $\{U_i\}, \{D_i\}$ separately linked in parallel chains across the network.⁵

By implementing a modified version of the DLCZ protocol, we have created, addressed, and controlled pairs (U_i, D_i) of atomic ensembles at each of two quantum nodes,⁶ thereby demonstrating entanglement distribution in a form suitable both for quantum network architectures and for entanglement-based quantum communication schemes. Specifically, two pairs of remote ensembles at two nodes are each prepared in an entangled state,⁷ in a heralded and asynchronous fashion, thanks to the conditional control of the quantum memories. The states of the ensembles are coherently transferred to propagating fields locally at the two nodes. The fields are arranged such that they effectively contain two photons, one at each node, whose polarizations are entangled, as verified by the violation of a Bell inequality. The effective polarization entangled state, created with favorable scaling behavior, is thereby compatible with entanglement-based quantum communication protocols.⁵

This work is supported by the NSF and by the DTO.

References

1. P. Zoller *et al.*, *Eur. Phys. J. D* **36**, 203 (2005).
2. J. I. Cirac *et al.*, *Phys. Rev. Lett.* **78**, 3221 (1997).
3. R. Miller, T. E. Northup, K. M. Birnbaum, A. Boca, A. D. Boozer, and H. J. Kimble, *J. Phys. B: At. Mol. Opt. Phys.* **38**, S551-S565 (2005).
4. A. D. Boozer, A. Boca, R. Miller, T. E. Northup, and H. J. Kimble, *Phys. Rev. Lett.* (accepted, March, 2007); available as quant-ph/0702248.
5. L.-M. Duan, M. Lukin, J.I. Cirac, and P. Zoller, *Nature* **414**, 413 (2001).
6. C.-W. Chou, J. Laurat, H. Deng, K. S. Choi, H. de Riedmatten, D. Felinto, and H. J. Kimble, *Science* (published online in *Science Express*, 5 April, 2007).
7. C.-W. Chou, H. de Riedmatten, D. Felinto, S. V. Polyakov, S. J. van Enk, and H. J. Kimble, *Nature* **438**, 828 (2005).

FREQUENCY COMPARISON OF Al^+ AND Hg^+ OPTICAL STANDARDS[‡]

T. ROSENAND*, D. B. HUME, L. LORINI[‡], P. O. SCHMIDT[§], T. M. FORTIER, J. E. STALNAKER, S. A. DIDDAMS, W. H. OSKAY[‡], W. M. ITANO, J. C. BERGQUIST, AND D. J. WINELAND

*National Institute of Standards and Technology,
325 Broadway, Boulder, CO 80305
E-mail: trosen@boulder.nist.gov

We measure the frequency ratio of two single ion frequency standards:^{1,2} $^{27}\text{Al}^+$ and $^{199}\text{Hg}^+$. Systematic fractional frequency uncertainties of both standards are below 10^{-16} , and the statistical measurement uncertainty is below 5×10^{-17} [see Fig. 1(a)]. Recent ratio measurements show a reproducibility that is better than 10^{-16} [see Fig. 1(b)].

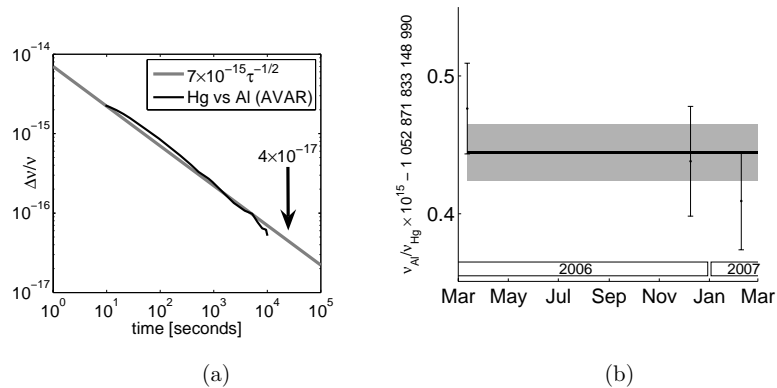


Fig. 1. Fractional stability of the ratio $\nu_{\text{Al}^+}/\nu_{\text{Hg}^+}$ (a). History of measurements of $\nu_{\text{Al}^+}/\nu_{\text{Hg}^+}$ (b).

[‡] Work supported by ONR and DTO.

[‡] Present address: Istituto Nazionale di Ricerca Metrologica, Torino, Italy

[§] Present address: Institut für Experimentalphysik, Universität Innsbruck, Austria

[‡] Present address: Stanford Research Systems, Sunnyvale, CA

References

1. T. Rosenband, P. O. Schmidt, D. B. Hume, W. M. Itano, T. M. Fortier, J. E. Stalnaker, K. Kim, S. A. Diddams, J. C. J. Koelemeij, J. C. Bergquist and D. J. Wineland, Observation of the $^1\text{S}_0 \rightarrow ^3\text{P}_0$ clock transition in $^{27}\text{Al}^+$, *arxiv:physics/0703067v2*, accepted for publication in *Phys. Rev. Lett.* (May, 2007)
2. W. H. Oskay, S. A. Diddams, E. A. Donley, T. M. Fortier, T. P. Heavner, L. Hollberg, W. M. Itano, S. R. Jefferts, M. J. Delaney, K. Kim, F. Levi, T. E. Parker and J. C. Bergquist, A single-ion optical clock with high accuracy, *Phys. Rev. Lett.* **97**, p. 020801 (2006).

ULTRACOLD STRONTIUM ATOMS IN AN OPTICAL LATTICE – QUANTUM MEASUREMENT AND CLOCK

A. D. LUDLOW, T. ZELEVINSKY, M. M. BOYD, S. BLATT, S. M. FOREMAN, G.
K. CAMPBELL, T. ZANON, AND J. YE[†]

*JILA, National Institute of Standards and Technology and University of Colorado, 440
UCB, Boulder CO 80309-0440 USA*

Ultracold atoms confined in an optical lattice offer an ideal platform for quantum manipulation and precision measurement. We report our recent development in the use of fermionic strontium for a precise and accurate optical atomic clock [1]. Atom-light interaction with coherence times approaching 1 s permits observation of the optical resonance with an unprecedented quality factor exceeding 2×10^{14} [2]. We will discuss the present limit of the clock instability of $\sim 2 \times 10^{-15}$ at 1 s, as well as appropriate steps for further improvement towards the quantum-projection-noise limit and beyond. The overall inaccuracy of such a clock is evaluated below the 7×10^{-16} fractional level. The clock frequency has also been measured against the NIST-F1 Cs fountain to a 1.1 Hz uncertainty, dominated by calibration of a microwave standard to the Cs fountain [3]. This system has the potential for very high stability and accuracy. Finally, we will describe an optical standard transfer scheme capable of making remote (tens of km) comparisons between optical frequency standards at instabilities below 10^{-17} at 1 s. We will present preliminary results of an optical comparison of the Sr standard to other optical standards in the Boulder area.

References

1. A. D. Ludlow *et al.*, “Systematic study of the ^{87}Sr clock transition in an optical lattice”, *Phys. Rev. Lett.* **96**, 033003 (2006).
2. M. M. Boyd *et al.*, “Optical Atomic Coherence at the 1-Second Time Scale”, *Science* **314**, 1430-1433 (2006).
3. M. M. Boyd *et al.*, “ ^{87}Sr lattice clock with inaccuracy below 1×10^{-15} ,” *Phys. Rev. Lett.* **98**, 083002 (2007).

[†] Email: Ye@jila.colorado.edu; Web: <http://jilawww.colorado.edu/YeLabs/>.

Poster No.	Title	Authors
1	MATTER-WAVE LOCALIZATION IN ANHARMONIC PERIODIC POTENTIALS	T. J. ALEXANDER , M. SALERNO, E. A. OSTROVSKAYA, YU. S. KIVSHAR
2	PRECISION MEASUREMENTS OF FREQUENCY, TIME AND DISTANCE WITH FREQUENCY COMBS GENERATED BY FEMTOSECOND LASERS	S.N. BAGAYEV, S.V. CHEPUROV, N.I. CHUNOSOV, V.I. DENISOV, V.M. KLEMENTYEV, I.I. KOREL, S.A. KUZNETSOV, B.N. NUSHKOV, M.V. OKHAPKIN, V.S. PIVTSOV, M.N. SKVORTSOV, A.V. TYAZHEV, V.F. ZAKHARYASH
3	COHERENT HETERODYNE-ASSISTED PULSED SPECTROSCOPY (CHAPS)	KENNETH G. H. BALDWIN, MITSUHIKO KONO, YABAI HE, RICHARD T. WHITE AND BRIAN J. ORR
4	AN OPTICAL LATTICE CLOCK BASED ON AN EVEN ISOTOPE OF NEUTRAL YTTERBIUM	Z. W. BARBER, C. W. OATES, J. E. STALNAKER, C. W. HOYT, AND L. HOLLBERG
5	Adiabatic beam-splitter pulses for atom interferometry	J. E. Bateman, M. D. Himsforth, R. Murray, S. Patel, and T. Fregarde
6	CHARACTERIZATION OF LASER COOLED AND TRAPPED ERBIUM ATOMS	ANDREW J. BERGLUND, SIU AU LEE, AND JABEZ J. MCCLELLAND
7	Progress Towards a Measurement of the Electric Dipole Moment of the Electron Using PbO	S. Bickman, P. Hamilton, Y. Jiang, A. Vutha, D. DeMille
8	GRAVITATIONAL PHYSICS WITH ATOM INTERFEROMETRY	GRANT BIEDERMANN, LOUIS DESLAURIERS, JASON HOGAN, DAVID JOHNSON, CHETAN MAHADESWARASWAMY, SEAN ROY, JOHN STOCKTON, KEN TAKASE, XINAN WU AND MARK KASEVICH
9	Zero-Down-Time Operation of Interleaved Atomic Clocks	G. W. Biedermann, K. Takase , X. Wu, L. Deslauriers, C. S. Roy, and M. A. Kasevich
10	Ground-state cooling and reversible state transfer in cavity QED	A. D. Boozer, A. Boca, R. Miller, T. E. Northup and H. J. Kimble
11	An optical clock based on levitating multiple-wave Bordé-Ramsey interferometers.	Christian J. Bordé and François Impens
12	REEXAMINATION OF 0g PURE LONGRANGE STATE OF Cs2: PREDICTION OF MISSING LEVELS IN THE PHOTOASSOCIATION SPECTRUM	Nadia BOULOUFA, Anne CRUBELLIER and Olivier DULIEU
13	Coherence properties of a Bose gas at the Bose-Einstein phase transition	T. Bourdel, S. Ritter, T. Donner, A. Å Ottl, F. Brennecke, M. K. Köhl, and T. Esslinger

Poster No.	Title	Authors
14	COLD ATOM CLOCKS IN SPACE: THE ACES MISSION CONCEPT AND STATUS	L. CACCIAPUOTI, C. SALOMON
15	PRECISE DETERMINATION OF h/m_{Rb} USING BLOCH OSCILLATIONS AND ATOMIC INTERFEROMETRY	MALO CADORET, ESTEFANIA DE MIRANDES, PIERRE CLADE, SAIDA GUELLATI-KHELIFA, CATHERINE SCHWOB, FRANÇOIS NEZ, LUCILE JULIEN AND FRANÇOIS BIRABEN
16	Optical-frequency-comb assisted measurements of atomic Helium transitions	P. CANCIO PASTOR , G. GIUSFREDI, P. DE NATALE, L. CONSOLINO and M. INGUSCIO
17	Cancellation of the collisional shift in caesium fountain clocks	W. Chalupczak , K. Szymaniec, E. Tiesinga, C. J. Williams, S. Weyers, R. Wynands
18	CORRELATED TUNNELLING OF INTERACTING ATOM PAIRS IN AN OPTICAL LATTICE OF DOUBLE WELLS	PATRICK CHEINET, SIMON FÖLLING, STEFAN TROTZKY, UTE SCHNORRBERGER, ROBERT SAERS, MICHAEL FELD, ARTUR WIDERA, TORBEN MÜLLER AND IMMANUEL BLOCH
19	GENERATION OF SINGLE CYCLE OPTICAL PULSES WITH CONSTANT CARRIER ENVELOPE PHASE	WEI-JAN CHEN, ZHI-MING HSIEH, SHU WEI HUANG, HOA-YU SU, A. H. KUNG
20	Multicomponent spinor atom laser generated by controllable Majorana transition	Xuzong Chen, Lin Xia, Xu Xu, Fan Yang, Wei Xiong, Juntao Li, Qianli Ma, Xiaoji Zhou and Hong Guo
21	APPROACHING THE HEISENBERG LIMIT IN AN ATOM LASER	J. D. CLOSE, N. P. ROBINS, C. FIGL, M. JEPPESEN, J. DUGUÉ, G. DENNIS, M. JOHNSON
22	SINGLE ATOM AND BEC DETECTION ON A MICROCHIP WITH AN INTEGRATED OPTICAL MICRORESONATOR	Y. COLOMBE, T. STEINMETZ, G. DUBOIS, F. LINKE, D. HUNGER T. W. HÄNSCH and J. REICHEL
23	NEAR-IR FREQUENCY COMB TO CHARACTERIZE SUB-DOPPLER SPECTROSCOPY OF ACETYLENE-FILLED OPTICAL FIBERS	KRISTAN L. CORWIN, KEVIN KNABE, RAJESH THAPA, KARL TILLMAN, ANDREW JONES, BRIAN R. WASHBURN, JEFFREY W. NICHOLSON AND MAN F. YAN
24	INTERACTIONS OF SPINOR MATTER-WAVE GAP SOLITONS	B. J. DABROWSKA-WUESTER, T. J. ALEXANDER , E. A. OSTROVSKAYA and YU. S. KIVSHAR
25	IMAGING THE BEAM PROFILE OF A METASTABLE ATOM LASER	R.G. DALL, L..J. BYRON, ,K.G.H. BALDWIN, A.G. TRUSCOTT, G. DENNIS, M. JEPPESEN, M.T. JOHNSON

Poster No.	Title	Authors
26	DECOHERENCE EFFECTS IN BOSE-EINSTEIN CONDENSATE INTERFEROMETRY	B J DALTON
27	ON-CHIP BOSE-EINSTEIN CONDENSATE INTERFEROMETER WITH 0.5 MM ARM LENGTH	QUENTIN DIOT, STEPHEN R. SEGAL, ERIC A. CORNELL, DANA Z. ANDERSON and MARA PRENTISS
28	DEVELOPMENT OF A NUCLEAR MAGNETIC RESONANCE GYROSCOPE	E.A. DONLEY, E. HODBY, S. KNAPPE, L. HOLLBERG, AND J. KITCHING
29	HIGH-RESOLUTION SPECTROSCOPY OF THE 88Sr^+ ION CLOCK TRANSITION	P. DUBE , A. A. MADEJ, J. E. BERNARD, and A. D. SHINER
30	COHERENT TRANSFER OF AN OPTICAL CARRIER THROUGH A LONG-DISTANCE FIBER LINK	S. M. FOREMAN, A. D. LUDLOW, M. M. BOYD, S. BLATT, T. ZELEVINSKY, G. K. CAMPBELL, T. ZANON, AND J. YE
31	A Magnesium Optical Clock	J. Friebe, K. Moldenhauer, M. Riedmann, T.E. Mehlstäubler, A. Voskrebenezv, A. Pape, G. Grosche, H. Schnatz, B. Lipphardt, E.M. Rasel and W. Ertmer
32	Molecular BEC of Lithium-6 in a Low Power Crossed Dipole Trap	J. Fuchs, G. Veeravalli, P.J. Dyke, G. Duffy, C.J. Vale, P. Hannaford and W.J. Rowlands
33	MEASUREMENT OF LIFETIME OF THE $2D_{5/2}$ STATE OF A SINGLE COLD 40Ca^+	KELIN GAO, HUA GUAN, BING GUO, QU LIU, AND XUEREN HUANG
34	ABSOLUTE OPTICAL FREQUENCY MEASUREMENTS IN 133Cs AND THEIR IMPACT ON ATOM INTERFEROMETRY AND THE FINE STRUCTURE CONSTANT	V. GERGINOV, K. CALKINS, C.E. TANNER, J.J. MCFERRAN, S. DIDDAMS, A. BARTELS, AND L. HOLLBERG
35	LASER PROBING MEASUREMENTS AND CALCULATIONS OF LIFETIMES OF THE $5d\ 2D_{3=2}$ AND $5d\ 2D_{5=2}$ METASTABLE LEVELS IN Ba II	J. GURELL, E. BIEMONT, K. BLAGOEV, V. FIVET, P. LUNDIN, S. MANNERVIK, L.-O. NORLIN, P. QUINET2, D. ROSTOHAR, P. ROYEN and P. SCHEF
36	Coupled motion in a three dimensional Brownian motor, realized in optical lattices	H. HAGMAN, P. SJOLUND, C. M. DION, S. J. PETRA, S. JONSELL AND A. KASTBERG
37	THE FERRUM-PROJECT: EXPERIMENTAL AND THEORETICAL TRANSITION RATES OF FORBIDDEN [ScII] LINES AND RADIATIVE LIFETIMES OF METASTABLE ScII LEVELS	H. HARTMAN, J. GUREL, P. LUNDIN2, P. SCHEF, A. HIBBERT, H. LUNDBERG, S. MANNERVIK, L-O. NORLIN and P. ROYEN

Poster No.	Title	Authors
38	DELTA-KICKED ROTOR EXPERIMENTS WITH AN ALL-OPTICAL BEC	F. HAUPERT AND M.D. HOOGERLAND
39	Rydberg Excitation of a Bose-Einstein Condensate, Collective and Coherent Dynamics	R. Heidemann, U. Raitzsch, V. Bendkowsky, B. Butscher, R. Löw and T. Pfau
40	COHERENT MANIPULATION OF ATOMS	M. D. HIMSWORTH , J. E. BATEMAN, S. PATEL, R. MURRAY and T. G. M. FREEGARDE
41	DECELERATION AND TRAPPING OF NEUTRAL POLAR MOLECULES	STEVEN HOEKSTRA AND GERARD MEIJER
42	COOLING, COHERENT MANIPULATIONS AND DECOHERENCE OF TWO-SPECIES TRAPPED-ION ARRAYS FOR QUANTUM INFORMATION PROCESSING	J. P. Home, J. D. Jost, J. Amini, J. J. Bollinger, R. B. Blakestad, J. Britton, R. J. Epstein, W. M. Itano, E. Knill, D. Leibfried, C. Ospelkaus, S. Seidelin, N. Shiga, J. H. Wesenberg, D. J. Wineland, R. Ozeri, C. Langer
43	Spin Dynamics in an Antiferromagnetic Spin-1 Condensate	S. Jung , L. D. Turner and P. D. Lett
44	MOLECULAR CLOCKS WITH ULTRA-COLD MOLECULES	MASATOSHI KAJITA
45	STRONG FIELD IONIZATION OF ALKALINE EARTH ATOMS	HUIPENG KANG, XIAOJUN LIU
46	DETAILED STUDY OF THE LASER COOLING PROCESS, AND OF THE VELOCITY DISTRIBUTION OF LASER COOLED ATOMS	A. KASTBERG , C. M. DION, H. HAGMAN, S. JONSELL, S. PETRA and P. SJOLUND
47	LASER-TRIGGERED ULTRAFast ELECTRON EMISSION FROM A SHARP TUNGSTEN TIP	C. KEALHOFER, P. HOMMELHOFF and M. A. KASEVICH
48	TOWARD MODE-LOCKED LASER COOLING OF NEW ATOMIC SPECIES	D. KIELPINSKI, M. PULLEN, J. CHAPMAN, M.J. MCDONNELL, AND E.W. STREED
49	POPULATION DYNAMICS OF ULTRACOLD RB RYDBERG ATOMS	H. KITSON AND W. J. ROWLANDS

Poster No.	Title	Authors
50	Heteronuclear Feshbach resonances in an ultracold Bose-Fermi Mixture	C. Klempt, T. Henninger, O. Topic, J. Will, W. Ertmer und J. Arlt
51	TUNABLE ALKALI LASERS FOR ATOMIC PHYSICS	RANDALL J. KNIZE and BORIS V. ZHDANOV
52	FOUR-WAVE MIXING IN THREE-LEVEL COLD ATOMS BY BICHROMATIC FIELD	L. B. KONG, X. H. TU, P. XU, J. WANG, Y.F.ZHU, AND M.S.ZHAN
53	COOLING A SINGLE-ATOM IN AN OPTICAL TWEEZER	A. M. LANCE, C. TUCHENDLER, Y. R. P. SORTAIS, G. MESSIN, A. BROWAEYS, P. GRANGIER
54	Towards a wire-mediated coupling of trapped ions	Tony Lee, Rob Clark, Hartmut Häffner
55	Quantum information processing with trapped ions at NIST	D. Leibfried, J. Amini, R.B. Blakestad, J.J. Bollinger, J. Britton, K.R. Brown, R. Epstein, J.P. Home, W.M. Itano, J.D. Jost, E. Knill, C. Langer], C. Ospelkaus, R. Ozeri, R. Reichle, S. Seidelin, N. Shiga, J. Wesenberg, and D.J. Wineland
56	OH Stark deceleration: magnetic trapping, precision measurement, and prospects for cavity-assisted laser cooling	Benjamin Lev, Brian Sawyer, Benjamin Stuhl, Mark Yeo, and Jun Ye
57	OBSERVATION OF THE DECONFINEMENT CROSSOVER IN A SUPERFLUID ARRAY FROM INSULATING 2D BEREZINSKI-KOSTERLITZ-THOULESS LAYERS TO A 3D ANISOTROPIC SUPERFLUID	WEI LI, HUI-CHUN CHIEN, AND MARK A. KASEVICH
58	Absolute frequency measurement of 2S-3S two-photon spectroscopy of $6,7\text{Li}$	Yu-Hung Lien, Jwo-Sy Chen, Chia-Hsiang Hsu, Yi-Wei Liu, Jow-Tsong Shy
59	AMPLIFIER DESIGN IMPLEMENTING HOLLOW-CORE PHOTONIC BANDGAP FIBER FOR FIBER-LASER BASED INFRARED FREQUENCY COMBS	JINGANG LIM, DANIEL V. NICKEL, BRIAN R. WASHBURN
60	Strontium Optical Lattice Clock: High Accuracy and Stability	A. D. Ludlow , T. Zelevinsky, M. M. Boyd, S. Blatt, S. Foreman, G. K. Campbell, M. Miranda, M. Martin, and J. Ye
61	PRECISE LASER SPECTROSCOPY AND MEASUREMENT ACROSS THE OPTICAL SPECTRUM USING OPTICAL FREQUENCY COMBS	A.A. MADEJ, J.E. BERNARD, P. DUBÉ, A. SHINER, J. JIANG, D. J. JONES, S. DRISSLER, A. CZAJKOWSKI

Poster No.	Title	Authors
62	Trapping of rubidium atoms by AC electric fields	Adela Marian, Sophie Schlunk, Peter Geng, Gerard Meijer and Wieland Schöllkopf, Allard P. Mosk
63	Frequency Comb Spectroscopy of Laser Cooled Rubidium-85	M. Maric, J.J. McFerran, and A.N. Luiten
64	DIRECT SPECTROSCOPY OF CESIUM IN A VAPOR CELL WITH A FEMTOSECOND LASER FREQUENCY COMB	Vela L. Mbele, Jason E. Stalnaker, Tara M. Fortier, Scott A. Diddams, Leo Hollberg, Vladislav Gerginov and Carol E. Tanner
65	A FUNDAMENTALLY MODE-LOCKED Yb-Er CO-DOPED FIBER LASER WITH A REPETITION RATE OF 860MHz	J. J. MCFERRAN , L. NENADOVIC, J. B. SCHLAGER and N. R. NEWBURY
66	COLD ATOM GRAVIMETRY	T. E. Mehlstäubler, J. LeGouet, S. Merlet, D. Holleville, A. Clairon, A. Landragin, F. Pereira Dos Santos
67	Transfer of coherence enhanced stimulated emission and electromagnetically induced absorption in Zeeman split atomic transitions	R. Meshulam, T. Zigdon, A. D. Wilson-Gordon, and H. Friedmann
68	SPECTRA OF BA AND BA+ IN SOLID AND LIQUID XE AND AR FOR BA TAGGING IN XE-136 DOUBLE BETA DECAY	BRIAN MONG, SHIE-CHANG JENG, KENDY HALL, CESAR BENITEZ-MEDINA, SHON COOK AND WILLIAM M. FAIRBANK, JR.
69	BOSE-EINSTEIN-CONDENSATE INTERFEROMETER ON AN ATOM CHIP WITH A LONG COHERENCE TIME	KEN'ICHI NAKAGAWA, MUNEKAZU HORIKOSHI
70	PROBING COLD ATOMS USING A TAPERED OPTICAL FIBER	SILE NIC CHORMAIC, MICHAEL MORRISSEY, THEJESH BANDI AND KIERAN DEASY
71	Laser Produced Spectra of SiC molecule in the region of 370 – 570 nm	K. S. Ojha, S. C. Singh and R. Gopal
72	Coherent atomic nano-beam	F. Perales, J. Robert, J. Baudon, M. Ducloy
73	Optical monitoring of molecular oxygen and water vapor in human sinuses using tunable diode laser spectroscopy	L. Persson , M. Andersson, M. Cassel-Engquist, T. Svensson, K. Svanberg, and S. Svanberg
74	BRAGG SPECTROSCOPY OF A 85RB BEC WITH TUNABLE INTERACTIONS	JUAN PINO, SCOTT PAPP, ROBERT WILD, DEBORAH JIN, ERIC CORNELL
75	Low noise RF and Optical Signals Derived from Stabilized Optical Frequency Combs	Qudsia Quraishi, Vela Mbele, Scott A. Diddams and Leo Hollberg

Poster No.	Title	Authors
76	Frozen and not-so-frozen Rydberg gases	M. Reetz-Lamour, T. Amthor, C. Giese, J. Denskat, and M. Weidemüller
77	Deterministic coupling of a single trapped atom to the mode of a high finesse optical resonator	S. Reick, W. Alt, I. Dotsenko, M. Khudaverdyan, A. Stiebeiner, and D. Meschede
78	Test of Special Relativity by Laser Spectroscopy and Fast Ions	Sascha Reinhardt, G. Saathoff, H. Buhr, L. A. Carlson, D. Schwalm, A. Wolf, S. Karpuk, C. Novotny, G. Huber, T. W. Hänsch, R. Holzwarth, Th. Udem, M. Zimmermann and G. Gwinner
79	Process tomography of ion trap quantum gates	M. Riebe, K. Kim, P. Schindler, T. Monz, P. O. Schmidt, T. K. Körber, W. Hänsel, H. Häffner, C. F. Roos, R. Blatt
80	Spiking optical patterns and synchronization of coupled semiconductor lasers	M. Rosenbluh
81	Photon emission of a single trapped ion into a cavity	C. Russo, F. Dubin, H. Barros, E.S. Philips, A. Stute, C. Becher, P.O. Schmidt and R. Blatt
82	SPINOR CONDENSATES AT FINITE TEMPERATURES	KAZIMIERZ M. RZAZEWSKI, MARIUSZ GAJDA, MIROSLAW BREWCZYK
83	QUANTUM TRANSPORT EFFECTS IN RATCHET-LIKE POTENTIALS AND OPTICAL MULTIPHOTON LATTICES	T. Salger, C. Geckeler, S. Kling, and M. Weitz
84	An atom-photon pair laser	Thomas Salzburger and Helmut Ritsch
85	A Miniature, Highly Sensitive Atomic Magnetometer Based on Suppression of Spin-Exchange Relaxation: Development and Applications	V. SHAH, S. KNAPPE, P.D.D. SCHWINDT, J. KITCHING
86	Influence of Externally Applied dc Electric and Magnetic Fields on Semiconductor- Photorefractivity	Dheeraj Sharma and Praveen Aghamkar
87	State-selective imaging of cold atoms using atomic coherence	D. V. SHELUDKO, S. C. BELL, S. SALIBA and R. E. SCHOLTEN
88	FABRICTION OF ATOM CHIPS	PETER D. D. SCHWINDT, MICHAEL MANGAN, CHRIS TIGGES, JAMES STEVENS, MATTHEW BLAIN
89	Quantum projection noise and squeezing with ions in a Penning-Malmberg trap.	N. Shiga, J. H. Wesenberg, W. M. Itano and J. J. Bollinger

Poster No.	Title	Authors
90	MACROSCOPIC ENTANGLEMENT OF A BOSE-EINSTEIN CONDENSATE ON A SUPERCONDUCTING ATOM CHIP	MANDIP SINGH
91	BOSE-EINSTEIN CONDENSATE ON A PERMANENT MAGNETIC LATTICE ON AN ATOM CHIP	M. SINGH, M. VOLK, A. AKULSHIN, R. McLEAN, A. SIDOROV AND P. HANNAFORD
92	EXPERIMENTAL DESIGN FOR EFFICIENT PHOTON-ATOM COUPLING IN FREE SPACE	M. Sondermann , H. Konermann, R. Maiwald, N. Lindlein, U. Peschel and G. Leuchs
93	BAYESIAN ESTIMATION OF DIFFERENTIAL INTERFEROMETER PHASE	JOHN K. STOCKTON and MARK A. KASEVICH
94	ABSOLUTE FREQUENCY STABILIZATION OF A LASER TO AN ION ABSORPTION LINE IN A DISCHARGE	ERIK W. STREED, GEOFFREY GENN, DAVID KIELPINSKI
95	INITIAL SPECTROSCOPY OF HfF+ FOR AN ELECTRON EDM SEARCH	R. STUTZ, A. LEANHARDT, L. SINCLAIR AND E. CORNELL
96	CRYOGENIC BUFFER-GAS COOLING AND CONFINEMENT OF PARAMAGNETIC ATOMS	ALEXANDER O. SUSHKOV and DMITRY BUDKER
97	Atom-Molecule Rabi Oscillations in a Mott Insulator	N. Syassen, D.M. Bauer, M. Lettner, D. Dietze, T. Volz, S. Dürr, and G. Rempe
98	YTTERBIUM SINGLE-ION OPTICAL FREQUENCY STANDARDS	CHR. TAMM, I. SHERSTOV, B. STEIN, B. LIPPHARDT, E. PEIK
99	CAVITY ENHANCED DIRECT FREQUENCY COMB SPECTROSCOPY	MICHAEL J. THORPE, DAVID BALSLEV-CLAUSEN, MATT KIRCHNER, BEN SAFDI, AND JUN YE
100	SPECTROSCOPY OF ATOM PAIRS AND COLD COLLISIONS	E. TIEMANN, H. KNÖCKEL, A. PASHOV, O. DOCENKO, M. TAMANIS, R. FERBER
101	Sharp Peak Density Solutions for Bose-Einstein condensate in approximate kinetic model	V. Tsurkov
102	VORTEX PROLIFERATION IN THE BEREZINSKII-KOSTERLITZ-THOULESS ON A TWO-DIMENSIONAL LATTICE OF BOSE-EINSTEIN CONDENSATES	S. TUNG, V. SCHWEIKHARD, AND E. CORNELL
103	Towards coherent matter-wave inertial sensors in microgravity	G. Varoquaux, J-F. Clement, J-P. Brantut, R. A. Nyman, A. Aspect, P. Bouyer, F. Pereira Dos Santos and A. Landragin, N. Zahzam, O. Carraz, Y. Bidet and A. Bresson

Poster No.	Title	Authors
104	SPECTROSCOPY ON ATOMIC RUBIDIUM AT 500 BAR BUFFER GAS PRESSURE: TOWARDS THERMAL EQUILIBRIUM OF COUPLED ATOM-LIGHT-STATES	U. VOGL and M. WEITZ
105	MULTIPLE FREQUENCY MODULATION FOR LOW-LIGHT ATOM MEASUREMENTS IN AN OPTICAL CAVITY	GEERT VRIJSEN, JONGMIN LEE, IGOR TEPER, ROMAIN LONG, ARI TUCHMAN, MARK KASEVICH
106	MANIFESTATION OF CONTINUOUS QUANTUM ZENO EFFECT BASED ON COLD ATOM INTERFEROMETRY	P.WANG, R.B.LI, J.WANG, H.W.XIONG, AND M.S.ZHAN
107	Progress toward trapping and coupling neutral atoms with a magnetic cantilever	Y.-J. Wang, M. Eardley, S. Knappe, L. Hollberg, J. Kitching and J. Moreland
108	Single-Atom Single-Photon Quantum Interface	T. Wilk , S. C. Webster, A. Kuhn and G. Rempe
109	MICROFABRICATION PROCESS DEVELOPMENT FOR ION TRAP CHIPS BASED ON PLANAR SILICA-ON-SILICON TECHNOLOGY	G. WILPERS, M. BROWNNUTT, P. GILL, A.G. SINCLAIR, R.C. THOMPSON
110	INTERFERENCE FRINGES OF TWO INITIALLY INDEPENDENT BOSE-EINSTEIN CONDENSATES BASED ON INTERACTION-INDUCED INTERFERENCE THEORY	Hongwei Xiong, Shujuan Liu and Mingsheng Zhan
111	High Resolution Stimulated Raman Spectroscopy for the D3/2 and D5/2 Metastable States Qubit in 40Ca+	Rekishu Yamazaki, Hideyuki Sawamura, Kenji Toyoda, Utako Tanaka and Shinji Urabe
112	GRAVITATIONAL SPLITTING OF A BEC IN A 10 CM RING	MATEUSZ ZAWADZKI, IAN NORRIS, AIDAN ARNOLD, AND ERLING RIIS
113	Transition from a Mott insulator to a two-dimensional superfluid in an optical lattice	MARTIN ZELAN, EMIL LUNDH, MAGNUS REHN, ROBERT SAERS AND ANDERS KASTBERG
114	Extending the frontiers of quantum gases to microgravity	T. C. Zoest, E.M. Rasel, W. Ertmer for the QUANTUS Team
115	Ca+ IONS FOR FREQUENCY METROLOGY	C. ZUMSTEG, C. CHAMPENOIS, P. DUBE, G. HAGEL, M. HOUSSIN, M.VEDEL, F.VEDEL, M. KNOOP

MATTER-WAVE LOCALIZATION IN ANHARMONIC PERIODIC POTENTIALS

T. J. ALEXANDER^{1,*}, M. SALERNO², E. A. OSTROVSKAYA¹, YU. S. KIVSHAR¹

¹*Nonlinear Physics Centre, Australian National University,
Canberra, ACT 0200, Australia*

²*Dipartimento di Fisica, "E.R. Caianiello" Università di Salerno,
I-84081 Baronissi (SA), Italy*

*E-mail: tja124@rsphysse.anu.edu.au
www.rsphysse.anu.edu.au/nonlinear

We demonstrate that subtle deviations from a harmonic periodic potential may lead to dramatic changes in the band gap structure and nature of the gap solitons and Bloch waves of a Bose-Einstein condensate in the lattice. In particular we reveal that a minimum in higher gaps occurs near the maximum in the first gap, allowing nontrivial mixed gap solitons to exist. Our results connect the currently disparate research into the effect of potentials across the fields of nonlinear optics and Bose-Einstein condensation.

Keywords: Bose-Einstein condensates; Gap solitons; Anharmonic potential;

The study of the effects of periodicity is of growing interest in different fields of physics ranging from condensed matter to optics and more recently to Bose-Einstein condensation. In the physics of Bose-Einstein condensates (BECs), a strong interest has developed around the use of optical lattices to manipulate and control condensate diffraction and localization [1]. Usually, optical lattices are produced by the interference of intersecting laser beams, and to a large extent they can be described by harmonic functions.

However, another well-known way to produce a lattice for cold atoms or BECs is to use periodic arrays of magnetic microtraps [2]. Thus with the advent of carefully engineered magnetic lattices it is now possible to consider BEC in a far wider range of potentials, even to the extent of lattices similar to those studied in optics.

Here we study the properties of generalized periodic potentials which vary between the two extreme cases of the so-called “dot” (Fig. 1(a)) and

“antidot” (Fig. 1(c)) lattices and which include the sinusoidal optical lattice potential as an intermediate case (Fig. 1(b)). We examine both one- and two-dimensional potentials and reveal the changes introduced to both the band structure and the localized states which may be found in the band gaps. We show that the optimum periodic potential for localization is not the typical sinusoidal optical lattice but that instead larger gaps are found in the anti-dot end of the spectrum of potentials (see Fig. 1). However, while the first gap opens, we show that higher gaps actually close due to a reversal of the symmetry of the band edge Bloch waves. We show that one consequence of this nontrivial opening and closing of the gaps is the mixed-gap soliton shown in Fig. 1(f) which exists as a surface state between two types of potential and localized in different gaps. Finally, we consider particle circulation through the different lattice structures, demonstrating “discrete” vortices in one limit, and quasi-continuous vortices in the other.

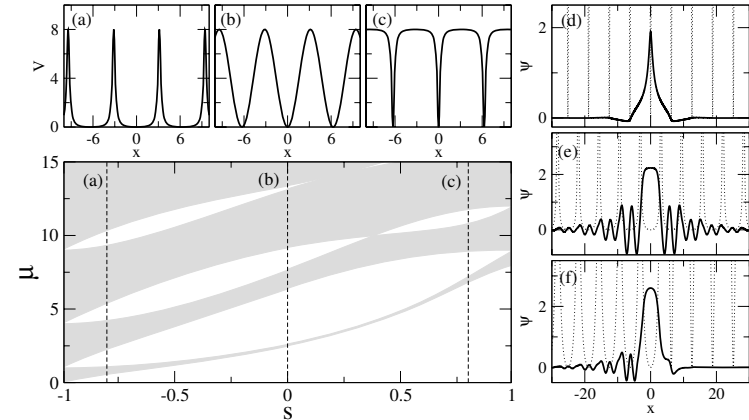


Fig. 1. Main panel: Opening and closing of gaps with change in potential shape from “dot” type (a), through sinusoidal (b) to “anti-dot” type (c). (d,e,f) Examples of 1st gap, 2nd gap, and mixed gap solitons respectively.

References

1. See, e.g., I. Bloch, Phys. World **17**(4), 25 (2004).
2. A. Günter et al, Phys. Rev. A **71**, 063619 (2005); S. Ghanbari, T.D. Kieu, A. Sidorov, and P. Hannaford, J. Phys. B **39**, 847 (2006)

**PRECISION MEASUREMENTS OF FREQUENCY, TIME AND
DISTANCE WITH FREQUENCY COMBS GENERATED BY
FEMTOSECOND LASERS***

S.N. BAGAYEV, S.V. CHEPUROV, N.I. CHUNOSOV, V.I. DENISOV,
V.M. KLEMENTYEV, I.I. KOREL, S.A. KUZNETSOV, B.N. NUSHKOV,
M.V. OKHAPKIN, V.S. PIVTSOV, M.N. SKVORTSOV, A.V. TYAZHEV,
V.F. ZAKHARYASH

Institute of Laser Physics SB RAS, prosp. Lavrentyeva 13/3, Novosibirsk, 630090, Russia

The recent results on the development of femtosecond frequency comb systems and their metrological application are reported.

Precision metrology of physical values has received a major boost with emergence of highly accurate broadband frequency combs generated either directly by mode-locked lasers or in special optical fibers.

In this report we review the research carried out at the Institute of Laser Physics SB RAS in the field of precision measurements of frequency, time and distance with frequency combs generated by femtosecond lasers. The comb systems based on various mode-locked lasers, such as the solid state Ti:Sapphire, Cr:Forsterite and Yb:KYW lasers as well as Er-fiber laser, developed at the Institute of Laser Physics are described.

The results of high precision frequency measurements of transitions in molecular iodine in the wavelength range of 515 nm by means of a frequency-stabilized infrared frequency comb from the mode-locked Cr:Forsterite laser are reported. Iodine transitions in this range feature a narrow linewidth (10 kHz) and can be used for establishment of an optical frequency standard with potential frequency instability on the order of 10^{-15} . A cw Yb:YAG laser at 1030 nm has been developed at the ILP SB RAS as a candidate for such a standard.

Future application of the developed comb systems for precision measurements of length and small amplitude oscillations is discussed. It is proposed to pass radiation from femtosecond laser through a perfect Fabry-Perot interferometer. The transmission maxima of the interferometer can be used as reference lines for absolute length measurements. The possibility of developing a unified frequency and length standard is shown. Also, theoretical and

* This work partially supported by grants 06-02-16286-a, 06-02-08069-ofi of the Russian Foundation for Basic Research and EOARD # 059001, Delivery Order 0028, CRDF RUP2-1510-NO-05.

experimental investigations of the measurement of small harmonic surface oscillations with the help of a femtosecond laser are presented. In this case, the radiation can be considered as a large number of spectral components that can act as separate channels for the measurements of displacements of an oscillating surface. These channels can be used to implement independent measurements and consequently to increase the signal-to-noise ratio. In the limit, if we could detect separately all beats between all laser modes, it would be possible to decrease the signal-to-noise ratio by a factor of \sqrt{N} , where N is the number of laser radiation modes.

In the past decade much attention has been paid to the spectral broadening of femtosecond pulses. Considering impressive effectiveness of this technique for high-precision spectroscopy, one should note that spectral broadening in fibers with strong nonlinear characteristics obviously affect stability of the femtosecond frequency comb. While noise characteristics of a stationary pulse trains generated by a stable mode-locked lasers are studied theoretically perfectly, there are still numerous questions regarding stability of the fiber outcoming radiation. So the major question is what are the main factors and parameters reducing frequency measurements accuracy. The influence of initial pulse train instability on the supercontinuum generated in optical fiber in presence of strong nonlinearity and dispersion effects is discussed. We also present a numerical study of spectral noise in pulse trains propagating through an optical fiber with high nonlinearity. It is shown that fluctuations of ingoing radiation, strongly affect the output spectral characteristics: spectral envelope and amplitudes of equidistant components in femtosecond comb.

COHERENT HETERODYNE-ASSISTED PULSED SPECTROSCOPY (CHAPS)

KENNETH G. H. BALDWIN[†] AND MITSUHIKO KONO

Atomic and Molecular Physics Laboratories, Research School of Physical Sciences and Engineering, Australian National University, Canberra, ACT 0200, Australia

YABAI HE, RICHARD T. WHITE^{*} AND BRIAN J. ORR

Centre for Lasers and Applications, Macquarie University, Sydney, NSW 2109, Australia

We describe a new pulsed laser spectroscopy technique that combines optical heterodyne detection with frequency binning. This method is used to demonstrate the high resolution capability (very close to the Fourier-transform limit) of a low-chirp, injection-seeded pulsed optical parametric oscillator, via Doppler-free two-photon excitation in cesium.

The bandwidth of pulsed lasers used for high-resolution measurements at high peak powers (lidar, nonlinear-optical spectroscopy, and frequency conversion into other wavelength regions *e.g.*, the vacuum ultraviolet) is limited fundamentally by the Fourier transform (FT) of the temporal pulse profile. Other spectroscopic limitations include frequency chirp during each pulse, fluctuations in temporal profiles, and shifts in the central frequency.

We have devised a new, more precise, pulsed laser-spectroscopic technique: Coherent Heterodyne-Assisted Pulsed Spectroscopy (CHAPS) [1]. We have applied CHAPS by using a low-chirp optical parametric oscillator (OPO) system [2] which employs a periodically-poled KTiOPO₄ crystal in a bow-tie cavity locked to the frequency of a narrowband cw laser that injection-seeds the nonlinear-optical process. When pumped with a single-longitudinal-mode 532-nm pulsed laser, the OPO generates narrowband signal and idler output radiation. In the experiments described here, we demonstrate that each OPO pulse has a nearly FT-limited optical bandwidth.

Optical-heterodyne detection (OHD) [2] is used to characterize each OPO output pulse. Part of the seed laser light is frequency-shifted by ~720 MHz

[†] Kenneth.Baldwin@anu.edu.au

^{*} Now at *Industrial Research Ltd, P.O. Box 31–310, Lower Hutt, New Zealand*

using an acousto-optic modulator, and is combined with the OPO pulse to create beats on a fast photodetector. A FT and sideband-filtering procedure then yields the frequency chirp, central frequency, and reconstructed temporal profile of each pulse.

When the OPO process is optimally phase-matched by temperature-tuning the peak gain to the seed laser wavelength, the total chirp during the OPO pulse (~23-ns FWHM) is <10 MHz. The OHD-determined optical bandwidth is then very close to the FT limit (~17 MHz).

To determine the OPO's spectroscopic bandwidth precisely, we have made a Doppler-free measurement of the very narrow (<2 MHz) two-photon excitation of the cesium 6S–8S transition [1]. We locked the 822.47-nm cw seed laser to the Doppler-free peak in one Cs cell, and then measured the OPO-excited Cs fluorescence from a second cell to obtain the spectroscopic linewidth.

We are able to remove the inhomogeneous broadening effect of pulse-to-pulse frequency jitter by exploiting the additional information provided by OHD. Every OHD beat frequency measurement yields the central frequency of the OPO signal pulse, which tends to jitter around the Cs resonance, owing to residual instabilities in the (locked) OPO cavity. In our novel CHAPS technique [1], we bin the resulting central frequency distribution to record spectra such as in Fig. 1(a), without actively scanning the seed wavelength or the OPO itself. By temperature tuning the OPO to operate very near the phase-matched (zero-chirp) condition we are able to minimize both the frequency distribution over many shots as well as the chirp of each individual OPO pulse.

We find that the OPO is indeed operating very close to the FT limit with a demonstrated minimum spectroscopic bandwidth of 18.0 ± 0.2 MHz. We expect that this OPO source and the novel heterodyne-assisted CHAPS method will prove very useful for high-precision pulsed spectroscopy, such as improved measurement of the ground-state Lamb shift in helium by two-photon excitation of the 1S–2S transition at ~120 nm [3].

References

1. M. Kono, K. G. H. Baldwin, Y. He, R. T. White, and B. J. Orr, *Opt. Lett.*, **30**, 3413 (2005); *J.O.S.A. B* **23**, 1181 (2006).
2. R. T. White, Y. He, B. J. Orr, M. Kono, and K. G. H. Baldwin, *Opt. Lett.* **28**, 1248 (2003); *J. Opt. Soc. Am. B* **21**, 1577 (2004); *J. Opt. Soc. Am. B* **21**, 1586 (2004); *Opt. Express* **12**, 5655 (2004).
3. S. D. Bergeson, K. G. H. Baldwin, T. B. Lucatorto, T. J. McIlrath, C. H. Cheng, and E. E. Eyler, *J. Opt. Soc. Am. B* **17**, 1599 (2000).

AN OPTICAL LATTICE CLOCK BASED ON AN EVEN ISOTOPE OF NEUTRAL YTTERBIUM

Z. W. BARBER*, C. W. OATES, J. E. STALNAKER, C. W. HOYT, AND L. HOLLBERG
 National Institute of Standards and Technology, 325 Broadway,
 Boulder 80305, USA

We report improvements and new measurements of an optical clock system based on the 1S_0 3P_0 transition in neutral ^{174}Yb at 578.4 nm. Included will be an absolute frequency measurement of this promising transition along with evaluation of some key systematic shifts. Absolute fractional uncertainties of well below 10^{-16} appear attainable with this system.

We are currently investigating the capabilities of an optical atomic clock that uses 10^4 neutral atoms confined tightly in a 1-D optical lattice¹. In contrast to most other lattice clock investigations^{2,3,4}, our work focuses on an even isotope⁵, ^{174}Yb . With no zero nuclear spin, even isotopes offer some potential advantages over their odd counterparts due to simpler structure (no Zeeman sublevels or optical pumping effects) and lack of first order sensitivity to magnetic fields and lattice polarization. However, in order to induce a non-zero transition probability for the clock transition in the even isotopes, it is necessary to use an auxiliary field in order mix a small fraction of $J=1$ states into the $J=0$ excited state of the clock transition. In our experiment, we use a 13 G magnetic bias field to provide the required mixing; when combined with probe light intensity of 60 mW/cm^2 , we achieve Rabi frequencies of about 5 Hz.

The atoms are loaded into the 1-D lattice with two stages of laser cooling. First, about 10^6 atoms from thermal beam fill a MOT (magneto-optic trap) based on the strong cooling transition at 399 nm, using InGaN diodes as the laser source. A frequency doubled Yb fiber laser at the 556 nm intercombination line allows us to transfer roughly half of atoms to a second MOT reducing the atom temperatures from 4 mK to 50 μK , the approximate depth of the potential wells of the optical lattice. The optical lattice consists of retroreflected, tightly focused light (waist = 30 μm , power = 1 W), whose wavelength is tuned near 759.35 nm, the value at which the ground and excited states experience nearly identical Stark shifts. We probe the atoms along the axis of tight confinement to suppress Doppler effects. We recently constructed a new probe system at 578 nm based on sum frequency of a 1.319 μm Nd:YAG laser and a 1.03 μm fiber laser. With 100 mW of each infrared source we generate 10 mW of yellow light in a periodically-poled non-linear waveguide. The frequency of the probe light is pre-stabilized to a high finesse (200,000), environmentally-isolated, vertically-mounted cavity. Below we show a scan over the resonance with a FWHM of 4 Hz, corresponding to a line Q of more than 10^{14} .

1

2

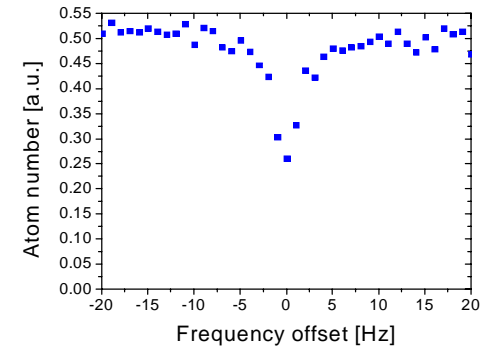


Figure 1. Scan of the optical clock transition in ^{174}Yb . The decrease in atom number reflects shelving of lattice-confined atoms through excitation by the probe laser at 578 nm.

Our most recent efforts have focused on the evaluation of key systematics. In particular we have improved our knowledge of the magic wavelength and evaluated the effect of a $J=0 \leftrightarrow J=0$ two photon transition that lies 0.3 nm away. Our preliminary measurements indicate that this effect contributes a shift of 0.2 Hz for our typical lattice intensities. Furthermore, we are investigating how this shift can be suppressed by use of circularly polarized lattice light.

References

1. Z. W. Barber, C. W. Hoyt, C. W. Oates, L. Hollberg, A. V. Taichenachev, and V. I. Yudin, *Phys. Rev. Lett.* **96**, 083002 (2006).
2. M. Takamoto, F.-L. Hong, R. Higashi, and H. Katori, *Nature (London)* **435**, 321 (2005).
3. A. Brusch, R. Le Targat, X. Baillard, M. Fouché, and P. Lemonde, *Phys. Rev. Lett.* **96**, 103003 (2006).
4. A. D. Ludlow, M. M. Boyd, T. Zelevinsky, S. M. Foreman, S. Blatt, M. Notcutt, T. Ido, and J. Ye, *Phys. Rev. Lett.* **96**, 033003 (2006).
5. X. Baillard, M. Fouché, R. Le Targat, P. G. Westergaard, A. Lecallier, Y. Le Coq, G. D. Rovera, S. Bize, and P. Lemonde, arXiv:physics/0703148 (2007).

Adiabatic beam-splitter pulses for atom interferometry

J. E. Bateman*, M. D. Himsforth, R. Murray, S. Patel, and T. Freearge

*School of Physics and Astronomy
University of Southampton
SO17 1BJ, United Kingdom
E-mail: jbateman@soton.ac.uk

The components of an interferometer are the mirrors and beam-splitters which, respectively, deflect, split and recombine the light. The equivalent elements in atom interferometry are provided by pulses of light which transfer the population between eigenstates and switch between eigenstates and superpositions.¹ These optical ‘mirrors’, ‘beam-splitters’ and ‘recombiners’ are traditionally provided by Rabi π and $\pi/2$ pulses which, while simple, are experimentally fragile.^{2,3} The remarkably robust process of adiabatic passage can approximate the mirror operation, but the extension of this technique to beam-splitters is not trivial. Specifically, a simple truncation of a pulse which would otherwise have caused full inversion does not exhibit the robustness of full adiabatic passage.

We investigate the possibility of extending adiabatic manipulation, including the characteristic robustness, to operations such as ‘half adiabatic passage’, to provide beam-splitters and recombiners. Pulses are designed by controlling the adiabatic parameter, which is a measure of how closely the operation approximates the adiabatic ideal, throughout the pulse including, crucially, the final extinction.

Using this technique, we obtain a pulse which is tolerant of experimental variations, the principle sources of which are expected to be variations in intensity across a beam profile and the different Doppler shifts of thermal atoms. Stability is compared with the $\pi/2$ pulse and examples given for a typical experiment. The progress of an experiment to implement these techniques is discussed.

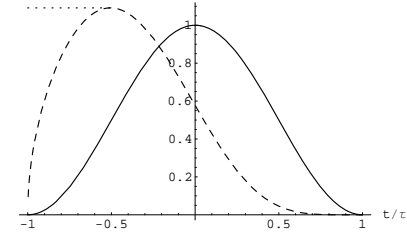


Fig. 1. Coupling strength (solid) and detuning (dashed) for a ‘beam-splitter’ pulse with an experimentally simple intensity modulation and an optimised detuning function.

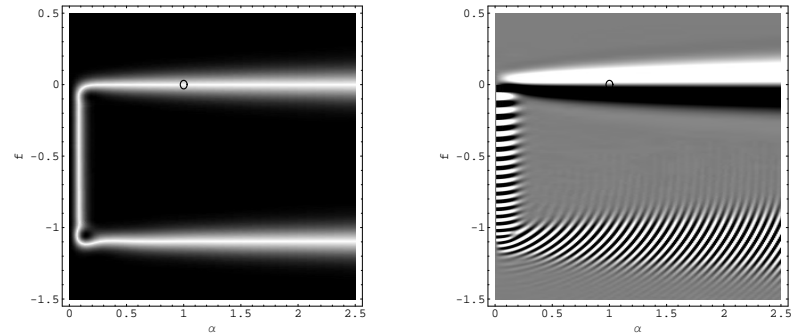


Fig. 2. The fidelity of superposition (left) and phase (right) resulting after application of an optimised ‘beam-splitter’ pulse whose deviation from the ideal, due to experimental variations, is parametrised by α and f , where α is the ratio of actual to expected coupling strength, and f is the detuning from resonance in natural units. Fidelity q , as expected, shows a narrow branch around $f = 0$ for which, above a minimum α , an equal superposition is created with relative phase $\sin \phi$ unaffected by changing α but strongly dependent on f . The unexpected lower branch, centred on $f = -1.09$, for which fidelity is high and phase is rapidly varying, will be discussed. White is high and black is low, and $q \equiv 1 - 2 \left| \frac{1}{2} - |\langle 0|\psi\rangle|^2 \right|$ and $\sin(\phi) \equiv \text{Im} \left(\frac{\langle 1|\psi\rangle}{\langle 0|\psi\rangle} \right)$. Results were obtained numerically.

References

1. J. Baudon, R. Mathevet and J. Robert, *J. Phys. B* **32**, R173 (1999).
2. B. W. Shore, K. Bergmann, A. Kuhn, S. Schieman, J. Oreg and J. H. Eberly, *Phys. Rev. A* **45**, p. 5297 (1992).
3. N. V. Vitanov, T. Halfmann, B. W. Shore and K. Bergmann, *Ann. Rev. Phys. Chem.* **52**, 763 (2001).

CHARACTERIZATION OF LASER COOLED AND TRAPPED ERBIUM ATOMS

ANDREW J. BERGLUND¹, SIU AU LEE², AND JABEZ J. MCCLELLAND¹

¹*Center for Nanoscale Science and Technology
National Institute of Standards and Technology
Gaithersburg, MD 20852, USA*

²*Department of Physics, Colorado State University
Ft. Collins, CO 80523, USA*

Owing to their unique electronic structure, rare-earth (lanthanide) elements exhibit unique optical properties particularly as solid-state laser materials. Even in free space, however, these elements exhibit rich, interesting dynamics, as seen in the recent demonstration of erbium magneto-optical trapping [J. J. McClelland and J. L. Hanssen, *Phys. Rev. Lett.* **96**, 14 (2006)]. Among its interesting properties, Er has a variety of accessible spectroscopic lines, including a broad ($\Delta\nu = 36$ MHz) 401 nm line, a narrow ($\Delta\nu = 8$ kHz) 841 nm line, and an ultra-narrow ($\Delta\nu = 2.1$ Hz), telecom-band 1299 nm line; it has naturally abundant bosonic and fermionic isotopes; furthermore, Er has high angular momentum ($J = 6$) and a large magnetic moment ($7 \mu_B$) in the ground state, making it amenable to sub-Doppler laser cooling and magnetic trapping. In this poster, we present our latest cooling and trapping results in this exciting new system. In particular, we demonstrate sub-Doppler MOT temperatures as low as 100 μ K and magnetically trapped sample temperatures as low as 30 μ K. Future prospects and challenges for our experiment are discussed.

Progress Towards a Measurement of the Electric Dipole Moment of the Electron Using PbO*

S. Bickman, P. Hamilton, Y. Jiang, A. Vutha, D. DeMille

*Physics Department, Yale University,
New Haven, CT 06511, USA*

**E-mail: sarah.bickman@yale.edu
http://pantheon.yale.edu/~dpm5*

S. Bickman

*DeMille Laboratory Group,
PO Box 208120
New Haven, CT 06511, USA
E-mail: sarah.bickman@yale.edu*

We have proposed and begun implementing an experiment to look for an electric dipole moment (EDM) of the electron using the metastable $a(1) \ ^3\Sigma^+$ state of the PbO molecule. A non-zero measurement of d_e within the next few orders of magnitude beyond the current limit of $|d_e| < 1.6 \times 10^{-27} \text{ e-cm}^1$ would be clear evidence for physics beyond the standard model. We will present recent results from and improvements to our experiment including a proof of principle for the experiment, recent data on the initial state preparation using simulated microwave Raman transitions, revised estimates of sensitivity to d_e based on the current experimental configuration, and progress towards data on an improved limit on d_e .

We are grateful for the support of NSF Grant No. PHY0244927.

Keywords: Electric dipole moment, electron, PbO

References

1. B.C. Regan, and Eugene D. Commins, and Christian J. Schmidt and David DeMille, *Phys. Rev. Lett.* **88**, 071805 (2002).

GRAVITATIONAL PHYSICS WITH ATOM INTERFEROMETRY

GRANT BIEDERMANN, LOUIS DESLAURIERS, JASON HOGAN, DAVID JOHNSON, CHETAN MAHADESWARASWAMY, SEAN ROY, JOHN STOCKTON, KEN TAKASE, XINAN WU AND MARK KASEVICH

Physics Department, Stanford University, Stanford, CA 94305

Recent measurements of Newton's constant G (1) and the development of high-accuracy gyroscopes (2) based on light-pulse atom interferometric methods indicate that next generation atom interferometric sensors show promise for competitive measurements of G , tests of the inverse square law, tests of the Equivalence Principle, and perhaps ground-based observation of post-Newtonian contributions to the metric (3).

In this work, we describe progress towards development of next generation atom interferometric sensors (shown in Fig. 1) for these measurements. Fig. 1a shows the apparatus under development for tests of the Equivalence Principle. This apparatus will compare the free-fall rates of evaporatively cooled Rb isotopes with the aim of achieving a 1 part in 10^{15} limit on the Equivalence Principle. Wavepackets will separate by more than 1 m during the interferometer interrogation sequence. Fig. 1b illustrates sensors under development to measure G with a precision approaching 10 ppm and to search for Yukawa-type deviations from the inverse-square law. Unlike previous measurements, this apparatus uses a horizontal configuration for the Raman interrogation beams in order to suppress possible systematic effects associated with source mass positioning. Novel detection methods have been developed to achieve the very high SNR levels required for these science goals (4).

1

2

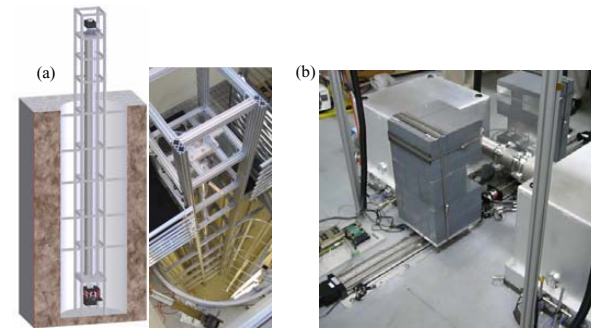


Fig.1 (a). Apparatus for tests of the Equivalence Principle and General Relativity. (b) Apparatus for measuring G and testing the inverse square law.

References

1. Jeff Fixler, Yale University PhD thesis, 2003; J. Fixler, G. T. Foster, J. M. McGuirk, and M. A. Kasevich, *Science* **315**, 74-77 (2007); A. Bertoldi, *et al.*, *Eur. Phys. J. D*, 271-279 (2006).
2. D. S. Durfee, Y. K. Shaham, and M. A. Kasevich *Phys. Rev. Lett.* **97**, 240801 (2006).
3. S. Dimopoulos, P. Graham, J. Hogan and M.A. Kasevich, *Phys. Rev. Lett.* **98**, 111102 (2007).
4. G. W. Biedermann, X. Wu, L. Deslauriers, K. Takase, and M. A. Kasevich, submitted to *Opt. Lett.*

Zero-Down-Time Operation of Interleaved Atomic Clocks

G. W. Biedermann, K. Takase*, X. Wu, L. Deslauriers, C. S. Roy, and M. A. Kasevich
*Department of Physics, Stanford University,
 Stanford, CA 94305, U.S.A.
 E-mail: ktakase@stanford.edu

Atom interferometers have demonstrated outstanding performance in sensing inertial and gravitational forces,¹⁻³ as well as unparalleled accuracy in the field of time-keeping.⁴⁻⁶ Most of these atom interferometers suffer from nonuniform coverage of the time axis due to discrete sampling. Consequently, phase noise in the reference oscillator results in an intermodulation error known as the Dick effect.⁷ We demonstrate a zero-down-time (ZDT) technique for eliminating the Dick effect in an atomic fountain clock by using a pair of clocks to alternately monitor a common local oscillator (LO) in a relay manner.

In our experiment, we operate two independent, compact Cesium fountain clocks by driving a microwave $\pi/2 - \pi/2$ Ramsey sequence on the $|F = 3, m_F = 0\rangle \rightarrow |F = 4, m_F = 0\rangle$ clock transition with an interrogation time of $T = 215$ msec. The two clocks are interleaved in time such that the first (second) $\pi/2$ -pulse for one clock and the second (first) $\pi/2$ -pulse for the other are simultaneously driven by the same LO.

We show that operation in ZDT mode with a noisy LO reduces cumulative phase errors due to the Dick effect over the use of a single clock. To demonstrate this, we add 300 mrad rms phase noise to the LO, which results in a random walk of the accrued phase error for each individual clock at a rate of ~ 0.5 rad/s^{1/2}. On the other hand, the ZDT output, given by the sum of the two clock outputs, exhibits 0.55 rad rms accumulated phase fluctuations over 200 s in contrast to 7.42 rad rms for each individual clock (see Fig. 1).

We also demonstrate a $1/\tau$ slope for the Allan deviation of the ZDT output, which is characteristic of the added phase noise. In contrast, phase fluctuations for a single clock average down as white frequency noise with a scaling of $1/\tau^{1/2}$. Therefore, the ZDT approach is advantageous for clocks

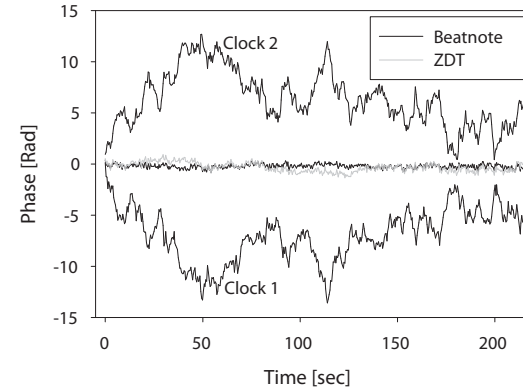


Fig. 1. Cumulative phase accrual of the two independent clocks demonstrating the perceived phase drift of the noisy LO due to incomplete sampling of the phase noise. The sum of the two clocks represents the ZDT quantity which largely removes the random walk drift. The phase accrual of a beatnote between the noisy LO and the master LO closely follows the ZDT.

dominated by phase noise in the LO.

Finally, we present a scheme for applying this ZDT technique to atom interferometer-based inertial sensors for continuous velocity measurements.

References

1. D. S. Durfee, Y. K. Shaham, and M. A. Kasevich, “Long-Term Stability of an Area-Reversible Atom-Interferometer Sagnac Gyroscope,” *Phys. Rev. Lett.* **97**, 240801 (2006).
2. J. B. Fixler *et al*, *Science* **315**, 74 (2007).
3. A. Peters, K. Y. Chung, and S. Chu, *Nature* **400**, 849 (1999).
4. W. H. Oskay *et al*, “Single-Atom Optical Clock with High Accuracy,” *Phys. Rev. Lett.* **97**, 020801 (2006).
5. U. Sterr *et al*, “The optical calcium frequency standards of PTB and NIST,” *C. R. Physique* **5**, 845 (2004).
6. G. Santarelli *et al*, *Phys. Rev. Lett.* **82**, 4619 (1999).
7. Dick G. J. *et al*, in “Proc. 19th Precise Time and Time Interval (PTTI) Applications and Planning Meeting,” pages 133–147 (1987).

Ground-state cooling and reversible state transfer in cavity QED

A. D. Boozer, A. Boca, R. Miller, T. E. Northup* and H. J. Kimble

*Norman Bridge Laboratory of Physics 12-33, California Institute of Technology,
Pasadena, CA 91125, USA*

**E-mail: northup@caltech.edu*

A single, trapped atom within a high-finesse optical resonator is cooled to the ground state of axial motion by way of resolved-sideband Raman cooling. Separately, we have demonstrated the reversible mapping of a coherent state of light to and from the hyperfine states of the atom, a significant step towards cavity-QED based quantum networks.

1. Cooling to the ground state of axial motion

Single atoms strongly coupled to the fields of optical cavities offer a promising setting for protocols in quantum information science.^{1,2} Following recent achievements for trapped ions³ and atoms in optical lattices,⁴ in which cooling to the ground state of motion has been an enabling step towards quantum control, we demonstrate localization to the ground state of axial motion for a single, trapped Cesium atom strongly coupled to the field of a high-finesse optical resonator.⁵

We drive coherent Raman transitions on the red vibrational sideband of the atom in order to cool its motion along the cavity axis. We employ an efficient state detection scheme in order to record the Raman spectrum, from which the resulting state of atomic motion is inferred. We find that the lowest vibrational level of the axial potential with zero-point energy $\hbar\omega_a/2k_B = 13 \mu\text{K}$ is occupied with probability $P_0 \simeq 0.95$.

2. Mapping quantum states between light and matter

One important goal in quantum information science is the realization of quantum networks, in which atomic internal states with long coherence times serve as ‘stationary’ qubits at nodes for local storage and manipulation, while optical fibers transport photons (‘flying’ qubits) over long distances between nodes.² In order to transfer quantum information between

stationary and flying qubits, quantum network protocols require the capability for reversible mapping of quantum states between light and matter. Although several groups have demonstrated single-photon generation,⁶⁻⁹ i.e. mapping from matter to light, no experiment has yet explicitly verified the reversibility of either the emission or the absorption process.

We report a significant advance toward the realization of quantum networks by demonstrating the reversible mapping of a coherent optical field to and from the hyperfine ground states of a single, trapped Cesium atom.¹⁰ We make use of a STIRAP process recently adapted to quantum fields in a high-finesse optical cavity.⁶ By adiabatically ramping *on* a classical field driving a single atom coupled to the cavity, a single photon can be coherently deposited into the cavity mode and thence emitted as a freely propagating pulse.^{2,6-8} Moreover, by ramping the classical field *off*, the state of an incident light pulse can be mapped back onto the atom.

We inject a coherent state of light with mean photon number $\bar{n} \simeq 1.1$ into the cavity and map it to a coherent superposition of $F = 3$ and $F = 4$ ground states with transfer efficiency 0.057; we then map the stored atomic state back to a field state. We verify the reversibility of the mapping process through interference between the final field state and a reference field that is phase-coherent with the original state, observing a fringe visibility of 0.46 ± 0.03 .

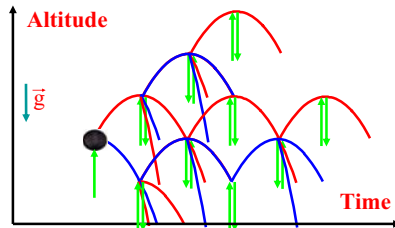
References

1. P. Zoller *et al.*, *Eur. Phys. J. D* **36**, 203 (2005).
2. J. I. Cirac, P. Zoller, H. J. Kimble, and H. Mabuchi, *Phys. Rev. Lett.* **78**, 3221 (1997).
3. C. Monroe *et al.*, *Phys. Rev. Lett.* **75**, 4011 (1995).
4. S. E. Hamann *et al.*, *Phys. Rev. Lett.* **80**, 4149 (1998); H. Perrin, A. Kuhn, I. Bouchoule, C. Salomon, *Europhys. Lett.* **42**, 395 (1998); V. Vuletic, C. Chin, A. Kerman, and S. Chu, *Phys. Rev. Lett.* **81**, 5768 (1998).
5. A. D. Boozer *et al.*, *Phys. Rev. Lett.* **97**, 083602 (2006).
6. J. McKeever *et al.*, *Science* **303**, 1992 (2004).
7. M. Keller *et al.*, *Nature* **431**, 1075 (2004).
8. M. Hijlkema *et al.*, *Nature Physics* **3**, 253 (2007).
9. P. Grangier, B. Sanders, and J. Vuckovic, eds., "Focus on Single Photons on Demand," *New J. Phys* **6** (2004).
10. A. D. Boozer *et al.*, quant-ph/0702248.

An optical clock based on levitating multiple-wave Bordé-Ramsey interferometers.

Christian J. Bordé and François Impens
 SYRTE, Observatoire de Paris, F-75014 Paris, France
<http://christian.j.borde.free.fr>

We propose a new concept of optical clock based on the levitation of a coherent atomic sample (such as a condensate). One shines a sequence of periodic $\pi/2$ laser pulses on the atomic cloud in the vertical direction. Each elementary sequence of four vertical $\pi/2$ pulses with counterpropagating pairs of copropagating waves provides a net vertical momentum transfer to the atomic sample which gives rise to its levitation if the pulse period is properly adjusted to compensate gravity. This process generates bouncing interferometers.



In fact, successive laser pulses split the condensate into a coherent superposition of an exponentially growing number of arms. In spite of the complexity of this matter-field structure, the resulting constructive interferences conserve the number of atoms for resonant frequencies provided that the atomic cloud is sufficiently coherent. Its motion in momentum space is periodic thanks to these wave interferences (matter-wave cavity in momentum space). The population of the levitating cloud is very sensitive to the laser frequency and the device can thus be used as an optical clock. Numerical simulations show that the central interference fringe sharpens fast as the condensate goes through its first bounces. We expect a very promising sensitivity for a great number of successive interferometers. This might require a transverse confinement of the cloud, which could be achieved thanks to an original matter-wave focusing scheme based on the interaction of atoms with laser waves of spherical wavefront.

REEXAMINATION OF 0_g^- PURE LONG-RANGE STATE OF Cs_2 : PREDICTION OF MISSING LEVELS IN THE PHOTOASSOCIATION SPECTRUM

Nadia BOULOUFA, Anne CRUBELLIER and Olivier DULIEU

Laboratoire Aimé Cotton, CNRS, bât 505, Campus d'Orsay, 91400 Orsay, France

A new investigation of the photoassociation (PA) spectrum of the external well of the 0_g^- potential of Cs_2 converging to the $(6s_{1/2} + 6p_{1/2})$ limit is performed, in order to resolve inconsistencies arising from a previously published work of our group [1].

The so-called 0_g^- ($6s_{1/2} + 6p_{3/2}$) pure long range molecular state of Cs_2 represents a case study, as the radiative decay of this state populated by PA of ultracold cesium atoms led to the first observation of stable ultracold molecules [2]. Furthermore, a reliable description of this state is crucial as it appears as a suitable intermediate step in the course of the formation of ground state molecules in their lowest $v = 0$ vibrational level.

The PA spectrum [2] of this state has been interpreted by our group using an analytic approach based on the asymptotic representation of long-range atom-atom interactions to extract an accurate potential curve of its outer potential well [3]. This potential does not allow one to reproduce the intensity pattern of the experimental spectrum. In addition, the van der Waals coefficient C_6 characterizing the long-range interaction between two ground state Cs atoms, as well as the triplet scattering length a_T values obtained in an other fully independent work of our group [1] are incompatible with the most precise available values.

The present work demonstrates that all these discrepancies are suppressed when we make a major modification in the assignment of the observed photoassociation lines corresponding to a shift of 2 units in the assignment of the vibrational levels of the 0_g^- outer well. We predict now that the lowest observed level is actually $v = 2$ and that two deeper levels, namely $v = 0$ and $v = 1$ have still to be discovered. The agreement between experimental and calculated energy positions is improved and the intensities calculated using the new potential extracted using the same approach

as in ref. [3] account well for all available data, see figure 1. New values of the van der Waals coefficient C_6 of the ground state and of the $6p^2P_{1/2}$ and $6p^2P_{3/2}$ atomic lifetimes are obtained, in agreement with available values but with a rather poor precision due to a strong interdependence of the parameters of the model. Only a more precise experimental study could allow one to improve the determination of these values.

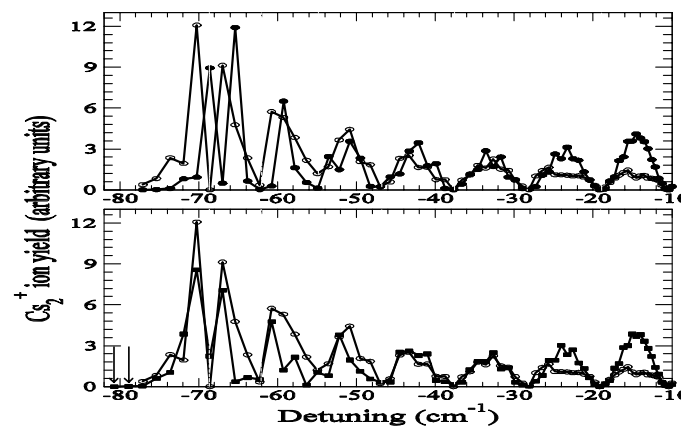


Figure1. Simulations of the PA spectrum, compared to the corresponding experimental spectrum. In both graphs, the experimental spectrum is displayed as open circles. In the upper graph, we show the simulation obtained with the 0_g^- potential of reference [3] (full circles); in the lower graph, we show similar calculations but with the 0_g^- potential of the present work (full squares)

References

- [1] C. Drag, B. Laburthe Tolra, B. T'Jampens, D. Comparat, M. Allegrini, A. Crubellier and P. Pillet, *Phys. Rev. Lett.*, **85**, 1408 (2000)
- [2] A. Fioretti, D. Comparat, C. Drag, C. Amiot, O. Dulieu, F. Masnou-Seeuws and P. Pillet, *Eur. Phys. J. D*, **5**, 389 (1999)
- [3] C. Amiot, O. Dulieu, R. F. Gutterres and F. Masnou-Seeuws, *Phys. Rev. A*, **66**, 052506 (2002)

Coherence properties of a Bose gas at the Bose-Einstein phase transition

T. Bourdel*, S. Ritter, T. Donner, A. Öttl, F. Brennecke, M. K. Köhl, and T. Esslinger

*ETH Zurich, Institute for Quantum Electronics
CH-8093, Zurich, Switzerland*

**E-mail: thomas.bourdel@insitutoptique.fr*

We probe the coherence properties of a Rubidium atomic cloud by monitoring the interferences between two atomic beams extracted at different locations. The atomic flux is detected with single atom resolution using a high finesse optical cavity.¹ Our experiment lies in the novel field of quantum atom optics, where correlations between atoms can be measured. Varying the distance between the output coupling regions allows us to precisely measure the first order correlation function of the cloud. We have observed the divergence of the correlation length in the critical regime, where phase fluctuations play a crucial role.² We have also investigated the formation of long range order as a non equilibrium cloud thermalizes and thereby crosses the phase transition.³ We can now transport the condensate into the high finesse cavity and explore this new strongly coupled quantum system.

References

1. T. Bourdel, T. Donner, S. Ritter, A. Öttl, M. Köhl, and T. Esslinger, Phys. Rev. A **73**, 043602 (2006).
2. T. Donner, S. Ritter, T. Bourdel, A. Öttl, M. Köhl, and T. Esslinger, Science **315**, 1556 (2007).
3. S. Ritter, A. Öttl, T. Donner, T. Bourdel, M. Köhl, and T. Esslinger, Phys. Rev. Lett. **98**, 090402 (2007).

**COLD ATOM CLOCKS IN SPACE:
THE ACES MISSION CONCEPT AND STATUS**

L. CACCIAPUOTI*

*Research and Scientific Support Department, European Space Agency,
Noordwijk ZH, 2200 AG, The Netherlands*

**E-mail: Luigi.Cacciapuoti@esa.int*

C. SALOMON

*Laboratoire Kastler Brossel, ENS, rue Lhomond 24,
Paris, 75005, France*

Atomic Clock Ensemble in Space (ACES)^{1,2} is an ESA mission in fundamental physics based on the performances of a new generation of atomic clocks operated in the microgravity environment of the International Space Station (ISS).

The heart of the ACES system is represented by two space clocks: the primary frequency standard PHARAO, based on laser cooled samples of Cs atoms, and the active hydrogen maser SHM. The good short-term performances of SHM are combined to the long-term stability and accuracy of the PHARAO clock to generate the on-board ACES time scale. The frequency reference delivered by ACES will reach fractional frequency instability and inaccuracy of few parts in 10^{16} . Distributed on ground by a time and frequency link in the microwave domain (MWL), the ACES clock signal will be used for the comparison of distant clocks, both space-to-ground and ground-to-ground. Based on these comparisons, ACES will perform tests of Einstein's theory of general relativity including an accurate measurement of the Einstein's gravitational red-shift, a search for time variations of fundamental constants, and tests of the Standard Model Extension (SME).

The planned mission duration is 18 months. During the first 6 months, the performances of SHM and PHARAO will be established. Thanks to the microgravity environment, the linewidth of the atomic resonance will be varied by two orders of magnitude (from 11 Hz to 110 mHz) and the 10^{-16} stability and accuracy level reached. In the second part of the mission,

the onboard clocks will be compared to a number of ground-based clocks operating both in the microwave and the optical domain.

The engineering models of the ACES clocks have been completed and are presently under test. The PHARAO clock, when driven in combination to a cryogenic sapphire oscillator, reaches a fractional frequency instability of $2.3 \cdot 10^{-13}$ at 1 s. The space hydrogen maser SHM, has already demonstrated an Allan deviation down to $1.5 \cdot 10^{-15}$ after 10^4 s of integration time.

Status, scientific objectives, and concept of the ACES mission will be presented and discussed in detail.

References

1. C. Salomon *et al.*, *C. R. Acad. Sci. Paris t.2 Séries IV*, 1313 (2001).
2. L. Cacciapuoti *et al.*, *Nucl. Phys. B* **166**, 303 (2007).

PRECISE DETERMINATION OF h/m_{Rb} USING BLOCH OSCILLATIONS AND ATOMIC INTERFEROMETRY

MALO CADORET, ESTEFANIA DE MIRANDES, PIERRE CLADE, SAIDA GUELLATI-KHELIFA, CATHERINE SCHWOB, FRANÇOIS NEZ, LUCILE JULIEN AND FRANÇOIS BIRABEN

Laboratoire Kastler-Brossel, ENS, CNRS, UPMC, 4 Place Jussieu, 75252 Paris Cedex 05, France

We determine accurately the ratio h/m_{Rb} from the measurement of the recoil velocity $v_r = \hbar k/m_{Rb}$ of a Rubidium atom absorbing or emitting a photon, combined with an accurate knowledge of the photon wavelength $\lambda = 2\pi/k$. From h/m_{Rb} we deduce a precise value of the fine structure constant α

$$\alpha^2 = \frac{2R_\infty m_{Rb} h}{c m_e m_{Rb}}$$

The key idea to precisely determine the recoil velocity, is to transfer to the atoms as many recoils as possible and to measure their velocity variation. For this purpose we start selecting from an ultracold Rb cloud a very narrow atomic velocity class of width $\approx v_r/50$. This selection is performed using a velocity sensitive stimulated Raman π pulse from $F=2, m_F=0$ to $F=1, m_F=0$ ground hyperfine states. Next, we transfer coherently to the selected atoms up to 1000 recoil velocities by means of Bloch oscillations with 99.95% transfer efficiency per oscillation. Finally, we measure the final atomic velocity distribution by scanning the frequency of a second Raman π pulse from $F=1$ back to $F=2$ state. We point the central velocity with an uncertainty of $\approx v_r/10000$. Adding several refinements to this basic protocol, in 2005 we did a precise measurement of h/m_{Rb} [1] with a relative statistical uncertainty of $8.8 \cdot 10^{-9}$. From a detailed analysis of the systematics, our deduced value of the fine structure constant was $1/\alpha = 137.03599884(91)[6.7 \cdot 10^{-9}]$. This value is in good agreement with the CODATA 2002 recommended value for α [2].

Recently, we have implemented an improved version of this experiment which takes advantage of Ramsey spectroscopy. We use an atomic interferometer consisting in two pairs of $\pi/2$ pulses which put the atom in a superposition of sixteen trajectories. Interference takes place when the spacing T_R between the $\pi/2$ pulses of each pair is equal (see Figure 1a) and Ramsey fringes are observed. The frequency resolution is now determined by the time within each pair of pulses (T_R) while the duration of each $\pi/2$ determines the

2

spectral width of the pulses. Hence, more atoms can contribute to the signal without sacrificing resolution.

In our interferometer all effective Ramsey k -wavevectors point in the same direction. The measurement then takes place by inserting as many Bloch oscillations as possible between the two sets of $\pi/2$ pulses. We measure the recoil frequency by precisely locating the center of the zero-order Ramsey fringe of the interferometer. Figure 1b shows a fringe pattern taken in 5 minutes with 3 ms between the $\pi/2$ pulses and 700 Bloch oscillations.

In the experiment, both Ramsey and Bloch beams are aligned along gravity. To get rid of the contribution of gravity to the determination of h/m_{Rb} we take alternate measurements of two conjugate interferometers (see Figure 1a) created by reversing the direction of the Bloch acceleration. Furthermore, a second pair of interferometers is created by reversing the direction of all the $\pi/2$ momentum impulses. This reversal helps cancelling many spatially dependant systematic effects, as light shifts or second order Zeeman shifts.

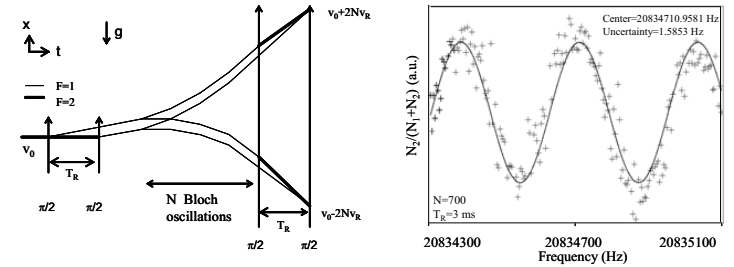


Figure 1a

Figure 1b

Figure 1. a) Double Ramsey interferometer to measure h/m_{Rb} . We show the interfering trajectories for the up and down directions of the Bloch acceleration. b) Fringe pattern of the interferometer.

Following this procedure we have recently performed a measurement of the ratio h/m_{Rb} which has led to a new determination of the fine structure constant α . We have carefully studied the systematic errors in this experiment. A detailed explanation and discussion will be presented in the poster.

References

1. P.Cladé, E.de Mirandes, M. Cadoret, S. Guellati-Khelifa, C.Schwob, F. Nez, L. Julien, and F.Biraben, *Phys. Rev. Lett* **97**, 170406 (2006).
2. P.Mohr, B. Taylor, *Rev. Mod. Phys.* **77**, 1 (2005).

Optical-frequency-comb assisted measurements of atomic Helium transitions

P. CANCIO PASTOR*, G. GIUSFREDI and P. DE NATALE

CNR-Istituto Nazionale di Ottica Applicata and LENS, Via N. Carrara 1,
Sesto Fiorentino, I-50019 Italy

*E-mail: pablo.canciopastor@inoa.it
www.inoa.it

L. CONSOLINO and M. INGUSCIO

LENS and Dipartimento di Fisica, Università di Firenze, Via N. Carrara 1,
Sesto Fiorentino, I-50019 Italy

Quantum-Electro-Dynamics (QED) theory of multielectron-bounded systems has quickly grown in the last decades due to the steep progress in computational facilities to perform detailed calculations.¹⁻³ Accurate tests of these results can be done by comparison with experimental measurements.⁴⁻⁷ Among these systems, perhaps the most accurately and largely studied is the simplest one: Helium atom. For a full exploitation of both experiment and theoretical data, it is important that they have a similar degree of accuracy. Fine structure constant can be determined by comparison of measurements and theoretical calculations of the 2^3P fine structure splittings.^{2,5,6} Isotope shift measurements can determine the nuclear charge radius difference between He isotopes.^{3,7} The strong hyperfine coupling of non-zero nuclear spin He isotopes (as ^3He) can be measured from hyperfine structure spectroscopy.⁷ Larger Lamb-shift contributions can be determined by absolute frequency measurements of visible-near IR He transitions.^{1,4} On the experimental side, the precision and accuracy of these spectroscopic measurements can be largely improved thanks to the Optical Frequency Comb Synthesizers (OFCS), as we have demonstrated for the $2^3S_1 \rightarrow 2^3P_{0,1,2}$ transitions at 1083 nm. This approach can be easily extended to other visible-near IR He transitions where the OFCS operates.

Here, we present an improved apparatus for precise and accurate He spectroscopy at 1083 nm. Basically, two diode lasers, phase-locked to the

nearest teeth of a fiber-OFCS, simultaneously probe two different He transitions. Scanning the OFCS repetition rate allowed us to directly measure the absolute frequency of the 1083 nm transitions and the frequency differences between them, with the accuracy of the GPS disciplined-quartz master oscillator of the OFCS. Moreover, in the frequency differences common systematics is cancelled, providing the possibility to measure small frequency shifts. We plan to use this system to study collisional shifts in BEC and ultracold degenerate He gases.

References

1. K. Pachucki *J. Phys. B* **35**, 3087 (2002). K. Pachucki *Phys. Rev. Lett.* **84**, 4561(2000).
2. G.W.F. Drake *Can. J. Phys.* **80**, 1195 (2002) and earlier references therein.
3. G.W.F. Drake *et al. Can. J. Phys.* **83**, 311 (2005).
4. P. Cancio, G. Giusfredi, P. De Natale, G. Hagel, C. de Mauro, M. Inguscio *Phys. Rev. Lett.* **92**, 023001 (2004) and *Phys. Rev. Lett.* **97**, 139903 (2006)
5. G. Giusfredi, P. De Natale, D. Mazzotti, P. Cancio, C. de Mauro, L. Fallani, G. Hagel, V. Krachmalnicoff and M. Inguscio *Can. J. Phys.* **83**, 301 (2005) and references there in.
6. T. Zelevinsky, D. Farkas, I and G. Gabrielse *Phys. Rev. Lett.* **95**, 203001 (2005)
7. P. Cancio Pastor, G. Giusfredi, D. Mazzotti, P. De Natale, V. Krachmalnicoff and M. Inguscio in *Laser Spectroscopy proceedings of the XVII international conference*, pp.52 (World Scientific, Singapore, 2005)

Cancellation of the collisional shift in caesium fountain clocks

W. Chalupczak*, K. Szymaniec

National Physical Laboratory, Hampton Road, Teddington, TW11 0LW, UK
*E-mail: witold.chalupczak@npl.co.uk

E. Tiesinga, C. J. Williams

Joint Quantum Institute and Atomic Physics Division, National Institute of Standards and Technology, 100 Bureau Drive, Gaithersburg, Maryland 20899-8423, USA

S. Weyers, R. Wynands

Physikalisch-Technische Bundesanstalt, Bundesallee 100, 38116 Braunschweig, Germany

A limiting factor for the accuracy of fountain clocks¹ are the collisions between the atoms, in particular for caesium, where the collision rate coefficients are large and in addition strongly depend on the collision energy.²

A typical Cs fountain standard operates with atoms cooled down to 1–2 μK at the time of launch. As the cloud expands during its ballistic flight, correlations build up between atomic position and velocity. In particular for atoms initially trapped in a small cloud (like in a MOT) very low effective collision energies can be reached even before the first Ramsey interaction³ (Fig. 1a). At low energies the collision rate coefficients for the clock states $|F = 3, m_F = 0\rangle$ and $|F = 4, m_F = 0\rangle$ differ in sign, which gives rise to a strong variation of the collisional shift if the relative weights of the clock states in the superposition state prepared during the first Ramsey interaction are varied.

Our experiments were performed on two independent primary standards: NPL-CsF1 at National Physical Laboratory and PTB-CSF1 at Physikalisch-Technische Bundesanstalt.⁴ The fraction of the population in a given clock state (e.g., $|4, 0\rangle$) was changed by adjusting the amplitude of the microwave field in the Ramsey cavity. The collisional frequency shift for atoms captured in a MOT varies linearly with the population fraction (Fig. 1b).

The collisional frequency shift is cancelled for a 30–40% fraction of $|4, 0\rangle$ atoms, which can be achieved experimentally with only a minor reduction of the fringe contrast and short-term stability of the fountain frequency standard. Our observations provide direct proof of the temperature-dependent model of the frequency shift developed in Ref. 2. Moreover, the possibility of cancelling the collisional shift may improve the effective short-term stability of a fountain standard and significantly shorten its averaging time.

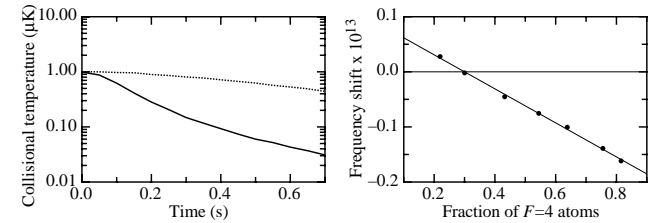


Fig. 1. (a) Evolution of the local energy during the ballistic flight for an initial temperature of 1 μK and initial cloud sizes of 1 mm (solid line) and 5 mm (dotted line). (b) Measurement of the collisional frequency shift in PTB-CSF1 as a function of population fraction in $|4, 0\rangle$ during the Ramsey time.

Typically, primary fountain frequency standards are tested at $n\pi/2$ microwave pulse area (n an odd integer) to check for potential frequency shifts due to, e.g., microwave leakage or cavity phase gradients. Usually the pulse area is adjusted to these values by maximizing the contrast of the central Ramsey fringe. We have experimentally demonstrated that in this case the clock state composition (and therefore the collisional shift) depends on n , if the average microwave power seen by the expanding atom cloud is different during the first and the second transition through the Ramsey cavity. The resulting strong collision-induced n -dependence of the output frequency can mask any potential effects due to leakage or cavity phase gradients.⁵

References

1. R. Wynands and S. Weyers, *Metrologia* **42**, S64 (2005).
2. P. J. Leo, P. S. Julienne, F. H. Mies and C. J. Williams, *Phys. Rev. Lett.* **86**, 3743 (2001).
3. W. Chalupczak and K. Szymaniec, *J. Phys. B* **40**, 343 (2007).
4. K. Szymaniec, W. Chalupczak, E. Tiesinga, C. Williams, S. Weyers and R. Wynands, *Phys. Rev. Lett.* **98**, 153002 (2007).
5. K. Szymaniec, W. Chalupczak, S. Weyers and R. Wynands, *IEEE Ultrason. Ferroel. Freq. Control*, to be published.

CORRELATED TUNNELLING OF INTERACTING ATOM PAIRS IN AN OPTICAL LATTICE OF DOUBLE WELLS*

PATRICK CHEINET, SIMON FÖLLING, STEFAN TROTZKY,
UTE SCHNORRBERGER, ROBERT SAERS, MICHAEL FELD, ARTUR WIDERA,
TORBEN MÜLLER AND IMMANUEL BLOCH

*Institut für Physik, Johannes Gutenberg Universität, Staudingerweg 7
55128 Mainz, Germany*

We study quantum mechanical tunneling of interacting atoms through a potential barrier in a lattice of double well potentials. For strong inter-atomic repulsion, an intriguing regime occurs for which independent tunneling of atoms is suppressed whereas correlated tunneling of atom pairs becomes the dominant tunneling process. We present the first direct measurement of such correlated tunneling events in cold quantum gases.

1. Introduction

The interplay between interaction energy and kinetic energy is the main parameter determining the ground state in strongly correlated systems of ultra-cold atoms in optical lattices. The simplest realization of such a system is a double well potential loaded with two interacting atoms. When the interaction dominates, independent tunnelling of atoms is suppressed due to energy conservation. However, a second order tunnelling process [1], leading to a correlated tunnelling of both atoms is still resonant and becomes the dominant tunnelling process.

2. Experimental setup

To investigate second order tunnelling processes, we load an ^{87}Rb Bose-Einstein condensate into a 3D lattice of double wells, containing each one or two atoms. We obtain the lattice of double wells on one axis by superposition of two standing waves with wavelengths of 765 nm and 1530 nm, with controlled relative phase. The dynamical control of the relative phase allows for a patterned loading of the atoms to one side of the double wells, before they are allowed to tunnel by lowering the short lattice power.

* This work is supported by the DFG, and the EU under the project MC-EXT QUASICOMBS.

3. Experimental results

We will present different results obtained with this setup. We present the first direct measurements of the full dynamics for single atoms as well as atom pairs in such a quantum mechanical junction. Tuning the tunnel matrix element J , we observe the crossover from the independently tunnelling regime to the interaction-dominated regime. By applying a controlled energy bias between the two wells (Figure 1), we could also bring the first order tunnelling process back to resonance for the two atom case, resulting in a conditional tunnelling. These results show the level of control achievable with our setup, which enables to engineer complex many-body systems. Adding the spin degree of freedom allows studying new phenomenon like spin exchange processes [2], for which we are getting the first results.

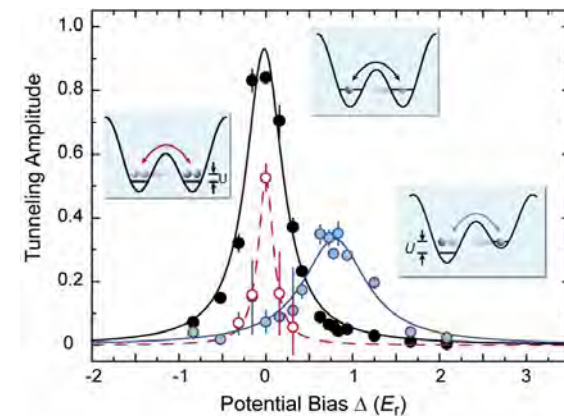


Figure 1. Tunneling amplitudes, for one and two atoms per junction, plotted as a function of an applied potential bias between the two wells. For one atom per junction (in black), any bias suppresses tunneling. For two atoms per junction, we find a correlated tunneling of atom pairs (in dashed red) in the unbiased case, and a conditional tunneling (in blue) of one atom, only in the presence of a second, when the bias is equal to the interaction energy.

References

1. Auerbach, A. *Interacting Electrons and Quantum Magnetism*, (Springer, Berlin, 1998).
2. Duan, L.-M., Demler, E. & Lukin, M. Controlling spin exchange interactions of ultracold atoms in an optical lattice. *Phys. Rev. Lett.* **91**, 090402 (2003).

GENERATION OF SINGLE CYCLE OPTICAL PULSES WITH CONSTANT CARRIER ENVELOPE PHASE

WEI-JAN CHEN, ZHI-MING HSIEH, SHU WEI HUANG, HOA-YU SU

Institute of Atomic and Molecular Sciences, Academia Sinica, Taipei, Taiwan 10617

A. H. KUNG*

Institute of Atomic and Molecular Sciences, Academia Sinica, Taipei, Taiwan 10617

Department of Photonics, National Chiao-Tung University, Hsinchu, Taiwan 300

We report the construction of a train of single cycle optical pulses with a constant carrier envelope phase from a nanosecond pulse that consists of a commensurate frequency comb of Stokes and anti-Stokes radiation generated by coherent modulation of room temperature H₂. Each single cycle pulse is 1.6 fs wide. The pulses are spaced by 8 fs apart in the pulse train.

Harris et. al. showed that molecular modulation is a viable approach to generating subfemtosecond pulses. In molecular modulation, the coherence of a molecule is driven with two intense laser beams to its maximum value. The strongly driven molecular coherence in turn modulates the incident laser frequency to produce a broad spectrum constituting many sidebands.[1] Then by carefully adjusting the phases of the components of this spectrum, a train of short laser pulses can be produced. A four-wave mixing cross-correlation scheme can be used to determine the temporal width of these pulses.[2]

With the help of two independently tunable pulse-amplified single-mode lasers, we have succeeded in generating in room temperature H₂ collinearly propagating Raman sidebands that have wavelengths that range from 1203 nm in the infrared to deep in the vacuum ultraviolet. The frequencies covered by these sidebands span over 4 octaves for a total of more than 70000 cm⁻¹ in the optical region of the spectrum.[3] We have carefully chosen the incident laser frequencies such that the generated spectrum of sidebands is commensurate. That is, the frequency ω_n of the nth sideband is an integral multiple of the modulating frequency ω_m . This commensurate spectrum then leads to the construction of ultrashort pulses with a constant carrier envelope phase (CEP).

* akung@pub.iams.sinica.edu.tw

Taking a subset of the generated sidebands, from 1203 nm to 344 nm and phase adjusting each sideband to correct for frequency dependent phase shifts that result from propagation through a dispersive medium, we have constructed a train of single-cycle constant CEP pulses. Each pulse has a single-cycle electric field half-width of about 0.5 fs and an envelope FWHM of 1.6 fs. The successful construction of the pulses is demonstrated by cross-correlation measurements using four-wave mixing in Xe that was employed by Shverdin[2]. Figure 1 shows the measured correlation signal as a function of time delay. Also shown is the simulated signal for pulses that has a constant CEP. Every waveform in the correlation is identical to the adjacent waveform. This is the signature for constant CEP pulses. For comparison, in figure 2 we show the measured and simulated cross-correlation signal from an incommensurate varying CEP pulse train obtained by deliberately changing the incident frequencies away from the commensurate condition.

These results represent the first single cycle pulses with a constant CEP produced in the optical region of the spectrum. By incorporating more sidebands from our spectrum, it will be possible to produce optical pulses in the attosecond or subfemtosecond time regime with this approach.

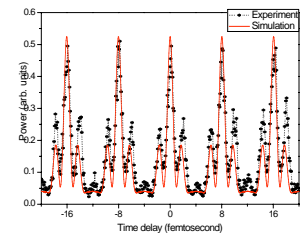


Figure 1. Cross-correlation signal from pulses with a *constant envelope phase*. Solid dots are measured data. Solid line is simulated results.

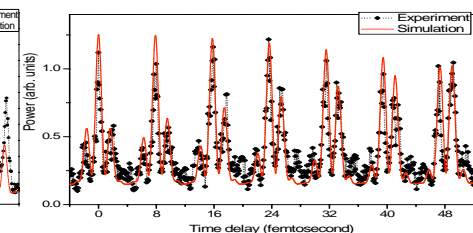


Figure 2. Cross-correlation signal from pulses with a *varying* envelope phase. Solid dots are measured data. Solid line is simulated results.

References

1. S. E. Harris and A. V. Sokolov, *Phys. Rev. Lett.* **81**, 2894 (1998).
2. M. Y. Shverdin, D. R. Walker, D. D. Yavuz, G. Y. Yin, and S.E. Harris, *Phys. Rev. Lett.* **94**, 033904 (2005).
3. Shu Wei Huang, Wei-Jan Chen, and A. H. Kung, *Phys. Rev. A* **74**, 063825 (2006).

Multicomponent spinor atom laser generated by controllable Majorana transition

Xuzong Chen*, Lin Xia, Xu Xu, Fan Yang, Wei Xiong, Juntao Li, Qianli Ma, Xiaoji Zhou and Hong Guo

School of Electronics Engineering and Computer Science, Peking University, Beijing 100871, Peoples Republic of China

*E-mail: xuzongchen@pku.edu.cn

<http://www.iqe.pku.edu.cn>

Multicomponent spinor of Rubidium atom laser is generated by the controllable Majorana transition in QUIC trap. Controllable Majorana transition in spinor BEC system has been realized by altering the rotation frequency of the magnetic field's direction. The population of spinor states can be conveniently manipulated by adjusting the turn-off time of the trap coils in experiment, which provides a new tool to manipulate quantum states. We demonstrate that the experiment results are agreed with the theoretical predication.

Keywords: Majorana Transition; Quantum Manipulation; Spinor BEC.

1. Introduction

Recent years, with the progress of research on atom lasers, the atom laser has been used to investigate the properties of Bose-Einstein condensates and to measure the gravitation with high precision. Majorana transition was first studied in 1932 by Majorana.¹ Some recent experiments did show the effects of Majorana transition, which are qualitatively observed.² We use Majorana transition to control the quantum state of atom lasers, where the order parameter is a vector rather than a scalar in common atom lasers.

2. Experiments and Analysis

We get samples of condensates in a compact low power quadrupole-Ioffe-configuration (QUIC) trap.³ We obtain atom lasers by producing pulsed atom laser with short rf radiation. The total number of atoms prepared in $m_F = 0$ state are about 4×10^4 . After the $m_F = 0$ atom laser is generated and falls down for 2 ms, the nonsynchronous process of the magnetic field

happens. The atom laser pulse will experience the reversion of the magnetic field's direction and the multicomponent spinor atom laser is generated [Fig.1(a)]. We can manipulate the distribution of the population by adjusting τ_i the switch-off time of Ioffe coil.

The experiments results of directly manipulating the quantum state of BEC is shown in Fig.1(b). The transition process is identical to that in Fig. 1(a).

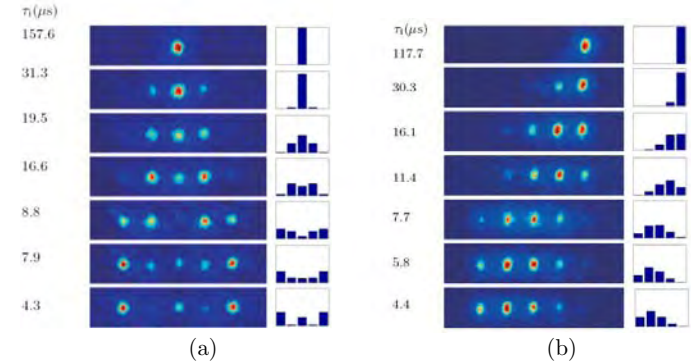


Fig. 1. (a)Generation of multicomponent spinor atom laser by Majorana transition: The $m_F = 0$ spinor state is prepared by producing pulsed atom laser with rf radiation. We can manipulate the distribution of the population by adjusting the switch-off time of Ioffe coil. The population distributions obtained from the analytical expression are shown in the bar charts. (b)Observation of different components of BEC after Majorana transition vs the turn-off time of Ioffe coil: The atoms are initially prepared in $|F = 2, m_F = 2\rangle$ state.

References

1. E. Majorana, *Nuovo Cimento* **9**, 43 (1932).
2. H. Ott, J. Fortagh, G. Schlotterbeck, A. Grossmann, and C. Zimmermann *et al.*, *Phys. Rev. Lett.* **87**, 230401 (2001).
3. Xiuquan Ma, Lin Xia, Fang Yang, Xiaoji Zhou, Yiqiu Wang, Hong Guo, and Xuzong Chen, *et al.*, *Phys. Rev. A.* **73**, 013624 (2006).

APPROACHING THE HEISENBERG LIMIT IN AN ATOM LASER

J. D. CLOSE, N. P. ROBINS, C. FIGL, M. JEPPESEN, J. DUGUÉ, G. DENNIS, M. JOHANSSON

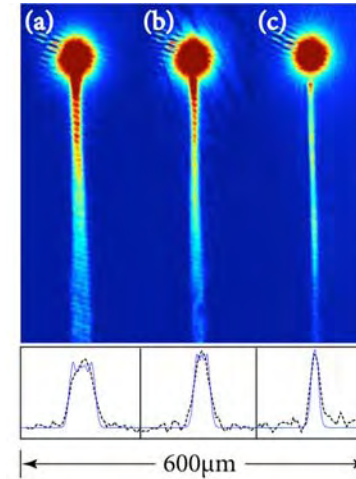
Australian Centre for Quantum Atom Optics and the Department of Physics, The Australian National University, Canberra, 0200, Australia.

We present experimental results showing the decreased divergence and improved spatial profile produced by Raman outcoupling an atom laser beam in comparison with RF outcoupling. We present a theoretical model to compare with the experimental results and find excellent agreement. The model predicts a limit to the beam quality of a Raman atom laser that is a factor of 1.3 above the fundamental (Heisenberg) limit.

Atom laser beams show great potential for use in studies of fundamental physics and in high precision measurements [1]. To fulfill this potential, it will be important to produce atom lasers that are diffraction limited, just as it was important for optical beams. A number of experimental works have shown that the beam quality of an atom laser is strongly affected by the interaction of the outcoupled atoms with the BEC from which it is produced [2-5]. As the atoms fall through the condensate, the repulsive interaction acts as a diverging lens to the outcoupled atoms. This leads to a divergence in the atom laser beam and a poor quality transverse beam profile. Such behavior may cause problems in, for example, mode matching an atom laser beam to a local oscillator in a precision measurement. Experiments on atom lasers in waveguides have produced beams with improved spatial profile [6], however, precision measurements with atom interferometry are likely to require propagation in free space.

In a recent Letter, it was shown that the quality of a free space atom laser is improved by outcoupling from the base of the condensate [2]. Our scheme enables the production of a high quality atom laser while outcoupling from the center of the condensate. This is desirable for a number of reasons. Outcoupling from the center allows the highest possible output flux for a given outcoupling rate and hence a lower classical noise level [7]. Outcoupling from the center allows the longest operating time (for a quasicontinuous atom laser) since the condensate can be drained completely. Outcoupling from the center minimizes the sensitivity of the output coupling to condensate excitations or external fluctuations.

In a recent Letter, we reported a continuously outcoupled atom laser where the output-coupler is a coherent multi-photon Raman transition [8]. In this scheme, the atoms receive a momentum kick from the absorption and emission of photons. They leave the condensate more quickly, so that adverse effects due to the mean-field repulsion from the condensate are reduced [9]. In the work presented here, we report a two-fold improvement in the beam quality M^2 over RF outcoupling. We have calculated the theoretical M^2 of the atom laser and find, that as the kick increases, the beam quality improves, and the quality asymptotes to that of a beam that does not interact with the condensate. The transverse velocity spread of the atom laser is equal to that of the condensate. We calculate this limit to be $M^2 = 1.3$ for our conditions, using the condensate wavefunction which is calculated numerically. We check this by propagating the atom laser using a kick sufficiently large that the mean field component of the transverse velocity spread is negligible. The limit of $M^2 = 1.3$ is greater than the Heisenberg limit, $M^2 = 1$, because the BEC, which is the source of the atom laser, is not a minimum uncertainty state due to the repulsive interactions between the atoms.



Sequence of atom laser beams showing the improved beam profile of a Raman atom laser. The atom laser beams were produced using RF (a) and Raman (b and c) transitions. The angle between the Raman beams was 30 degrees in (b) and 140 degrees in (c), corresponding to a kick of 0.3-cm/s and 1.1-cm/s respectively. Below: Comparison of experimental (dashed) and theoretical (solid) beam profiles 500 microns below the BEC. The height of each theoretical curve has been scaled to match experimental data.

1. M.A. Kasevich, *Science* **298**, 1363 (2002).
2. J.-F. Riou *et al.* *Phys. Rev. Lett.* **96**, 070404 (2006).
3. M. Köhl *et al.* **72**, 063618 (2005).
4. T. Busch, M. Köhl, T. Esslinger, and K. Mølmer, *Phys. Rev. A* **65**, 043615 (2002).
5. Y. Le Coq *et al.* *Phys. Rev. Lett.* **87**, 170403 (2001).
6. W. Guerin *et al.* *Phys. Rev. Lett.* **97**, 200402 (2006).
7. N. P. Robins, A. K. Morrison, J. J. Hope and J. D. Close, *Phys. Rev. A* **72**, 031606 (2005).
8. N. P. Robins *et al.* *Phys. Rev. Lett.* **96**, 140403 (2006).
9. E. W. Hagley *et al.* *Science* **283**, 1706 (1999).

SINGLE ATOM AND BEC DETECTION ON A MICROCHIP WITH AN INTEGRATED OPTICAL MICRORESONATOR

Y. COLOMBE^{1,*}, T. STEINMETZ^{1,2}, G. DUBOIS¹, F. LINKE¹, D. HUNGER²,
T. W. HÄNSCH² and J. REICHEL¹

¹Laboratoire Kastler Brossel, Département de Physique de l'École Normale Supérieure,
24 rue Lhomond, 75231 Paris Cedex 05, France
*E-mail: yves.colombe@kb.ens.fr

²Max-Planck-Institut für Quantenoptik and
Sektion Physik der Ludwig-Maximilians-Universität München,
Schellingstr. 4, 80799 München, Germany

We report on experiments where we couple atoms to the mode of a miniaturized optical Fabry-Perot cavity integrated on an atom chip. The cavity is formed by two optical fiber facets and lies $150\mu\text{m}$ below the surface of the atom chip. It is $39\mu\text{m}$ long, has mode waist $w_0 = 3.9\mu\text{m}$ and a finesse $\mathcal{F} = 36000$. The small volume of the cavity mode leads to a very high atom-photon coupling rate $g_0 = 2\pi \times 213\text{MHz}$, which exceeds both the cavity decay rate $\kappa = 2\pi \times 53\text{MHz}$ and the atom spontaneous emission rate $\gamma = 2\pi \times 3\text{MHz}$. The cooperativity parameter $C_0 = g^2/(2\kappa\gamma)$, which is often used to characterize the atom-field coupling strength, reaches the remarkably high value of 140.

This strong coupling makes it possible to detect single ^{87}Rb atoms passing through the cavity mode, as shown in Fig. 1. In this experiment a $T < 1\mu\text{K}$ atomic cloud is trapped 1.25mm away from the cavity and then released into a magnetic waveguide crossing the cavity mode. We also demonstrate the preparation and the detection of atomic samples trapped inside the cavity, with a mean atom number of a few units.

In a second series of experiments we observe the collective coupling of N Bose-condensed atoms with the cavity mode. The energies of the coupled atoms-photon eigenmodes are splitted by the vacuum Rabi frequency $2g = 2\sqrt{N}g_0$, as is shown on Fig. 2 where the number of trapped atoms is varied. Using a red-detuned dipole beam that is resonant with the cavity mode, we also show that the high confinement and the precise positioning

provided by the atom chip allows to resolve individual anti-nodes of the dipole standing wave, and to tune the coupling of the atoms to the cavity.

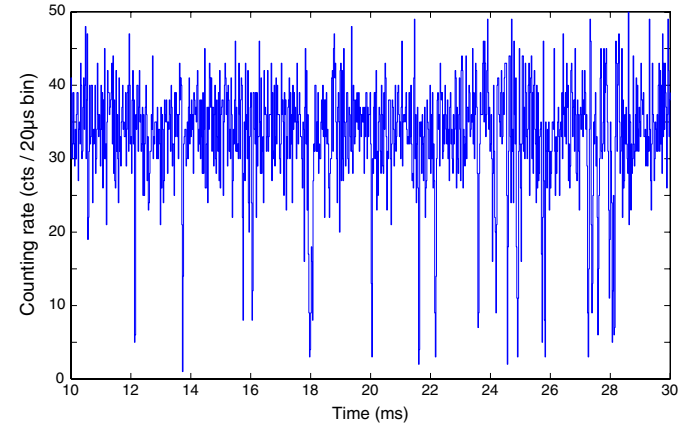


Fig. 1. Optical transmission of the cavity showing transits of single atoms magnetically guided on the atom chip.

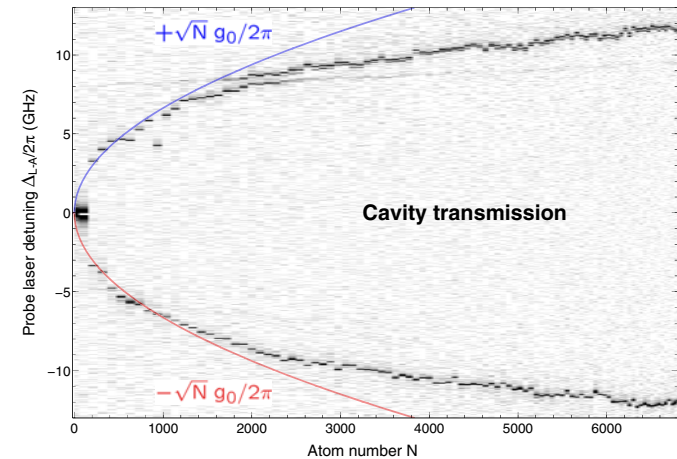


Fig. 2. Evolution of the vacuum Rabi splitting of the coupled atoms-cavity system as the number of atoms is varied. For $N < 3000$ the atoms form a Bose-Einstein condensate.

NEAR-IR FREQUENCY COMB TO CHARACTERIZE SUB-DOPPLER SPECTROSCOPY OF ACETYLENE-FILLED OPTICAL FIBERS*

KRISTAN L. CORWIN[†], KEVIN KNABE, RAJESH THAPA, KARL TILLMAN, ANDREW JONES, AND BRIAN R. WASHBURN

Department of Physics, Kansas State University, 116 Cardwell Hall
Manhattan, KS 66503, USA

JEFFREY W. NICHOLSON AND MAN F. YAN

OFS Laboratories, 19 Schoolhouse Rd., Somerset NJ 08873, USA

We have stabilized a near-infrared frequency comb based on a Cr:forsterite laser with prisms for dispersion compensation. This comb exhibits a narrower carrier-envelope frequency beatnote than a previously published result in a chirped-mirror Cr:forsterite laser. In addition, we report on recent efforts to create portable sub-Doppler frequency references based on acetylene-filled hollow photonic bandgap fiber. We have developed a novel technique for simplifying the spectroscopy inside these fibers, called the “reflected pump” technique.

1 Cr:forsterite laser

Optical frequency combs are typically based on Ti:sapphire lasers, but near-infrared frequency combs are particularly useful for measurements in the telecommunications bands. Cr:forsterite lasers based on chirped-mirror dispersion compensation have previously been stabilized, using the self-referencing technique [1]. In that case, the carrier-envelope offset beatnote (f_0) was observed to be ~ 6 MHz. In contrast, in our prism-based laser we observe significantly narrower widths (~ 1.5 MHz), although the pump lasers in the two cases are nearly identical. Possible explanations will be explored. Furthermore, the laser has been stabilized using feedback to both the pump power and the prism insertion. The comb will be stabilized to synthesizers that are in turn referenced to a GPS-disciplined Rb clock. Then, it will be compared to laser frequencies that are stabilized to the sub-Doppler spectra described below [2], in order to characterize the stability of these novel frequency references.

2 Fiber-based acetylene spectroscopy

We will use this comb to characterize optical frequency references based on acetylene-filled hollow photonic bandgap optical fibers [2]. The technique involves pump-probe spectroscopy with two counter-propagating beams. When this spectroscopy is performed

* This work is supported by the NSF award No. ECS-0449295 and by the AFOSR, award No. FA9550-05-1-0304.

[†] Dr. Corwin’s E-mail address is corwin@phys.ksu.edu.

inside a hollow photonic bandgap fiber that is spliced to a solid-core fiber, the reflections from the splice can create interference fringes that degrade the signal. However, as shown in Fig. 1 below, we have exploited that reflection to create the probe beam, thus simplifying the spectroscopic technique considerably. We compare the resulting signals from the simplified “reflected pump” technique to those of more conventional methods. Furthermore, we have used rf modulation techniques to peak-lock a diode laser to the sub-Doppler feature [3].

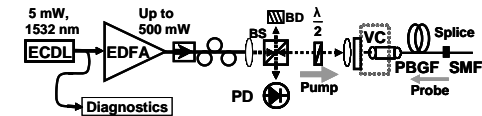


Figure 1. a) Schematic of the “reflected pump” technique for saturated absorption inside photonic bandgap fiber. The output of a tunable diode laser is amplified by an EDFA, passes through an isolator and non-polarizing beamsplitter, and is coupled through a window into a photonic bandgap (PBG) fiber with a core diameter of $20 \mu\text{m}$. The end of the PBG fiber is inside the vacuum chamber (VC), and can be evacuated to less than 1 mTorr. The VC and PBG fiber are then filled to between 100 and 1000 mTorr. The saturated absorption spectra are viewed as a voltage on the photodetector (PD).

Next, we will make measurements of the locked diode laser frequency using the stabilized comb. The long-term and short-term stability of the lock will be assessed.

Acknowledgements

We thank Scott Diddams, Henry Kapteyn, Nathan Newbury, Kendall Read, Kurt Vogel, and Larry Weaver for helpful discussions.

References

- [1] K. Kim *et al.*, “Stabilized frequency comb with a self-referenced femtosecond Cr:forsterite laser,” *Opt. Lett.*, **30**, 932 (2005).
- [2] R. Thapa, K. Knabe, M. Faheem, A. Naweel, O. L. Weaver, and K. L. Corwin, “Saturated absorption spectroscopy of acetylene gas inside large-core photonic bandgap fiber,” *Opt. Lett.* **31**, 2489 (2006).
- [3] J. L. Hall, L. Hollberg, T. Baer, and H. G. Robinson, “Optical heterodyne saturation spectroscopy,” *Appl. Phys. Lett.*, **39**, 680 (1981).

INTERACTIONS OF SPINOR MATTER-WAVE GAP SOLITONS

B. J. DABROWSKA-WUESTER, T. J. ALEXANDER*, E. A. OSTROVSKAYA and
YU. S. KIVSHAR

*Nonlinear Physics Centre, Australian National University,
Canberra, ACT 0200, Australia*

**E-mail: tja124@rsphysse.anu.edu.au
www.rsphysse.anu.edu.au/nonlinear*

We consider the interaction of spinor gap solitons in a Rb^{87} Bose-Einstein condensate. We demonstrate that by controlling the phase and relative amplitude of different spin components soliton switching and guiding may be achieved, and even a complete transformation of the output spin state.

Keywords: Spinor Bose-Einstein condensates; Gap solitons; Soliton interactions

Collisions between vector (composite) solitons are known from optics to possess unique features, including the emergence of different solitons after the collision process and energy exchange between components during the collision [1]. However, past studies have only considered lattice-free solitons. In Bose-Einstein condensates solitons in a lattice and multicomponent condensates bring new physics at different levels. Solitons existing solely due to the lattice, known as gap solitons, are an important class of solutions which can be localized and mobile even when the interparticle interaction is repulsive. Multicomponent condensates come in a number of guises, but perhaps the most intriguing and physically complex are the multicomponent spinor condensates, in which a number of spin hyperfine components are populated and atoms are free to change their spin nature through a parametric conversion between spin states.

In this work we show that the interaction of spinor gap solitons display a myriad of effects in which ultimately the direction and spin state after the collision can be controlled by the input state. We demonstrate matter-wave switching behaviour, conversion between ferromagnetic and antiferromag-

netic solitons and “shepherding” of weaker components by dominant components. Underlying all these effects are the phase dependent conversion processes and interactions between components.

Our analysis is conducted using the Gross-Pitaevskii formalism in the semi-classical regime. We have shown previously that gap solitons in a Rb^{87} condensate, localized by a balance of the nonlinearity and the modified diffraction in the lattice, can be either ferromagnetic or antiferromagnetic in character, despite the overall ferromagnetic nature of Rb^{87} [2]. We examine here the variety of interactions which are possible with mobile gap solitons. The dynamics of the interaction, including the energy exchange and direction of motion can be carefully controlled by modifying the relative phases and amplitudes of the components. In this way fusion, repulsion or switching behaviour may be observed. As an example Fig. 1 demonstrates how a dominant out-of-phase component induces an overall repulsion between solitons, with some particle exchange occurring between the attractive components before they are drawn apart. This interaction may actually change the overall spin state of the final gap soliton, through a fusion of different spin states. This process allows for the possibility of manipulating the spin nature of a condensate without the need for external magnetic fields.

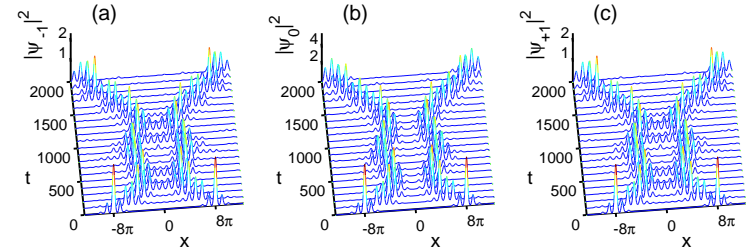


Fig. 1. Interaction of two anti-ferromagnetic solitons, showing energy conversion between the $\Psi_{\pm 1}$ components and guiding by the Ψ_0 component

References

1. Yu. S. Kivshar and G. P. Agrawal, *Optical solitons* (Academic Press, San Diego, 2003).
2. B. J. Dabrowska-Wuster, E. A. Ostrovskaya, T. J. Alexander and Yu. S. Kivshar, *Phys. Rev. A* **75**, 023617 (2007).

IMAGING THE BEAM PROFILE OF A METASTABLE ATOM LASER

R.G. DALL, L.J. BYRON, K.G.H. BALDWIN, A.G. TRUSCOTT
*ARC Centre of Excellence for Quantum-Atom Optics,
 Research School of Physical Sciences and Engineering,
 Australian National University, Canberra, ACT 0200, Australia.*

G. DENNIS, M. JEPPESEN, M.T. JOHANSSON
*ARC Centre of Excellence for Quantum-Atom Optics,
 Department of Physics, The Australian National University, Canberra, ACT 0200,
 Australia*

In our experiment we condense metastable helium (He^*), typically reaching the transition temperature for Bose Einstein condensation (BEC) with around ten million atoms [1]. Recently, we have created a metastable atom laser by using radio frequency (RF) output coupling to create a matter wave beam from our condensate. In our experiment, the size of the condensate is large compared to the gravitational sag of the magnetic trap. This is due to the relatively large s-wave scattering length for He^* in combination with the tight confinement that is possible. For such a system RF output coupling leads to output coupling surfaces which are oblate spheroids, rather than planes as is the case of previously studied atom lasers. This output coupling geometry leads to a 'fountain' effect, in which atoms output coupled above the trap centre experience an upward force. Since the output coupling surface is symmetric around the centre of the magnetic trap, the result is that initially the output coupled atom cloud contains atoms going both upward and downward. This creates unusual dynamics, in which some atoms 'fountain' up and then drop back through the condensate. The resulting transverse atom laser profiles exhibit a forbidden region for those atoms that have an initial upward velocity. Since these atoms pass back through the condensate they feel an enormous mean field repulsion and are pushed off axis, creating a shadow in the atom laser beam.

We image the transverse profile of the metastable atom laser beam using a micro-channel plate and phosphor screen detector located about 4 cm below our condensate. The output beam is only well collimated and approximately Gaussian if the atoms are outcoupled from the very bottom of the BEC. If the atoms are coupled out near the centre of the condensate they experience a repulsive force from the atoms in the BEC, resulting in large lensing and the appearance of "caustics" on the edge of the beam. Furthermore, a forbidden region is observed in the centre of the beam [2]. Fig. 1 shows an image of our atom laser beam outcoupled from the centre of the BEC.

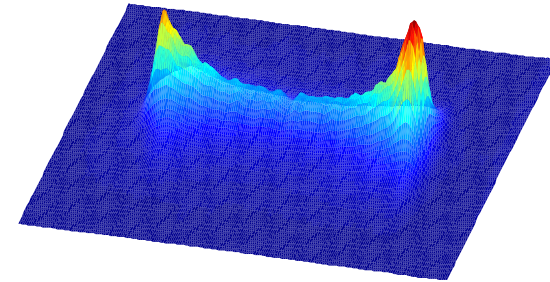


Fig 1. Transverse profile of a He^* atom laser beam. The atoms are output coupled from the centre of the condensate resulting in large lensing due to atom-atom interactions. Note the appearance of caustics near the edge of the beam and a forbidden region in the centre of the beam.

References

1. R.G. Dall and A.G. Truscott, *Optics Communications* **270**, 255 (2007).
2. R.G. Dall, L.J. Byron, G. Dennis, M.T. Johansson, M. Jeppesen and A.G. Truscott, *in preparation*.

DECOHERENCE EFFECTS IN BOSE-EINSTEIN CONDENSATE INTERFEROMETRY

B J DALTON

*ARC Centre for Quantum-Atom Optics
and
Centre for Atom Optics and Ultrafast Spectroscopy
Swinburne University of Technology
Melbourne, Victoria 3122, Australia
Email: bdalton@swin.edu.au*

Recently a generalised two-mode theory of double-well BEC interferometry was developed [1] using the quantum principle of least action, and based on allowing for possible fragmentations of the original BEC into two modes - which may be localised in each well. Though restricted to small boson numbers, the theory gave self consistent coupled equations for the mode functions (generalised Gross Pitaeviskii equations) and for the amplitudes (matrix equations) describing BEC fragmentation. The mode functions depend on the relative importance of the fragmentation amplitudes, which themselves depend on the mode functions. However, only intra-condensate bosonic interactions and dephasing processes were treated, and not decoherence processes associated with elementary collective excitations (Bogoliubov) and single boson excitations (thermal modes).

In the present paper, a more complete theory of decoherence and dephasing effects in BEC interferometry is now developed for determining the quantum correlation functions [2] used in describing interferometric effects. A generalised phase space method mapping the density operator onto a distribution functional is used [3], with the highly occupied condensate modes described via a generalised Wigner representation (the bosons in condensate modes behave like a classical mean field), and the basically unoccupied non-condensate modes described via a positive P representation (these bosons should exhibit quantum effects). The functional Fokker-Planck equation (FFPE) for the distribution functional is based on the truncated Wigner approximation [3]. The FFPE are replaced by coupled Ito stochastic equations for condensate and non-condensate field functions, and contain deterministic and random noise terms. Stochastic averages of the field functions then give the quantum correlation functions.

References

- [1] B J Dalton, *J. Mod Opt.* **54**, 615 (2007).
- [2] R Bach and K Rzazewski, *Phys. Rev. A* **70**, 063622 (2004).
- [3] M J Steele *et al.*, *Phys. Rev. A* **58**, 4824 (1998).

ON-CHIP BOSE-EINSTEIN CONDENSATE INTERFEROMETER WITH 0.5 MM ARM LENGTH

QUENTIN DIOT, STEPHEN R. SEGAL, ERIC A. CORNELL AND DANA Z. ANDERSON

*Department of Physics and JILA, University of Colorado and the National Institute of Standards and Technology,
University of Colorado, Campus Box 440, Boulder, CO 80309*

MARA PRENTISS

Physics Department, Harvard University, Cambridge, MA 02138

ALEX A. ZOZULYA

Department of Physics, Worcester Polytechnic Institute, 100 Institute Road, Worcester, Massachusetts 01609

We demonstrate a chip-based Michelson interferometer for Bose-Einstein condensates in which a harmonic trap reflects the atoms. The condensate is split by diffraction from momentary exposure to an off-resonant standing light field. The two clouds propagate in opposite directions along a waveguide having a weak (4 Hz) harmonic axial confinement. The condensates reflect from the axial potential at classical turning points separated by about 1 mm. Upon returning to the trap center, the two clouds are recombined by a second exposure to the standing light field. The resulting three clouds are allowed to remain in the guide for a brief time. The atoms are then released from the guide and imaged after 15 ms of ballistic expansion. The total propagation time can be set to 120 or 240 ms.

We investigate the conditions that maximize the interference signal by adjusting the phase overlap between the clouds. We show that inside each cloud, the phase stays relatively flat for durations of at least 240ms. At this point, external noise sources randomize the relative phase between the clouds and the phase scatters widely from shot to shot. In order to track the coherence of the recombined atoms over large sets of data, we have implemented the Principal Component Analysis of a series of many images. This method does not require any assumptions for the shape of the clouds and makes a rigorous treatment of small signals possible.

Work supported by DARPA Defense Sciences Office and the NSF

DEVELOPMENT OF A NUCLEAR MAGNETIC RESONANCE GYROSCOPE

E.A. DONLEY, E. HODBY, S. KNAPPE, L. HOLLBERG, AND J. KITCHING
NIST Time and Frequency Division, 325 Broadway, Boulder, CO, USA

1. Introduction

Rotation can be sensed using a precision measurement of the Larmor precession of noble-gas nuclei [1]. The nuclei are polarized via spin-exchange optical pumping with spin-polarized Rubidium atoms, which are also used as a magnetometer to sense the noble-gas nuclear precession. We are taking a new look at the feasibility of NMR Gyroscopes in light of recent developments in chip-scale atomic clocks [2], which rely on similar technologies. The hope is that NMR can be used together with micro-electro-mechanical systems technology to develop a high-performance gyroscope that can be miniaturized.

2. Experimental Results

Various types of spectroscopic measurements of the spin-precession of ^{129}Xe and ^{131}Xe nuclei contained in a 1mm^3 vapor cell have been performed. The fundamental sensitivity limits of the measurements have been studied. Measurements of the resonance linewidth versus temperature have yielded information about the wall interactions in the vapor cell. These and other measurements will be presented in detail.

Acknowledgments

This work was supported by DARPA and is a contribution of NIST, an agency of the US government, and is not subject to copyright.

References

1. J.M. Andres, *United States Patent 3,214,683* (1965), B.C. Grover, E. Kanegsberg, J.G. Mark, and R.L. Meyer, *United States Patent 4,157,495* (1979).
2. S. Knappe et al., *Appl. Phys. Lett.* **85** 1460-1462 (2004).

HIGH-RESOLUTION SPECTROSCOPY OF THE $^{88}\text{Sr}^+$ ION CLOCK TRANSITION

P. DUBÉ*, A. A. MADEJ, J. E. BERNARD, and A. D. SHINER

*Institute for National Measurement Standards,
National Research Council, Ottawa, ON, K1A 0R6, Canada*

**E-mail: pierre.dube@nrc-cnrc.gc.ca*

We present recent results on the high-resolution spectroscopy of the $^{88}\text{Sr}^+$ ion. We have improved the linewidth of our probe laser system and have observed 5 Hz Fourier transform limited linewidths at 445 THz (resolution of 1×10^{-14}) on a Zeeman component of the $5s^2S_{1/2} - 4d^2D_{5/2}$ “clock” transition of $^{88}\text{Sr}^+$.

Keywords: Ultra-stable laser, single-ion, optical frequency standard, high resolution spectroscopy, thermal expansion.

1. Introduction

An optical frequency standard can have very high stability compared to a microwave clock because of the high frequency and narrow linewidth of its reference transition. The quality factor, $Q = \nu_0/\Delta\nu$, of an optical reference transition based on either trapped single ions or lattices of spatially confined neutral atoms is typically 10^{14} or higher. For example, the $5s^2S_{1/2} - 4d^2D_{5/2}$ transition of $^{88}\text{Sr}^+$ has a linewidth of $\Delta\nu = 0.4$ Hz at $\nu_0 = 445$ THz, which provides a line Q of 10^{15} . Probing of such narrow resonances requires a suitably stable and narrow linewidth laser source. The frequency characteristics of the probe laser system are ultimately determined by the mechanical stability of the reference optical resonator used to stabilize the laser.¹⁻⁵

2. Probe Laser System

A commercial diode laser at 674 nm is frequency narrowed and stabilized using a cascade of two Fabry-Perot resonators. The first resonator ($\Delta\nu = 100$ kHz) is used for pre-stabilization of the diode laser, and the second resonator ($\Delta\nu = 3.7$ kHz) is the ultra-stable reference that determines the final frequency characteristics of the probe laser system.

The spacer and mirrors of the reference resonator are made of ultra-low expansion glass. This ULE cavity and its support structure are each mounted on Viton O-rings for decoupling from external vibrations. To further reduce vibrations from the floor, the optical table is floated during the high-resolution experiments.

The reference cavity is made exceptionally immune to thermal fluctuations by using two-stage temperature stabilization, and by setting the vacuum chamber temperature at the value where the thermal expansion coefficient of the ULE cavity on its support structure is “zero.” We have measured this temperature for our system using a steady-state method. Such a measurement was possible because of the small and predictable drifts of the ULE spacer over long periods of time (months). A temperature of $5.45(1)^\circ\text{C}$ was found for our particular sample of ULE glass.

3. High-Resolution Spectroscopy of $^{88}\text{Sr}^+$

The performance of the probe laser system was investigated by scanning across a Zeeman component of the $5s^2S_{1/2} - 4d^2D_{5/2}$ transition of a trapped and laser cooled single ion of $^{88}\text{Sr}^+$. The stabilized light from the probe laser system was sent to the trapped-ion apparatus with a fiber equipped with a phase-noise cancellation system.^{6,7} A linewidth of 5 Hz was observed,⁸ representing a fractional frequency resolution of 1×10^{-14} . It is worth noting that a typical scan across the width of the Zeeman component took about three minutes during these measurements without requiring drift cancellation.

References

1. B. C. Young, F. C. Cruz, W. M. Itano and J. C. Bergquist, *Phys. Rev. Lett.* **82**, 3799(May 1999).
2. A. D. Ludlow, X. Huang, M. Notcutt, T. Zanon-Willette, S. M. Foreman, M. M. Boyd, S. Blatt, and J. Ye, *Opt. Lett.* **32**, 641 (2007).
3. H. Stoehr, F. Mensing, J. Helmcke, and U. Sterr, *Opt. Lett.* **31**, 736 (2006).
4. M. Notcutt, L.-S. Ma, J. Ye and J. L. Hall, *Opt. Lett.* **30**, 1815 (2005).
5. S. A. Webster, M. Oxborrow, and P. Gill, *Opt. Lett.* **29**, 1497 (2004).
6. B. C. Young, R. J. Rafac, J. A. Beall, F. C. Cruz, W. M. Itano, D. J. Wineland and J. C. Bergquist, Hg^+ optical frequency standard: Recent progress, in *Laser Spectroscopy XIV International Conference*, eds. R. Blatt, J. Eschner, D. Leibfried and F. Schmidt-Kaler (World Scientific, Singapore, 1999).
7. L.-S. Ma, P. Jungner, J. Ye and J. L. Hall, *Opt. Lett.* **19**, 1777 (1994).
8. P. Dubé, A. A. Madej, J. E. Bernard, and A. D. Shiner, $^{88}\text{Sr}^+$ single-ion optical frequency standard, in *Proceedings of the 2006 International Frequency Control Symposium and Exposition*, (Miami, Florida, USA, 2006).

COHERENT TRANSFER OF AN OPTICAL CARRIER THROUGH A LONG-DISTANCE FIBER LINK

S. M. FOREMAN, A. D. LUDLOW, M. M. BOYD, S. BLATT, T. ZELEVINSKY, G. K. CAMPBELL, T. ZANON, AND J. YE

*JILA, National Institute of Standards and Technology, and University of Colorado
Department of Physics, Boulder, Colorado 80309-0440, USA*

J. E. STALNAKER AND S. A. DIDDAMS

*National Institute of Standards and Technology
325 Broadway, MS 847, Boulder, Colorado 80305*

An optical carrier frequency of 282 THz, corresponding to a wavelength of 1064 nm, is transmitted through an urban-installation fiber optic network that can be configured in a 3.5- or 7.0-km length. The optical phase delay fluctuations of the fiber link are compensated by using a method similar to that of Ref. [1], where the in-loop error signal is formed by a heterodyne beat between a local copy of the input light and light that has been retro-reflected from the remote tip of the fiber, traveling a total distance of 7 or 14 km, respectively. Feedback to an acousto-optic modulator (AOM) placed just in front of the fiber link is used to precompensate for the link's passive frequency fluctuations.

The 7-km link allows the "local" and "remote" ends of the fiber to be collocated, so that light exiting the remote end can be directly compared against the local reference in order to characterize the actively-stabilized fiber link in an out-of-loop fashion. A transfer instability (see Fig. 1(b)) of 6×10^{-18} at 1-s averaging time is recovered, averaging down to 3×10^{-19} at 1000-s averaging time, limited by slow fluctuations of the out-of-loop optical path length. A heterodyne beat between input and output ends of the 7-km link reveals a resolution-bandwidth-limited linewidth of 1 mHz and a phase noise corresponding to a timing jitter of 0.08 fs, integrated from 10 mHz to 10 MHz.

A 25-km fiber spool was also inserted into the 7-km urban fiber link, for a net 32-km (one-way) transfer. For this scheme, a transceiver configuration was used at the remote end instead of a simple retroreflection, in order to enhance the power and distinguish the round-trip light from reflections of the incident

2

light inside the fiber. Similar instability was achieved as for the 7-km link, again limited by the out-of-loop measurement system which was more complicated for the transceiver configuration. A 1-mHz relative linewidth between ends of the link was again recovered, with a lower signal-to-noise ratio.

As a first application of the fiber link, the 3.5 km link has been used to remotely compare two independent ultrastable-cavity-stabilized lasers operating at 698 (local) and 1126 nm (remote), with a femtosecond frequency comb at each end of the fiber link in order to transfer the 698-nm laser's stability to the 1064-nm transfer laser, and to compare the transferred 1064-nm light to the 1126-nm laser. A heterodyne beat between one mode of the remote comb and the transferred 1064-nm light had a resolution-limited linewidth of 1 Hz, as shown in Fig. 1(b).

This phase-stable optical fiber link will help to allow important intercomparisons of next-generation optical atomic clocks, and find important applications for very-long-baseline interferometry and the synchronization of components in large accelerator-based advanced light sources.

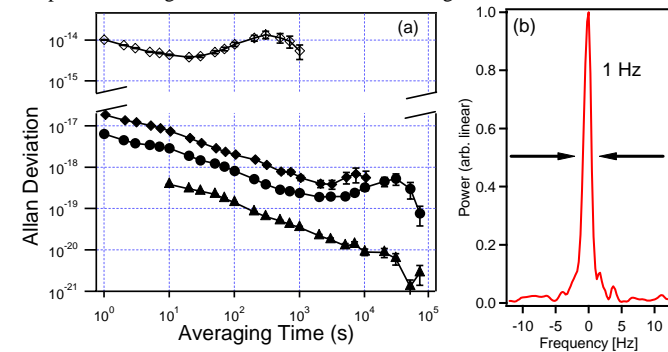


Figure 1. (a) Allan deviations for the various fiber links. Open circles at the top are typical of the passive instability of either the 7- or 32-km link. Closed diamonds are the measured out-of-loop instability of the 32-km system using a transceiver configuration. Closed circles show the 7-km transfer instability. Closed triangles are a measurement of the in-loop signal while being used to stabilize either the 7- or 32-km link, divided by a factor of 2 for a fair comparison against the one-way transfer instability shown by the other curves. (b) Remote ultrastable-cavity intercomparison. A 698-nm laser is effectively heterodyned against a 1126-nm laser via a 3.5-km urban fiber link and two femtosecond frequency combs to span the spectral gaps to the 1064-nm transfer laser, revealing a 1-Hz resolution-bandwidth-limited linewidth as measured at 1064 nm.

References

1. L.-S. Ma, P. Jungner, J. Ye, and J. L. Hall, *Opt. Lett.* **19**, 1777 (1994).

A MAGNESIUM OPTICAL CLOCK

J. FRIEBE, K. MOLDENHAUER, M. RIEDMANN, T.E. MEHLSTÄUBLER, A. VOSKREBENZEV, A. PAPE, E.M. RASEL AND W. ERTMER[†]

*Institut für Quantenoptik – Leibniz Universität Hannover, Welfengarten 1
Hannover, 30167, Germany*

G. GROSCHE, H. SCHNATZ, B. LIPPARDT

*Arbeitsgruppe 4.31, Physikalisch-Technische Bundesanstalt Braunschweig, Bundesallee
100, Braunschweig 38116, Germany*

We report on the progress towards an optical clock based on magnesium. The absolute frequency value of the intercombination transition $3^1S_0 \rightarrow 3^3P_1$ of ^{24}Mg was measured with a Ramsey-Bordé beam interferometer. The optical frequency of about 655 THz, generated with a pre-stabilized diode laser with sub-kHz linewidth, was compared with a primary Cs Frequency standard of the PTB via a fiber femtosecond laser. Suppression of first order Doppler effect has been achieved by applying beam reversal technique¹. With this method we reached an uncertainty of 1 part in 10^{11} which is dominated by residual Doppler effect in first and second order. In the past we have demonstrated² a spectroscopic resolution of 290 Hz with cold atoms leading to a short term stability of $8 \cdot 10^{-14}$ in one second. This stability is mainly limited by residual motion of the atoms at temperatures slightly above the Doppler cooling limit at 2 mK. In the case of bosonic Mg it is difficult to advance towards even lower temperatures in the microkelvin range. Standard sub-Doppler cooling schemes are not applicable because of the non-magnetic ground state. We investigate novel methods to lower the temperatures of magnesium atoms. One promising method is based on a coherent two photon-process which provides higher velocity selectivity. The method extends standard Doppler cooling based on the transition $3^1S_0 \rightarrow 3^1P_1$ by coupling the excited state with an additional laser to the 1D_2 level. This gives the possibility to modify the population in the intermediate state 3^1P_1 and thus the mechanical light force, which in our experiments is actually dominated by the photons of the strong cooling transition. The force profile in all three dimensions can

[†] Work supported by DLR 50 WM 0346, Germany.

be modified with one additional laser beam exciting the $^1P_1 \rightarrow ^1D_2$ transition. In a 1D molasses configuration temperatures as cold as 500 μK could be realized, which means a reduction of one order of magnitude. This makes the experimental implementation easy, especially in a 3D-MOT. There, temperatures of 1 mK were reached with an additional cooling time of only 1ms and a high transfer efficiency of more than 60%. The observed temperatures could be matched with theoretical predictions by assuming a higher diffusion due to imperfections of the UV laser beams. For eliminated technical heating we extrapolate temperatures of 200 μK and 600 μK in the 1D molasses and MOT configuration respectively. Our model, indicates that the lifetime of the upper state limits the achievable temperature which is restricted in the present case to about 50 μK .

References

1. A. Morinaga, F. Riehle, J. Ishikawa, J. Helmcke, "A Ca Optical Frequency Standard: Frequency Stabilization by Means of Nonlinear Ramsey Resonances", *Appl. Phys. B* **48**, 165 (1989)
2. J. Keupp et al., "A high-resolution Ramsey-Bordé spectrometer for optical clocks based on cold Mg atoms", *Eur. Phys. J D* **36**, 289 (2005)

Molecular BEC of Lithium-6 in a Low Power Crossed Dipole Trap

J. Fuchs, G. Veeravalli, P.J. Dyke, G. Duffy, C.J. Vale, P. Hannaford
and W.J. Rowlands

*ARC Centre of Excellence for Quantum-Atom Optics and Centre for Atom Optics and
Ultrafast Spectroscopy, Swinburne University of Technology,
Melbourne, Australia 3122
E-mail: jfuchs@swin.edu.au

Recent investigations by several groups¹⁻³ have demonstrated that it is possible to produce a highly stable molecular BEC of ${}^6\text{Li}_2$ molecules composed of fermionic atoms, which exhibit lifetimes of some tens of seconds, compared to typically 1 ms or less for quantum degenerate molecular gases obtained from bosonic atoms. We report the production of our first molecular Bose-Einstein condensates of lithium-6 dimers in a low power crossed optical dipole trap.

Initially, we load a magneto-optical trap (MOT) with typically 10^8 atoms from a slowed atomic beam. We then transfer up to 400000 atoms into an optical dipole trap with an almost equal spin mixture in the two lowest hyperfine states. The optical dipole trap is formed using light from a 25 W VersaDisk Yb:YAG laser at 1030 nm. It consists of a 15 W beam with a waist of about $30 \mu\text{m}$ crossed with a 13 W beam at about 80 degrees. To increase the number of condensed molecules the second beam has a waist of about $100 \mu\text{m}$.

Evaporative cooling is achieved by reducing the laser power near the broad Feshbach resonance at 834 G. By tuning to the low magnetic field side (770 G) of the Feshbach resonance molecules are formed through three-body recombination at sufficiently low temperatures. Further evaporation leads to the creation of a molecular BEC. After reducing the laser power by a factor of about 1000 in 3 s we have observed more than 10000 condensed molecules. During the evaporation the temperature decreases from about $100 \mu\text{K}$ to below 100 nK.

References

1. S. Jochim, M. Bartenstein, A. Altmeyer, G. Hendl, S. Riedl, C. Chin, J. Hecker Denschlag and R. Grimm, *Science* **302**, 2101 (2003).
2. M.W. Zwierlein, C.A. Stan, C.H. Schunck, S.M.F. Raupach, S. Gupta, Z. Hadzibabic and W. Ketterle, *Phys. Rev. Lett.* **91**, 250401 (2003).
3. T. Bourdel, L. Khaykovich, J. Cubizolles, J. Zhang, F. Chevy, M. Teichmann, L. Tarruell, S. Kokkelmans and C. Salomon, *Phys. Rev. Lett.* **93**, 050401 (2004).

MEASUREMENT OF LIFETIME OF THE $^2D_{5/2}$ STATE OF A SINGLE COLD $^{40}\text{Ca}^+$

KELIN GAO[†], HUA GUAN, BING GUO, QU LIU, AND XUEREN HUANG

State Key Laboratory of Magnetic Resonance and Atomic and Molecular Physics, Wuhan Institute of Physics and Mathematics, and Center for Cold Atom Physics, Chinese Academy of Sciences, Wuhan 430071, P. R. China

[†]*E-mail: klgao@wipm.ac.cn*

Trapped and cold $^{40}\text{Ca}^+$ ion is one of promising candidate of future optical frequency standards. In this paper we will give the lifetime measurement of the Ca in the small Paul trap in our laboratory recently.

A miniature Paul trap with a ring ($r_0=0.8\text{mm}$) and two endcaps ($2z_0=2\text{mm}$) electrodes with two compensation electrodes was developed for trapping single Ca ions [1].

The cooling laser at 397 nm and repumping laser at 866nm available for trapped Ca^+ ions are carried out with a commercial single-mode laser diode. The laser at 729nm for the clock transition $S_{1/2}-D_{5/2}$ is also a Titanium-Sapphire laser (Coherent MBR-110).

Single cold $^{40}\text{Ca}^+$ ion was loaded in a Paul trap directly and the probability of loading only single ion was above 50%. The signal-to-noise ratio (S/N) and the storage time of single ion have been improved by locking the cooling and repumping lasers to Fabry-Perot interferometers and Optogalvanic (OG) signals respectively[2], and by minimizing the micromotion. From the single ion fluorescence spectrum, the ion temperature was estimated to be about 5mK [3].

The lifetime of $^3D_{5/2}$ was measured by analyzing statistically the signal of a number of quantum jumps of single ion. The result we obtained accorded with others' results which have been published.

References

1. SHU Hua-Lin, GUAN Hua, HUANG Xue-Ren, LI Jiao-Mei, GAO Ke-Lin: *Chin. Phys. Lett.* **22**, 1641 (2005)
2. SHU HuaLin , GUO Bin , GUAN Hua, LIU Qu, HUANG XueRen , GAO KeLin: *Chin. Phys. Lett.* (2007)(in press)
3. H. Guan , B. Guo , G.L.Huang , H.L.Shu, X.R.Huang , and K.L.Gao: *Optics Communications* (2007) (in press)

ABSOLUTE OPTICAL FREQUENCY MEASUREMENTS IN ^{133}Cs AND THEIR IMPACT ON ATOM INTERFEROMETRY AND THE FINE STRUCTURE CONSTANT

V. GERGINOV, K. CALKINS, C.E. TANNER[†]

Department of Physics, University of Notre Dame, 225 Nieuwland Science Hall
Notre Dame, Indiana 46556-5670 USA

J.J. MCFERRAN

School of Physics, The University of Western Australia, 35 Stirling Highway
Nedlands, 6009, Australia

S. DIDDAMS, A. BARTELS, AND L. HOLLBERG

Time and Frequency Division, National Institute of Standards and Technology
325 Broadway M.C. 847
Boulder, Colorado 80305-5670, USA

High resolution laser spectroscopic measurements of the $6s\ ^2S_{1/2} \rightarrow 6p\ ^2P_{1/2}$ (D_1) and $6s\ ^2S_{1/2} \rightarrow 6p\ ^2P_{3/2}$ (D_2) transitions in neutral ^{133}Cs were performed in a highly collimated thermal atomic beam using a femtosecond laser frequency comb and narrow-linewidth CW diode lasers. The diode lasers were mixed with the output of a femtosecond laser frequency comb referenced to a stabilized hydrogen maser calibrated with a Cs fountain clock. The diode lasers probed optical transitions between pairs of ground state and excited state hyperfine levels. A photodiode was used to detect the excited state decay fluorescence. The first order Doppler shift was eliminated by orienting the laser beam in a direction perpendicular to the atomic beam with a precision of 5×10^{-6} radians. Optical frequencies for all possible pairs of hyperfine levels were measured independently, from which the line centroids and excited state hyperfine splittings were obtained for both the D_1 and D_2 transitions. For the D_2 transition differences between optical frequencies agreed with previously completed more precise measurements of the hyperfine splittings. For the D_1 line, a new value for the $6p\ ^2P_{1/2}$ state hyperfine splitting was also obtained. We used the D_1 results, in combination with the results of an atom interferometry experiment by Wicht et al. to calculate the fine-structure constant based on the atom recoil approach, $\alpha^{-1} = 137.0360000(11)$. Our optical frequency results in cesium represent significant improvements in both precision and accuracy when compared with previous measurements for these quantities. The absolute optical frequencies of the D_1 and D_2 lines of cesium and other alkalis play important roles in the interpretation of current and pending atom interferometry experiments in cesium.

[†] Work partially supported by grant PHY99-87984 of the US National Science Foundation.

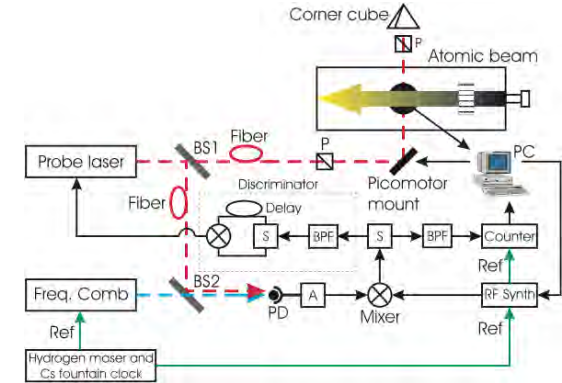


Figure 1. Experimental setup for optical frequency measurements.

Table 1. Summary of ^{133}Cs Results: optical frequencies, [1, 2] and hyperfine splittings [3].

$6s\ ^2S_{1/2} F_g \rightarrow 6p\ ^2P_{3/2} F_x D_2$	$6s\ ^2S_{1/2} F_g \rightarrow 6p\ ^2P_{1/2} F_x D_1$
$f_{43}=351\ 721\ 508\ 210.5(5.5)$ kHz	$f_{43}=335\ 111\ 370\ 129.1(3.4)$ kHz
$f_{44}=351\ 721\ 709\ 496.9(5.5)$ kHz	$f_{44}=335\ 112\ 537\ 852.7(3.3)$ kHz
$f_{45}=351\ 721\ 960\ 585.7(5.5)$ kHz	$f_{45}=335\ 120\ 562\ 760.8(3.4)$ kHz
$f_{32}=351\ 730\ 549\ 621.5(5.5)$ kHz	$f_{33}=351\ 730\ 700\ 845.9(5.5)$ kHz
$f_{33}=351\ 730\ 700\ 845.9(5.5)$ kHz	$f_{34}=335\ 121\ 730\ 484.4(3.3)$ kHz
$f_{34}=351\ 730\ 902\ 133.2(5.6)$ kHz	
$f_{D_2}=351\ 725\ 718\ 474.4(5.1)$ kHz	$f_{D_1}=335\ 116\ 048\ 748.1(2.4)$ kHz
$\Delta f_{23}=151\ 224.7(1.6)$ kHz	
$\Delta f_{34}=201\ 287.1(1.1)$ kHz	$\Delta f_{34}=1\ 167\ 723.6(4.8)$ kHz
$\Delta f_{45}=251\ 091.6(2.0)$ kHz	

We obtained the fine structure constant from $\alpha^2 = R_\infty c \frac{m_p}{m_e} \frac{m_{\text{Cs}}}{m_p} \frac{f_{\text{ref}}}{(f_{33}+f_{43})^2}$ using $\frac{f_{\text{ref}}}{2} = 15\ 006.276\ 88(23)$ Hz from reference [4] other references cited in [2].

References

1. V. Gerginov, C. E. Tanner, S. Diddams, A. Bartels, L. Hollberg, Phys. Rev. A **70**, 042505 (2004).
2. V. Gerginov, K. Calkins, C. E. Tanner, J. J. McFerran, S. Diddams, A. Bartels, L. Hollberg, Phys. Rev. A **73**, 032504 (2006).
3. V. Gerginov, A. Derevianko, C. E. Tanner, Phys. Rev. Lett. **19**, 072501 (2003).
4. A. Wicht, J. M. Hensley, E. Sarajlic, S. Chu, Phys. Scr. T **102**, 82 (2002).

**LASER PROBING MEASUREMENTS AND
CALCULATIONS OF LIFETIMES OF THE $5d\ ^2D_{3/2}$ AND
 $5d\ ^2D_{5/2}$ METASTABLE LEVELS IN Ba II**

J. GURELL¹, E. BIÉMONT^{2,3}, K. BLAGOEV⁴, V. FIVET², P. LUNDIN¹,
S. MANNÉRIK¹, L.-O. NORLIN⁵, P. QUINET^{2,3}, D. ROSTOHAR³, P. ROYEN¹
and P. SCHEF¹

¹*Department of Physics, Stockholm University, AlbaNova University Center,
SE-10691 Stockholm, Sweden*

²*Service d'Astrophysique et de Spectroscopie Université de Mons-Hainaut, 20 Place du
Parc B-7000 Mons, Belgium*

³*Institut de Physique Nucléaire, Atomique et de Spectroscopie (IPNAS) Université de
Liège, Sart Tilman, Bât. B15 B-4000 Liège, Belgium*

⁴*Institute of Solid State Physics, Bulgarian Acad. of Sciences, 72 Tzarigradsko
Chaussee, BG-1784 Sofia, Bulgaria*

⁵*Department of Physics, Royal Institute of Technology, AlbaNova University Center,
SE-10691 Stockholm, Sweden*

The lifetimes of the metastable $5d\ ^2D_{3/2}$ and $5d\ ^2D_{5/2}$ levels in Ba II have been measured with a Laser Probing Technique (LPT)^{1,2} at the ion storage ring facility CRYRING³ located in the Manne Siegbahn Laboratory in Stockholm, Sweden. The lifetime of the $5d\ ^2D_{3/2}$ level proved to be the longest lifetime ever measured with this technique utilizing fast ion beams, $\tau = 89.4 \pm 15.6$ s, and to the best of our knowledge it constitutes the longest lifetime ever measured in a storage ring. Also the $5d\ ^2D_{5/2}$ level has a lifetime of the order of tens of seconds which was determined to be $\tau = 32.0 \pm 4.6$ s. These new measurements are also supported by our new pseudo-relativistic Hartree-Fock calculations⁴ resulting in $\tau = 82.0$ s and $\tau = 31.6$ s respectively.

These lifetimes have been measured previously by several groups but the experimental lifetimes resulting from the different studies are inconsistent. For the $5d\ ^2D_{3/2}$ level, the measurements of Schneider and Werth⁵ and of Yu et al.⁶ differ by a factor of four and, for the $5d\ ^2D_{5/2}$ level, the results of Plumelle et al.⁷ are larger than those of Nagourney et al.⁸ and of Madej et al.⁹ by about 50%. One possible reason for the existing discrepancies might be the difficulty to monitor and measure both the col-

lisional excitation of the ions and the collisional quenching. A method for correcting for both these effects have been developed and used in previous LPT measurements^{10,11} up to lifetimes of 28 s in Ti II.¹² The value of the $5d\ ^2D_{3/2}$ lifetime presented in this study shows good agreement with both the experimental result of Yu et al.⁶ and also with several calculated values.¹³⁻¹⁵ The measured lifetime of the $5d\ ^2D_{5/2}$ level is also in agreement with several previous measurements⁷⁻⁹ and calculations.^{7,8,13-15}

References

1. Lidberg J., Al-Khalili A., Norlin L.-O., Royen P., Tordoir X., Mannérik S., Nucl. Instrum. Methods B **152**, 157 (1999).
2. Mannérik S., Phys. Scr. **T105**, 67-75 (2003).
3. Manne Siegbahn Laboratory homepage at <http://www.msi.se>.
4. Cowan R.D., *The Theory of Atomic Structure and Spectra*, (Univ. California Press, Berkeley, 1981).
5. Schneider R., Werth G., Z. Phys. A **293**, 103 (1979).
6. Yu N., Nagourney W., Dehmelt H., Phys. Rev. Lett. **78**, 4898 (1997).
7. Plumelle F., Desaintfusien M., Duchene J.L., Audoin C., Opt. Commun. **34**, 71 (1980).
8. Nagourney W., Sandberg J., Dehmelt H., Phys. Rev. Lett. **56**, 2797 (1986).
9. Madej A.A., Sankey J.D., Phys. Rev. A **41**, 2621 (1990).
10. Mannérik S., Lidberg J., Norlin L.-O., Royen P., Phys. Rev. A **56** R1075 (1997).
11. Mannérik S., Ellmann A., Lundin P., Norlin L.-O., Rostohar D., Royen P., Schef P., Phys. Scr. **T119**, 49-54 (2005).
12. Hartman H., Rostohar D., Derkatch A., Lundin P., Schef P., Johansson S., Lundberg H., Mannérik S., Norlin L.-O., Royen P., J. Phys. B **36** L197 (2003).
13. Dzuba V.A., Flambaum V.V., Ginges J.S.M., Phys. Rev. A **63**, 062101 (2001).
14. Gopakumar G., Merlitz H., Chaudhuri R.K., Das B.P., Mahapatra U.S., Mukherjee D., Phys. Rev. A **66**, 032505 (2002).
15. Guet C., Johnson W.R., Phys. Rev. A **44**, 1531 (1991).

Coupled motion in a three dimensional Brownian motor, realized in optical lattices

H. HAGMAN, P. SJÖLUND, C. M. DION, S. J. PETRA, S. JONSELL AND A.

KASTBERG

*Umeå University,
Department of Physics,
90187 Umeå,
Sweden*

Brownian motors (BM) are small devices who convert random fluctuations into directed motion. The general requirements for a BM to work is that the system is spatially or temporally asymmetric and brought out of thermal equilibrium.

Our BM are based on cold atoms in a double optical lattice. The symmetry originates from a combination of a relative spatial phase (RSP) between the lattices and unequal transfer rates between them. This gives our BM an inherent possibility to induce drifts in an arbitrary direction in three dimensions. This is in contrast with many other BMs, which are typically controllable only in one direction.

Since the potentials are coupled in all three dimension is the multi dimensional RSP dependency non-trivial. This dependency has therefore been measured, see figure 1a, and a full control of our BM is gained. To qualitatively understand our BM, we have performed semi-classical simulation. Even though the main features of BM are reproduced does the pattern of the induced drifts minima differ, see figure 1b. This calls for a full quantum model to explain our BM. Such a model is under construction.

The induced drift dependency on the inequality in the transfer rates, the diffusion and the potential height, also has been carefully investigated. Induced drifts in arbitrary directions with controllable speeds up to a few mm/s has been evident.^{1,2}

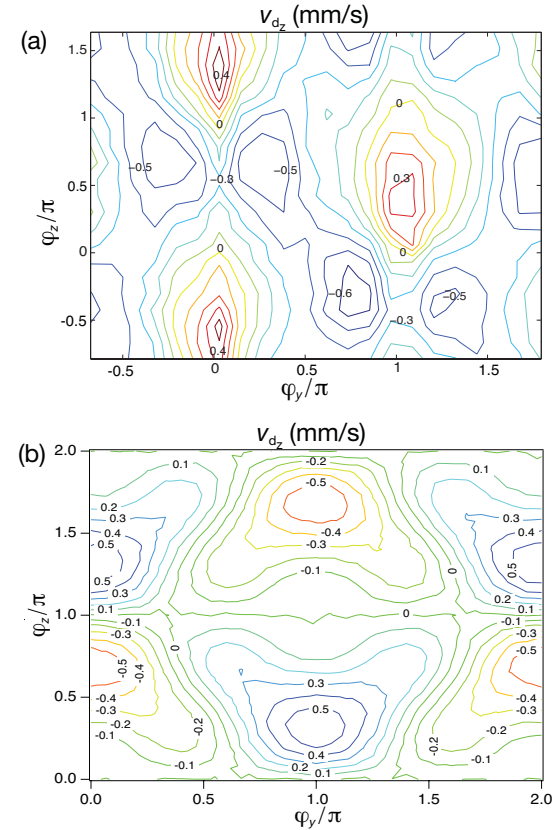


Fig. 1. False color contour plots of the induced drift along the vertical z axes as a function of the relative spatial phase in z and y from (a) measurements, and (b) simulations.

References

1. P. Sjölund, S. J. Petra, C. M. Dion, S. Jonsell, M. Nylén, L. Sanchez-Palencia and A. Kastberg, *Phys. Rev. Lett.* **96**, p. 190602 (2006).
2. P. Sjölund, S. J. H. Petra, C. M. Dion, S. Jonsell, H. Hagman and A. Kastberg (accepted for publication in *Euro. Phys. J. D*).

**THE FERRUM-PROJECT: EXPERIMENTAL AND
THEORETICAL TRANSITION RATES OF FORBIDDEN
[ScII] LINES AND RADIATIVE LIFETIMES OF
METASTABLE ScII LEVELS**

H. HARTMAN¹, J. GURELL², P. LUNDIN², P. SCHEF², A. HIBBERT³,
H. LUNDBERG⁴, S. MANNERVIK², L-O. NORLIN⁵ and P. ROYEN²

¹*Lund Observatory, Lund University, Box 43, SE-221 00 Lund, Sweden*

²*Department of Physics, Stockholm University, AlbaNova University Center,
SE-106 91, Stockholm, Sweden*

³*Department of Applied Mathematics and Theoretical Physics, The Queens University
of Belfast, Belfast BT7 1NN, Northern Ireland*

⁴*Department of Physics, Lund Institute of Technology, Box 118, SE-221 00, Lund,
Sweden*

⁵*Physics Department, Royal Institute of Technology, AlbaNova University Center,
SE-106 91, Stockholm, Sweden*

In many plasmas, long lived metastable levels are primarily depopulated by collisions. In low-density regions, however, radiative decays through forbidden transition channels will be more important and can be observed. If the atomic transition data is known, these lines are indicators of physical plasma conditions and can be used for abundance determination.¹ Transition probabilities can be derived by combining relative intensities between the decay channels, so called branching fractions (BFs), and the radiative lifetime of the common upper level.² We use this approach for forbidden [ScII] lines along with new calculations.

Neither BFs for forbidden lines nor lifetimes for metastable levels are easily measured in the laboratory. Therefore, astrophysical BFs measured in Space Telescope Imaging (STIS) spectra of the strontium filament of Eta Carinae are combined with lifetime measurements using a laser probing technique^{3,4} on a stored ion beam at the CRYRING⁵ facility in Stockholm, Sweden. These lifetimes are used to derive the absolute transition probabilities (A-values). New theoretical transition probabilities and lifetimes are calculated using the CIV3 code.

We report experimental lifetimes for the ScII levels $3d^2 \ ^3P_{0,1,2}$ with

lifetimes 1.28, 1.42 and 1.15 s respectively and transition probabilities for lines from these levels down to the ground state $3d4s \ a^3D$. New calculations for these forbidden [ScII] lines and metastable lifetimes are also presented.

References

1. Johansson S. et al., Physica Scripta, **T100**, 71 (2002).
2. Hartman H., Johansson S., Lundberg H., Lundin P., Mannervik S. and Schef P., Physica Scripta, **T119**, 40 (2005).
3. Mannervik S., Phys. Scr. **T105**, 67-75 (2003).
4. Mannervik S., Ellmann A., Lundin P., Norlin L.-O., Rostohar D., Royen P., Schef P., Phys. Scr. **T119**, 49-54 (2005).
5. Manne Siegbahn Laboratory homepage at <http://www.msi.se>.

DELTA-KICKED ROTOR EXPERIMENTS WITH AN ALL-OPTICAL BEC

F. HAUPERT AND M.D. HOOGERLAND*

Department of Physics, University of Auckland,
Auckland, New Zealand

*E-mail: m.hoogerland@auckland.ac.nz
www.phy.auckland.ac.nz/staff/mdh

We report the construction of an all-optical BEC, and initial experiments demonstrating some features of the δ -kicked rotor.

Keywords: Delta-kicked rotor, All-Optical BEC

1. The All-Optical BEC

We create an all optical Bose-Einstein Condensate (BEC) using a method similar to the one used by Barrett *et al.*¹ A crossed pair of CO₂ laser beams, with waist diameters of 80 μm ($1/e^2$) forms a dipole trap, which is overlapped with a magneto-optical trap for rubidium-87 atoms in an ultra high-vacuum environment. Both laser beams are derived from a single 25 W CO₂ laser, but are orthogonally polarised. The power in both beams is controlled by an AOM, and is 10 W per beam initially. By gradually reducing the laser power, we force evaporative cooling of the atoms down to the BEC transition. At this point, we have about 10^5 atoms at a temperature of 60 nK. The temperature is hence much smaller than the recoil energy for rubidium, which is 180 nK.

2. δ -kicked rotor

The atoms are then periodically subjected to a potential which varies as the cosine of the position.

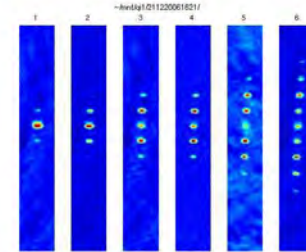
$$V = \kappa \cos 2kx \sum_n f(t - nT)$$

with κ the kick strength, and T the kick period. The potential is achieved by using a standing laser field, which is detuned by ~ 2 GHz from the D_2

transition, at a wavelength of $\lambda = 2\pi/k = 780$ nm. For an ideal correspondence to the classical δ -kicked rotor, the function $f(t)$ is a δ -function. In this experiment, $f(t)$ is a square profile laser pulse with a duration much less than the period. This system forms a quantum-mechanical equivalent of the classical kicked rotor.

It is well-known that the classical kicked rotor, for sufficient kick strength, is a chaotic system. Hence, the variance of the velocity distribution (the energy) should grow quadratically with the number of kicks. In the quantum-mechanical equivalent, quantum coherences inhibit the energy growth after a certain number of kicks.²

However, at a particular kick period, known as the *quantum resonance*, a manifestation of the Talbot effect can be observed. The first kick effectively acts as a diffraction grating for the atomic wave, and will split it into a number of momentum component states. If the phase accumulated by these momentum components during the time the laser is off exactly equals 4π , the wave function is identical to the wave function just after the laser pulse, and the second laser pulse will add coherently to the first, leading again to quadratic energy growth with the number of kicks. In the figure, we show the atomic momentum distribution after 1–6 kicks, at a kick period equal to this quantum resonance. The momentum difference between two adjacent clouds is $2\hbar k$. At the conference, we will present more detailed measurements for different kick periods and kick strengths.



References

1. M. D. Barrett, J. A. Sauer, M. S. Chapman, Physical Review Letters 87 (1) (2001) 010401–010404.
2. S. Fishman, *Quantum Chaos, Proceedings of the International School of Physics “Enrico Fermi”, Varenna, 1991*, G. Casati, I. Guarneri, and U. Smilansky eds, North-Holland, New York, (1993).

Rydberg Excitation of a Bose-Einstein Condensate, Collective and Coherent Dynamics

R. Heidemann*, U. Raitzsch, V. Bendkowsky, B. Butscher, R. Löw and T. Pfau

5. Physikalisches Institut, University of Stuttgart, Germany

*E-mail: r.heidemann@physik.uni-stuttgart.de

www.pi5.uni-stuttgart.de

We present our experimental results on Rydberg excitation of magnetically trapped Rubidium atoms. In a thermal cloud of a few microKelvin we observe coherent, collective and strongly blocked excitation induced by the van der Waals interaction among the Rydberg atoms. The reversibility of the excitation dynamics was measured with an echo type technique for various densities of ground state atoms and excitation times. With this experiments we prove the coherence of the excitation and gain insight into the dephasing due to interactions. We further observed a signature of the phase transition to a Bose-Einstein condensate in the fraction of excited Rydberg atoms when cooling the thermal cloud below T_c .

The van der Waals interaction energy of two Rydberg atoms separated by 10 micrometres can be in the range of MHz which leads to a blockade of the photo-excitation-process when the interaction energy is larger than the linewidth of the excitation process. This defines the radius of a blockade sphere within which only one excitation is created.

In our experiments using the high density of ground state atoms in a magnetic trap, several thousand atoms are located within one blockade sphere. As the excitation can be located at any of the N available atoms the state is described by the collective state:

$$|\psi_e\rangle = \frac{1}{\sqrt{N}} \sum_{i=1}^N |g_1, g_2, g_3, \dots, e_i, \dots, g_N\rangle, \quad (1)$$

where g_k indicates an atom numbered k in the ground state and e_i atom i in the excited state. Therefore in this strong blockade regime the ensemble is excited collectively and oscillates with the collective Rabi frequency $\sqrt{N}\Omega_0$ between the ground state and the collective excited state $|\psi_e\rangle$. Our sample consists of many blockade spheres which have due to the inhomogeneous

density different collective Rabi frequencies. Therefore the Rabi-oscillations get out of phase and are not detectable in the total Rydberg atom number. Still the time scale of this integrated excitation scales with the square root of the density and linear with the Rabi frequency. We have observed the collective coherent behaviour of the excitation in a thermal cloud with this scaling of the excitation rate with the collective Rabi-frequency $\sqrt{N}\Omega_0$.¹

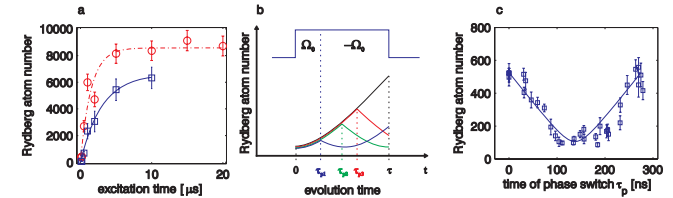


Fig. 1. **a** Rydberg population as a function of excitation time for two different densities of ground state atoms. The Rydberg atom number saturates due to van der Waals blockade. **b** Schematic of the pulse sequence. At a variable time τ_p during an excitation pulse of constant duration τ , the phase of the driving field for Rydberg-excitation is switched by π , equivalently to inverting Ω_0 to $-\Omega_0$. The coloured curves show the excitation dynamics for the whole sample during the pulse sequence for some values of τ_p . **c** Rydberg atom number as a function of τ_p . The reversal of the excitation reduces the population by 80% at the point where τ_p equals half of the excitation time $\tau = 275$ ns. This proves the coherent nature. The solid line is a hyperbolic fit as a guide to the eye.

By inverting the phase of the excitation light, we coherently reversed the excitation process (see Fig. 1) and proved the coherent dynamics. We observed a density dependent decrease in the efficiency of reversal, which we attribute to a dephasing due to the irreversibility of the van der Waals interaction.²

We further observed a signature of the phase transition to a Bose-Einstein condensate in the fraction of excited Rydberg atoms when cooling the thermal cloud below T_c . In a next step we plan to use the phase coherence of a Bose-Einstein condensate in interferometric experiments to investigate the expected strong correlations.

References

1. R. Heidemann, U. Raitzsch, V. Bendkowsky, B. Butscher, R. Löw and T. Pfau, *quant-ph/0701120* (2007).
2. U. Raitzsch, V. Bendkowsky, B. Butscher, R. Löw, R. Heidemann and T. Pfau, *in preparation* (2007).

COHERENT MANIPULATION OF ATOMS

M. D. HIMSWORTH*, J. E. BATEMAN, S. PATEL, R. MURRAY and T. G. M. FREEGARDE

*School of Physics and Astronomy, University of Southampton,
Southampton, SO17 1UN, UK*

**E-mail: mdh@phys.soton.ac.uk
www.phys.soton.ac.uk*

We present an experiment to coherently manipulate the centre of mass momentum of an atomic cloud to implement a variety of as yet untested cooling schemes (including amplified Doppler cooling¹ and Interferometric cooling²), as well as atom interferometry experiments, using apparatus which is computer programmable and hence allows for implementation of as yet unconsidered experiments.

The technique of Amplified Doppler cooling enhances traditional Doppler cooling by using coherent manipulation to impart additional momentum before sponatenous emission can occur. The technique will allow the compact deceleration of beams with reduced transverse heating. Theoretical predictions suggest it should be possible to reduce the temperature by approximately a factor of two for each spontaneous emission event, providing an exponential speed up compared to traditional Doppler cooling.

In Interferometric cooling, an ensemble of atoms placed in a superposition will evolve in phase due to their momentum, including the center of mass term. By recombining the two 'arms' of the interferometer at a time later, the atom will either be in an excited or ground state. The absorption (or stimulated emission) of a photon will cause the atom to recoil away (towards) the photon's wavevector direction. This leads to a velocity dependant force.

Both of these schemes reduce the reliance of the cooling mechanism on a closed transition: the former by increasing the momentum imparted for each spontaneous emission event, a large number of which will empty the cooling transition, and the latter by allowing the possibility of operating across a manifold of levels using broadband techniques such as Adiabatic Rapid

Passage. The reduced reliance on a closed transition means these schemes can, in principle, be applied to the direct optical cooling of molecules.

The apparatus consists of a Magneto-Optical Trap for Rubidium-85, the trapping and repump beams of which can be extinguished in ~ 100 ns using AOMs, and a 1W diode laser, detuned from resonance by \sim GHz, with a chain of acousto- and electro- optical components to produce counter propagating Raman beams with intensity and detuning which can be arbitrarily scuplted with sub-microsecond resolution.

References

1. T. Freegarde, G. Daniell and D. Segal, *Phys. Rev. A* **73**, 033409 (2006).
2. M. Weitz and T. Hänsch, *Europhys. Lett.* **49**, 302 (2000).

DECELERATION AND TRAPPING OF NEUTRAL POLAR MOLECULES

STEVEN HOEKSTRA AND GERARD MEIJER

Molecular Physics Department, Fritz-Haber-Institut der Max-Planck-Gesellschaft, Faradayweg 4-6, 14195 Berlin, Germany

We have been exploring and exploiting the possibility of slowing down and trapping neutral molecules by the use of time-varying inhomogeneous electric fields. The decelerated beams of molecules have been loaded into a variety of traps. In these traps, electric fields are used to keep the molecules confined in a region of space where they can be studied in complete isolation from the (hot) environment. Recent experiments include the far-infrared optical pumping of these polar molecules due to blackbody radiation and the demonstration of a molecular synchrotron.

Getting full control over both the internal and external degrees of freedom of molecules has been an important goal in molecular physics during the last decades. Arrays of time-varying, inhomogeneous electric fields are used to reduce in a stepwise fashion the forward velocity of molecules in a beam. With this so-called 'Stark decelerator', the equivalent of a LINear ACcelerator (LINAC) for charged particles, one can transfer the high phase-space density that is present in the moving frame of a pulsed molecular beam to a reference frame at any desired velocity; molecular beams with a computer-controlled velocity and with a narrow velocity distribution, corresponding to sub-mK longitudinal temperatures, can be produced [1]. These decelerated beams offer new possibilities for collision studies [2], for instance, and enable spectroscopic studies with an improved spectral resolution; first proof-of-principle studies have been performed. These decelerated beams have also been used to load ND_3 molecules and OH radicals in an electrostatic trap at a density of 10^7 mol/cm^3 and at temperatures around 50 mK [3]. Trapping of vibrationally excited OH ($v=1$) radicals has enabled a direct measurement of the infrared radiative lifetime [4], and optical pumping of neutral molecules due to blackbody radiation has been investigated [5]. Ground-state molecules have been trapped in a novel AC electric field trap, decelerated molecular beams have been injected in a prototype molecular synchrotron [6], and, using micro-structured electrode arrays, a switchable mirror for neutral molecules has been constructed and tested.

1

2

In figure 1 the operation of the Stark decelerator is illustrated by the deceleration and trapping of OD radicals. OD radicals are created by photodissociation of supersonically expanded deuterated nitric acid, and subsequently decelerated in a Stark decelerator. The slowed molecules are trapped in an electrostatic trap, and the population in the different rotational states is probed by laser-induced fluorescence detection. In the inset the arrival of undecelerated OD molecules followed by the steady signal of the trap-loaded OD molecules is shown, up to 20 ms after production of the molecules. We have detected the trapped molecules up to 15 s.

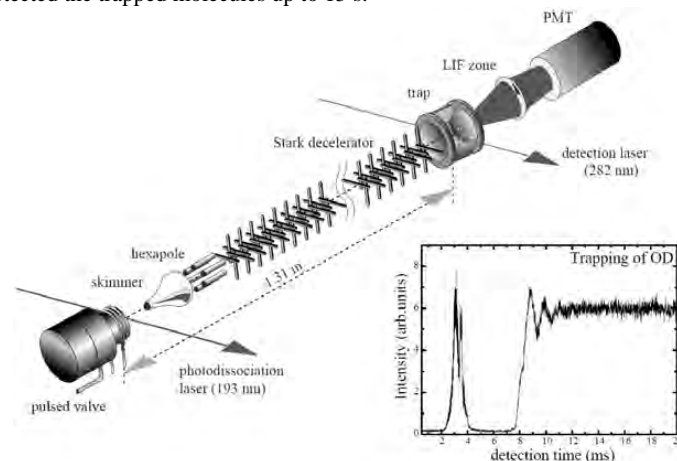


Figure 1: Electrostatic deceleration and trapping of OD radicals

References

1. H.L. Bethlem, G. Berden, and G. Meijer, *Phys. Rev. Lett.* 83, 1558 (1999)
2. J.J. Gilijamse, S. Hoekstra, S.Y.T. van de Meerakker, G.C. Groenenboom, and G. Meijer, *Science* 313, 1617 (2006)
3. H. L. Bethlem, G. Berden, F.M.H. Crompvoets, R.T. Jongma, A.J.A. van Roij and G. Meijer, *Nature* 406, 491 (2000)
4. S.Y.T. van de Meerakker, N. Vanhaecke, M.P.J. van der Loo, G.C. Groenenboom, and G. Meijer, *Phys. Rev. Lett.* 95, 013003 (2005)
5. S. Hoekstra, J.J. Gilijamse, B. Sartakov, N. Vanhaecke, L. Scharfenberg, S.Y.T. van de Meerakker, and G. Meijer, *Phys. Rev. Lett.* 98, 133001 (2007)
6. C.E. Heiner, D. Carty, G. Meijer, and H.L. Bethlem, *Nature Physics* 3, 115 (2007)

**COOLING, COHERENT MANIPULATIONS AND
DECOHERENCE OF TWO-SPECIES TRAPPED-ION
ARRAYS FOR QUANTUM INFORMATION PROCESSING.**

J. P. Home, J. D. Jost, J. Amini, J. J. Bollinger, R. B. Blakestad, J. Britton, R. J. Epstein, W. M. Itano, E. Knill, D. Leibfried, C. Ospelkaus, S. Seidelin, N. Shiga, J. H. Wesenberg and D. J. Wineland.

*Time and Frequency Division, National Institute of Standards and Technology
Boulder, CO, U.S.A.*

*E-mail: jhome@boulder.nist.gov
<http://tf.nist.gov/ion/index.htm>

R. Ozeri

*Weizmann Institute of Science
Rehovot, 76100, Israel*

C. Langer

*Lockheed Martin
Palmdale, CA, U.S.A.*

We present results from experiments towards development of a scalable ion trap quantum information processor. The realization of such a scalable processor depends on the ability to implement fault-tolerant techniques. These require the ability to move information around the processor while retaining the ability to perform high fidelity quantum gates. For trapped ions, one approach is to move the ions themselves through an array of microtraps^{1,2} One challenge in this scheme is that the ions' motion may be heated by the transport processes. In addition, fluctuations of the electric field at the position of the ions leads to ambient heating. Since the fidelity of two qubit trapped ion gates are sensitive to the ions' temperature, it is necessary to cool the motion of the qubit ions prior to gates, while preserving the stored quantum information. In our experiments, we perform sympathetic cooling by adding coolant $^{24}\text{Mg}^+$ ions to the $^9\text{Be}^+$ qubits. We report recent work involving ground state sympathetic cooling and coherent manipulations with two-species arrays of multiple ions.

In addition, we have experimentally and theoretically investigated the gate error due to spontaneous photon scattering, which represents a fundamental limit to the fidelity of logic gate operations implemented using Raman transitions. We find that in the limit where the detuning of the Raman laser from the excited states is larger than their fine structure splitting, spin-relaxation due to spontaneous Raman scattering is dramatically reduced relative to Rayleigh scattering due to an interference effect between scattering paths.³ In this regime, the limiting factor for two-qubit gate fidelity becomes decoherence of the motional state due to Rayleigh scattering. We show that with high laser power, for realistic trap frequencies of ~ 10 MHz the error rate from this source can in theory be reduced to below 10^{-4} per gate, which is below current threshold estimates for fault-tolerant quantum computation.^{4,5}

Finally we have devised a new method to measure heating rates of trapped ions by observing the fluorescence during Doppler re-cooling. This method offers two advantages over traditional Raman thermometry.⁶ It requires less complex laser systems and does not require the ions to be in the Lamb-Dicke regime. Both the Doppler re-cooling and Raman thermometry methods have been compared in studies of heating rates for a range of microfabricated traps.

1. Acknowledgements

Work supported by DTO. J.H. acknowledges funding from the Lindemann Fellowship.

References

1. D. J. Wineland, C. Monroe, W. M. Itano, D. Leibfried, B. E. King and D. M. Meekhof, *J. Res. Natl. Inst. Stand. Technol.* **103**, 259 (1998).
2. D. Kielpinski, C. Monroe and D. Wineland, *Nature* **417**, 709 (2002).
3. R. Ozeri, C. Langer, J. D. Jost, B. L. DeMarco, A. Ben-kish, B. R. Blakestad, J. Britton, J. Chiaverini, W. M. Itano, D. Hume, D. Leibfried, T. Rosenband, P. Schmidt and D. J. Wineland, *Phys. Rev. Lett.* **95**, p. 030403 (2005).
4. E. Knill, R. Laflamme and W. H. Zurek, *Science* **279**, 342 (1998).
5. A. M. Steane, *Phys. Rev. A* **68**, p. 042322 (2003).
6. F. Diedrich, J. C. Bergquist, W. M. Itano and D. J. Wineland, **62**, 403 (1989).

Spin Dynamics in an Antiferromagnetic Spin-1 Condensate

S. Jung*, L. D. Turner and P. D. Lett

National Institute of Standards and Technology, MS 8424,
Gaithersburg, Maryland 20899, USA

*E-mail: sebastian.jung@nist.gov

We observe coherent spin dynamics and measure ground state populations in an antiferromagnetic spin-1 Bose-Einstein condensate. At a critical value of the quadratic Zeeman shift, the oscillations display a resonance in oscillation period.

Keywords: spin dynamics; spin-1; sodium.

The coherent nature of atomic collisions in degenerate quantum gases has been demonstrated in an array of recent experiments. Coherent collisions in spinor condensates are of particular interest because of the rich dynamics that become possible when internal degrees of freedom are included. We present the first experimental study of coherent spin dynamics in a Bose-Einstein condensate of antiferromagnetic, spin-1 sodium atoms. The antiferromagnetic $F = 1$ case is distinct from the ferromagnetic one both in the structure of the ground-state magnetic phase diagram and in the spinor dynamics. Both cases can exhibit a regime of slow, anharmonic spin oscillations; however, this behavior is predicted over a wide range of initial conditions only in the antiferromagnetic case.¹

We produce a Bose-Einstein condensate of 10^5 ^{23}Na atoms in the $F = 1$ state in a crossed dipole trap. The condensate is initially fully polarized, with all atoms in the $m_F = 1$ Zeeman sublevel. We apply a magnetic field in order to vary the quadratic Zeeman shift, whose competition with the spin-mixing rate determines the spin dynamics. By applying an RF field resonant with the linear Zeeman shift to drive magnetic dipole transitions, we change the spin state of the sample. We then observe spin dynamics by measuring magnetic sublevel populations at different times using Stern-Gerlach separation of components and absorption imaging.

We initiate spin dynamics by suddenly driving the atomic spin state away from equilibrium using the RF field. Following this sudden state

change, we observe oscillations in the magnetic sublevel populations. We then measure the amplitude and period of oscillation over a range of different magnetic fields.

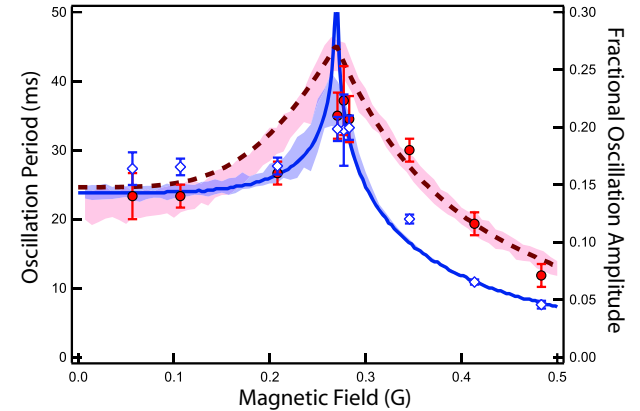


Fig. 1. Period (diamonds) and amplitude (circles) of spin oscillations as a function of applied magnetic field following a sudden change in spin state. The solid and dashed lines are theoretical predictions of the period and amplitude, respectively. The shaded regions indicate one standard deviation above and below the mean result expected when the fluctuations in magnetic field and density are modeled.

In Figure 1, we plot experimental results and theoretical predictions of the period and amplitude of oscillation as a function of magnetic field. We observe a peak in period and amplitude near to the theoretically predicted value of the critical magnetic field. As shown in the figure, the oscillation period at low magnetic field is insensitive to magnetic field fluctuations. The period depends sensitively only upon the value of the spin interaction coefficient c_2 and the density. The coefficient c_2 is proportional to the difference in scattering lengths $a_2 - a_0$, where a_2 (a_0) is the scattering length for collision processes with total coupled spin $F = 2$ ($F = 0$). We determine a value of $a_2 - a_0 = (5.34 \pm .58)a_B$. It constitutes the most precise measurement to date of this quantity in sodium.

References

1. W. Zhang, D.L. Zhou, M.-S. Chang, M.S. Chapman and L. You, J. Phys. Rev. A **72**, 013602 (2005).

MOLECULAR CLOCKS WITH ULTRA-COLD MOLECULES

MASATOSHI KAJITA

National Institute of Information and Communications Technologys
Koganei, Tokyo 184-8795, JAPAN

A molecular clock using magnetically trapped ^{24}MgH molecules is proposed. The inelastic collision rate was estimated to be 3-4 orders smaller than elastic collision rate, therefore evaporative cooling is easy. There is no Zeeman shift with $|\nu=0, N=0, F=1, M=1\rangle \rightarrow |\nu=2, N=0, F=1, M=1\rangle$ transition frequency, because the Zeeman coefficient does not depend on the vibrational state. The uncertainty of clock transition can potentially be reduced to 10^{-17} . This molecular clock is useful to measure the variation of the electron to proton mass ratio.

1. Introduction

Possible variations in nature's fundamental constants are currently a very popular topic of research. The precise measurement of the molecular vibrational rotational transition frequency is useful to measure the variance in electron to proton mass ration.

This paper discusses the feasibility of a molecular clock based on the ^{24}MgH $|\nu=0, N=0, F=1, M=1\rangle \rightarrow |\nu=2, N=0, F=1, M=1\rangle$ transition frequency (83 THz). Here ν , N , and F are the quantum numbers of the vibrational state, rotational state, and hyperfine state, respectively. M denotes the trajectory of F parallel to the magnetic field. ^{24}MgH molecules are trapped by magnetic field after precooling using buffer gas¹. The molecular temperature is reduced by evaporative cooling. As shown below, Zeeman shift does not exist with this transition. The two photon absorption spectrum using two counter-propagating laser lights is free from the Doppler broadening.

2. Elastic and inelastic collision between trapped ^{24}MgH molecules

Evaporative cooling is possible only when the collision loss rate is much less than the elastic collision rate. Collision loss is caused by the inelastic collision that changes the electron spin direction. Elastic and inelastic collision cross sections were estimated using a simplified method shown in Reference 2. Elastic collision is mainly caused by the electric dipole-induced dipole interaction and inelastic collision is mainly caused by the magnetic dipole-dipole interaction.

1

2

Figure 1 plots the elastic and inelastic collision cross sections between ^{24}MgH molecules in the $|\nu=0, F=1, M=1\rangle$ state as a function of the collision kinetic energy, taking the magnetic field 100 G. The inelastic collision rate is more than three orders smaller than the elastic collision rate. Therefore, evaporative cooling seems easy for magnetically trapped ^{24}MgH molecule.

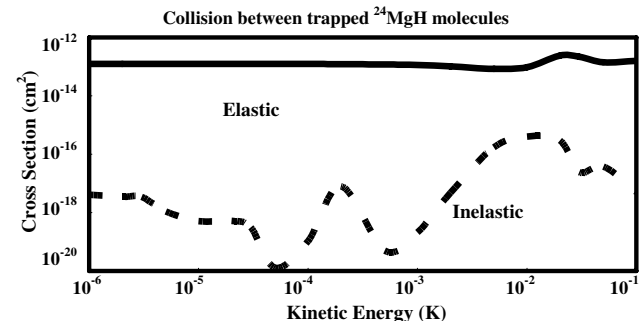


Fig.1: Elastic and inelastic collision cross sections as a function of the collisional kinetic energy.

3. Shift of the clock transition frequency

The Zeeman energy shift of ^{24}MgH molecules in the $|\nu=0, F=1, M=1\rangle$ state is given by $\Delta_Z = \mu_B (g_e + g_p)B/2$, where μ_B is the Bohr magneton, B is the magnetic field, and $g_{e,p}$ are the g-factors of the electron and proton, respectively. Δ_Z does not depend on the vibrational state and there is no Zeeman shift with the $|\nu=0, N=0, F=1, M=1\rangle \rightarrow |\nu=2, N=0, F=1, M=1\rangle$ transition.

The frequency shift is actually dominated by the AC-Stark shift caused by the probe laser and the collision shift. The AC-Stark shift is estimated to be in the order of $2 \times 10^{-14} (II_S)$, where I is the power density of probe laser and I_S is the saturation power density. The collision shift is in the order of $2 \times 10^{-26} n$ (n is molecular density with the unit of cm^{-3}) when the molecular temperature is lower than 1 mK.

The frequency shift is in the order of 10^{-17} assuming $(II_S) < 10^{-3}$ and $n < 10^9/\text{cm}^3$. This frequency uncertainty is low enough to measure the variance of electron-proton mass ratio (estimated to be $10^{-15}/\text{year}$).

References

1. J. D. Weinstein et al., *Nature* **395**, 148 (1998).
2. M. Kajita, *Phys. Rev.* **A74**, 032710 (2006).

STRONG FIELD IONIZATION OF ALKALINE EARTH ATOMS

HUIPENG KANG, XIAOJUN LIU

*State key Laboratory of Magnetic Resonance and Atomic and Molecular Physics,
Chinese Academy of Sciences, Wuhan 430071, China*

The behavior of atoms in intense femtosecond laser field has been under active investigation[1]. A multitude of novel effects have been revealed, such as above-threshold ionization (ATI), high harmonic generation (HHG) and nonsequential ionization (NSI). Extensive study on noble gases indicate a rescattering picture be responsible for the nonsequential ionization caused by electron correlation[2]. However, recent experiments performed on alkaline earth atoms exhibit different ionization behavior from that of noble gas atoms[3], suggesting other different ionization mechanisms. With a newly established photoelectron spectrometer based on time-of-flight principle, strong field ionization of alkaline earth atoms is investigated. We focus on double ionization dynamics of alkaline earth atoms subject to ultrashort intense fs laser pulses. The light intensity is chosen in a regime where non-sequential double ionization dominates. The electron-ion coincidence technique allows a detailed exploration of underlying ionization dynamics. Some preliminary results will be presented.

References

1. M Protopapas, C H Keitel and P L Knight, *Rep. Prog. Phys.* **60**, 389(1997).
2. P. B. Corkum, *Phys. Rev. Lett.* **71**, 1994 (1993).
3. G. D. Gillen, M. A. Walker, and L. D. Van Woerkom, *Phys. Rev.* **A64**, 043413 (2001).

**DETAILED STUDY OF THE LASER COOLING PROCESS,
AND OF THE VELOCITY DISTRIBUTION OF LASER
COOLED ATOMS**

A. KASTBERG*, C. M. DION, H. HAGMAN, S. JONSELL,
S. PETRA and P. SJÖLUND

Department of Physics, Umeå University, SE-90187 Umeå, Sweden
* E-mail: anders.kastberg@physics.umu.se

L. SANCHEZ-PALENCIA

*Laboratoire Charles Fabry de l'Institut d'Optique,
CNRS and Univ. Paris-Sud, Campus Polytechnique, RD 128,
F-91127 Palaiseau cedex, France*

R. KAISER

*Institut Non Linéaire de Nice,
1361 route des Lucioles, F-06560 Valbonne, France*

Laser cooling in optical lattices is often believed to be a solved problem. In particular, this is the case for the ‘lin⊥lin configuration’ for multilevel atoms, where the famous Sisyphus cooling model is relevant.¹ This is remarkable, since already from the outset of that theory, it was obvious that it explained many of the features of laser cooling, and provided great insight, but also that some of the results from the Sisyphus model are based on strong approximations (*e.g.* spatial averaging) that deviate from real situations.²

There have been many reports where basic properties of laser cooling have been performed, for example a linear scaling between steady-state temperature and light shift accompanied by an abrupt turn-off at low light shifts (see *e.g.*³ and references therein). However, experimental findings have also clearly shown that the model is too simplified for a complete description of laser cooling. In particular, the rate of cooling does not correspond to the model,^{4–6} and the emerging velocity distribution shows deviations from the expected ones.^{7–10} There have also been studies based on quantum simulations that show discrepancies with analytical models.^{2,6,11}

Deviations from Gaussian distributions are obtained from the seminal semi-classical model¹ when velocity-dependent nonlinear terms are not neg-

ligible and an analytic solution of the equation of motion yields a Tsallis distribution.¹² However, this model explicitly neglects the spatial modulations of the potential and thus the trapping of atoms in the potential wells, which is a crucial ingredient.

Through experiments with a high resolution velocity probe, and numerical simulations, we show that the velocity distribution, when atoms are laser cooled in an optical lattice, is bimodal. That is, at relatively high light shifts, where laser cooling is typically applied, essentially all atoms are trapped at potential sites, and the velocity distribution has the appearance of a *slightly* truncated Gaussian. If the light shift is lowered, towards and beyond the point where laser cooling has been believed to break down, a mode with untrapped atoms will appear. By the dissipation processes involved, atoms are continuously shifting between being localized (trapped mode) and moving around in the lattice (untrapped mode). Even at very low light shifts, a majority of the atoms are in the trapped mode, but the overall velocity distribution will be strongly influenced by the untrapped ones.

We also investigate the momentum diffusion of untrapped atoms for signs of non-ergodic behavior.

References

1. J. Dalibard and C. Cohen-Tannoudji, *J. Opt. Soc. Am. B* **6**, 2023 (1989).
2. Y. Castin, J. Dalibard and C. Cohen-Tannoudji, The limits of sisyphus cooling, in *Light Induced Kinetic Effects on Atoms, Ions, and Molecules*, eds. L. Moi, S. Gozzini, C. Gabbanini, E. Arimondo and F. Strumia (ETS Editrice, Pisa, 1991).
3. S. Chu, *Rev. Mod. Phys.* **70**, 685 (1998); C. Cohen-Tannoudji, *ibid.* **70**, 707 (1998); W. D. Phillips, *ibid.* **70**, 721 (1998).
4. G. Raithel, G. Birkl, A. Kastberg, W. D. Phillips and S. L. Rolston, *Phys. Rev. Lett.* **78**, 630 (1997).
5. L. Sanchez-Palencia, M. Schiavioni, F.-R. Carminati, F. Renzoni and G. Grynberg, *J. Opt. Soc. Am. B* **20**, 925 (2003).
6. C. M. Dion, P. Sjölund, S. J. H. Petra, S. Jonsell and A. Kastberg, *Europhys. Lett.* **72**, 369 (2005).
7. H. Katori, S. Schlipf and H. Walther, *Phys. Rev. Lett.* **79**, 2221 (1997).
8. J. Jersblad, H. Ellmann and A. Kastberg, *Phys. Rev. A* **62**, 051401 (2000).
9. L. Sanchez-Palencia, P. Horak and G. Grynberg, *Eur. Phys. J. D* **18**, 353 (2002).
10. J. Jersblad, H. Ellmann, K. Støchkel, A. Kastberg, L. Sanchez-Palencia and R. Kaiser, *Phys. Rev. A* **69**, 013410 (2004).
11. T. Bergeman, *Phys. Rev. A* **48**, R3425 (1993).
12. E. Lutz, *Phys. Rev. A* **67**, 051402(R) (2003).

LASER-TRIGGERED ULTRAFAST ELECTRON EMISSION FROM A SHARP TUNGSTEN TIP

C. KEALHÖFER*, P. HOMMELHOFF and M. A. KASEVICH

*Department of Physics, Stanford University,
Stanford, CA 94305, USA*

**E-mail: ckealhof@stanford.edu*

A low-power (~ 600 mW) 8-fs pulsed Ti:Sapph laser oscillator has been used to generate electron emission from sharp tungsten tips. By studying the non-linearity of the electron emission as a function of laser power and DC bias field, we infer that the electron emission process is prompt.^{1,2} If the photon energy is below the effective work function of the metal, electrons can be emitted due to multiphoton excitation (in the low power limit) or optical field emission (in the high power limit). This latter process can be thought of as electrons tunneling out of the metal in the electric field of the laser. The emission in this case is a non-linear function of the laser electric field and may only occur during one half of the optical cycle. For 800 nm light, this corresponds to sub-femtosecond emission times.

Normally, the quasistatic approximation used to study optical field emission holds for cases where the Keldysh parameter, γ , is much less than one (the multiphoton regime, in contrast, is characterized by $\gamma \gg 1$). In the case of our experiment, however, $\gamma \sim 1$. In order to better understand this system, we developed a simple numerical model by integrating the Schrödinger equation for a single electron tunneling from a surface state in the presence of the laser field. The model provides a reasonable fit to our data (nonlinearity as a function of bias voltage). Furthermore, it predicts that the electron emission is confined to only part of each laser cycle, so that the temporal profile of the electron emission consists of one or more sub-femtosecond pulses, even for intermediate values of γ . This is consistent with recent theoretical and experimental work on tunnel ionization in atoms, for which the electron emission is shown to be sub-laser cycle even in the intermediate regime.^{3,4} As the emitter size is on the order of nanometers, an electron source based on optical field emission can be highly localized in both space

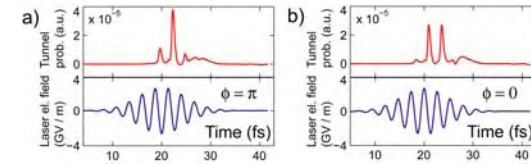


Fig. 1. Simulation results showing sub-optical cycle electron emission for 3-cycle laser pulses of different carrier envelope phase.

and time. Some possible applications of such a source include generation of femtosecond x-ray pulses, ultrafast electron microscopy, and electron interferometry.

References

1. P. Hommelhoff, C. Kealhofer, and M. A. Kasevich, *Phys. Rev. Lett.* **97**, 247402 (2006)
2. P. Hommelhoff, Y. Sortais, A. Aghajani-Talesh, and M. A. Kasevich, *Phys. Rev. Lett.* **96**, 077401 (2006)
3. G. L. Yudin and M. Y. Ivanov, *Phys. Rev. A* **64**, 013409 (2001)
4. M. Uiberacker et al., *Nature* **446**, 631 (2007)

TOWARD MODE-LOCKED LASER COOLING OF NEW ATOMIC SPECIES

D. KIELPINSKI*, M. PULLEN, J. CHAPMAN, M.J. MCDONNELL, AND E.W. STREED

Centre for Quantum Dynamics, Griffith University, Brisbane, Nathan QLD 4111, Australia

**E-mail: d.kielpinski@griffith.edu.au*

The pulse train from an ultrafast mode-locked laser has two properties which in combination make it a good tool for laser cooling. First, the nonlinear conversion efficiency for femtosecond to picosecond long pulses approaches unity, allowing access to wavelengths in the deep UV region of the spectrum. Secondly, the phase coherence between pulses in the pulse train allows excitation of two-photon transitions at rate equal to a CW laser of the same average power. These two properties acting together mean that ultrafast lasers can be used for cooling of species with transitions in the deep UV, such as the chemically interesting species H, C, N, O and Cl. Here we describe work toward implementation of the mode-locked cooling scheme described in "Laser cooling of atoms and molecules with ultrafast pulses," D. Kielpinski. Phys. Rev. A, 73, 063407 (2006). We have trapped and crystallized Yb⁺ ions by standard laser cooling for a proof of principle experiment. The mode-locked laser source for the proof of principle is a Ti:sapphire laser for cooling on the two-photon 871 nm transition in Yb⁺. This laser has achieved high pulse repetition rate, low pump threshold, and carrier-frequency stability at a relatively narrow optical bandwidth. We describe our high-power 515 nm fibre laser source for "magic wavelength" dipole trapping of hydrogen and discuss plans for cooling a dipole-guided beam of atomic hydrogen with a mode-locked fibre laser.

POPULATION DYNAMICS OF ULTRACOLD RB RYDBERG ATOMS

H. KITSON AND W. J. ROWLANDS

*Centre for Atom Optics and Ultrafast Spectroscopy, Swinburne University of Technology,
Melbourne 3122, Australia*

We report on recent experiments investigating the lifetimes of highly excited nd -states ($n=12-37$) of ultracold rubidium atoms. The lifetime of Rydberg states at finite temperature is not determined solely by spontaneous decay rates, but is influenced by the redistribution of atomic populations amongst nearby states via interaction with blackbody radiation [1].

Our work uses time-resolved ionization detection of ultracold Rydberg atoms produced in a standard Rb magneto-optical trap (MOT). A single focused beam from a high-energy tunable MOPO laser is used for both the Rydberg excitation and subsequent photoionization. A channeltron is used to detect atomic ions as the frequency of the laser is scanned, resulting in a resonantly-enhanced ionization spectrum which is used to identify the atomic energy levels. Rydberg lifetimes were measured by recording the time-resolved ion signals, consisting of ionization by the photoionization beam and the MOT light.

Although the Rydberg atoms are created in a state-selective process, the ion signal decay is not simply due to radiative transitions from a single state. The ambient blackbody radiation allows transitions to neighbouring Rydberg states, and it is this population redistribution and subsequent decay that must be considered. We have modeled the population dynamics, using two different forms for the blackbody interaction [2] [3]. Comparison of our experimental lifetime data to the model provides limits on the validity for the two approaches to the blackbody interaction.

References

1. K.M.F. Magalhaes, A.L. de Oliveira, R.A.D.S. Zanon, V.S. Bagnato and L.G. Marcassa, *Opt. Com.* **184**, 385 (2000). A. L. Oliviera, M. W. Mancini, V. S. Bagnato and L. G. Marcassa, *Phys. Rev. A* **65**, 031401 (2002).
2. J.W. Farley and W.H. Wing, *Phys. Rev. A* **23**, 2397 (1981).
3. Constantine E. Theodosiou, *Phys. Rev. A* **30**, 2881 (1984).

HETERONUCLER FESHBACH RESONANCES IN AN ULTRACOLD BOSE-FERMI MIXTURE

C. Klempt, T. Henninger, O. Topic, J. Will, W. Ertmer and J. Arlt

*Institut für Quantenoptik; Leibniz Universität Hannover,
Welfengarten 1, 30167 Hannover, Germany*

The methods developed for the production of quantum degenerate Bose and more recently Fermi gases now also allow for the production and examination of heteronuclear quantum degenerate gases. Within our experiments, bosonic ^{87}Rb atoms are used to cool an ensemble of fermionic ^{40}K atoms to joint quantum degeneracy. This opens a vast research area, including the investigation of interactions within these mixtures and the production of cold K-Rb molecules via magnetic Feshbach resonances.

In our experimental apparatus, both atomic species are cooled and trapped in a dual magneto-optical trap, where $8 \cdot 10^9$ Rb and $1 \cdot 10^8$ K atoms are captured. These samples are transferred into a movable magnetic quadrupole trap and physically transported into a magnetic QUIC trap. Within the magnetic trap, the Rubidium atoms are evaporatively cooled and thermalize with the Potassium atoms. Since a freely adjustable magnetic field is desirable for further investigations, the atoms are loaded into a dipole trap shortly before reaching quantum degeneracy. Dipole traps created from single and dual foci have been investigated and a final number of $1.5 \cdot 10^6$ Rb and $1.5 \cdot 10^6$ K atoms at a temperature of 800 nK was obtained. Within this trap, rapid adiabatic passages are used to prepare mixtures of arbitrary spin states via radio (K) and microwave (Rb) frequency ramps.

Applying a homogeneous magnetic field of up to 600G allows for the investigation of heteronuclear Feshbach resonances in this mixture. We have recently been able to observe 28 resonances in 10 stable spin configurations. In combination with results from molecular spectroscopy, this allows for a large

2

improvement of the molecular potential. The structure of these resonances opens new possibilities for the control of the interactions.

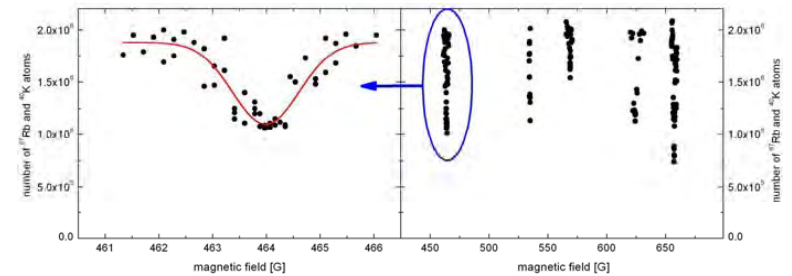


Figure: Observation of a heteronuclear Feshbach resonance.

Precise control of the Feshbach resonances will allow for the investigation of weakly bound molecules. The transfer of these molecules into deeply bound states is one the major current goals in this novel field of quantum chemistry.

TUNABLE ALKALI LASERS FOR ATOMIC PHYSICS

RANDALL J. KNIZE and BORIS V. ZHDANOV

US Air Force Academy, 2354 Fairchild Dr., Ste. 2A31, USAF Academy, CO
80840, Phone: 719-3332109, Fax: 719-3337098, Email:
randy.knizer@usafa.af.mil

Abstract: We present a narrowband tunable Cesium vapor laser pumped with a continuous wave narrowband laser diode array that can have various applications in experimental atomic physics and laser spectroscopy.

Keywords: Atomic gas lasers, Alkali lasers

Tunable lasers are an important tool in most experiments concerning laser spectroscopy, laser cooling, optical pumping of spin polarized gases and other experiments in atomic physics. The most common laser sources for such experiments are dye lasers, Ti:Sapphire lasers and optical diodes. Maximum output power of these sources is usually less than 5 W which can be a limitation. Recently developed diode pumped Alkali vapor lasers [1,2] have demonstrated an output power of 13 W and can be scaled to higher powers. In this paper we present our results demonstrating single mode tunable Cs atomic vapor laser which can find wide applications in atomic physics.

Cs vapor laser as well as other Alkali lasers (e.g. Rb, K) operate using three-level pump scheme suggested by Konefal [3]. An optical pump source with a wavelength corresponding to the D2 line ($6S_{1/2} \rightarrow 6P_{3/2}$) excites Cs atoms to the $6P_{3/2}$ state. A buffer gas (usually ethane) provides fast population transfer from the $6P_{3/2}$ state to the $6P_{1/2}$ state that creates population inversion and lasing on the D1 transition ($6P_{1/2} \rightarrow 6S_{1/2}$).

There has been a significant progress in Alkali lasers development during the last several years. Cs laser with 81% slope efficiency [4], Rb laser with 59% slope efficiency [5] and Potassium laser with 20% slope efficiency [6] were demonstrated. Lasers of different types (Ti:Sapphire, single frequency diode lasers) were used as pump sources for Alkali lasers. To generate a high output power (10 – 100 W), high power diode lasers or arrays must be used. The first diode pumped alkali (Cs) laser [1] demonstrated such possibility – a 41% slope efficiency was obtained. The most powerful diode pumped alkali (Cs) laser has a demonstrated output power of 13 W and a total optical efficiency of 62% [7].

Using buffer gases for atomic states mixing in alkali vapors leads to broadening of the atomic energy levels corresponding to the lasing transition $P_{1/2} \rightarrow S_{1/2}$ that allows tuning of the lasing wavelength. For example, for the Cs laser with 500 torr of Ethane buffer gas, the broadening is about 10 GHz. We demonstrated a Cs ring laser operating on single transverse and single

longitudinal mode with a linewidth less than 3 MHz which can be fine tuned in the range of about 14 GHz (from 894.5863 nm to 894.6250 nm). The same result can be obtained for other alkali vapor lasers, operating in different spectral range.

References

1. T. Ehrenreich, B. Zhdanov, T. Takekoshi, S. P. Phipps, and R. J. Knize, "Diode Pumped Cesium Laser", *Electronics Letters* 41(7), 47-48 (2005).
2. R. Page, R. Beach, V. Kanz, and W. Krupke, "Multimode-diode-pumped gas (alkali-vapor) laser", *Opt. Lett.* 31(3), 353-355 (2006).
3. Z. Konefal, "Observation of collision induced processes in rubidium-ethane vapour", *Opt. Comm.* 164, 95-105 (1999).
4. B. V. Zhdanov, T. Ehrenreich and R.J. Knize, "Highly Efficient Optically Pumped Cesium Vapor Laser", *Optics Communications* 260(2), 696-698 (2006)
5. W.F. Krupke, R.J. Beach, V.K. Kanz, and S.A. Payne, "Resonance Transition 795-nm Rubidium Laser", *Optics Letters* 28(23), 2336-2338 (2003).
6. B. Zhdanov, C. Maes, T. Ehrenreich, A. Havko, N. Koval, T. Meeker, B. Worker, B. Flusche, and R.J. Knize, "Optically Pumped Potassium Laser", *Optics Communications*, vol. 270, no.2, pp. 353-355, 15 February 2007
7. B. Zhdanov and R.J. Knize, "Laser Diode Array pumped Cesium laser with 13 W output", *CLEO/QELS 2007 Conference*, May 6-11, 2007, Baltimore, MD, USA, Presentation no.: CPDB2

FOUR-WAVE MIXING IN THREE-LEVEL COLD ATOMS BY BICHROMATIC FIELD

L. B. KONG¹, X. H. TU¹, P. XU¹, J. WANG¹, Y.F.ZHU², AND M.S.ZHAN^{1†}

¹State Key Laboratory of Magnetic Resonance and Atomic and Molecular Physics, Wuhan Institute of Physics and Mathematics, and Center for Cold Atom Physics, Chinese Academy of Sciences, Wuhan 430071, P. R. China

²Department of Physics, Florida International University, Miami, Florida 33199, USA

†E-mail: mszhan@wipm.ac.cn

Laser induced coherence can modify linear and nonlinear optical processes in atomic medium. Electromagnetically induced transparency (EIT), a quantum coherence effect, has been proposed to eliminate the linear absorption and, at the same time, to obtain large nonlinear susceptibility. In recent experimental demonstrations of four-wave mixing (FWM) with EIT in cold atoms^{1,2}, a four-level double- Λ system coupled by three lasers, one weak light with two strong lasers can generate a new FWM signal with large efficiency. In this work, we compose a symmetrical double- Λ configuration in a three-level system coupled by a bichromatic field and a weak light, and report the experimental observation of FWM signal in three-level cold rubidium atoms. The Energy-level structure of ⁸⁵Rb atom and laser coupling scheme are shown in Figure 1 (a). For the weak light, there exhibit a series of transparent windows at multiple frequencies as shown in Figure 2 (a), which is called bichromatic electromagnetically induced transparency and has been experimentally studied by us³. With the backward-wave geometry of the coupling laser beams as shown in Figure 1 (b), we found that the maximum FWM conversion efficiency occurs under the symmetrical coupling of the bichromatic field. Under our experimental condition, the measured maximum conversion efficiency was about 18%. Due to the simple and completely symmetrical configuration, we find that the coherence and enhanced nonlinearity of this system should have useful applications in slow light propagation and quantum information processing.

1

2

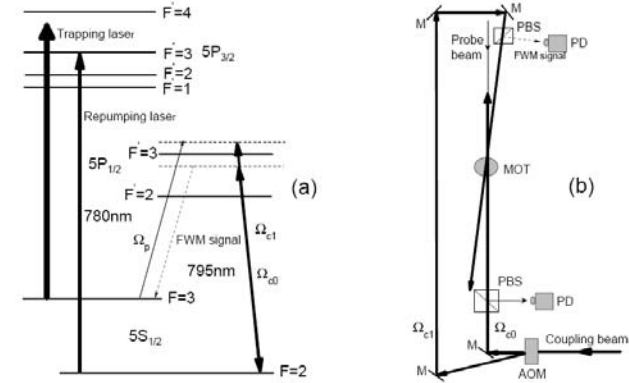


Figure 1: (a) Energy-level structure of ⁸⁵Rb and laser coupling scheme. (b) Schematic diagram of the experimental setup. M, mirror; PBS, polarizing beam splitter; PD, photodiode; AOM, acousto-optic modulator.

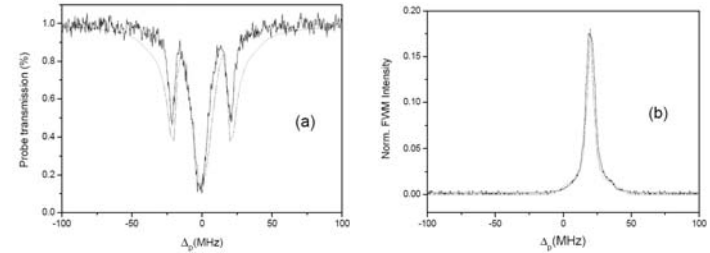


Figure 2. (a) Measured (solid line) and calculated (dotted line) probe transmission, and (b) measured (solid line) and calculated (dotted line) FWM signal (normalized relative to the probe intensity) versus the probe frequency detuning. The system is under the symmetrical coupling condition of $\Delta = (\omega_{c0} + \omega_{c1})/2 - \omega_{23} = 0$ and $\Omega_{c1}/2\pi = \Omega_{c0}/2\pi = 12\text{MHz}$, $\Omega_p/2\pi = 0.8\text{MHz}$.

References

1. Danielle A. Braje, Vlatko Balic, Sunil Goda, G.Y. Yin, and S. E. Harris, Phys. Rev. Lett. 93, 183601 (2004).
2. Hoonsoo Kang, Gessler Hernandez, and Yifu Zhu, Phys. Rev. A 70, 061804 (2004).
3. J. Wang, Yifu Zhu, K. J. Jiang, and M. S. Zhan, Phys. Rev. A 68, 063810 (2003).

COOLING A SINGLE-ATOM IN AN OPTICAL TWEEZER

A. M. LANCE[†], C. TUCHENDLER, Y. R. P. SORTAIS, G. MESSIN, A. BROWAEYS,
P. GRANGIER

*Laboratoire Charles Fabry de l'Institut d'Optique, CNRS, Univ. Paris-sud, Campus
Polytechnique, RD 128, 91127 Palaiseau Cedex, France[‡]*

Trapped cold neutral atoms have promising applications in quantum information processing, as well as fundamental atom-optic research. We are interested in investigating small numbers of cold ^{87}Rb atoms trapped in a microscopic optical dipole trap, as well as using this system to isolate and manipulate single atoms. To achieve these goals, we are currently investigating techniques for cooling a single atom in an optical tweezer towards the ground state of the trap.

We have built an optical system designed to capture and observe a single neutral atom in an optical dipole trap, created by focusing a laser beam at 850 nm using a large numerical aperture (N.A.=0.5) aspheric lens [1], as shown in Figure 1(a). This optical system is diffraction limited over a broad spectral range (~ 200 nm) with a large transverse field (± 25 μm). The optical tweezer, created at the focal point of the lens, is able to trap single ^{87}Rb atoms and to detect them individually with large collection efficiencies. We observe the fluorescence of the trapped atoms at 780 nm with a CCD camera with low read-out noise, as well as an avalanche photodiode (APD) as shown in Figure 1(b). The histogram of this measured fluorescence in Figure 1(c) shows that we can discriminate between the presence and absence of an atom within in 10 ms with a confidence of better than 99%.

We are currently investigating techniques for cooling the single atom in the dipole trap. We have used an optimized cooling sequence to achieve a single atom temperature of $T_{\text{atom}} = 30.0$ μK for an optical trap depth of 2.8 mK. We are currently investigating the effect on the temperature of the trapped atom after adiabatically lowering the depth of the dipole trap. Figure 1(d) shows the preliminary experimental results of the temperature of the single atom after the

2

dipole trap has been adiabatically lowered from an initial depth of $U_{\text{initial}} = 2.8$ mK to a variable final trap depth U_{final} , in a constant cooling time of 2.5 ms. Using this technique, we have measured a lowest temperature of $T_{\text{atom}} = 0.4$ μK , corresponding to a final trap depth of $U_{\text{final}} = 2$ μK .

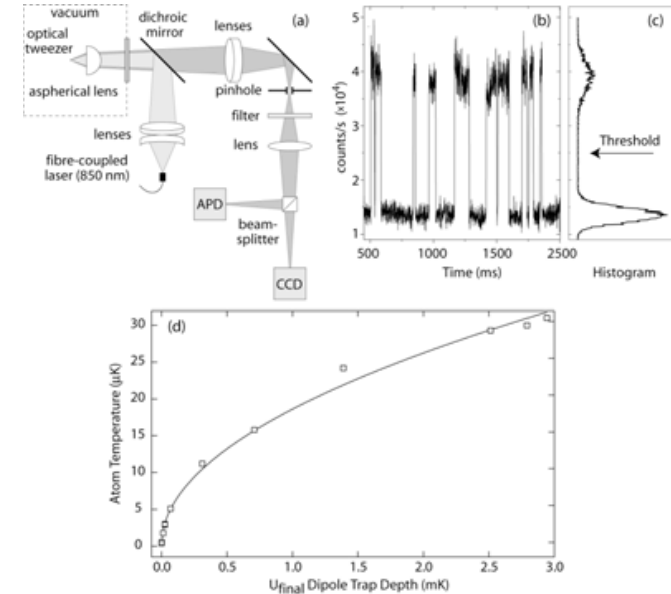


Figure 1. (a) Schematic of the single-atom trapping experiment. (b) Fluorescence of the single atom measured by the avalanche photo diode. Each point corresponds to a 10 ms time bin. (c) Histogram of the measured fluorescence recorded over 100s. (d) Preliminary experimental results of the temperature of the single atoms in the dipole trap after the trap depth has been adiabatically lowered from an initial depth of $U_{\text{initial}} = 2.8$ mK to a final depth U_{final} .

References

1. Y. R. P. Sortais, H. Marion, C. Tuchendler, A. M. Lance, M. Lamare, P. Fournet, C. Armellin, R. Mercier, G. Messin, A. Browaeys, P. Grangier, *Phys. Rev. A* **75**, 013406 (2007).

[†] Electronic address: andrew.lance@institutoptique.fr.

[‡] Laboratoire Charles Fabry is a "Unité Mixte de Recherche" of Institut d'Optique Graduate School, Centre National de la Recherche Scientifique, and Université Paris-Sud.

Towards a wire-mediated coupling of trapped ions

Tony Lee¹, Rob Clark², Hartmut Häffner¹

¹*Institute for Quantum Optics and Quantum Information, Innsbruck, Austria*

²*Research Laboratory of Electronics and Department of Physics, Massachusetts Institute of Technology, Cambridge, USA*

An oscillating trapped ion induces oscillating image charges in the trap electrodes. If this current is sent to the electrodes of a second trap, it influences the motion of an ion in the second trap. This inter-trap coupling may be used for scalable quantum computing, cooling ion species that are not directly accessible to laser cooling, for the non-invasive study of superconductors, and for coupling an ion-trap quantum computer to a solid-state quantum computer, e.g. a system of Josephson junctions.

We have set up a planar Paul trap with the goal to demonstrate this inter-trap coupling. In this trap, single calcium ions are confined 800 μm above the trap surface. With a piezo translation stage a wire can be brought close to the ions ($< 100 \mu\text{m}$) to study the interaction between the wire and the ion(s). We present first results of the wire's influence on the ion trapping.

Finally, we will discuss more theoretical aspects; the most relevant sources of decoherence are heating (e.g. Johnson noise) and dephasing of the electronic wave function inside the wire. However, using superconducting transmission lines, a coherent current transport over macroscopic distances ($>1 \text{ mm}$) is possible. In addition, Johnson noise heating would be greatly reduced, and the coherent coupling of two ions would become feasible. The expected time for a complete exchange of the ionic motional states is 1 ms for an ion-wire distance of 50 μm .

Quantum information processing with trapped ions at NIST*

D. Leibfried[†], J. Amini, R.B. Blakestad, J.J. Bollinger, J. Britton, K.R. Brown, R. Epstein, J.P. Home, W.M. Itano, J.D. Jost, E. Knill, C. Langer[‡], C. Ospelkaus, R. Ozeri[‡], R. Reichle[§], S. Seidelin, N. Shiga, J. Wesenberg, and D.J. Wineland
*Time and Frequency Division, National Institute of Standards and Technology,
Boulder, CO 80305, USA*
[†]*E-mail: dil@boulder.nist.gov*

Atomic ions confined in an array of interconnected traps represent a potentially scalable approach to quantum information processing. All basic requirements have been experimentally demonstrated in one and two qubit experiments. The remaining task is to scale the system to many qubits while minimizing and correcting errors in the system. While this requires extremely challenging technological improvements, no fundamental roadblocks are currently foreseen. The poster will give a survey of recent experimental progress at NIST in practically implementing quantum algorithms with up to 6 qubits. It will also discuss some new approaches to minimizing the overhead of laser beam control in large scale implementations.

* Work supported by DTO.

[#] present address: Lockheed Martin, Palmdale CA, USA

[‡] present address: Weizmann Institute of Science, Rehovot, Israel

[§] present address: Universität Ulm, Ulm, Germany

OH Stark deceleration: magnetic trapping, precision measurement, and prospects for cavity-assisted laser cooling

Benjamin Lev, Brian Sawyer, Benjamin Stuhl, Mark Yeo, and Jun Ye

*JILA, National Institute of Standards and Technology and the University of Colorado
Department of Physics, University of Colorado, Boulder, Colorado 80309-0440, USA
E-mail: benlev@jila.colorado.edu*

The experimental realization of large samples of ultracold, ground state polar molecules would be a major breakthrough for research in ultracold collisions and chemistry, quantum information processing, and the study of novel states of matter. To accomplish this goal, our research employs a Stark decelerator to slow a supersonic expansion of OH in its rovibronic ground state. At the decelerator's terminus, a 30 mK OH packet of density 10^4 cm^{-3} is caught and confined in a magnetic quadrupole trap. An adjustable electric field of sufficient magnitude to completely polarize the OH is superimposed on the trap in either a quadrupole or homogenous field geometry. The trap dynamics deviate from that governed by simple addition of the fields forces on OH's magnetic and electric dipoles. Confinement of cold polar molecules in a magnetic trap, leaving large, adjustable electric fields for control, is an important step towards the study of low energy dipole-dipole collisions. The cold molecular packets produced via Stark deceleration have enabled us to perform precision microwave spectroscopy of the OH ground state structure, which serves as an important system for constraining variation of fundamental constants and for molecular quantum information processing. Future experiments will require much colder molecules, and we will briefly discuss prospects for cavity-assisted laser cooling of OH.

OBSERVATION OF THE DECONFINEMENT CROSSOVER IN A SUPERFLUID ARRAY FROM INSULATING 2D BEREZINSKII-KOSTERLITZ-THOULESS LAYERS TO A 3D ANISOTROPIC SUPERFLUID

WEI LI, HUI-CHUN CHIEN, AND MARK A. KASEVICH

Physics Department, Stanford University, Stanford, CA 94305

Although the past decade has seen significant advances in understanding the mechanism for high-temperature superconductivity in the cuprates, a definitive understanding of these materials remains elusive. There is recent evidence that electron pairing occurs at temperatures above the observed superconducting transition temperatures. In this case, superconductivity is associated with the phase ordering of adjacent layers of interacting bosons. Such a system can be studied with ultra-cold bosonic atoms in a one-dimensional optical lattice.

In this work, we use Bose-Einstein condensed ^{87}Rb atoms confined in a far-detuned one-dimensional optical lattice (1) to investigate a finite temperature deconfinement transition from insulating two-dimensional Berezinskii-Kosterlitz-Thouless (BKT) layers (2,3) to a three dimensional anisotropic superfluid. Using the renormalization group methods of Ref. 4, we obtain quantitative agreement with theory for the observed superfluid fraction and transition temperature as a function of the tunable tunnel coupling between adjacent lattice planes. For deep lattices, where tunneling between layers is frustrated, we observe universal BKT behavior, as illustrated in Fig. 1. In addition to interferometric probes of long range phase order, we demonstrate superfluid flow with direct transport measurements.

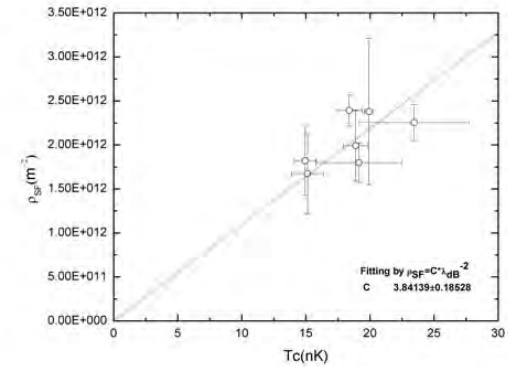


Fig.1 The two-dimensional superfluid density ρ_{SF} vs. transition temperature T_c for various lattice depths. A fit to $\rho_{\text{SF}}=C*\lambda_{\text{dB}}^{-2}$ yields $C = 3.84$ (0.18).

References

1. W. Li, A. K. Tuchman, H.C. Chien, and M. A. Kasevich, Phys. Rev. Lett. **98**, 040402 (2007).
2. Berezinskii, V. L. Sov. Phys. JETP **34**, 610-616 (1972).; J. M. Kosterlitz, D. J. Thouless, J. Phys. C **6** 1181-1203 (1973).
3. Hadzibabic, Z. and Kruger, P. and Cheneau, M. and Battelier, B. and Dalibard, J.B., Nature **441**, 1118 - 1121 (2006).
4. L. Benafatto, C.Castellani and T. Giamarchi Phys. Rev. Lett. **98**, 117008 (2007).

Absolute frequency measurement of 2S-3S two-photon spectroscopy of ${}^6,7\text{Li}$

Yu-Hung Lien, Jwo-Sy Chen, Chia-Hsiang Hsu, Yi-Wei Liu, Jow-Tsong Shy
Department of Physics, National Tsing Hua University, Hsinchu, 30013, Taiwan

The absolute frequency measurement of 2S-3S two-photon transition of ${}^6,7\text{Li}$ has been pursued by the combination of laser induced fluorescence on an atomic beam and an optical frequency comb for frequency measurement. The preliminary results are acquired and show some discrepancies from previous results. Further investigations are in progress.

Keywords: lithium, two-photon, absolute frequency measurement

1. Introduction

Being the simplest three-electron system, lithium atom serve as the playground of many studies such as higher order relativistic and QED corrections and so on. One of the latest advances is the determination of nuclear charge radius of lithium isotopes by 2S-3S two-photon spectroscopy.^{1,2} However, the transition frequencies are measured by indirect approach. In order to pursue better accuracy, the absolute frequencies of 2S-3S two-photon transitions of ${}^6,7\text{Li}$ are directly measured by an optical frequency comb in our laboratory.

2. Setup and Preliminary Results

A 735 nm Ti:sapphire laser is used in the experiment. The light is split for the ratio 10–90%. The strong beam is chopped by a 510 Hz optical chopper and then directed into the chamber. The weak beam is further split for frequency measurement, linewidth reduction and power calibration. The linewidth reduction is achieved by stabilizing laser frequency on a cavity whose finesse is ≈ 20 .

An atomic beam system is set up for two-photon spectroscopy of lithium. A stainless steel oven for lithium is heated to 450 °C to generate the lithium beam. The interaction chamber is differentially pumped to 8×10^{-6} torr.

The 735 nm laser beam is perpendicular to the atomic beam and focused on the intersection. The intensity is about $2.7 \times 10^3 \text{ W/cm}^2$. A mirror ($R = 25 \text{ cm}$) is used to reflect the beam backward. The induced 2P–2S fluorescence is collected by a lens and detected by a PMT.

The frequency measurement is accomplished by an optical frequency comb (OFC). This OFC is based on a femtosecond Ti:sapphire laser (Giga-jet 20) whose repetition frequency is about 1 GHz and pulse width is about 35 fs. The spectrum of femtosecond laser is expanded by a photonic crystal fiber. The offset frequency is locked by f-2f self-referencing scheme. Both the repetition and offset frequency are referenced to a GPS disciplined Rb frequency standard (PRS10) whose accuracy is about 10^{-12} . The frequency of 735 nm light is first determined up to GHz accuracy by a wavemeter and then heterodyning with OFC to determine the residue. The beat frequency is counted by an universal counter.

The spectrum of ${}^7\text{Li}$ 2S-3S F=2–2 is shown in Fig. 1. The scan rate of laser frequency is about 1.6 MHz/s. The preliminary laser frequencies for F=2–2 and F=1–1 two-photon transitions are 407,808,974.87(13) and 407,809,283.21(21) MHz respectively. There exist several MHz discrepancy with the best previous results.¹ Further investigation is under way and the final results will be presented at the conference.

References

1. B. A. Bushaw, W. Nörtershäuser, G. Ewald, A. Dax and G. W. F. Drake, *Phys. Rev. Lett.* **91**, p. 043004 (2003).
2. R. Sánchez, W. Nörtershäuser, G. Ewald, D. Albers, J. Behr, P. Bricault, B. A. Bushaw, A. Dax, J. Dilling, M. Domsby, G. W. F. Drake, S. Götze, R. Kirchner, H. J. Kluge, T. Kühl, J. Lassen, C. D. P. Levy, M. R. Pearson, E. J. Prime, V. Ryjkov, A. Wojtaszek, Z. C. Yan and C. Zimmermann, *Phys. Rev. Lett.* **96**, p. 033002 (2006/01/27).

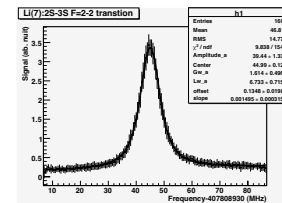


Fig. 1. Spectrum of ${}^7\text{Li}$ 2S-3S F=2–2 two-photon transition.

AMPLIFIER DESIGN IMPLEMENTING HOLLOW-CORE PHOTONIC BANDGAP FIBER FOR FIBER-LASER BASED INFRARED FREQUENCY COMBS

JINGANG LIM, DANIEL V. NICKEL, BRIAN R. WASHBURN
 Department of Physics, Kansas State University, 116 Cardwell Hall
 Manhattan, KS 66503, USA

Infrared frequency combs based on mode-locked erbium-doped fiber lasers typically require an external amplifier since the pulses directly from the laser have insufficient peak power to generate an octave-spanning supercontinuum for self-referencing. Here we implement a unique, all-fiber erbium-doped fiber amplifier that uses hollow-core photonic bandgap fiber for pulse compression. Through a combination of experiment and numerical simulations we have demonstrated temporal compression in the hollow-core photonic bandgap fiber, thus increasing the pulse's peak power.

1 Introduction

Mode-locked erbium-doped fiber lasers produce the ideal frequency comb for infrared optical frequency metrology [1, 2]. By phase-locking the repetition rate, f_r , and the carrier-envelope offset frequency, f_{CEO} , to a stable RF or optical frequency, the resulting comb can be used as spectral ruler for measuring infrared optical frequencies [3].

One difficulty that fiber-laser based frequency combs have compared to their solid-state counterparts is that pulses directly from the laser do not have enough peak power to generate the octave bandwidth for f_{CEO} detection. External amplification is used to increase the pulse energy and decrease the pulse duration. This is accomplished using an erbium-doped fiber (EDF) amplifier [1] of three fiber sections (Fig. 1a). The first section contains a single-mode fiber (SMF) which has anomalous dispersion at 1550 nm. This section chirps the pulses before they are injected into the normal dispersion EDF section. Here the pulses experience gain but the normal dispersion prevents solitonic spectral broadening from occurring. In the post-chirp SMF section the dispersion is again anomalous and nonlinear solitonic effects are used to temporally compress the amplified pulses. Typically pulses can be temporally compressed by over 30% and experience larger than 10 dB gain.

Although this amplifier can produce short pulses, it does not efficiently use the bandwidth produced by nonlinear interactions in the EDF. The solitonic fiber nonlinearities in the post-chirp section cause pulse distortions and degrade the compression from the transform-limit. Instead of using nonlinear methods for pulse compression, we replace the nonlinear SMF with a hollow core photonic bandgap fiber (PBGF) in the post-chirp section. The effective nonlinearity of the PBGF is ~ 1000 times less than that of SMF since the pulse propagates in air in the PBGF, but it also exhibits anomalous dispersion ($-11 \times 10^{-5} \text{ fs}^2/\text{nm}$) for temporal compression. We have

2

demonstrated pulse compression with an EDF amplifier implementing hollow-core PBGF for pulse compression. Furthermore, we have numerically modeled nonlinear pulse propagation by solving the nonlinear Schrödinger equation for propagation in the SMF, EDF, and PBGF sections.

2 Numerical and Experimental Results of Pulse Compression

The numerical and experimental results involve the amplification and temporal compression of 209 fs full-width at half-maximum (FWHM) pulses from an erbium-doped figure-eight laser. Numerical solutions to the nonlinear Schrödinger equation were performed to understand the pulse evolution through the amplifier. Care was taken to include the effects of dispersion, nonlinearity, gain, and gain dispersion. Figure 1b shows a numerical solution that illustrates pulse compression. The pulse propagates through 6 m of EDF and is compressed to 50 fs after 0.3 m of PBGF.

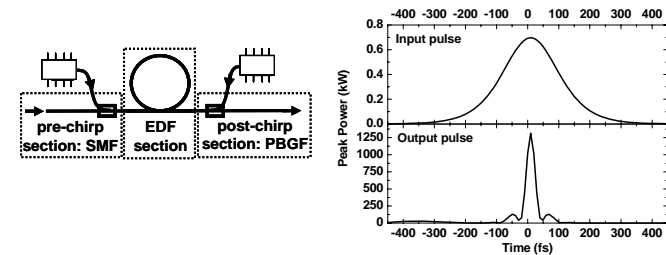


Figure 1. a) Schematic of the amplifier. b) Numerical simulation of pulse compression in the fiber amplifier. Top: the input, 210 fs transform-limited pulse from the figure-eight laser. Bottom: Output pulse from the amplifier showing temporal compression to 50 fs FWHM.

A series of experiments measured the pulse compression produced by an all-fiber amplifier design where the PBGF was directly spliced to the EDF [4]. The pulse duration was measured before the amplifier, after the EDF and after the PBGF. The duration increased from 210 fs to 800 fs in the EDF and the pulse was compressed to 110 fs in the PBGF. The difficulty in experimentally obtaining the 50 fs pulses arises due to a technical inability to cut off millimeter lengths of the PBGF.

References

1. B. R. Washburn, S. A. Diddams, N. R. Newbury, J. W. Nicholson, M. F. Yan, and C. G. Jørgensen, *Opt. Lett.* **29**, 250 (2004).
2. T. R. Schibli, K. Minoshima, F.-L. Hong, H. Inaba, A. Onae, H. Matsumoto, I. Hartl, and M. N. Fermann, *Opt. Lett.* **29**, 2467 (2004).
3. R. Fox, B. R. Washburn, N. R. Newbury, and L. Hollberg, *App. Opt.* **44**, 7793 (2005).
4. R. Thapa, K. Knabe, K. L. Corwin, and B. R. Washburn, *Opt. Express* **14**, 9576 (2006).

Strontium Optical Lattice Clock: High Accuracy and Stability

A. D. Ludlow* , T. Zelevinsky, M. M. Boyd, S. Blatt, S. Foreman, G. K. Campbell, M. Miranda, M. Martin, and J. Ye

*JILA, National Institute of Standards and Technology and University of Colorado
440 UCB Boulder CO 80309-0440 USA*

**E-mail: ludlow@colorado.edu*

We report recent developments in an optical atomic clock based on neutral strontium confined in an optical lattice. We first describe the accuracy evaluation of such a clock to the 7×10^{-16} fractional level. Furthermore, we measure the absolute clock frequency against the NIST-F1 Cs fountain to a 1.1 Hz uncertainty, dominated by the Cs-calibration of the hydrogen maser used for the measurement. These results were facilitated by interrogation of the Sr clock transition with a linewidth as small as 1.8 Hz.

As has been long anticipated, these optical systems have the potential for very high stability, even at shorter time scales. We discuss our current estimates of the clock instability at a few 10^{-15} at 1 second as well as appropriate steps for further improvement towards quantum-projection-noise-limited operation. We also describe an optical standard transfer scheme capable of making remote (tens of km) comparisons between optical frequency standards at instabilities below 10^{-17} at 1 second. We discuss preliminary results of a remote optical comparison of the Sr standard to other NIST optical standards in the Boulder area³ using this transfer system and we consider important features for continued improvement of overall clock performance in the near future.

References

1. M. M. Boyd et al., Phys. Rev. Lett. 98, 083002 (2007).
2. A. D. Ludlow et al., Phys. Rev. Lett. 96, 033003 (2006).
3. C. W. Oates et al., 2006 IEEE International Frequency Control Symposium and Exposition, 74-79 (June 2006).

**PRECISE LASER SPECTROSCOPY AND MEASUREMENT
ACROSS THE OPTICAL SPECTRUM USING OPTICAL
FREQUENCY COMBS**

A.A. MADEJ, J.E. BERNARD, P. DUBÉ, A. SHINER

*Frequency and Time Group, Institute for National Measurement Standards, National
Research Council of Canada, 1200 Montreal Rd., Ottawa, Ontario, K1A 0R6, Canada*

J. JIANG, D. J. JONES, S. DRISSLER

*Department of Physics and Astronomy, University of British Columbia, Vancouver, BC,
V6T 1Z1, Canada*

A. CZAJKOWSKI

*Department of Physics, University of Ottawa, 150 Louis Pasteur, Ottawa, Ontario,
K1N 6N5, Canada*

We present experimental results dealing with recent work in the application of optical frequency comb technology for the precise measurement of reference spectral lines in atomic and molecular systems spanning from 0.4 to 1.5 μm .

1. Introduction:

The development of mode-locked laser based optical frequency comb technology has opened new possibilities in precision laser spectroscopy. Using a high quality atomic time standard as a reference, the measurements performed by such systems are frequently limited solely by the precision and accuracy of the laser spectroscopic probe system used to investigate the atomic or molecular sample.

2. Measurements of Rb Reference Transitions at 422nm:

Although the resonance transitions of the alkali atoms have been extensively studied and used for the verification of detailed atomic structure calculations and fundamental constant studies[1], measurements of the longer-lived, higher lying states have been performed at significantly lower accuracies. Recently, we have developed a 422 nm diode laser based Rb spectrometer probing the $5s\ ^2S_{1/2}$ - $6p\ ^2P_{1/2}$ transition using saturation spectroscopy with

accuracies at the 10's of kHz level. We have extended the range of our NRC Ti:Sapphire based optical frequency comb system by frequency offset locking a frequency doubled 844 nm diode laser system to the 422 nm probe laser. Twelve transition components for the ^{85}Rb and ^{87}Rb isotopes were measured for this system representing a four orders of magnitude improvement in the knowledge of this transition frequency. The lines obtained at 422 nm are among the most accurately known reference lines in the violet region of the spectrum.

3. Infrared Reference Wavelengths Measured Using a Fiber Based Frequency Comb System:

A self-referenced mode-locked fiber laser system using a stretched pulse erbium doped fiber laser was developed. The comb is capable of measuring laser sources from 1 to 2 μm wavelengths. The system was applied to the measurement of reference lines in $^{12}\text{C}_2\text{HD}$ of the $2\nu_1$ band between 1512 nm and 1537 nm. A cavity enhanced saturation absorption spectrometer was employed in the work, which had been used in the measurement of other isotopes of acetylene [2]. Accuracies of several lines were obtained at a level of 1.3 kHz (7×10^{-13}) and a total of 55 new lines were measured for an improvement of over 10^3 in accuracy. The results provide additional high quality reference lines for the telecom region of the spectrum together with improved values of the ground state constants.

4. Comb Based Measurement of the Sr^+ 445 THz Clock Transition:

The $\text{Sr}^+ 5s\ ^2S_{1/2} - 4d\ ^2D_{5/2}$ transition at 445 THz has been extensively studied by our group and that of NPL and has been selected as a secondary realization of the second. Recently, we have been able to resolve the reference transition at the level of better than 5 Hz (1×10^{-14}) using an improved probe laser system. The NRC Ti:Sapphire frequency comb has been used in optical frequency measurements yielding inaccuracies at the few Hz level of this clock transition [3]. We will describe the extension of the fiber laser comb for the measurement of the 445 THz radiation and its operation for extended periods thus creating true clockworks for the next generation optical time standards.

References:

1. Th. Udem, J. Reichert, R. Holzwarth, and T.W. Hansch, *Phys. Rev. Lett.* **82**, 3568-3571 (1999).
2. A.A. Madej, A.J. Alcock, A. Czajkowski, J.E. Bernard, and S. Chepurov, *J. Opt. Soc. Am B* **23**, 2200-2208 (2006) and references therein.
3. P. Dubé, A.A. Madej, J.E. Bernard, L. Marinet, J.-S. Boulanger, and S. Cundy, *Phys. Rev. Lett.* **95**, 033001 (2005).

Trapping of rubidium atoms by AC electric fields

Adela Marian, Sophie Schlunk, Peter Geng, Gerard Meijer and Wieland Schöllkopf
*Fritz-Haber-Institut der Max-Planck-Gesellschaft,
 Berlin, D14195, Germany*

Allard P. Mosk
*Mesa⁺ Institute for Nanotechnology, University of Twente,
 Enschede, The Netherlands*

We have demonstrated trapping of cold ground-state ^{87}Rb atoms in a macroscopic AC electric trap.¹ Such an AC electric trap has been previously used to confine polar molecules.² In addition, electrodynamic trapping of Sr atoms has also been demonstrated on an atom chip.³ The operation principle of an AC electric trap for neutral particles⁴ is analogous to that of the Paul trap for ions. A potential energy surface is created with a saddle point at the trap center, resulting in attractive forces (focusing) in one direction and repulsive forces (defocusing) along the other two directions. The electric field configuration is then switched to a second one in which the roles of the forces are reversed. Alternating between these two configurations at the appropriate frequency leads to dynamic confinement of the particles. The calculated potential-well depths for Rb are on the order of $10\ \mu\text{K}$.

In the experiment, the Rb atoms are cooled in a standard MOT loaded from a Zeeman slower. After loading the atoms into a spatially overlapped quadrupole magnetic trap, a density on the order of $10^{10}\ \text{atoms}/\text{cm}^3$ and a temperature of about $100\ \mu\text{K}$ are measured. The cold Rb cloud is then transferred, by physically moving the magnetic field coils, into a second vacuum chamber housing the AC trap. High voltage is applied to the four AC trap electrodes after ensuring that the magnetic field is completely off.

We have observed trapping of about 10^5 atoms at a switching frequency of 60 Hz with trap lifetimes on the order of 5 s. Absorption images of the Rb cloud taken at various phases of the AC switching cycle show changing shapes, reflecting the focusing and defocusing forces acting on the atoms along the r and z directions (see Fig. 1). In addition, we have observed

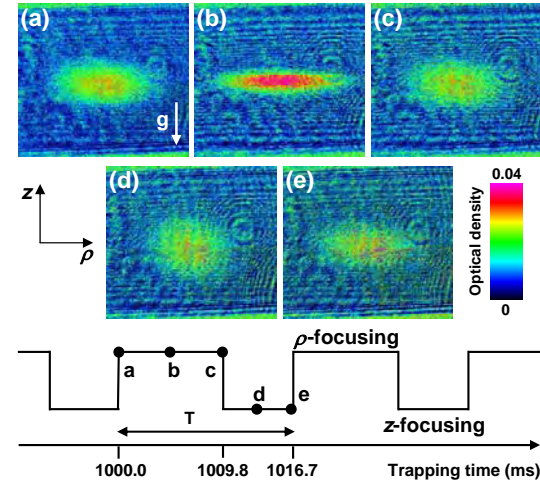


Fig. 1. Absorption images of the Rb cloud at different times within the 61st switching cycle, i.e., at the beginning, middle, and end of the ρ -focusing (a-c) and at the middle and end of the z -focusing (d,e) phase. The corresponding times are indicated in the switching pattern; the switching frequency is 60 Hz, giving a period of $T = 16.7$ ms. The image area is $2.2 \times 2\ \text{mm}^2$, such that the field of view covers exactly the space between the two ring electrodes. Each image is obtained by averaging 100 pictures and the corresponding optical density is indicated by the color scale.

a strong dependence of the number of trapped atoms on the switching frequency, in agreement with trajectory calculations.

Acknowledgments

This work is part of the research program of the “Stichting voor Fundamenteel Onderzoek der Materie (FOM)”. A. M. is a research fellow of the Alexander von Humboldt Foundation.

References

1. S. Schlunk *et al.*, <http://arxiv.org/abs/physics/0702119> (2007), accepted for publication in *Phys. Rev. Lett.*
2. J. van Veldhoven, H. L. Bethlem, and G. Meijer, *Phys. Rev. Lett.* **94**, 083001 (2005).
3. T. Kishimoto *et al.*, *Phys. Rev. Lett.* **96**, 123001 (2006).
4. E. Peik, *Eur. Phys. J. D* **6**, 179 (1999).

Frequency Comb Spectroscopy of Laser Cooled Rubidium-85

M. Maric, J.J. McFerran, and A.N. Luiten
*Physics M013, University of Western Australia,
 Nedlands, WA 6009, Australia*
 *E-mail: andre@physics.uwa.edu.au
www.fsm.physics.uwa.edu.au

We will report accurate laser spectroscopy of the Rubidium D₁ line using a continuous wave laser that has been frequency stabilized to a frequency comb.

Keywords: Laser Spectroscopy, Rubidium, Frequency Comb

Frequency combs emitted by mode-locked lasers (MLL) are providing the basis for a revolution in laser spectroscopy by giving a means for simple and accurate optical frequency measurements. An MLL generates a set of optical signals with frequencies given by $f_n = f_0 + n f_r$, where the two frequencies f_0 (offset frequency) and f_r (repetition rate) are readily measurable. We will make use of an optical frequency comb to perform accurate spectroscopic measurements on the $5P_{1/2}$ level of laser cooled ^{85}Rb atoms. The hyperfine splitting of this level is known only at the 7-40 kHz level with a large discrepancy between the results from the two leading groups.^{1,2} The use of a laser cooled sample, in contrast to the vapour measurements of the past, avoids collisional shifts and eliminates peak pulling from nearby cross-over peaks. In our first spectroscopic measurement we used the frequency comb directly on the atoms. In the second technique we frequency locked a continuous-wave tunable laser to a mode of the frequency comb and used this stronger cw signal to drive the optical transition.

The Ti:sapphire MLL produces pulses with a spectral width of 20nm centered on 805 nm overlapping the D₁ and D₂ lines of Rubidium. This laser interrogates a Rb magneto-optical trap (MOT) that holds approximately 10^7 atoms at a temperature of around $100\mu\text{K}$. For the initial direct comb experiments a 1 s cooling and preparation phase left atoms in the $5S_{1/2}$, $F=3$ ground state (see Fig. 1a). This was followed by 3 ms interaction between the pulse train and atoms, and then a read-out phase to measure the number of atoms left in the initial state. The MLL repetition rate was scanned

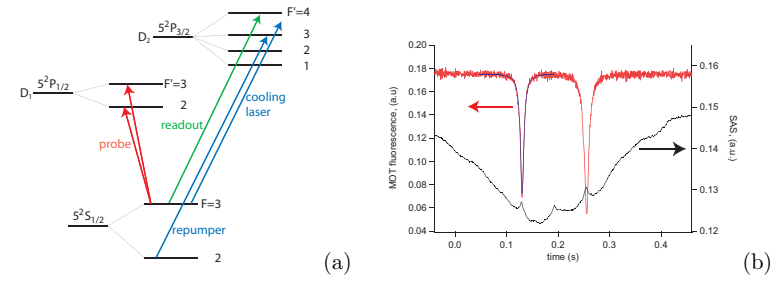


Fig. 1. (a) Simplified schematic of the energy levels of Rb. In addition, we show the cooling and repumper laser that form the Rb MOT, the probe laser provided by an optical frequency comb or the stabilized cw Ti:S laser. The read-out laser was used to measure the number of atoms left after interrogation (b) Preliminary results of MOT fluorescence as a cw laser is scanned through the D₁ line. The second trace shows the saturated absorption spectrum of a Rb vapour cell.

over 20 kHz (optical tuning range of around 7 GHz) in 10Hz steps and narrow dark resonances were observed when a mode of the MLL induces a transition. It was not possible to stabilize the offset frequency of the comb in this experiment as all the comb power was needed to drive transitions in the laser cooled sample.³ The absence of stabilization causes indeterminable optical frequency shifts at the level of a few MHz over the duration of the experiment.

In order to overcome this issue a tunable cw Ti:S laser was stabilized with a frequency-locked loop⁴ to a mode of the comb with a fractional frequency instability of around 10^{-12} . In addition, the optical comb mode frequencies were stabilized to better than 10^{-13} by locking the repetition rate to a H-maser referenced synthesizer, and the offset frequency using the self-referencing technique.³ In this case we observed strong and narrow absorption features as the cw laser is scanned across the D₁ line. A preliminary measurement of the MOT fluorescence is shown in Fig. 1b. We will present frequency measurements at the conference.

References

1. G.P. Barwood, P. Gill, W.R.C. Rowley, *Appl. Phys. B* **53**, 142-147 (1991).
2. D. Das, V. Natarajan, *Eur. Phys. J. D.* **37**, 313-317, (2006).
3. S. T. Cundiff, Jun Ye, *Rev. Modern Phys.* **75**, 325-342, (2003).
4. T Stace, AN Luiten, RP Kovacich, *Meas. Sci. Technol.* **9**, 1635-1637, (1998).

DIRECT SPECTROSCOPY OF CESIUM IN A VAPOR CELL WITH A FEMTOSECOND LASER FREQUENCY COMB

Vela L. Mbele¹, Jason E. Stalnaker, Tara M. Fortier, Scott A. Diddams*, Leo Hollberg, Vladislav Gerjinov² and Carol A. Tanner²

National Institute of Standards and Technology, 325 Broadway MS 847, Boulder, CO 80305,

¹National Metrology Institute of South Africa, P.O. Box 395, Pretoria, 0001, and the School of Physics, University of the Witwatersrand, Private Bag 3, WITS, 2050, RSA,

²Department of Physics, University of Notre Dame, Notre Dame, Indiana 46556-5670
*E-mail: sdiddams@boulder.nist.gov

We excite, using a comb of modes from a mode-locked Ti: Sapphire laser, the low lying even parity states $8s\ ^2S_{1/2}$, $9s\ ^2S_{1/2}$, and $7d\ ^2D_{3/2,5/2}$ in a neutral cesium vapor at room temperature. The output from a single femtosecond frequency comb is split, focused and sent counterpropagating to the atomic vapor. Laser induced fluorescence of the decay from $7p$ states is detected by a photo multiplier tube (PMT). Figure 1(a) shows the

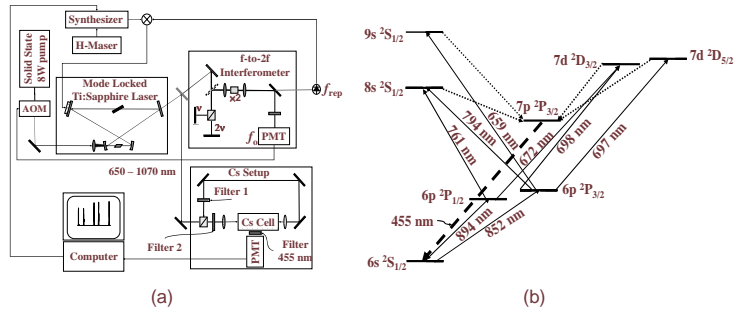


Fig. 1. The experimental arrangement, and the energy diagram of the states excited in this work.

experimental setup and Fig. 1(b) the states excited with their excitation pathways and decay scheme. The collected spectrum is rich, containing no

fewer than 90 resonance peaks and a broad background. The narrow peaks are due to stepwise excitation of two-photon transitions by the counterpropagating light fields. Filtering the light beams selects only comb modes near specific atomic transitions, allowing for the isolation and identification of the excited states. Using a simple two-photon transition probabilities equation¹ the spectra can be simulated. Figure 2(a) shows the entire collected fluorescence spectrum (without filters), and Fig. 2(b) shows the collected and calculated 9S spectra. Using nonlinear least squares fitting routines we extract the center of gravity frequencies with statistical fractional uncertainties $< 10^{-10}$. The hyperfine electric quadrupole coupling for the $7D$ states is measured for the first time, to our knowledge. The total uncertainties are estimated not to exceed 100 kHz for the absolute frequencies. These uncertainties are comparable to a recent report² of the $8S$ state, and represent two orders of magnitude improvements in measurements of the other states.³⁻⁵

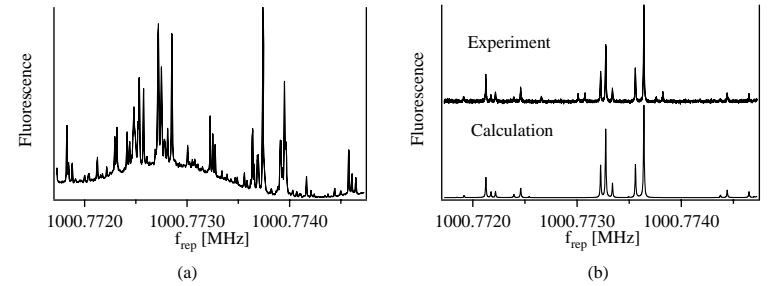


Fig. 2. The spectrum collected without filtering the counterpropagating light beams is shown in (a), while (b) shows the collected and calculated 9S spectra.

References

1. W. Demtröder, *Laser Spectroscopy: Basic Concepts and Instrumentation*, third edn. (Springer, New York, 2003).
2. P. Fendel, S. D. Bergeson, T. Udem and T. W. Hänsch, *Optics letters* **32**, 701 (2007).
3. G. Hagel, C. Nesi, L. Jozefowski, C. Schwob, F. Biraben and A. Bartels, *Optics Comm.* **160**, 1 (1999).
4. K.-H. Weber and C. J. Sansonetti, *Phys. Rev. A* **35**, 4650 (1987).
5. E. Arimondo, M. Inguscio and P. Violino, *Rev. Mod. Phys.* **49**, 31 (1977).

A FUNDAMENTALLY MODE-LOCKED Yb-ER CO-DOPED FIBER LASER WITH A REPETITION RATE OF 860 MHz

J. J. MCFERRAN*, L. NENADOVIĆ, J. B. SCHLAGER and N. R. NEWBURY

*Optoelectronics Division, NIST, 325 Broadway,
Boulder, CO 80305, U.S.A.*

**E-mail: mcferran@boulder.nist.gov*

We report on the development of a passively mode-locked Yb-Er co-doped fiber laser with a repetition frequency, f_{rep} , of 860 MHz. The laser, centered at 1.54 μm , exhibits a single pulse per round trip and is free of Q-switching.

Keywords: Ytterbium; Erbium; Mode-locked laser; Fiber laser.

High repetition rate mode-locked lasers are advantageous in experiments requiring large mode spacing between comb elements, such as Fourier transform spectroscopy, frequency metrology and telecommunication applications. The high repetition rate laser described here uses a gain medium of phosphosilicate fiber co-doped with Yb and Er ions and has a core-pumped geometry. This fiber's application to mode-locked lasers appears rather infrequently. In one instance the Yb-Er fiber laser contained a semiconductor saturable absorber mirror (SAM),¹ where a fundamental f_{rep} of 295 MHz was achieved. In another development the saturable absorber is formed from single-walled carbon nanotubes,² where $f_{rep}=5$ GHz was produced. While this approach seems very promising, the robustness of the carbon nanotubes needs to be improved before mode-locked lasers based on the technology become reliable.³

The laser here is composed of 8 cm of Yb-Er co-doped fiber spliced to 2.5 cm of single-mode fiber (SMF). A standing wave cavity is formed between a SAM at one end and a partially reflective (95%) mirror at the input of the Yb-Er fiber, which acts as the output coupler. The light exiting the SMF is collimated, then focused by a second lens onto the SAM, where the spot size is $\sim 2.0 \mu\text{m}$ in radius. The gain fiber is driven by an optically pumped semiconductor laser with $\lambda = 977$ nm. The optical power reaching the fiber laser cavity is ~ 380 mW.

The SAM has a modulation depth of ~ 0.1 to facilitate mode-locking.

Its saturation fluence is $\sim 25 \mu\text{J}/\text{cm}^2$, relaxation time constant ~ 2 ps, non-saturable loss $\sim 10\%$, and the group delay dispersion is $\sim -2000 \text{ fs}^2$ at 1540 nm. Dispersion measurements of the Yb-Er fiber give $\beta_2 = +14.0 \pm 0.2 \text{ ps}^2/\text{km}$ at 1540 nm. Combined with the dispersion of the SMF and the SAM, the net group delay dispersion of the laser is $\sim -660 \text{ fs}^2$.

Fig. 1a shows a train of pulses emitted from the Yb-Er laser. The pulses exhibit constant amplitude indicating cw mode-locked behaviour. The microwave spectrum of Fig. 1b shows the f_{rep} signal and its harmonics out to high frequency. The uniform intensity of the harmonics indicates single pulse per round trip propagation.

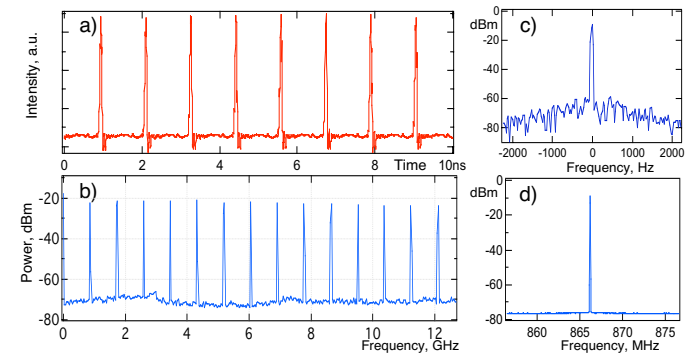


Fig. 1. a) Pulse train from the $f_{rep}=866$ MHz Yb-Er fiber laser; b), c) and d) RF spectra of light from the Yb-Er laser with rbw of 3 MHz, 30 Hz and 10 kHz, respectively.

Examining f_{rep} more closely (and offset to 0 Hz) we see the narrow feature shown in Fig. 1c (res. bw = 30 Hz). Fig. 1d displays f_{rep} with a span of 20 MHz, demonstrating the absence of sidebands associated with Q-switching. At present the spectral width of the pulses is limited by the bandwidth of the gain medium and this limits the pulse width to ~ 1.7 ps. Loss changes to the cavity have had little influence of the spectral output, however, attempts at gain flattening with filters may prove to be an effective means of manipulating the spectral width.

References

1. B. Collings, *et al.*, *IEEE J. Sel. Top. Quantum Electron.* **3**, 1065 (1997).
2. S. Yamashita, *et al.*, *IEEE Photonics Technol. Lett.* **17**, 750 (2005).
3. T. Schibli, *et al.*, *Opt. Express* **13**, 8025 (2005).

Cold atom gravimetry

T.E. Mehlstäubler, J. LeGouët, S. Merlet, D. Holleville, A. Clairon,

A. Landragin, F. Pereira Dos Santos

*SYRTE, Observatoire de Paris, 61 avenue de l'observatoire
75014 Paris, France*

* E-mail: tanja.mehlstaubler@obspm.fr
<http://lne-syrte.obspm.fr/>

Atom interferometers have shown in the past to be sensitive devices for the accurate measurement of acceleration,¹ rotation^{2,3} and gravity gradients,⁴ reaching performances of present state-of-the-art instruments. This turned them on one side into interesting candidates for applications such as gravity field mapping and inertial navigation,⁵ but as well into powerful instruments to address fundamental questions in physics, testing the equivalence principle or measuring the fine-structure constant.^{6,7} For ultra-sensitive measurements, space borne interferometers utilizing degenerate quantum gases are pursued.⁸

To push the limits of performance we are studying a ground based atom interferometer, used to measure absolute gravitational acceleration, and detail systematic effects, influencing the long term stability. Our experiment represents a compact portable gravimeter based on laser cooled rubidium atoms, which will be used in the Watt-Balance project of the LNE in Paris for the redefinition of the kg. Up to 10^7 atoms are loaded into a magneto-optical trap within 50 ms and cooled to temperatures of $2 \mu\text{K}$. The released and free falling atoms are brought into a coherent superposition of spatially separated internal states by stimulated Raman transitions. In a Mach-Zehnder type interferometer geometry with dark time T between the pulses the atoms collect a phase shift at the output port given by $\Delta\phi = \phi(0) - 2\phi(T) + \phi(2T)$, which is in ideal case related to g by $\Delta\phi = k_{eff}gT^2$. Our experiment permits to resolve the interferometric signal with a high sensitivity of $2 \times 10^{-8} \text{ g/Hz}^{\frac{1}{2}}$, currently limited only by vibrational noise. Digital filtering of the sismometer data, that are simultaneously recorded, promises a further reduction by a factor 2.

With a resolution of a few μGal we investigate the influence of several systematic effects such as residual magnetic field gradients, 1 and 2 photon light shifts, RF chirp, Coriolis forces and optical aberrations onto the phase shift of the interferometric signal and its effect on the long term stability of our measurement. In differential measurements with reversed k -vector the influence of some contributions (e.g. B-fields or light shift) can be separated, however strongly depends on a careful overlap of the atomic trajectories. With an improved interferometer scheme we prove a rejection of 10^3 in the differential measurement. The comparison of our atom interferometer with a commercial FG5 and A10 gravimeter is discussed.

Further on, we present the new vacuum chamber that is currently built in our lab. Here, larger optical access and the implementation of an optical dipole trap will allow for a better control of atomic residual velocities and thus a further improved accuracy.

References

1. A. Peters, K.Y. Chung and S. Chu, *Metrologia* **38**, 25 (2001).
2. T.L. Gustavson, P. Bouyer, M.A. Kasevich, *Phys. Rev. Lett.* **78**, 2046 (1997).
3. F. Yver-Leduc *et al*, *J. Opt. B* **5**, 136 (2003).
4. J.M. McGuirk *et al*, *Phys. Rev. A* **65**, 033608(2002).
5. N. Yu, J.M. Kohel, J.R. Kellogg and L. Maleki, *Appl. Phys. B* **84**, 647 (2006).
6. A. Wicht, J.M. Hensley, E. Sarajlic and S. Chu, *Phys. Scr.* **T102**, 82 (2002).
7. P. Clade *et al*, *Phys. Rev. Lett.* **96**, 033001 (2006).
8. R.A. Nyman *et al*, *Appl. Phys. B* **84**, 673 (2006).

Transfer of coherence enhanced stimulated emission and electromagnetically induced absorption in Zeeman split

$F_g \rightarrow F_e = F_g - 1$ atomic transitions

R. Meshulam, T. Zigdon, A. D. Wilson-Gordon, and H. Friedmann

Department of Chemistry, Bar-Ilan University, Ramat Gan 52900, Israel

We show that the probe absorption spectrum in multi-tripod systems, formed when a *weak* σ polarized pump and a tunable π polarized probe laser interact with an $F_g \rightarrow F_e = F_g - 1$ transition [see Fig. 1(a) and (b)], in the presence of a weak magnetic field, is characterized by two interfering stimulated Raman features separated by an electromagnetically induced absorption (EIA) peak at line center.

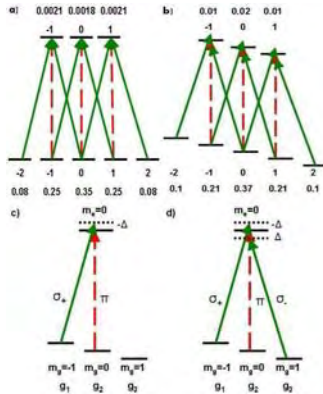


Fig. 1. Energy-level scheme for (a) and (b) $F_g = 2 \rightarrow F_e = 1$ in D_2 line of ^{85}Rb , (c) and (d) $F_g = 1 \rightarrow F_e = 0$ in D_2 line of ^{87}Rb . In (a) and (b), the populations of the Zeeman sublevels are written on the multi-tripod schemes for the parameters $V_1/\Gamma = 1$, $\Gamma_{gg}/\Gamma = 0.0005$, $\gamma/\Gamma = 0.001$, and $N = 10^{12}$ atoms cm^{-3} , with $B = 0$ in (a) and $B = 1\text{G}$ in (b). In (c), the pump is σ_+ polarized (Λ system) whereas in (d) the pump is σ_- polarized (tripod system).

At moderate pump intensities, the stimulated Raman features resemble electromagnetically induced transparency (EIT), windows as observed by Lezama *et al.* (see Fig. 8 of¹). However at higher pump Rabi frequencies, they appear as *stimulated emission peaks* centered near the Raman frequencies, which gradually become weaker and move towards line center as the pump becomes more intense. We show that both the central absorption peak and the stimulated emission peaks result from the combined effects of interfering stimulated Raman features and transfer of coherence (TOC) from the excited state to the ground state. TOC has previously been shown to lead to EIA in degenerate $F_g \rightarrow F_e = F_g + 1$ transitions,^{2,3} due to incomplete population trapping in the Zeeman sublevels of the ground state. Such incomplete population trapping also occurs in multi-tripod systems, when the degeneracy is lifted by applying a weak magnetic field [see Figs. 1(a) and (b)].

The origin of the stimulated emission peaks can be understood by considering a simple near-degenerate Λ system, such as the one shown in Fig. 1(c) formed when a near-degenerate $F_g = 1 \rightarrow F_e = 0$ transition is pumped by a near-resonant σ_+ polarized pump of frequency ω_1 , and probed by a tunable π polarized probe of frequency ω_2 . It can be shown both analytically and numerically, that when the pump is sufficiently weak so that optical pumping cannot completely overcome the repopulation of state $m_g = -1$ from the reservoir, stimulated emission appears at the Raman resonance frequency. When the pump is changed from σ_+ to σ_- polarization, under the same conditions, a tripod system is obtained [Fig. 1(d)] whose probe absorption spectrum consists of two stimulated emission peaks at the Raman frequencies, separated by a sharp EIA peak. At higher pump intensities, all the population is pumped into the $m_g = 0$ sublevel, and two EIT windows are obtained.⁴

References

1. A. Lezama, S. Barreiro, A. Lipsich and A. M. Akulshin, *Phys. Rev. A* **61**, 013801 (1999).
2. A. V. Taichenachev, A. M. Tumaikin and V. I. Yudin, *Phys. Rev. A* **61**, 011802(R) (1999).
3. C. Goren, A. D. Wilson-Gordon, M. Rosenbluh and H. Friedmann, *Phys. Rev. A* **67**, 033807 (2003).
4. C. Goren, A. D. Wilson-Gordon, M. Rosenbluh and H. Friedmann, *Phys. Rev. A* **69**, 063802 (2004).

SPECTRA OF BA AND BA⁺ IN SOLID AND LIQUID XE AND AR FOR BA TAGGING IN XE-136 DOUBLE BETA DECAY*

BRIAN MONG, SHIE-CHANG JENG, KENDY HALL, CESAR BENITEZ-MEDINA, SHON COOK AND WILLIAM M. FAIRBANK, JR.

*Physics Department, Colorado State University,
Fort Collins CO 80523-1875, USA*

FOR THE THE EXO COLLABORATION

As a step toward in-situ single ¹³⁶Ba daughter detection in neutrinoless double beta decay, we report spectra of Ba atoms in solid argon and xenon and Ba⁺ ions in liquid xenon.

To achieve a neutrino mass sensitivity of 0.01 eV in neutrinoless double beta decay, an isotopically enriched sample of ton size and zero background is required. In the Enriched Xenon Observatory (EXO) experiment, it is proposed that detection of the ¹³⁶Ba daughter ion from ¹³⁶Xe double beta decay by laser fluorescence will provide an additional signature leading to zero background [1]. This may occur in liquid xenon (LXe) at the decay site [2], after trapping the ion in solid xenon (SXe) on a cold fiber probe sent to the decay site, or in a linear trap after release from a probe removed from the detector. In this paper we report progress toward single Ba or Ba⁺ detection in LXe and SXe.

Absorption and emission spectra for Ba atoms in solid argon (SAr) and SXe have been taken by co-depositing Ba and Ar or Xe in high vacuum on a sapphire window or single-mode fiber cooled by a cryostat to around 15K. Results for SAr are shown in Figure 1. At low temperature, triplet absorption features from

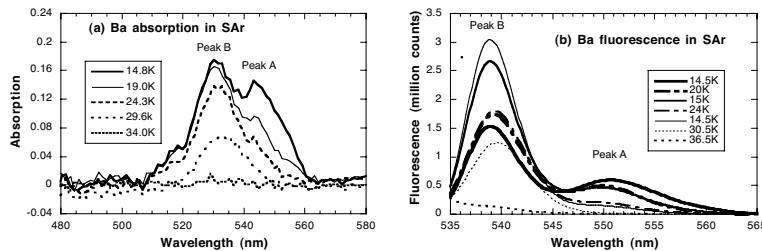


Figure 1. Absorption and emission spectra of 10^{13} Ba atoms in solid argon at different temperatures.

* This work is supported by the Department of Energy grant number DE-FG02-03ER41255.

two different lattice sites are observed. Two interesting temperature dependences are apparent. First, as the temperature is raised to 24K, site A absorption and emission converts to signal from site B. This is evidence for irreversible annealing of the lattice. Second, as the temperature is further raised, the fluorescence decreases, but then recovers as the temperature is lowered. This is likely a reversible temperature-dependent change in fluorescence efficiency. At around 34K, near the temperature where the SAr layer evaporates, absorption and emission disappear. Similar results are obtained in solid xenon, except that the corresponding temperatures are about 1.5x as high. Current work is focused on doing Ba in SAr and SXe spectroscopy on the end of a single mode fiber first using 10^7 atoms and then being able to detect one Ba atom. We are also preparing to do spectroscopy of Ba⁺ ions deposited in SAr and SXe.

Excitation and fluorescence spectra of $\sim 10^8$ Ba⁺ ions flowing in an electric field through LXe after creation by laser ablation above the surface are shown in Figure 2. Significant features are (a) the expected two or three broad peaks of the 6s-6p transition near the gas phase transitions (shown by arrows) and (b) a broader and red-shifted emission spectrum, which probably includes both the 6p-6s and 6p-5d transitions.

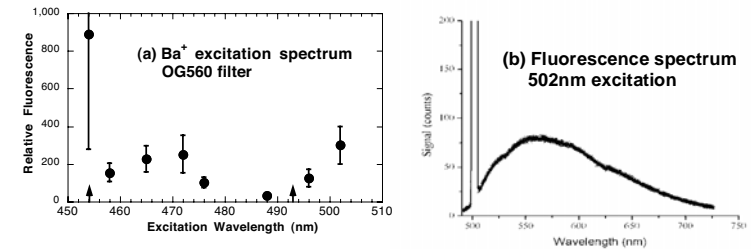


Figure 2. Excitation and emission spectra of 10^8 Ba⁺ ions in liquid xenon at 170K.

From observations to date, detection of single Ba atoms in SXe or single Ba⁺ ions in LXe or SXe is very promising with increased laser power and detection efficiency, repumping with a red laser to overcome population buildup in the 5d state and improved filtering to reduce stray light.

References

1. M. Danilov et al., *Phys. Lett. B* **480**, 12 (2000).
2. M. K. Moe, *Phys. Rev. C* **44**, R931 (1991).

BOSE-EINSTEIN-CONDENSATE INTERFEROMETER ON AN ATOM CHIP WITH A LONG COHERENCE TIME*

KEN'ICHI NAKAGAWA, MUNEKAZU HORIKOSHI†

Institute for Laser Sciencet, University of Electro-Communications, 1-5-1 Chofugaoka, Chofu, 182-8585, Japan

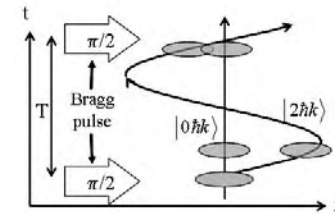
We demonstrate an atom interferometry with a long coherence time using Bose-Einstein condensates of ^{87}Rb atoms on an atom chip. Dephasing of wave packets due to the trap potential is reduced by applying two Bragg laser pulses with a time interval T equal to the oscillation period of the magnetic trap. We observe a high contrast ($\sim 30\%$) interference fringe signal for $T = 58$ ms.

Recently many attentions have been paid to atomic interferometry using Bose-Einstein condensates in a trap or waveguide because of its inherent long interrogation time [1-4]. However, the various dephasing effects due to the atom-atom interaction and/or the trap potential limit the maximum interrogation time [1-4]. Although the atom-atom interaction can be reduced by lowering the atomic density or using a number squeezed state of atoms [2,3], the dephasing due to the trap potential is still a problem for the realization of long interrogation time [4]. In this paper, we present a novel interferometer using Bose-Einstein condensates with a long interrogation time of more than 50 ms.

The experimental setup and procedure are similar to those of our previous experiment [4][5]. Bose-Einstein condensates of about 3×10^3 ^{87}Rb atoms in the $|F = 2, m_F = 2\rangle$ state is loaded into a micro magnetic trap on an atom chip [5]. The axial trap frequency (ν_{axial}) is about 17 Hz (or 10 Hz) and the radial trap frequency is 60 Hz. We use a Bragg diffraction of atoms using two off-resonance counter-propagating laser beams as a beam splitter for the atom [4]. A first $\pi/2$ Bragg laser pulse splits a condensate into two momentum components $|0\hbar k\rangle$ and $|2\hbar k\rangle$ ($k=2\pi/\lambda$, $\lambda \sim 779$ nm) (Fig. 1). The $|2\hbar k\rangle$ component starts to oscillate in a trap potential. If the anharmonicity of the trap potential is enough small, the collective mode motion of the condensate is hardly excited during the

2

oscillation and the dephasing due to the atom-atom interaction can be minimized. When the $|2\hbar k\rangle$ component returns to the initial position, a second $\pi/2$ pulse is applied to recombine these two components. If the time interval T between two pulses is equal to the trap oscillation period ($= 1/\nu_{\text{axial}}$), the dephasing due to the trap potential is cancelled and a high contrast ($\sim 30\%$) interference signal is observed for $T = 58$ ms (Fig. 2 (a)). When we increase the time interval T to 97 ms ($\nu_{\text{axial}} = 10$ Hz), an interference fringe is washed out (Fig. 2 (b)). We attribute this contrast degradation to the external vibrational noise which randomly modulates the optical phase of the Bragg pulses. Further improvements in the vibrational isolation will allow to realize an interrogation



time of longer than 100 ms.

Figure 1. A schematic diagram of the interferometer.

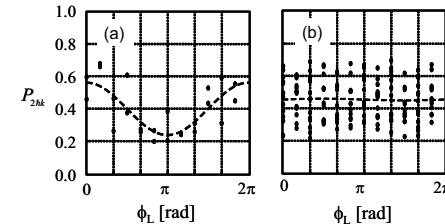


Figure 2. Interference fringe signals for $T = 58$ ms (a) and $T = 97$ ms (b).

References

1. O. Garcia et al., Phys. Rev. A 74, 031601(R) (2006).
2. G.-B. Jo et al., Phys. Rev. Lett. 98, 030407 (2007).
3. Wei Li et al., Phys. Rev. Lett. 98, 040402 (2007).
4. M. Horikoshi et al., Phys. Rev. A 74, 031602(R) (2006).
5. M. Horikoshi et al., Appl. Phys. B 82, 363 (2006).

* This work was partly supported by a Grant-in-Aids for Science Research (17340120) from the Ministry of Education, Science, Sports and Culture, and a Ground-based Research Program for Space Utilization promoted by Japan Space Forum.

† Present address: The University of Tokyo, Bunkyo-ku, Tokyo 113-8656, Japan.

PROBING COLD ATOMS USING A TAPERED OPTICAL FIBER*

SÍLE NIC CHORMAIC

*Physics Department, University College Cork, Cork, Ireland and
Photonics Centre, Tyndall National Institute, Prospect Row, Cork, Ireland*

MICHAEL MORRISSEY, THEJESH BANDI AND KIERAN DEASY†

*Department of Applied Physics and Instrumentation, Cork Institute of Technology,
Bishopstown, Cork, Ireland and
Photonics Centre, Tyndall National Institute, Prospect Row, Cork, Ireland*

We present our recent results on the use of the evanescent field from a tapered optical fiber to probe cold, rubidium atoms contained in a magneto-optical trap. We have used a UHV compatible nanopositioning motor in order to move the fiber through the trap region. Photons scattered by the atoms are coupled into the fiber and detected using a single photon counting module. This technique has allowed us to gather information on the size of the atomic cloud and to estimate the refractive index of the sample.

1. Introduction

Interest in the design and realization of micro-optics components to manipulate and control cold atomic samples has increased in recent years. One such component – the tapered optical fiber – has been theoretically shown to be a useful tool for trapping and guiding atoms [1]. Tapered optical fibers are fabricated by a heat-and-pull technique, while ensuring that the transmission through the fiber remains quasi-lossless during the pulling process. As the taper is formed, the core-cladding interface responsible for guiding the light within the fiber is replaced by a cladding-air interface. This leads to a significant portion of the light being guided outside the confines of the fiber, creating an exponentially decaying evanescent field. In order to be useful for atom optics, it is important that the wavelength of the light guided by the fiber be comparable to the diameter of the taper waist. In addition, if the fiber is too small, it has been shown that light will no longer be guided but will rather be lost outside of

* This work is funded by Science Foundation Ireland under grant 02/IN1/128.

† Work supported by the Irish Research Council for Science, Engineering and Technology through the Embark Initiative.

the fiber. This places strict limits on the size of taper suitable for atom optics experiments.

2. Experimental Details

In our experiments, we are interested in probing samples of magneto-optically trapped rubidium atoms through the photons in the evanescent field of a fiber taper. Our setup is configured such that a $1\ \mu\text{m}$ fiber taper, mounted on a nanopositioning, UHV compatible stage (Fig. 1), can be translated through the cloud of atoms, thereby enabling us to study the profile of the atomic cloud and to estimate several associated parameters, such as the refractive index. We use single-mode 780 nm fiber, tapered using a heat-and-pull rig as described in [2]. The fiber has a typical transmission of 85% and no loss was recorded during the pump down and bake out of the vacuum system. The number of atoms interacting with the evanescent field depends on the atomic cloud density and the fiber waist. We are currently considering light scattered from the atoms and coupled into the fiber, which leads to very low light levels. A single photon counting module is being used to monitor the coupled light into the fiber.

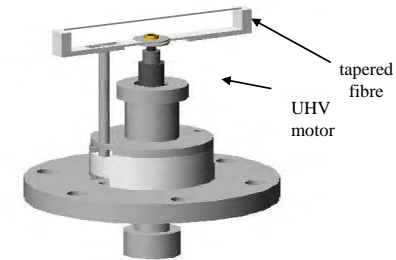


Figure 1. Schematic of the fiber taper mounted on the nanopositioning motor.

References

1. V. I. Balykin, K. Hakuta, F. Le Kien, J. Q. Liang, and M. Morinaga, *Phys. Rev. A* **70**, 011401 (2004).
2. J. M. Ward, D. G. O'Shea, B. J. Shortt and S. Nic Chormaic, *Rev. Sci. Instrum.* **77**, 083105 (2006).

LASER PRODUCED SPECTRA OF SiC MOLECULE IN THE REGION OF 370 – 570 NM

K. S. OJHA

Laser & Spectroscopy Laboratory, Department of Physics
University of Allahabad, Allahabad, 211002, India

R. GOPAL

Laser & Spectroscopy Laboratory, Department of Physics
University of Allahabad, Allahabad, 21002, India

The emission spectra of SiC molecule are reinvestigated in the region of 370 – 570 nm using laser ablation technique. About 120 bands are recorded in this region and analyzed into two band systems $G^3\Pi-X^3\Pi$ and $G^3\Pi-A^3\Sigma^-$. The determined molecular constants of $X^3\Pi$, $A^3\Sigma^-$ and $G^3\Pi$ states are in close agreement to that reported by earlier workers.

1. Introduction

SiC molecule is of astrophysical importance since it is observed in carbon stars, stellar atmospheres and in the interstellar molecular clouds. Ebben *et al.*[1] observed seven bands of $C^3\Pi-X^3\Pi$ system in the region of 384 – 442 using laser vaporization technique and modified the vibrational and rotational constants of the $C^3\Pi$ and $X^3\Pi$ states. Butenhoff *et al.*[2] reported LIF spectroscopic investigation of $C^3\Pi-X^3\Pi$ band system and observed nine bands including first seven bands reported by Ebben *et al.*[1] and modified vibrational constants. Grutter *et al.*[3] observed three band systems $A^3\Sigma^-X^3\Pi$, $B^3\Sigma^+X^3\Pi$ and $C^3\Pi-X^3\Pi$ of SiC molecule in 5^0K neon matrices in absorption.

2. Experimental Setup

The SiC rod target is clamped inside the chamber with a rotating and translating target. The 120 mJ energy of 355 nm of Nd: YAG laser is focused using a convex lens of focal length 50 cm inside the ablation chamber. The produced plasma is allowed to cool adiabatically and the radiation from the cooled plasma is collected on the entrance slit of TRIAX 320 M monochromator. The spectra are recorded using 1200 grs/mm grating blazed at 330 nm and the bands of SiC molecule are appeared at 220 ns delay time.

E – Mail:kspectra12@yahoo.co.in

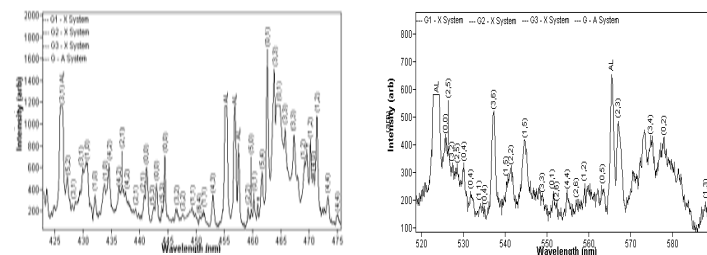
2

3. Results

Laser produced spectra of SiC molecule are reinvestigated in the region of 370 – 570 nm. The recorded spectra consist of about 120 bands and classified into two band systems $G^3\Pi-X^3\Pi$ (previously assigned as C–X) and $G^3\Pi-A^3\Sigma^-$. Out of 120 bands, 98 bands including the 9 bands reported by previous workers are assigned to three sub systems of G–X system. The remaining 22 bands are assigned to G–A system. Total 98 bands of G–X system are analyzed into $\Delta v = 0, \pm 1, \pm 2, \pm 3, \pm 4, + 5, + 6, + 7$ and $+ 8$ sequences while the 22 bands of G–A system are analyzed into $\Delta v = 0, \pm 1, \pm 2, + 3, + 4$ and $+ 5$ sequences. The molecular constants of $X^3\Pi$, $G^3\Pi$ and $A^3\Sigma^-$ states are modified and are given in Table 1. A portion of spectra are shown in figures 1 and 2.

Table 1. Molecular constants of SiC molecule.

State	T_e	ω_e	$\omega_e x_e$	$\omega_e y_e$
$C^3\Pi$	22830.19	615.80	9.75	0.05
$A^3\Sigma^-$	3691.36	862.20	4.92	-0.25
$X^3\Pi$	0.00	965.20	5.95	0.58



Figures 1 and 2. Laser produced spectra of SiC molecule

Acknowledgments

The authors are thankful to Department of Science & Technology, New Delhi (India) for financial support.

References

1. M.Ebben, M.Drabbels and J.J.ter Meulen, *J.Chem.Phys.*, **95(4)**, 2292 (1991).
2. T. J. Butenhoff and E. A. Rohlffing, *J. Chem. Phys.*, **95 (6)**, 3939 (1991).
3. M. Grutter, P. Freivogel and J. P. Maier, *J. Phys. Chem.A*, 101, 275 (1997).

Coherent atomic nano-beam

F. Perales¹, J. Robert², J. Baudon¹, M. Ducloy¹

(1) *Laboratoire de Physique des Lasers (UMR-CNRS 7538), Université Paris 13, Avenue J.B. Clement, 93430-Villetaneuse, France*

(2) *Laboratoire Aimé Cotton (UPR-CNRS 3321), Université Paris-Sud, Bât. 505, 91405-Orsay cedex, France*

Because of their wide range of applications high-brightness, narrow-aperture and large-coherence atom beams have been actively developed. Possible applications are coherent atom optics experiments, atomic lithography or deposition at a sub-micrometric scale as well as (after slowing) loading of atomic traps and further production of Bose-Einstein condensates. In most cases, the tools used to manipulate the external atomic motion are various 1D and 2D material masks, resonant or quasi-resonant laser beams and light standing waves, electric or magnetic fields [1]. Spatial resolution is generally limited by beam diffraction. Indeed material wave packets spread during the propagation in free space due to velocity-position uncertainty relations. These diffraction phenomena put fundamental limits to the focusing accuracy in atomic and optical lithography: focusing can be improved only at the expense of field depth. We propose here a novel way of generating a matter wave which spreads very slightly as it propagates. This is obtained by fashioning an atom beam profile inside a special type of Stern-Gerlach atomic interferometer [2, 3]. It is the atomic counterpart of the bi-refringent crystal-plate interferometer, where the atom spin plays the role of the light polarisation. The peculiar transverse profile (a narrow central bright fringe surrounded by a wide dark one), as provided by adequate matter refraction indices, i.e. an adequate magnetic field configuration, closely resembles a Lorentzian profile. This profile, contrary to a Gaussian profile, is much less sensitive to diffraction because of its smoother wings. In spite of a size as small as a few tens of nm, this profile remains almost identical during propagation, and diverges much less than Gaussian beams. In a sense, it is the equivalent for matter waves of Bessel beams in light propagation [4].

The field configuration able to produce the phase-shift required to get the adequate profile consists of two adjacent opposite quadrupoles (within which the magnetic gradient G is radial and constant), and a homogeneous magnetic field b added to the second one. Under such conditions Zeeman sub-levels (M) accumulate along a straight-line trajectory at a distance ρ from the axis, the phase-shift $M\Phi$, with $\Phi = C v^{-1} G (\sqrt{\rho^2 + (b/G)^2} - \rho)$, where v is the atom velocity and C a constant. The width $\Delta\rho$ (FWHM) of the corresponding beam profile (in $\sin^2\Phi$) is given by width $\Delta\rho$ of the central peak (FWHM) is given by: $\Delta\rho = 3b/(2G)$. As the field b is aimed to produce a phase-shift $\pi/2$ over a path of few cm, its magnitude is small (\sim mGauss). Hence, even with a modest gradient, it is possible to get a width of a few tens of nm, e.g. $\Delta\rho = 15$ nm for $G = 10^2$ Gauss/mm.

Numerical simulations based upon the Huygens-Fresnel integral show that, in the so-called saturation regime, the final amplitude on the observation screen at a distance r from the axis is the product of the Gaussian amplitude $u_G(r)$ obtained when the interferometer is absent, by an "interferometric factor" $[1 + (\omega r)^2]^{-1/2}$, where ω is proportional to the magnetic gradient. The use of the device as a lithographic tool or a probe of composite surfaces obviously implies that a target is placed beyond the phase object, at least at a few mm from what we called "observation screen". Therefore the free propagation of the beam beyond the

interferometer needs to be examined. Calculations show that the width of the beam profile Δr increases with the distance Z beyond the end of the device much slower than the width of the diffraction pattern of a simple circular hole or a Gaussian profile of a diameter comparable to the initial width of the Lorentzian profile (twice 50 nm in the present case) (see fig.1). Such a type of almost "non-diffracting" beam, rather similar to the so-called "Bessel beams" in light optics [4], is of a great practical interest in so far as it allows us to leave some free space (few cm) between the interferometer and the target. It is worth noting that, in the present device, the atoms do not interact with material walls, contrarily to what would happen with a diaphragm of a diameter as small as 100 nm. As the angular aperture of the beam is extremely small, the brightness defined as $\mathcal{W} = (F/A) \Delta\Omega^{-1} (v/\delta v)$, where F is the atom flux, A the beam cross section, $\Delta\Omega$ the solid angle of divergence and $\delta v/v$ the relative velocity spread, is generally higher than those previously obtained (\mathcal{W} of a few 10^{20} atoms/s/mm²/str).

References

- [1] For a review, see: D. Meschede and H. Metcalf, *J. Phys. D: Appl. Phys.*, **36**, R17 (2003) and references therein ; S. Nowak, T. Pfau, J. Mlynek, *Microelectronic Engineering* **35** (1-4): 427-430, (1997) ; M. Cashen and H. Metcalf, *J. Opt. Soc. Am. B* **20**, 915 (2003)
- [2] J. Robert *et al.*, *J. Phys II, France* **4**, 2061 (1994) ; B. Viaris de Lesegno *et al.*, *Eur. Phys. J.D.* **23**, 25 (2003)
- [3] F. Perales, J. Robert, J. Baudon, M. Ducloy, *Europhysics letters*, in press (2007)
- [4] J. Durnin, *J.O.S.A. A*, **4**, 651 (1987); J. Durnin, J.J. Miceli Jr and J.H. Eberly, *Phys. Rev. Lett.*, **58**, 1499 (1987); N. Trappe, R. Mahon, W. Lanigan, J.A. Murphy, S. Withington, *Infrared Physics & Technology*, **46**, 233 (2005)

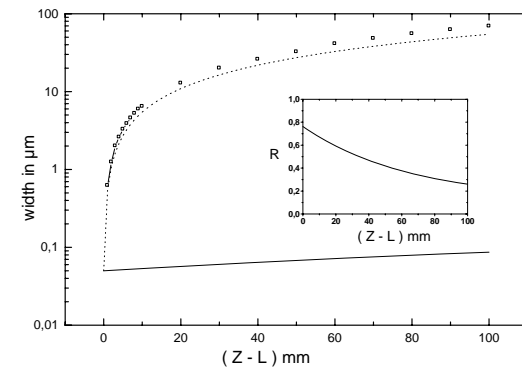


Fig.1. Free evolution of the peak width beyond the interferometer and the screen plane located at $z = L$. ($Z > L = 1.1$ m). Full line: present quasi-Lorentzian profile at position L (diameter at $1/e^3$: 100 nm, $G = 240.66$ Gauss/mm), half width to $1/e^3$ 1_{\max} as a function of the distance $Z - L$. Dotted line: Gaussian source at L (diameter at $1/e^3$: 100 nm), evolution of the half width to $1/e^3$. Open squares: circular hole at $z = L$ (diameter 100 nm), evolution of the half width to the first zero of the diffraction pattern. *Inset*: relative intensity as a function of the distance for the quasi-Lorentz source. Note the slow decrease of R . (From Ref. [3])

Optical monitoring of molecular oxygen and water vapor in human sinuses using tunable diode laser spectroscopy

L. Persson*, M. Andersson, M. Cassel-Engquist, T. Svensson,
K. Svanberg, and S. Svanberg

Medical Laser Centre, Lund University, P.O. Box 118, SE-221 00 Lund, Sweden

*E-mail: linda.persson@fysik.lth.se, <http://www-atom.fysik.lth.se>

We present spectroscopic measurements of molecular oxygen and water vapor within human maxillary sinuses, including gas exchange between nasal cavity and sinus. Volunteers with and without sinus problems were compared, and significant differences were observed.

Annually 37 million people in US get diagnosed with sinusitis (sinus inflammation).¹ Being air filled in a healthy state, sinuses become filled with liquid during sinusitis. Antibiotics are sometimes utilized without a firm diagnosis. X-ray computerized tomography (CT) is a good modality, but uses ionizing radiation and is expensive. Therefore, there is a need for a new non-invasive method to support and complement already existing ones.²

In this report, we present a new spectroscopic method to investigate the human sinuses. The technique is based on tunable diode laser spectroscopy. Pigtailed DFB lasers are repetitively wavelength-tuned across a molecular oxygen absorption line around 760 nm and a water vapor absorption line around 935 nm. High sensitivity is achieved by imposing a modulation on the laser driver current and employing second-harmonic lock-in detection. The light is split into two optical fibers in order to allow balanced detection to suppress common noise such as laser noise and optical interference fringes. One of the fibers goes directly to a detector while the other fiber is brought to a position close to the sinus of the volunteer, and the scattered light is detected on the other side of the sinus. A so-called equivalent mean path length, L_{eq} , is estimated corresponding to the distance that light has to travel in ambient air to yield the same oxygen absorption imprint.³

Fig. 1a shows a CT image of a volunteer with constantly recurring sinus-problems. Measurements were performed on this volunteer as well as on a

volunteer with no history of sinus problems. In Fig. 1b the average L_{eq} on both left and right maxillary sinuses of the two volunteers are presented for measurements during ten days. It can clearly be seen that a significant difference in the signal level is obtained between the two volunteers. The status of the passages between the nasal cavity and the sinuses was investigated by flushing N_2 into the nostril during a certain time while continuously measuring L_{eq} . The volunteer with sinus problem did not show any different signal level during the flush of N_2 , while on the healthy volunteer a decrease of the oxygen level was recorded. The reinvasion of oxygen was also recorded after ending the N_2 flush; see Fig. 1c. We are also able to monitor molecular H_2O and have demonstrated O_2 signals normalized on H_2O to yield the absolute O_2 concentration.⁴

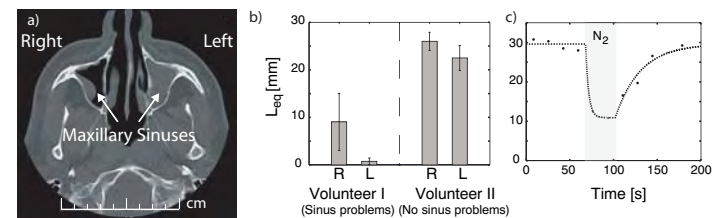


Fig. 1. a) CT-image of volunteer I with constantly recurring sinus-problem. b) Recorded L_{eq} from the maxillary sinuses of volunteer I and II together with one standard deviation. c) Monitored L_{eq} when flushing with N_2 of left maxillary of volunteer II.

In conclusion, we have shown the feasibility of sinus investigation by using a spectroscopic method based on balanced detection of oxygen and water vapor absorption. The possibility to study the gas exchange between the nasal cavity and the maxillary sinuses was also successfully demonstrated. To investigate the clinical use of the method, a clinical trial is planned.

References

1. Health Matters, Sinusitis, Nat. Inst. of Allergy and Infectious Diseases (US Dept. of Health and Human Services, Bethesda, 2005).
2. L. Persson, K. Svanberg and S. Svanberg, *Appl. Phys. B* **82**, 313 (2006).
3. L. Persson, F. Andersson, M. Andersson and S. Svanberg, *In press, Appl. Phys. B* (2007).
4. L. Persson, M. Andersson, M. Cassel-Engquist, K. Svanberg and S. Svanberg, Gas monitoring in human sinuses using tunable diode laser spectroscopy, Submitted to Journal of Biomedical Optics, (2007).

BRAGG SPECTROSCOPY OF A ^{85}Rb BEC WITH TUNABLE INTERACTIONS

JUAN PINO, SCOTT PAPP, ROBERT WILD, DEBORAH JIN, ERIC CORNELL

*JILA, University of Colorado, 440 UCB
Boulder, CO 80309, USA*

Bragg spectroscopy has been shown to be not only a useful tool in mapping the dispersion relation of a Bose Einstein condensate, but also in identifying the energetic contributions of the interparticle interactions within the condensate. By preparing a Bose condensed gas of ^{85}Rb atoms, we have experimental control of these interactions via the magnetically tunable Feshbach resonance. We report on recent experiments, including the role of many body effects on the dispersion relation of our condensate in the regime where na^3 is no longer small.

Low noise RF and Optical Signals Derived from Stabilized Optical Frequency Combs

Qudsia Quraishi^{1,2}, Vela Mbele^{1,3}, Scott A. Diddams¹ and Leo Hollberg^{1*}

¹National Institute of Standards and Technology, 325 Broadway MS 847, Boulder, CO 80305,

²Department of Physics, University of Colorado, Boulder, CO 80305

³National Metrology Institute of South Africa, P.O. Box 395, Pretoria, 0001, and the School of Physics, University of the Witwatersrand, Private Bag 3, WITS, 2050, RSA,

*E-mail: leo.hollberg@nist.gov

We generate low phase noise radio frequency (RF) and optical frequencies using the discretely spaced optical frequencies emitted by pulsed Titanium:Sapphire (Ti:S) lasers [Fig. 1(a)]. We study the phase noise properties of the RF and optical signals when two of the Ti:S laser's free parameters are electronically controlled, namely, the spacing between emitted optical frequencies f_{rep} and the uniform offset of all of the modes f_0 [Fig. 1(b)].¹⁻³

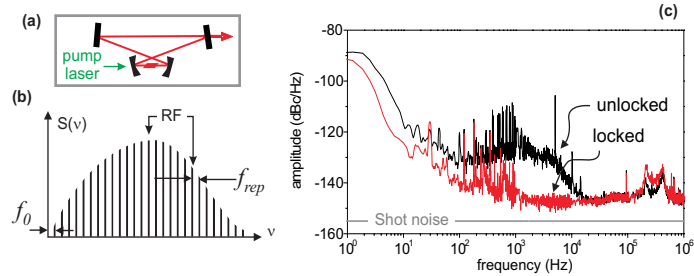


Fig. 1. (a) a 1 GHz repetition rate Ti:S laser (b) optical frequency comb and (c) amplitude noise on an RF signal at 10 GHz derived from an optical frequency comb when f_0 is locked and unlocked.

We demonstrate that the amplitude noise, for an RF signal derived from the optical frequency comb [Fig. 1(b)], is strongly correlated to the Ti:S pump laser amplitude noise. We see that phase locking f_0 is tantamount

to amplitude noise control of the Ti:S's pump laser and serves to mitigate deleterious effects of amplitude noise on microwave signals derived from frequency combs. Therefore, amplitude noise on the pump causes amplitude (and phase) noise on f_0 and in turn on the microwave signal derived from the repetition rate of the comb. Figure 1(c) shows the reduction of the amplitude noise on a 10 GHz carrier derived from the frequency comb when only f_0 is phase locked.

Additionally, we show that we can employ a stabilized optical frequency comb for high resolution spectroscopy. Using a high resolution spatial disperser [a virtually imaged phase array (VIPA) in combination with a diffraction grating] we are able to resolve, and record the power of, individual comb modes [Fig. 2(a)] with a spacing of 3 GHz. When a I_2 gas sample is placed within the spectrometer we observe absorption of individual comb modes [Fig. 2(b)].⁴ This approach provides high spectral resolution over broad bandwidth with simple and rapid data acquisition.

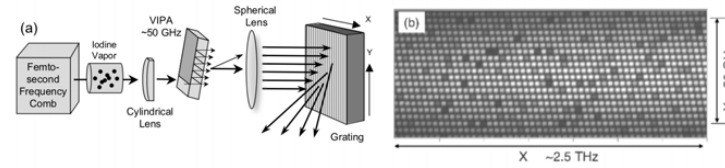


Fig. 2. (a) Schematic of the high resolution VIPA spectrometer and (b) two dimensional CCD image of the power of individual comb modes (spaced by 3 GHz). The absorption by I_2 is marked by the appearance of dark regions (where light regions correspond to full transmission of the mode).

References

1. S. A. Diddams, T. Udem, J. C. Bergquist, *et al.*, *Science* **293**, 825 (2001).
2. Th. Udem, R. Holzwarth and T. W. Haensch, *Nature* **416**, p. 233 (2002).
3. A. Bartels, C. W. Oates, L. Hollberg and S. Diddams, *Opt. Lett.* **29**, p. 1081 (2004).
4. S. A. Diddams, L. Hollberg and V. Mbele, *Nature* **445**, p. 627 (2007).

Frozen and not-so-frozen Rydberg gases

M. Reetz-Lamour*, T. Amthor, C. Giese, J. Denskat, and M. Weidemüller

Physikalisches Institut, Universität Freiburg,
Hermann-Herder-Str. 3, 79108 Freiburg, Germany

*E-mail: m.rlamour@physik.uni-freiburg.de
http://quantendynamik.physik.uni-freiburg.de

Due to the long-range character of the interaction between highly excited atoms, the dynamics of an ultracold gas of Rydberg atoms is entirely determined by van-der-Waals and dipole-dipole interactions. One outstanding property is the tunability of interaction strength and character which allows one to explore the transition from a weakly coupled two-body system to a strongly coupled many-body system. While the gas is ultimately unstable against autoionization there is a sufficiently large time window to study coherent processes and many-body entanglement in the frozen gas. In a recent series of experiments we studied both coherent phenomena in an ultracold gas of Rydberg atoms and important decoherence mechanisms.

Our experiment starts from a magneto-optically trapped cloud of ^{87}Rb atoms. Exciting into Rydberg states by narrow-bandwidth cw-lasers we achieve excitation efficiencies exceeding 90%¹ by using stimulated adiabatic passage and recently succeeded in driving synchronous Rabi oscillations of a mesoscopic ensemble of about 100 atoms between the atomic ground state and the Rydberg state.² One spectacular effect of Rydberg–Rydberg interactions is the dipole blockade, *i.e.* the inhibition of multiple Rydberg excitations in a confined volume induced by dipole interactions. We observe a suppression of Rydberg excitation as a local dipole blockade in a macroscopic and in a structured mesoscopic ensemble.^{2,3} Rydberg atoms can be seen as a prototype system to investigate resonant energy transfer processes, which play an important role *e.g.* in many biological systems (Förster processes). We present a model describing the many-body character of this energy transfer in a frozen gas and compare it with density-dependent measurements.⁴ The good agreement underlines the coherent character of the resonant energy transfer. Ultimately, cold Rydberg gases are unstable as the

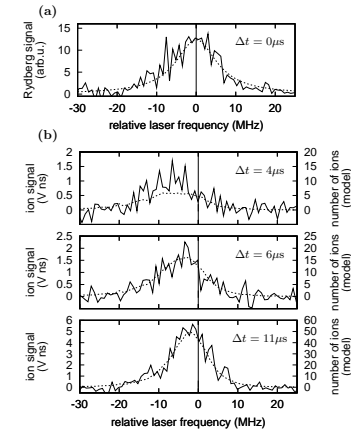


Fig. 1. Spectroscopic signature of atomic motion induced by long-range van der Waals forces.⁵ (a) Excitation resonance of the $60\text{D}_{5/2}$ state. (b) Evolution of the Penning ionization signal for different interaction times compared to Monte-Carlo simulations (dotted) which describe the atomic motion due to long-range van der Waals forces.

attractive interaction between atoms can lead to acceleration, collisions, and finally Penning ionization. We present spectroscopically resolved measurements of the ionization dynamics, which allow us to follow the acceleration of the atoms due to van-der-Waals interactions in real time.⁵ Comparison with a model as shown in Fig. 1 yields the strength of the interaction, which agrees well with predictions.⁶ Decay processes and many-body effects can lead to ionizing collisions even for repulsive interactions.

References

1. J. Deiglmayr, M. Reetz-Lamour, T. Amthor, S. Westermann, K. Singer, A. L. de Oliveira and M. Weidemüller, *Opt. Comm.* **264**, p. 293 (2006).
2. M. Reetz-Lamour, J. Deiglmayr, T. Amthor and M. Weidemüller, *in prep.* (2007).
3. K. Singer, M. Reetz-Lamour, T. Amthor, L. Marcassa and M. Weidemüller, *Phys. Rev. Lett.* **93**, p. 163001 (2004).
4. S. Westermann, T. Amthor, A. L. de Oliveira, J. Deiglmayr, M. Reetz-Lamour and M. Weidemüller, *Eur. Phys. J. D* **40**, p. 37 (2006).
5. T. Amthor, M. Reetz-Lamour, S. Westermann, J. Denskat and M. Weidemüller, *Phys. Rev. Lett.* **98**, p. 023004 (2007).
6. K. Singer, J. Stanojevic, M. Weidemüller and R. Côté, *J. Phys. B* **38**, p. S295 (2005).

Deterministic coupling of a single trapped atom to the mode of a high finesse optical resonator

S. Reick*, W. Alt, I. Dotsenko, M. Khudaverdyan, A. Stiebeiner, and D. Meschede

Institute for Applied Physics, University of Bonn, D-53225, Germany

**E-mail: s.reick@iap.uni-bonn.de, www.iap.uni-bonn.de*

A single neutral atom is trapped in a standing-wave optical dipole trap and transported deterministically into the mode of a high-finesse optical resonator. We detect the continuous coupling of the atom to the cavity mode for more than two seconds.

Cavity QED experiments provide unique possibilities for studying atom-photon interaction at a fundamental level. Furthermore, neutral atom systems are a promising candidate for quantum information processing. In our experiment we explore the coupling of a small, controlled number of neutral caesium atoms to the mode of a high-finesse optical cavity (finesse $F \approx 10^6$, estimated cooperativity parameter $C_1 = g^2/(2\kappa\gamma) = 146$).

Using a number-triggered loading process¹ we transfer a pre-determined number of atoms, ranging from one single atom to several atoms, from a magneto-optical trap into a standing wave dipole trap. Subsequently, the atoms are transported into the center of the cavity mode with sub-micrometer precision² using our "optical conveyor belt" technique.³

A probe laser is coupled into the empty cavity and its transmission is detected. A single atom transported into the cavity mode shifts the cavity out of resonance with respect to the probe laser, which can be observed as a reduced laser transmission, see fig. 1.

In this way we can observe a single atom coupled to the cavity mode for several seconds. The time-dependent transmission signal allows us to infer information about the dynamics of the atom-cavity system, especially about the variation of the coupling strength g . We study how the localization of the atom with respect to the cavity field can be optimized, with the goal to reach a constant atom-photon-coupling, which is a fundamental requirement for entangling two atoms via a cavity-mediated interaction.

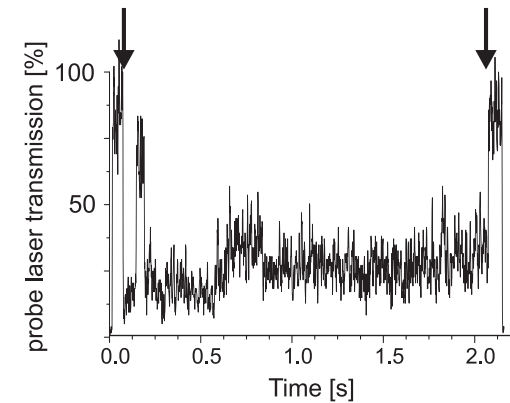


Fig. 1. Transmission of the probe-laser through the high-finesse cavity. The arrows indicate the points of time when a single atom is transported into and out of the cavity mode, respectively. We attribute the variation in transmission during the observation time to a corresponding variation in the average coupling rate g .

References

1. L. Förster, W. Alt, I. Dotsenko, M. Khudaverdyan, D. Meschede, Y. Miroshnychenko, S. Reick and A. Rauschenbeutel, *New J. Phys.* **8**, p. 259 (2006).
2. I. Dotsenko, W. Alt, M. Khudaverdyan, S. Kuhr, D. Meschede, Y. Miroshnychenko, D. Schrader and A. Rauschenbeutel, *Phys. Rev. Lett.* **95**, p. 033002 (2005).
3. S. Kuhr, W. Alt, D. Schrader, M. Müller, V. Gomer and D. Meschede, *Science* **293**, p. 278 (2001).

Test of Special Relativity by Laser Spectroscopy and Fast Ions

Sascha Reinhardt, G. Saathoff, H. Buhr, L. A. Carlson, D. Schwalm and A. Wolf

*Max Planck Institut für Kernphysik
Heidelberg, Germany*

S. Karpuk, C. Novotny and G. Huber

*Johannes Gutenberg Universität Mainz
Mainz, Germany*

T. W. Hänsch, R. Holzwarth, Th. Udem and M. Zimmermann

*Max Planck Institut für Quantenoptik
Garching, Germany*

G. Gwinner

*University of Manitoba
Winnipeg, Canada*

Nowadays it is not possible to describe all known interactions in one single theory. For the electromagnetic, weak and strong interaction quantum field theory and for the gravitation General Relativity is used. New theories like String theory or quantum gravity are currently under development to overcome this handicap. In these new theories the violation of Lorentz invariance is possible, which is part of quantum field theory and General Relativity as well. At the heavy ion test storage ring in Heidelberg the time dilation is tested by Lithium ions, that are stored with a velocity of 3% or 6.4% speed of light. Using saturation spectroscopy methods the transition frequency of the ions can be measured and compared on a 10^{-10} level. These measurements leads to improved upper limits for parameters used by test theories containing a possible violation of Lorentz invariance.

Keywords: Special Relativity, Lorentz invariance, Time dilation, Heavy ion storage ring, Saturation spectroscopy

Time dilation is introduced by Special Relativity and describe how time goes by in a moving frame compared to a frame in rest. In the rest frame the

laser frequency is stabilized on hyperfine structure lines of iodine molecules used as clocks to measure time and the moving frame is given by ${}^7\text{Li}^+$ ions at a velocity v of 3% or 6.4% speed of light c and time is measured by measuring the transition frequency of the Lithium ions. In the ion frame the laser frequency is Doppler shifted. To excite the ions with a transition frequency ν_0 a laser beam propagating anti-parallel to the ions must has a frequency $\nu_a = \nu_0\gamma(1 - \beta)$ ($\beta = v/c$, $\gamma = 1/\sqrt{1 - \beta^2}$) and a laser beam propagating parallel to the ions must has a frequency $\nu_p = \nu_0\gamma(1 + \beta)$. The product of the laser frequencies leads to an equation without a velocity dependence $\nu_a\nu_p/\nu_0^2 = 1$. To describe deviations from this equation an ε can be added. The shape and interpretation of ε depends on the used test theory (like RMS¹ or SME²).

The experiment starts with Lithium ions that are accelerated to the desired velocity. The ions are injected and stored in the test storage ring in Heidelberg (circumference 55.4 m) and to obtain a high quality beam with a small velocity distribution and divergence an electron cooler is used. On a straight section with a length of about 10 m the laser- and ion-beams are overlapped. The transition wavelength in rest of the ions are 548.5 nm and the laser wavelengths are 532 nm/514 nm (parallel) and 565 nm/585 nm (anti-parallel) for 3% c /6.4% c respectively. The antiparallel laser is tuned in frequency (≈ 200 MHz) and the fluorescence of the ions are detected by several photomultipliers distributed over the straight section. If both lasers interacts with the same velocity class, a dip in the fluorescence signal is observed with a linewidth in the order of the natural linewidth (3.7 MHz). Including all relevant systematics $\sqrt{\nu_a\nu_p}$ can be determined on a 100 kHz level ($\hat{=}10^{-10}$). With these measurements it is possible to improve several earlier values and limits by a factor of two to four.³⁻⁶

References

1. R. Mansouri and R. U. Sexl, *Gen. Rel. Grav.* **8**, p. (7)497;(7)515;(10)809 (1977).
2. D. Colladay and V. A. Kostelecký, *Phys. Rev. D*, **55**, 6760 (1997); **58**, 116002 (1998).
3. G. Saathoff, S. Karpuk, U. Eisenbarth, G. Huber, S. Krohn, R. M. Horta, S. Reinhardt, D. Schwalm, A. Wolf and G. Gwinner, *Phys. Rev. Lett.* **91**, 190403/1 (2003).
4. E. Riis, A. G. Sinclair, O. Poulson, G. W. F. Drake, W. R. C. Rowley and A. P. Levick, *Phys. Rev. A* **49**, p. 207 (1994).
5. C. D. Lane, *Phys. Rev. D* **72**, 016005/1 (2005).
6. M. Hohensee, A. Glenday, C.-H. Li, M. E. Tobar and P. Wolf, *Phys. Rev. D* **75**, p. 049992(E) (2007).

Process tomography of ion trap quantum gates

M. Riebe¹, K. Kim¹, P. Schindler¹, T. Monz¹, P. O. Schmidt¹, T. K. Körber¹,
W. Hänsel¹, H. Häffner², C. F. Roos², R. Blatt^{1,2}

¹*Institut für Experimentalphysik, Universität Innsbruck, A-6020 Innsbruck, Austria*

²*Institute for Quantum Optics and Quantum Information, Innsbruck, Austria*

Characterizing the building blocks of a quantum computer is of central interest as it allows to predict a quantum computer's performance for concatenated operations. Furthermore, a detailed knowledge of the imperfections of the basic operations helps to identify shortcomings and thus forms an excellent basis to optimize the building blocks itself. One such crucial building block for quantum information processing is a controlled-NOT quantum gate.

We perform quantum process tomography of two different implementations of a controlled-NOT gate operation with trapped ions. In both cases we find fidelities exceeding 90%. Furthermore, the advantage of amplitude-shaped laser pulses over simple square pulses is quantified with process tomography. Finally, we show that the fidelity of two concatenated controlled-NOT operations agrees with the estimation based on the process tomography of a single gate operation.

Spiking optical patterns and synchronization of coupled semiconductor lasers

M. Rosenbluh

Department of Physics, Bar-Ilan University, Ramat Gan 52900, Israel

The output intensity of a semiconductor laser, having external feedback is known to possess chaotic intensity fluctuations. When two such lasers are coupled one to another, the chaotic fluctuations of the two lasers can become highly synchronized. The synchronization can be of various types; simultaneous-isochronal (zero time lag), leader-laggard in which each laser assumes either a leader or a laggard role, anticipated synchronization and achronal synchronization where each laser has equal probability to be a leader or a laggard. Our group over has recently explored the various region of synchronization and the statistics and dynamics of the chaotic signals.¹⁻³ The time resolved spike statistics of a solitary and two mutually interacting chaotic semiconductor lasers whose chaos is characterized by apparently random, very short intensity spikes, as shown in Fig. 1. Repulsion between two successive spikes is observed, and for long time intervals between spikes, the distribution of the intervals is a Poisson distribution. The spiking pattern is highly periodic over time windows corresponding to the optical length of the external cavity, with a slow change of the spiking pattern as time increases. When zero-lag synchronization between the two lasers is established, the statistics of the nearly perfectly matched spikes are not altered. In recent work⁴ we have shown how two lasers can be synchronized isochronally, without any delay in their fluctuating output intensity. The synchronization, as measured by the normalized correlation function, is surprisingly robust as was demonstrated in an experiment in which the communication between the two chaotic lasers was terminated. As shown in Fig. 2, the laser signals, nevertheless remained isochronally synchronized for times much longer than the solitary laser feedback delay time, τ . After the lasers desynchronized, they could be rapidly resynchronized (on a time scale of order τ) by reestablishing the communication between them. In re-

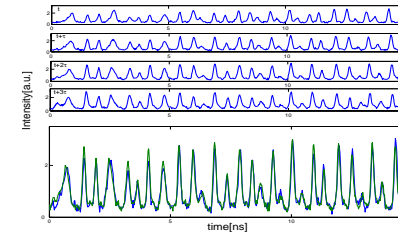


Fig. 1. The intensity trace of a solitary chaotic laser for a 15 ns time window followed by plots of the same laser intensity after a time τ , 2τ , and 3τ with $\tau = 23.55$ ns, the feedback delay time. The laser was operating slightly over threshold with a reflected power of a few % of the laser output intensity. (b) The intensity trace at time $t + \tau$ (green) and at time $t + 2\tau$ (blue) demonstrating the slowly decaying periodicity of the spiking pattern.

lated work² with secure optical communication in mind, we have also shown that over a significant operational phase space, two mutually coupled semiconductor lasers can synchronize to each other very well while an attacker (unidirectional listener) laser can not synchronize nearly as well with the chaotic signal. The demonstration of a long persistence of the correlation while the lasers are not communicating leads us to expect that these effects will play an important role in advanced secure communications using mutually chaotic lasers.

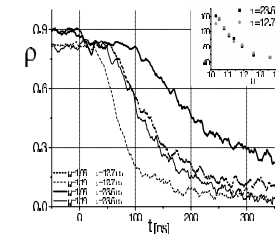


Fig. 2. The zero time lag correlation of the fluctuating output intensity of two lasers after the communication between them is terminated.

References

1. N. Gross *et al.*, *Opt. Comm.* **267**, p. 464 (2006).
2. E. Klein *et al.*, *Phys. Rev. E* **74**, 046201 (2006).
3. E. Klein *et al.*, *Phys. Rev. E* **73**, 066214 (2006).
4. I. Kanter *et al.*, *Phys. Rev. Lett.* **98**, 154101 (2007).

Photon emission of a single trapped ion into a cavity

C. Russo¹, F. Dubin¹, H. Barros¹, E.S. Philips², A. Stute¹, C. Becher³, P.O.

Schmidt^{*,1} and R. Blatt¹

¹*Institut für Experimentalphysik, Universität Innsbruck,
Technikerstr. 25, A-6020 Innsbruck, Austria*

**E-mail: Piet.Schmidt@uibk.ac.at
www.quantumoptics.at*

²*Department of Atomic and Laser Physics, Clarendon Laboratory,
Parks Road, Oxford OX1 3PU, United Kingdom*

³*Technische Physik, Universität des Saarlandes, Postfach 151150, D-66041
Saarbrücken, Germany*

We present results on the statistical properties of light emitted by a single atom into the mode of a high-finesse cavity. We were able to observe a transition from photon bunching to anti-bunching in the arrival times of the photons by changing simple experimental parameters.

We trap a single $^{40}\text{Ca}^+$ ion in a linear Paul trap. Perpendicular to the axis of the trap, two mirrors form a high-finesse cavity ($\mathcal{F} \approx 70000$) as shown in Fig. 1(a). The cavity can be moved with respect to the ion's position in the trap to maximize atom-cavity coupling within the standing wave of the cavity. The length of the cavity is stabilized using a transfer lock scheme. A single ion typically stays in the trap for several hours, well exceeding the required experiment time.

We generate photons in the cavity mode continuously by exploiting cavity-stimulated Raman transition between the $|S\rangle$ ground and $|D\rangle$ metastable states as shown in Fig. 1(b). Pump laser and cavity are detuned from the $|P\rangle$ state by 400 MHz. A repumping laser transfers the ion from the $|D\rangle$ to the $|P\rangle$ state from which it decays spontaneously back into the $|S\rangle$ ground state. Applying all lasers continuously, a cycle between atomic states is obtained which adds a photon to the cavity mode for each $|S\rangle \rightarrow |D\rangle$

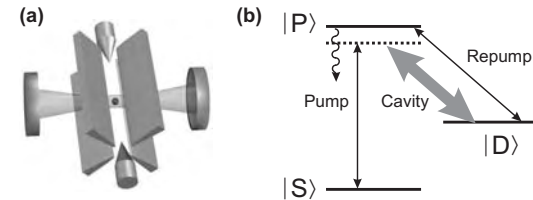


Fig. 1. (a) Experimental setup: a single $^{40}\text{Ca}^+$ ion is trapped in a linear Paul trap surrounded by a high-finesse optical cavity. (b) Simplified level scheme of a $^{40}\text{Ca}^+$ ion. Cavity-assisted Raman transitions are driven using a pump laser. Re-initialization of the ion is achieved via repumping to the $|P\rangle$ state, followed by spontaneous emission to the $|S\rangle$ state.

transition. The photons leaking out of the cavity at a rate of ≈ 50 kHz are analyzed using a Hanbury Brown & Twiss setup. We present intensity correlation functions, $g^{(2)}(\tau)$, which exhibit photon bunching and anti-bunching character, depending on the intensity and detuning of the pump and repump lasers. The results are well understood with a model taking into account all involved atomic levels and two nearly-degenerate orthogonal modes of the cavity. A variation of the scheme using pump laser pulses allows for the implementation of a deterministic single photon source.

Acknowledgments

We acknowledge stimulating discussions with H. Ritsch and T. Salzburger. This work is supported by the Austrian Science Fund (FWF), by the European Commission (SCALA, CONQUEST networks), and by the Institut für Quanteninformation GmbH.

SPINOR CONDENSATES AT FINITE TEMPERATURES

KAZIMIERZ M. RZAZEWSKI
*Center for Theoretical Physics
Warsaw, Poland*

MARIUSZ GAJDA
*Institute of Physics,
Warsaw, Poland*

MIROSLAW BREWCZYK
*University of Bialystok
Poland*

We consider a spinor condensate of 87Rb atoms in its $F = 1$ hyperfine state at finite temperatures. To this end we use our classical fields approximation. Spin textures, breaking of chiral symmetry and coherence is than studied.

QUANTUM TRANSPORT EFFECTS IN RATCHET-LIKE POTENTIALS AND OPTICAL MULTIPHOTON LATTICES

T. Salger¹, C. Geckeler¹, S. Kling¹, and M. Weitz^{1,2}

1. *Institut für Angewandte Physik, Universität Bonn, Wegelerstr. 8, D-53115 Bonn, Germany*

2. *Physikalisches Institut, Universität Tübingen, Auf der Morgenstelle 14, D-72076 Tübingen, Germany*

We report experimental results on transport properties of Bose-Einstein condensates in periodic optical potentials of variable asymmetry. By studying Landau-Zener tunneling and Bloch oscillations, we have explored the band structure of both ratchet-type asymmetric and symmetric optical potentials. In earlier work, quantum transport in “conventional” sinusoidal lattices has proven to be a powerful technique for characterisation of the band structure. To realize lattice potentials of variable asymmetry, we superimpose a conventional lattice potential of $\lambda/2$ spatial periodicity with a fourth-order optical potential of $\lambda/4$ spatial periodicity. The high periodicity lattice is realized using dispersive properties of multiphoton Raman transitions. To study quantum transport in such Fourier-synthesized lattice potentials, the periodic potential is accelerated. We observe a sinu-

soidal dependence of the tunneling rate between the first and second excited Bloch band. If the phase difference between the two harmonics reaches 180° , nearly all atoms were observed to tunnel to the higher Bloch band, while the tunneling decreases for other phase values, as shown in Fig. 1a. Two extremes at minimal and maximal tunneling have been investigated more in detail by variation of the potential depth of the optical standing wave, yielding results as shown in Fig. 1b. For a phase difference near 0° a simple exponential dependence of the tunneling rate on the potential depth is observed. In contrast, for a phase difference of 180° , the tunneling rate reaches its maximum at a two-photon potential value different from zero. In subsequent experiments, we also studied Bloch oscillations in accelerated lattices with $\lambda/2$ and $\lambda/4$ spatial periodicities. The frequency of the Bloch oscillation is directly connected to the spatial variation of the corresponding lattice potential. Of special interest are investigations of the effective atom mass, which for the multiphoton lattice near the band edge reaches considerable smaller values compared to a conventional optical standing wave at comparable potential depth.

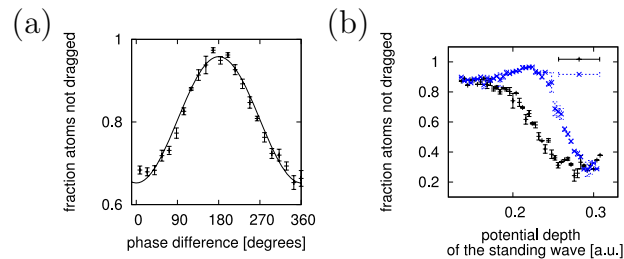


Fig. 1. (a) Phase dependency of the number of atoms tunneling between the first and second excited Bloch band. (b) Dependence of the tunneling rate on the potential depth of the optical standing wave for a phase difference between two- and four-photon potentials of 0° (x) and 180° (+).

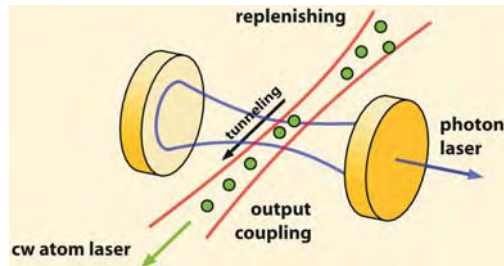
An atom-photon pair laser

Thomas Salzburger and Helmut Ritsch

*Theoretical Physics, University of Innsbruck,
Innsbruck, Tirol, Austria*

**E-mail: ab_Helmut.Ritsch@uibk.ac.at*

We study the quantum dynamics of an ultracold atomic gas in a deep optical lattice within an optical high- Q resonator. The atoms are coherently illuminated with the cavity resonance tuned to a blue vibrational sideband, so that photon scattering to the resonator mode is accompanied by vibrational cooling of the atoms. This system exhibits a threshold above which pairwise stimulated generation of a cavity photon and an atom in the lowest vibrational band dominates spontaneous scattering and we find a combination of optical lasing with a buildup of a macroscopic population in the lowest lattice band. Including output coupling of ground-state atoms and replenishing of hot atoms into the cavity volume leads to a coherent, quantum correlated atom-photon pair source very analogous to twin light beam generation in a nondegenerate optical parametric oscillator.



References

1. T. Salzburger and H. Ritsch, Phys. Rev. Lett. **93**, 063002 (2004).
2. C. Maschler and H. Ritsch, Phys. Rev. Lett. **95**, 260401 (2005).

Work supported by the Austrian Science Fund FWF: (S1512,P17709).

A Miniature, Highly Sensitive Atomic Magnetometer Based on Suppression of Spin-Exchange Relaxation: Development and Applications

V. SHAH, S. KNAPPE, P.D.D. SCHWINDT*, J. KITCHING

*National Institute of Standards and Technology
Boulder, CO 80305, USA*

**current address: Sandia National Laboratories
MS-1082, PO Box 5800, Albuquerque, NM 87185*

**E-mail: vshah@nist.gov*

1. Abstract

We demonstrate an atomic magnetometer with a sensitivity of $70 \text{ fT}/\sqrt{Hz}$ based on a millimeter-scale microfabricated alkali vapor cell and a single low power laser. This result represents an improvement by a factor of over 100 in sensitivity over previous measurements made using microfabricated vapor cells and suggests that simple non-cryogenic alternatives to high-Tc SQUID magnetometers are feasible for low field applications.

The key physics that underlies the improvement in sensitivity here is the suppression of spin relaxation originating from spin-exchange collisions between the alkali atoms^{1,2} and the generation of a large atomic coherence at low magnetic field strengths. Magnetic sensors based on this technology would have important practical applications, including: highly sensitive geophysical surveys, environmental monitoring, security, lower-cost sensors for biomedical applications such as magnetic resonance imaging and satellite-based measurements of magnetic fields. Here, we discuss the use of such an atomic magnetometer in remote NMR detection³ based on micro-fluidics.

References

1. W. Happer and H. Tang, *Phys. Rev. Lett.* **31**, 273(Jul 1973).
2. I. Kominis, T. Kornack, J. Allred and M. Romalis, *Nature* **422**, 596 (2003).
3. S. Xu, V. Yashchuk, M. Donaldson, S. Rochester, D. Budker and A. Pines, *PNAS* **103**, 12668 (2006).

Influence of Externally Applied dc Electric and Magnetic Fields on Semiconductor- Photorefractivity

Dheeraj Sharma and Praveen Aghamkar
 Department of Applied Physics
 Guru Jambheshwar University, Hisar 125001, INDIA
 Telephone: +91-1662-263176, 9416355455,
 Fax: 91-1662-263240
 E-mail: khushi_cha@rediffmail.com

Photorefractive effect [PRE] is identified as one of the most important nonlinear optical phenomena in many semiconductors. Today, semiconductors are the most sophisticated, sensitive and ultrafast nonlinear materials due to their compactness, provision of material relaxation time and highly advanced fabrication technology. The present paper deals with the theoretical investigation of PR- characteristic parameters such as space charge electric field, gain coefficient and diffraction efficiency in semi-insulating semiconductors like GaAs:Cr and CdTe :V in presence of applied dc electric (E_0) and magnetic (B_0) fields. A critical dependence of E_0 and B_0 on the real and the imaginary part of the space charge field has been noticed. The numerical estimation have been made for GaAs: Cr at 77K duly irradiated by 1.06 μ m Nd:YAG laser. It is noticed that an externally applied electric and magnetic fields substantially modify magnitude and sign of the real and imaginary part of the space charge electric field. In particular, we obtained space charge electric field $\sim 7 \times 10^5$ V/m at $E_0=10^4$ V/m and $B_0=640$ Guass, this value is nearly three-order larger in the absence of E_0 and B_0 . The gain coefficient and diffraction efficiency also enhances. These results are good qualitatively in agreement with theory and experiment [2]. In conclusion, photorefractive-semiconductor in presence of externally applied dc electric and magnetic fields may be used as efficient dynamic holograms.

Keywords: Photorefractivity, Semiconductors, External Electric and Magnetic Fields, Band Charge Transport Model, Space Charge Electric field.

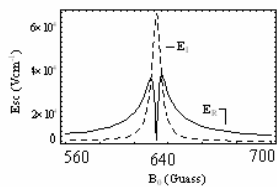


Fig. 1 B_0 V/s E_{sc} (real, imaginary)

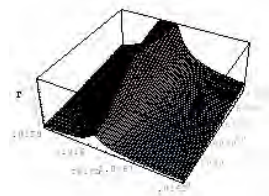


Fig. 2 Gain V/s E_0 V/s θ

References:

1. N.V.Khukhtarev, V.Markov, S.Odulov, M.Soskin and V.Vinetskii, *Ferroelectrics*, **22**, 949,1979.
2. J.E.Millerd, E.M.Garmine and A.Partovi, in *Photorefractive Effects and Materials*, ed. D.D.Nolte (Boston, Kluwer Academic, 1995), pp312-372.

State-selective imaging of cold atoms using atomic coherence

D. V. SHELUDKO, S. C. BELL, S. D. SALIBA and R. E. SCHOLTEN*

*School of Physics, The University of Melbourne,
VIC 3010, Australia*

*E-mail: r.scholten@physics.unimelb.edu.au

Imaging cold atom samples provides interesting opportunities for studying not only the external atomic distribution, but also the internal atomic state, particularly for atoms prepared in a coherent state. We have previously developed techniques for off-resonant imaging of a cold atom cloud without optical elements, computationally extracting the atomic column density map from a diffraction pattern. We are now combining two lasers and three states, in Λ , V , and cascade configurations, to explore atomic coherence via two-dimensional imaging and to image the spatial distribution of non-ground-state atoms.

We have developed a minimally destructive imaging technique to determine the fraction and distribution of excited-state Rb atoms in a magneto-optical trap (MOT). The work has been motivated by a general interest in probing atomic coherence states and related phenomena such as electromagnetically induced transparency and slow light,¹ and coherent frequency up-conversion.² These phenomena have typically been studied using techniques without spatial resolution, and imaging offers the potential for obtaining much greater information. Combining diffraction-based phase imaging with control of the internal state of the imaged atoms using a probe laser, we can explore techniques for enhancing the imaging (e.g. by modifying the refractive index), or for directly measuring the control process itself.

Our approach is based on off-resonance diffraction contrast imaging (DCI) of cold atom clouds.³ The diffracted intensity pattern of an off-resonant probe is recorded with a conventional absorption imaging apparatus, but with lens defocused, or entirely without a lens or other imaging optic elements. The atomic column density is then extracted computationally from the diffracted intensity distribution. DCI is quantitative and less sensitive to experimental imprecision compared to conventional absorption imaging or classical phase imaging.

We have extended the method to imaging excited-state atom distribu-

tions, in particular Rb atoms in a MOT. The atoms are excited from 5S to 5P states by 780 nm trapping and cooling beams, and imaged on the 5P to 5D transition by a 776 nm probe laser beam. To extract the excited atom distribution from the diffraction pattern, we must know the complex refractive index (atomic susceptibility) for the 5P–5D transition. The atomic state is, however, perturbed by the trapping light: we effectively have a three-level atom with two coupling fields, in a cascade or ladder type atomic coherence system. We have used an optical Bloch equation approach⁴ to determine the 776 nm susceptibility (Fig. 1). Autler-Townes splitting of the 776 nm

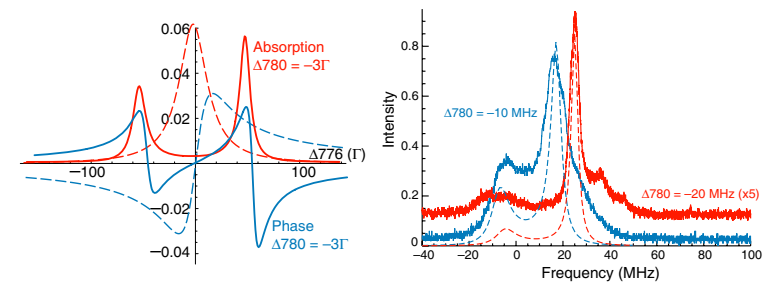


Fig. 1. Left: Calculated phase and absorption on the 776 nm transition for a three-level model of Rb (left). Right: Theoretical (dashed) and experimental (solid) 420 nm fluorescence in the MOT for 780 nm cooling beam detunings of -10.0 ± 0.5 and -20 ± 3 MHz.

transition is clearly evident, and supported by experimental measurements of 420 nm fluorescence via the 5D–6P–5S decay path. We are now applying this knowledge to extract images of the distribution of excited-state atoms.

References

1. M. O. Scully and M. S. Zubairy, *Quantum Optics* (Cambridge University Press, 1997).
2. T. Meijer, J. D. White, B. Smeets, M. Jeppesen and R. E. Scholten, *Opt. Lett.* **31**, 1002 (April 2006).
3. L. D. Turner, K. F. E. M. Domen and R. E. Scholten, *Phys. Rev. A* **72**, p. 1403 (2005).
4. L. P. Maguire, R. M. W. van Bijnen, E. Mese and R. E. Scholten, *J. Phys. B: At. Mol. Opt. Phys.* **39**, 2709 (2006).

FABRICTION OF ATOM CHIPS

PETER D. D. SCHWINDT,* MICHAEL MANGAN, CHRIS TIGGES, JAMES STEVENS, MATTHEW BLAIN

Sandia National Laboratories, PO Box 5800
Albuquerque, NM 87185, USA

Much like laser cooling in the 1990's, "atom chip" technology today is rapidly gaining popularity as a convenient and powerful approach to achieving precise control over atom's motion and internal state. While great success has been achieved in magnetically manipulating the atoms, integrating optical elements onto the atom chip is an active area of research. Premier applications for these "optoatomic circuits" can be foreseen in both quantum information science¹ and in quantum sensors.²

At Sandia, our efforts are focused on fabricating high quality atom chips forming magnetic traps and guides in combination with open access optical cavities. Typically, the conductors used for atoms chip have been copper and gold to allow the highest possible current density.³ However, aluminum has a conductivity only 15% less than gold, and Sandia has an established Al metallization process for making small feature size, multilayer structures (less than 1 μm). The Al conductors are formed on a Si substrate and are imbedded in

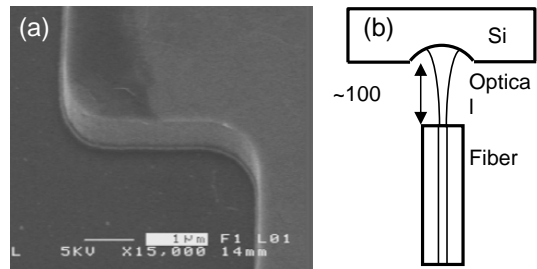


Figure 1. (a) Scanning electron microscope image of 2.5 μm thick Al (0.5% Cu) wire before it is imbedded in SiO_2 . (b) Schematic of the miniature optical cavity.

* Email: pschwin@sandia.gov

SiO_2 which is polished flat. Gold or dielectrics will be deposited to form a mirror for a mirror magneto-optical trap.

In a parallel effort, we are developing optical cavities compatible with the processing for the Al conductors. Having a lithographic process that allows an array of low mode volume optical cavities on an atom chip is critical for quantum information processing in neutral atoms. In a design similar to Ref. [4], one side of the optical cavity is formed by a hemispherical void etched into Si and the other by the tip of the optical fiber. Both will be coated with a dielectric stack to form a relatively high finesse optical cavity. The Si divot will be suspended so that the cavity length can be tuned by electrostatic actuation. We will present details on the design, fabrication, and characterization of the conductors and optical cavities.

References

1. H. Mabuchi, M. Armen, B. Lev, M. Loncar, J. Vuckovic, H. J. Kimble, J. Preskill, M. Roukes, and A. Scherer, *Quantum Information and Computation*, **1**, 7 (2001).
2. Y.-J. Wang, D. Z. Anderson, V. M. Bright, E. A. Cornell, Qu. Diot, T. Kishimoto, M. Prentiss, R. A. Saravanan, S. R. Segal and S. Wu, *Phys. Rev. Lett.* **94**, 090405 (2005). T. Schumm, S. Hofferberth, L. M. Andersson, S. Wildermuth, S. Groth, I. Bar-Joseph, J. Schmiedmayer, P. Kruger, *Nature Physics*, **1**, 57 (2005).
3. J. Fortágh, C. Zimmermann, *Rev. of Mod. Phys.* **79**, 235-289 (2007).
4. M. Trupke, E.A. Hinds, S. Eriksson, E.A. Curtis, Z. Moktadir, E. Kukharenska, M. Kraft, *Appl. Phys. Lett.* **87**, 211106 (2005). C.O. Gollasch, Z. Moktadir, M. Kraft, M. Trupke, S. Eriksson, E.A. Hinds, *J. Micromech. Microeng.* **15**, S39-S46 (2005).

Quantum projection noise and squeezing with ions in a Penning-Malmberg trap.

N. Shiga[◇]*, J. H. Wesenberg, W. M. Itano and J. J. Bollinger

*Trapped ion group, NIST,
Boulder, 80305, USA*

[◇] *E-mail: shiga@boulder.nist.gov*

We describe plans and summarize initial progress towards making spin squeezed states with up to ~ 1000 ${}^9\text{Be}^+$ ions in a Penning-Malmberg trap. We use the ground-state electron spin-flip transition, which in the 4.5 T magnetic field of the trap has a transition frequency of 124 GHz, as the ion qubit. With a 30 mW Gunn diode oscillator we have observed π -times as short as 100 μs .

We have realized projection noise limited spectroscopy¹ on this transition—a prerequisite for demonstrating spin squeezing (Figure 1). For entangling the ions we plan to use a generalization of the few ion qubit phase gate developed at NIST² to generate an $\exp(i\chi J_z^2 t)$ interaction between all of the ion qubits. This interaction can be implemented on a single plane of ions³ with a motional sideband, stimulated Raman transition. We have observed fast (1 ms) magnetic field fluctuations of our magnet through spin-echo spectroscopy. These fluctuations limit the amount of time that can be used to apply the squeezing.

References

1. W.M. Itano, et al., Phys. Rev. A **47**, 3554 (1993).
2. D. Leibfried, et al., Nature **438**, 639 (2005).
3. T.B. Mitchell, et al., Science **282**, 1290 (1998).

*Supported by a DOD MURI program administrated by ONR

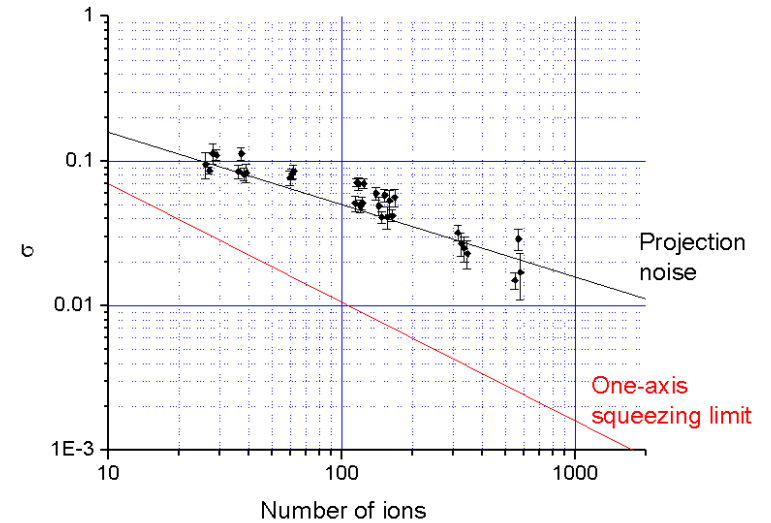


Fig. 1. Standard deviation σ of the measured J_z as a function of ion number N

MACROSCOPIC ENTANGLEMENT OF A BOSE-EINSTEIN CONDENSATE ON A SUPERCONDUCTING ATOM CHIP

MANDIP SINGH

*Centre for Atom Optics and Ultrafast Spectroscopy and
ARC Centre of Excellence for Quantum-Atom Optics
Swinburne University of Technology, Melbourne, Australia 3122*

A Schrödinger cat state lies at the heart of quantum mechanics in both fundamental and philosophical contexts. In recent years there has been ground breaking progress in the field of manipulation of Bose-Einstein condensates on atom chips. Also the field of superconducting circuits is progressing rapidly in terms of technological implementation and realization of quantum coherent control [1, 2]. Atom chips based on superconductor substrates and wires have been implemented [3, 4]. In this paper we present a practically implementable scheme which combines the two emerging fields of micro-manipulation of a Bose-Einstein condensate on an atom chip and quantum coherent dynamics in superconductor circuits in order to realise a macroscopic entanglement of a Bose-Einstein condensate. Our idea is based on coupling a superconductor flux loop to a Bose-Einstein condensate in a magnetic trap on an atom chip. We treat the superconductor flux loop in quantum superposition of two flux states. Our scheme also provides a platform to realise entangled atoms interferometry through a Bose-Einstein condensate on an atom chip.

References

1. J.R. Friedman, V. Patel, W. Chen, S.K. Tolpygo, and J.E. Lukens, *Nature*, **406**, 43 (2000).
2. C. H. Van der Wal, A.C.J. ter Haar, F.K. Wilhelm, R.N. Schouten, C.J.P.M. Harmans, T.P. Orlando, S. Lloyd, and J.E. Mooij, *Science*, **290**, 773 (2000).
3. T. Nirrengarten, A. Qarry, C. Roux, A. Emmert, G. Nogues, M. Brune, J.-M. Raymond, and S. Haroche, *ArXiv: quant-ph/0610019v2*.
4. T. Mukai, C. Hufnagel, A. Kasper, T. Meno, A. Tsukada, K. Semba, and F. Shimizu, *ArXiv:cond-mat/0700142v1*.

BOSE-EINSTEIN CONDENSATE ON A PERMANENT MAGNETIC LATTICE ON AN ATOM CHIP

M. SINGH, M. VOLK, A. AKULSHIN, R. McLEAN, A. SIDOROV AND
P. HANNAFORD

*Centre for Atom Optics and Ultrafast Spectroscopy and
ARC Centre of Excellence for Quantum-Atom Optics,
Swinburne University of Technology, Melbourne, Australia 3122*

In recent years there has been ground breaking progress in the field of manipulation of Bose-Einstein condensates on an atom chip. Chip-based magnetic traps made from permanent magnetic films are attractive for their low heating rates and high intrinsic stability. We report the realisation of a Bose-Einstein condensate of ^{87}Rb on an atom chip incorporating a permanent magnetic lattice. The magnetic lattice is produced by a perpendicularly magnetised magnetic film ($\text{Gd}_{10}\text{Tb}_6\text{Fe}_{80}\text{Co}_4$) deposited on a $10\ \mu\text{m}$ period grooved structure on a Si substrate. The BEC is initially created in a Z-shaped wire trap far from the lattice and then moved closer to the film in order to load the lattice. We aim to study the quantum coherent dynamics of the condensate on the magnetic lattice.

EXPERIMENTAL DESIGN FOR EFFICIENT PHOTON–ATOM COUPLING IN FREE SPACE

M. Sondermann*, H. Konermann, R. Maiwald, N. Lindlein, U. Peschel and G. Leuchs#

*Institute of Optics, Information and Photonics, Max Planck Research Group,
University of Erlangen-Nuremberg,
91058 Erlangen, Germany*

** E-mail: msondermann@optik.uni-erlangen.de,*

E-mail: leuchs@physik.uni-erlangen.de

We propose a design of an experiment in which a single photon is coupled with a single atomic ion in such a way that an incident photon is absorbed with a probability close to one before reemission. The experiment is adaptable to other systems such as neutral atoms, single molecules or quantum dots.

Keywords: spontaneous emission; quantum optics; quantum information

The spontaneous emission of a photon by a two-level quantum system in its excited state is a fundamental processes in quantum optics in particular and in physics in general. This process has been studied for almost a century and it is characterized by an exponential decay to the ground state with a probability equal to one.¹ If the single photon can be coupled to the two-level system, e.g. a single atom, such that it is absorbed for certain, one has realized time reversal of spontaneous emission.

Strong coupling of light to single atoms has been demonstrated inside high finesse resonators² as well as efficient attenuation of laser radiation by a single trapped ion³ and a single molecule in a cryogenic matrix.⁴ In contrast to previous investigations, it is our goal to effectively couple light and matter in *free space*. This shall be achieved by shaping the incident light in such a way that it best resembles the inverse of an outgoing dipole wave emitted by a single atom/ion with respect to temporal/spectral shape, intensity distribution and polarization.

The proposed experimental setup is as follows: An atomic ion is trapped by a radio-frequency trap consisting of two needle-like electrodes. The feasibility of such a trap has been shown recently.⁵ The ion is cooled to its

motional ground state via Doppler-cooling. The center of the trap is located in the focus of a deep parabolic mirror with the trap electrodes positioned on the optical axis of the mirror. By use of radial polarization⁶ and a suitable phase and intensity distribution⁷ of the incident light one will be able to excite the ion with a spatial radiation pattern that provides almost the complete far field pattern of a linear dipole in the location of the mirror focus. The finite extension of the parabolic mirror results in an incomplete coverage of the dipole radiation pattern. Therefore, the remainder of the radiation pattern is provided by deflecting a part of the incident radiation directly towards the ion by a diffractive optical element. In a first trial, the ion will be excited by light pulses with an average photon number much smaller than one. To this purpose, an exponentially increasing pulse shape will be cut out of a coherent continuous wave laser beam. The time constant is chosen to match the life time of the upper state of the two-level system. The resulting pulse is subsequently attenuated until the desired average photon number per pulse is obtained.

For the demonstration of spontaneous emission reversal, we choose an ion with only one decay channel out of the excited state. Considering dipole selection rules and experimental feasibility, doubly ionized ytterbium is the medium of choice.

The central element of the proposed setup is the mode converter described above containing a parabolic mirror and a diffractive optical element. Potential applications range from quantum information applications to 4π -microscopy in a novel geometry.

References

1. V. Weisskopf and E. Wigner, *Z. Phys.* **63**, 54 (1930).
2. Q. A. Turchette, C. J. Hood, W. Lange, H. Mabuchi and H. J. Kimble, *Phys. Rev. Lett.* **75**, 4710 (1995).
3. D. J. Wineland, W. M. Itano and J. C. Bergquist, *Opt. Lett.* **12**, 389 (1987).
4. I. Gerhardt, G. Wrigge, P. Bushev, G. Zumofen, M. Agio, R. Pfaf and V. Sandoghdar, *Phys. Rev. Lett.* **98**, p. 033601 (2007).
5. L. Deslauriers, S. Olmschenk, D. Stick, W. K. Hensinger, J. Sterk and C. Monroe, *Phys. Rev. Lett.* **97**, p. 103007 (2006).
6. S. Quabis, R. Dorn, M. Eberler, O. Glöckl and G. Leuchs, *Opt. Comm.* **179**, 1 (2000).
7. N. Lindlein, R. Maiwald, H. Konermann, M. Sondermann, U. Peschel and G. Leuchs, *Laser Physics* (2007), submitted.

BAYESIAN ESTIMATION OF DIFFERENTIAL INTERFEROMETER PHASE

JOHN K. STOCKTON* and MARK A. KASEVICH

*Physics Dept., Stanford University,
Stanford, CA 94305, USA*

**E-mail: jks@stanford.edu*

We apply Bayesian logic¹ to optimally estimate the differential phase in a discrete time, dual interferometer measurement. This maximum likelihood method is particularly relevant to the case of a gravity gradiometer, where the gravity gradient between cold-atom fountain interferometers can be estimated from the differential phase, despite the presence of large common phase (acceleration) fluctuations. Given an accurate model, the bias-free algorithm we present is optimal and leverages experimental knowledge of the system noise, classical or quantum, to outperform other typical estimators, including ellipse-fitting techniques.^{2,3}

References

1. E. T. Jaynes and G. Larry Bretthorst, *Probability Theory: The Logic of Science*, (Cambridge University Press, 2003).
2. G. T. Foster, J. B. Fixler, J. M. McGuirk, and M. A. Kasevich, "Method of phase extraction between coupled atom interferometers using ellipse-specific fitting," *Opt. Lett.*, **27**, 951-953 (2002).
3. A. Fitzgibbon, M. Pilu, and R.B. Fisher, "Direct least square fitting of ellipses," *Pattern Analysis and Machine Intelligence, IEEE Transactions on* **21**, 476-480 (1999).

ABSOLUTE FREQUENCY STABILIZATION OF A LASER TO AN ION ABSORPTION LINE IN A DISCHARGE

ERIK W. STREED, GEOFFREY GENN, DAVID KIELPINSKI

Centre for Quantum Dynamics, Griffith University, Nathan QLD 4111 AUSTRALIA

Ion trap quantum computing experiments require laser systems with an absolute frequency stability of a few MHz tuned near specific atomic transitions. We have constructed a tunable diode laser system for Yb⁺ at 369.5 nm and stabilized it to the ion absorption signal from a hollow cathode discharge lamp. The laser is a Littrow configuration external cavity laser diode consisting of a 372 nm (room temperature) Nichia GaN laser diode cooled to -16°C and a 3600 g/mm holographic diffraction grating. The grating feedback provides a coarse tuning range of 1.6 nm. The unstabilized laser has a linewidth of 6.4 MHz (1sec) and a long term drift of <700 MHz. Simultaneous sweeping of grating displacement and diode current produces a mode hop free tuning range of 30 GHz. The laser frequency is stabilized using a two stage technique. First the laser is side locked to a Fabry-Perot (FP) cavity (1GHz FSR, Finesse 33), reducing the linewidth to 1.8 MHz (1 sec). The long term drift of the FP cavity length is then stabilized to the Yb⁺ absorption line in a hollow cathode discharge lamp using the Dichoric Atomic Vapor Laser Lock (DAVLL) method. Prior to this spectroscopy an acousto-optical modulator (AOM) shifts the frequency of the laser light with respect to the spectroscopy signal by +160 MHz. The uniform external magnetic field of 900 G applied to split the Zeeman sublevels is shielded by the lamp to 200 G at the ions. Ion absorption signals are observed in lamps with Ne buffer gas but not in those with He buffer gas. The dichoric absorption signal is detected by chopping the laser power at 100 kHz with the AOM and demodulating with a lockin amplifier, low pass time constant 100 ms. This laser system is used to cool ¹⁷⁴Yb⁺ ions in a linear RF trap to crystallization.

INITIAL SPECTROSCOPY OF HfF^+ FOR AN ELECTRON EDM SEARCH

R. STUTZ, A. LEANHARDT, L. SINCLAIR AND E. CORNELL

JILA, NIST and Department of Physics, University of Colorado, Boulder, CO 80309

The $^3\Delta_1$ state of HfF^+ is an attractive system for probing the electron electric dipole moment^{1,2}, due to its small Ω -doublet splitting and large enhancement of an external electric field. Recent theoretical work^{3,4} identifies the two lowest lying states as $^1\Sigma$ and $^3\Delta_1$, with a spacing comparable to the theoretical uncertainties. Experimentally, we wish to measure transitions from these low lying states to excited singlet and triplet Π states, which are predicted to lie 10,000-15,000 cm^{-1} above the ground state. These higher lying Π states should be well mixed by spin orbit interactions, thus making them useful intermediate levels for two-photon transitions between the $^1\Sigma$ and $^3\Delta_1$ states in our proposed electron EDM experiment.

References

1. R. Stutz and E. Cornell, *Bull. Am. Soc. Phys.* **49**, 76 (2004).
2. L. Sinclair, J. Bohn, A. Leanhardt, P. Maletinsky, E. Meyer, R. Stutz and E. Cornell, *36th Meeting of the Division of Atomic, Molecular, and Optical Physics(DAMOP)*, poster M6.00119 (2005) .
3. E. Meyer, J. Bohn, M. Deskevich, *Phys Rev A*, **73**, n6, 062108 (2006).
4. A. Petrov, N. Mosyagin, T. Isaev, A. Titov, arXiv: physics/0611254v2.

CRYOGENIC BUFFER-GAS COOLING AND CONFINEMENT OF PARAMAGNETIC ATOMS.*

ALEXANDER O. SUSHKOV

Department of Physics, University of California at Berkeley, Berkeley, California 94720-7300, USA

DMITRY BUDKER

Department of Physics, University of California at Berkeley, Berkeley, California 94720-7300, USA

and Nuclear Science Division, Lawrence Berkeley National Laboratory, Berkeley, California 94720, USA

Atomic vapor clouds of a number of paramagnetic atoms (Li, Rb, Ag, Au) have been produced by laser ablation in high-density buffer gas (He, N₂, Ne) in a wide range of temperatures ($4\text{K} < T < 300\text{K}$). The paramagnetic atoms thermalize with the buffer gas within a few collisions, and are spatially confined by the slow diffusion rates. Paramagnetic vapor densities of 10^{11} cm^{-3} are achieved in 10 cm^3 volume, and vapor lifetimes in excess of 100 ms are observed. Typical buffer-gas densities are 10^{18} cm^{-3} . There are two main mechanisms leading to loss of paramagnetic atoms: diffusion out of experimental volume dominates for low buffer-gas densities, and the onset of triple collisions, leading to clusterization, is the dominant loss mechanism at high buffer-gas densities. The techniques of laser spectroscopy, optical pumping and non-linear magneto-optical rotation are now being applied to these paramagnetic atoms at temperatures far lower than those needed to maintain an appreciable saturated vapor pressure necessary for vapor cell-based experiments. This system may find applications in a number of precision experiments and devices, such as an atomic magnetometer and searches for permanent electric dipole moments.

* This work is supported by NSF.

Atom-Molecule Rabi Oscillations in a Mott Insulator

N. Syassen*, D.M. Bauer, M. Lettner, D. Dietze, T. Volz, S. Dürr, and G. Rempe

*Max-Planck-Institute für Quantenoptik, Hans-Kopfermann-Str. 1,
85748 Garching, Germany*

**E-mail: niels.syassen@mpq.mpg.de*

Ultracold molecular gases have the potential for a variety of interesting applications, *e.g.*, in precision measurements or in quantum simulations. As precision measurements are usually best performed in terms of frequency measurements, atom-molecule Rabi oscillations open up promising opportunities in this direction. Specifically, it was proposed recently that measurements of atomic scattering properties with moderate accuracy might be used to perform sensitive tests for drifts of fundamental constants [1].

Here, we report on the experimental observation of time-resolved Rabi

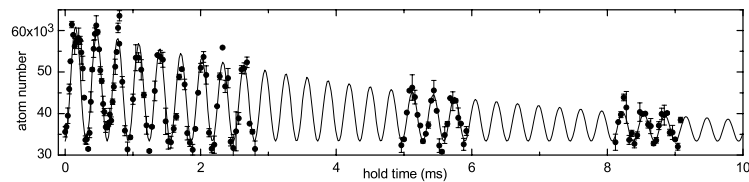


Fig. 1. Time-resolved Rabi oscillations between the atomic and the molecular state. The experimental data (●) show the number of entrance-channel atoms.

oscillations up to the 29th cycle between an atomic and a molecular state near a Feshbach resonance (Fig. 1). As compared to earlier experiments [2], we observe oscillations with large amplitude. The experiment uses a Mott insulator of ⁸⁷Rb in an optical lattice and a Feshbach resonance near 414 G. The frequency and amplitude of the oscillations depend on magnetic field in a way that is well described by a two-level model. The observed density dependence of the oscillation frequency agrees with the theoretical expectation. We confirmed that the state produced after a half-cycle contains

exactly one molecule at each lattice site [3]. In addition, we show that the molecules cannot dissociate at energies corresponding to band gaps in the optical lattice [4].

References

1. C. Chin and V. V. Flambaum, Phys. Rev. Lett. **96**, 230801 (2006).
2. E.A. Donley, N.R. Claussen, S.T. Thompson, and C.E. Wiemann, Nature **417**, 529 (2002).
3. T. Volz, N. Syassen, D.M. Bauer, E. Hansis, S. Dürr, and G. Rempe, Nature Phys. **2**, 692 (2006).
4. N. Syassen, D.M. Bauer, M. Lettner, D. Dietze, T. Volz, S. Dürr, and G. Rempe, arXiv:0704.2155v1 (2007).

YTTERBIUM SINGLE-ION OPTICAL FREQUENCY STANDARDS

CHR. TAMM, I. SHERSTOV, B. STEIN, B. LIPPARDT, E. PEIK

*Physikalisch-Technische Bundesanstalt, Bundesallee 100, 38116 Braunschweig,
Germany*

A single laser-cooled ion confined in a radiofrequency trap is a nearly ideal reference for an optical frequency standard. The ion $^{171}\text{Yb}^+$ has two transitions from its $^2\text{S}_{1/2}$ ground state that are attractive reference transitions: an electric-quadrupole transition to the $^2\text{D}_{3/2}(\text{F}=2, m_{\text{F}}=0)$ level at 436 nm which has a natural linewidth of 3.1 Hz, and an electric-octupole transition to the $^2\text{F}_{7/2}(\text{F}=3, m_{\text{F}}=0)$ level at 467 nm. The natural linewidth of the latter transition is in the nanohertz range so that the achievable resonance quality factor is practically limited only by the short-term frequency stability of the employed probe laser and by the heating rate of the trapped ion.

Recently we have measured the frequency of the $^{171}\text{Yb}^+$ 436 nm quadrupole transition with a total relative uncertainty of $2.0 \cdot 10^{-15}$ [1]. The unperturbed transition frequency has been recommended as a secondary realization of the SI second [2]. The 467 nm octupole transition has been investigated spectroscopically at NPL (Teddington, UK) [3].

Precise comparisons between the frequencies of the 436 nm and the 467 nm transitions of Yb^+ over a period of a few years can be used for a highly sensitive, model-independent search for temporal variations of the fine structure constant α [4]. In a local frequency comparison based on a femtosecond frequency comb generator, the ratio of the transition frequencies can be measured with an accuracy that is independent of the limitations of microwave frequency standards and of long-distance time transfer techniques.

2

In order to enable local frequency comparisons between the two Yb^+ transition frequencies, we are presently developing a standard based on the 467 nm octupole transition. In this contribution, we discuss recent results and perspectives for the two Yb^+ standards.

Work supported in part by Deutsche Forschungsgemeinschaft through SFB407 and by grant RFP-1-06-08 of the Foundational Questions Institute (fqxi.org).

- [1] T. Schneider, E. Peik, Chr. Tamm, Phys. Rev. Lett. 94, 230801 (2005); Chr. Tamm, B. Lipphardt, H. Schnatz, R. Wynands, S. Weyers, T. Schneider, E. Peik, IEE Trans. IM-56, 601 (2007).
- [2] P. Gill, F. Riehle, Proc. 20th European Frequency and Time Forum (Braunschweig 2006), p. 282.
- [3] P.J. Blythe, S.A. Webster, H.S. Margolis, S.N. Lea, G. Huang, S.-K. Choi, W.R.C. Rowley, P. Gill, R.S. Windeler, Phys. Rev. A 67, 020501 (2003).
- [4] V.A. Dzuba, V.V. Flambaum, M.V. Marchenko, Phys. Rev. A 68, 022506 (2003); E. Peik, B. Lipphardt, H. Schnatz, Chr. Tamm, S. Weyers, R. Wynands, physics/0611088 (2006).

CAVITY ENHANCED DIRECT FREQUENCY COMB SPECTROSCOPY

MICHAEL J. THORPE, DAVID BALSLEV-CLAUSEN, MATT KIRCHNER,
BEN SAFDI, AND JUN YE

*JILA, National Institute of Standards and Technology
and University of Colorado Department of Physics,
University of Colorado, Boulder, CO 80309-0440, USA*

Cavity enhanced direct frequency comb spectroscopy (DFCS) combines the broad bandwidth and precision frequency capabilities of the frequency comb with the high sensitivity to optical loss of a high finesse optical cavity. Precise control of an optical frequency comb allows the individual comb components to be coherently coupled to corresponding resonance modes of the high finesse optical cavity. By constructing the cavity from broad bandwidth, and low dispersion reflectors, large spectral bandwidths ranging from 15% to 40% of the center optical frequency can be efficiently coupled. The long cavity lifetime dramatically enhances the effective interaction between the light field and intra cavity matter, making it a very sensitive approach for measurement of optical losses. The light transmitted from the cavity is spectrally resolved with a virtually-imaged phased-array spectrometer to recover the optical loss information with resolutions ranging from a gigahertz to several kilohertz. Recent experiments conducted in our laboratory have demonstrated the use of cavity enhanced DFCS for trace detection of molecular components within a host gas and the mapping of the quantum state distribution of cold molecules in a supersonic beam. In both cases, the wide bandwidth and ultra sensitive nature of the femtosecond enhancement cavity enable real time detection of multiple molecular species in a massively parallel fashion, greatly reducing the time required for molecule and state identification. The poster presents: The underlying physics of the coupling between a femtosecond comb and an external optical cavity; the experimental implementation of the cavity-enhanced DFCS with corresponding results illustrating the capabilities of the current systems, and finally our visions for future scientific explorations using these unique techniques.

SPECTROSCOPY OF ATOM PAIRS AND COLD COLLISIONS

E. TIEMANN, H. KNÖCKEL

Leibniz Universität Hannover, Welfengarten 1, 30167 Hannover, Germany

A. PASHOV

Department of Physics, Sofia University, 5 James Bourchier Blvd, 1164 Sofia, Bulgaria

O. DOCENKO, M. TAMANIS, R. FERBER

Department of Physics and Institute of Atomic Physics and Spectroscopy, University of Latvia, 19 Rainis Boulevard, Riga LV-1586, Latvia

High resolution spectra of polar alkalis are combined with data of cold collisions like Feshbach resonances to obtain precise molecular potentials with which highly reliable predictions of further cold collision properties or of formation paths of deeply bound cold molecules can be made.

Keywords: Laser spectroscopy, cold collisions

1.

By the recent developments on cold atomic ensembles, cold atomic collisions, Feshbach resonances at zero kinetic energy and finally cold molecules, the need for precise spectroscopy on diatomic alkalis gained a high importance. Most researchers discovered that the spectroscopic effort on such species stopped some time ago and moreover, just before that energy range where the interest of the community for ultracold atoms starts. During the last years we used laser fluorescence excitation in combination with high resolution Fourier transform spectroscopy to study the complete energy interval of binding potentials for the coupled system of singlet-triplet states of the atomic ground state asymptote.

We will report in this poster the wide application on homo and heteronuclear molecules(e.g. $NaRb$, $NaCs$,² $LiCs$, and $LiRb$) to derive precise data which are able to model ultra cold collisions reliably including

resonance structure. The spectra show clearly hyperfine structure and the singlet-triplet coupling by hyperfine interaction, which is taken into account by coupled channels calculations during the evaluation.

In recent developments we included also in our fitting process the observed Feshbach resonances, for which we give the well developed example of KRb .

The next steps of experimental development will be the application of molecular beams to increase the accuracy of the modeling. First positive results using Franck-Condon pumping to reach the molecular levels located directly at the atomic ground state asymptote were obtained for Na_2 ¹ some years ago. Recently, we succeeded in observing NaK in the beam.

References

1. C. Samuelis, E. Tiesinga, T. Laue, M. Elbs, H. Knöckel, and E. Tiemann. Cold atomic collisions studied by molecular spectroscopy. *Phys. Rev. A*, 63:012710, 2000.
2. example NaCs: O. Docenko, M. Tamanis, J. Zaharova, R. Ferber, A. Pashov, H. Knöckel, E. Tiemann *J. Phys. B: At. Mol. Opt. Phys.*, 39, S929-S943, 2006.

Sharp Peak Density Solutions for Bose–Einstein condensate in approximate kinetic model

V. Tsurkov

*School of Computer & Information Sciences, Georgia Southwestern State University,
Americus, GA 31709, USA
E-mail: tsurkov@usa.net
http://cis.gsw.edu/*

We consider the density response of rare degenerate Bose–gas with respect to small perturbations of temperature. The so-called BKV model of kinetic Boltzmann equation is used. The numerical solution demonstrates the sharp density behavior similar to one in the case of hydrodynamic conservation laws.

Keywords: Bose–Einstein condensate; kinetic equations; sharp peak density solutions.

1. Background.

We consider the approximate BKV–model¹ of Boltzmann kinetic equations without external forces

$$\frac{\partial f}{\partial t} + \mathbf{v} \frac{\partial f}{\partial \mathbf{r}} = \nu (f_e - f) \quad (1)$$

($\nu = \text{const}$) where f_e is the Bose–Einstein distribution of ideal degenerate gas.

In the case of spherical symmetry, when the distribution $f = f(\mathbf{r}, \mathbf{v}, t)$ depends on three coordinates and time, where $r = |\mathbf{r}|$, $v = |\mathbf{v}|$, and $s = \mathbf{r}\mathbf{v}/rv$, Eq. (1) becomes

$$\frac{\partial f}{\partial t} + v \left(s \frac{\partial f}{\partial r} + \frac{1-s^2}{r} \frac{\partial f}{\partial s} \right) = \nu (f_e - f) \quad (2)$$

where the macroscopic variables ρ , \mathbf{V} and T depend only on r ($\mathbf{V} = V\mathbf{r}/r$, where $V = V(r)$ and $|V| = |\mathbf{V}|$).

We have the initial condition

$$f(r, s, v, t)|_{t=0} = f_e(\rho_0(r), V_0(r), T_0(r), s, v) \quad (3)$$

where $\rho_0(r)$, $V_0(r)$, $T_0(r)$ are given functions.

2. Main result.

For each discrete time step, Eq. (2) is solved in two stages. First, we solve Eq. (2) without right part. Second, we take into account the right part of Eq. (2) which accounts for particle collisions. Function f_e depends on variables $\rho(r)$, $V(r)$, $T(r)$, that are defined by means of three integrals of f with respect to s and v and, consequently, depend on t .

Following Refs. 2–4, we took initial values $\rho_0(r) = \rho_0 = \text{const}$, $V_0(r) = 0$ and set a temperature perturbation as a power function of the radius $T_0(r) = T_0 \cdot \min(1, 1 - C_1(1 - (C_2 r/R)^\beta))$. The temperature T_0 was set below the critical. The size of the perturbation area was several times less than the sphere radius (parameter $C_2 = 4$). Parameter C_1 , that specifies the magnitude of temperature perturbation, was set to 0.25. The parameter of β was taken in the range 0.5 . . . 2.5. The computations were stopped when the perturbation reached the boundary of the considered sphere.

We obtained a sharp density peak in the sphere center for all β from the interval considered. The density as a function of r has sharp peaks, the density peak in the sphere center being significantly greater than that of the degenerate Fermi–gas (corresponding computations for the Fermi–gas were also carried out).

This is in agreement with results of Refs. 2–4.

References

1. Cercignani C. *Theory and application of the Boltzmann equation*. (Scottish Academic Press, Edinburgh–London, 1978).
2. V.I. Tsurkov. *Comput. Math. Math. Phys.* **11**, 488 (1971).
3. Tsurkov V.I. *Majorant Catastrophe of Eulerian Gas Dynamics Equations for Bosons* (Felicity Press, USA, 1998).
4. V.I. Tsurkov. *J. Low Temp. Phys.* **138**, 717 (2005).

VORTEX PROLIFERATION IN THE BEREZINSKII-KOSTERLITZ-THOULESS ON A TWO-DIMENSIONAL LATTICE OF BOSE-EINSTEIN CONDENSATES

S. TUNG, V. SCHWEIKHARD, AND E. CORNELL

*JILA, National Institute of Standards and Technology and University of Colorado, and
Department of Physics, University of Colorado
Boulder, CO 80309-0440*

A two-dimensional array of Josephson-coupled Bose-Einstein condensates is created by loading a Bose-Einstein condensate into a two-dimensional optical lattice. By tuning Josephson (tunneling) energy J and thermal energy T , vortex proliferation in the Berezinskii-Kosterlitz-Thouless regime is observed. As long as the Josephson energy exceeds the thermal energy, the array is vortex-free. With decreasing J/T , vortices appear in the system in ever greater numbers. We confirm thermal activation as the vortex formation mechanism, and obtain information on the size of the bound vortex pairs as J/T is varied.

Towards coherent matter-wave inertial sensors in microgravity

G. Varoquaux*, J-F. Clément, J-P. Brantut, R. A. Nyman, A. Aspect and P. Bouyer

*Laboratoire Charles Fabry de l'institut d'Optique,
Campus Polytechnique, RD 128, 91127 Palaiseau, France*

**E-mail: gael.varoquaux@institutoptique.fr*

F. Pereira Dos Santos and A. Landragin

*LNE-SYRTE, UMR8630, Observatoire de Paris,
61 avenue de l'Observatoire, 75014 Paris, France*

N. Zahzam, O. Carraz, Y. Bidet and A. Bresson

*Office National d'Étude et de Recherches Aérospatiales,
Chemin de la Lumière, 91761 Palaiseau, France*

We present our progress on developing atom-interferometric inertial sensors in microgravity.

The use of ultracold atomic gases as a source for matter-wave interferometry allows high signal-to-noise ratio due to high densities and narrow momentum-spectra. To avoid inhomogeneities of external potential, propagation between beam splitters in an atom interferometer is usually achieved via free-fall. The precision of an interferometric measurement is limited in current high-precision experiments by the propagation time of the atoms, itself limited by the free expansion of the atomic cloud in the vacuum chamber. The use of a Bose-condensed cloud dramatically reduces the ballistic expansion and allows for long propagation times.

In the presence of gravity, accessing such long fall times requires very large vacuum system. We present progress on transportable atom-interferometry apparatuses that can be used on an airplane, in ballistic flights, to perform measurements in microgravity.

A novel laser source using standard fibered telecom components and frequency doubling to rubidium wavelength (780nm) allows for compact and transportable laser sources suitable for laser cooling and coherent manipulation of atoms in a noisy environment. A cold-atom apparatus has been built to test coherent-splitting of laser-cooled rubidium clouds in ballistic

flights. It has been tested to produce a magneto-optical trap during a flight campaign late March.

In addition, a more complex apparatus is under construction to allow rapid cooling to degeneracy in a microgravity parabola. A mixture of quantum degenerate gases, bosonic ^{87}Rb and fermionic ^{40}K , will be used in a Raman-pulse interferometer for accelerometry.

High density samples such as Bose-condensed gases used for long time of flight measurements suffer from important interaction effects, giving rise to systematic shifts in interferometric measurements. Fermionic degenerate gases have a broad momentum distribution but negligible collisions. We plan to study the importance of interaction shifts in our ^{87}Rb bosonic sample using a Fermi gas of ^{40}K .

We will present some technical achievements in our experimental apparatuses, give an outline of some possible microgravity measurements and an estimation of the experimental limits.

SPECTROSCOPY ON ATOMIC RUBIDIUM AT 500 BAR BUFFER GAS PRESSURE: TOWARDS THERMAL EQUILIBRIUM OF COUPLED ATOM-LIGHT-STATES

U. VOGL* and M. WEITZ

*Institut für Angewandte Physik, Universität Bonn,
Wegelerstraße 8, D-53115 Bonn, Germany*

**E-mail: vogl@iap.uni-bonn.de
www.iap.uni-bonn.de/ag-weitz*

In usual experiments in atomic physics the observed linewidth of the fluorescence is many orders of magnitude below the room temperature, so that the excitation profile is widely unaffected by the statistical distribution function. We report on experiments in which by near 500 bar buffer gas pressure in a high pressure cell, linewidths of a few nanometers of the rubidium D-lines are reached (Fig. 1). With high light intensities of the exciting laser light the resonance lines are additionally power-broadened above values of $k_B T$ ($\simeq 1.1 \cdot 10^{13}$ Hz at 510 K cell temperature). In this parameter range we observe a strong asymmetry of the fluorescence line, in which the blue wings of the lines are strongly enhanced. More clear evidence is obtained when extrapolating the observed fluorescence signals to infinite laser power (Fig. 2), as in this limit spontaneous decay processes, driving the system out of equilibrium, are negligible. We interpret the data as evidence for the coupled atom-light states (dressed states) to reach thermal equilibrium. The thermalisation is here realized by atom-buffer gas collisions. Rate equations for the coupled atom-light system under frequent buffer gas collisions indicate strong deviations from the usual excitation spectrum when the system reaches thermal equilibrium. Our data agree reasonably well with this predictions. For the future, we expect interesting new experiments on the collective dynamics of hybrid atom-light-quasiparticles (polaritons) in this novel high pressure system.

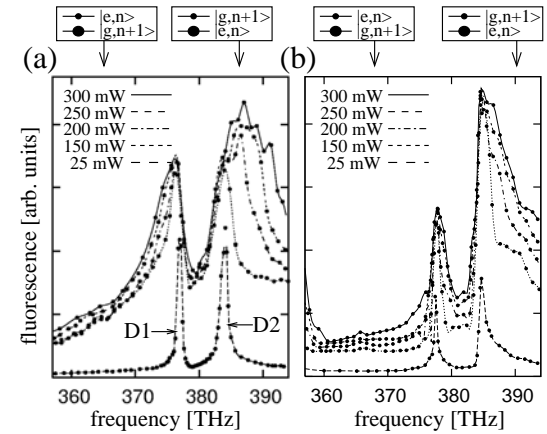


Fig. 1. Fluorescence spectrum of the rubidium D-lines at 500 bar argon (a) and 400 bar helium (b) buffer gas pressure for different optical beam powers. The small drawings on the top indicate the population of the dressed states on the red and blue side of the electronic transition respectively.

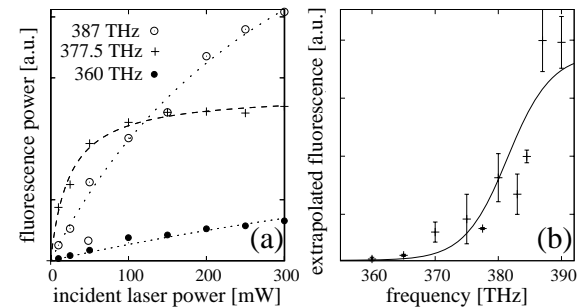


Fig. 2. (a) fluorescence of rubidium atoms at 400 bar helium buffer gas as a function of optical power for different laser frequencies. The experimental data has been fitted with the expected saturation dependence of our model. (b) Expected atomic fluorescence at infinite laser power, obtained from extrapolation curves as in (a), versus laser frequency. The shown error bars were obtained from the extrapolation fits. The data has been fitted with a Fermi-Dirac distribution, as expected for thermal equilibrium of the two-level dressed state system.

MULTIPLE FREQUENCY MODULATION FOR LOW-LIGHT ATOM MEASUREMENTS IN AN OPTICAL CAVITY*

GEERT VRIJSEN, JONGMIN LEE, IGOR TEPER, ROMAIN LONG†, ARI TUCHMAN, MARK KASEVICH

Physics Department, Stanford University, 382 Via Pueblo Mall
Stanford, CA 94305-4060

We present a frequency modulation scheme to dispersively detect atoms in a high finesse optical cavity at low light levels with immunity to cavity length fluctuations. Simultaneous use of multiple cavity resonances provides common mode noise rejection.

1. Motivation

Non-destructive detection of cold atom clouds is a promising method for the generation of atomic squeezed states¹, which can improve the performance of atomic clocks and interferometers². An optical cavity reduces the spontaneous emission rate of an atomic ensemble by the square root of the cavity finesse for a give signal-to-noise ratio³, thereby increasing the attainable degree of squeezing over free space atoms. While techniques have been developed for both dispersive detections at low light levels⁴, as well as noise-immune measurements in optical cavities^{5,6}, these requirements have not previously been simultaneously met.

2. Method

Multiple modulation sidebands, each matched to a different cavity resonance, are used to provide common mode noise rejection. The high-intensity carrier is kept off-resonant from the cavity modes to maintain low light levels while providing photon-shot noise limited detection in the cavity reflection. We use this method to measure the optical phase shift of a detuned sideband interacting with the atomic cloud. Atoms are prepared in the cavity using standard laser cooling techniques.

* This work is supported by DARPA and the MURI on Quantum Metrology sponsored by the Office of Naval Research.

† Present address: Laboratoire Kastler Brossel, Département de Physique de l'École Normale Supérieure, 24 Rue Lhomond, 75231 Paris Cedex 05, France.

3. Result

In the far-detuned limit, $\delta\nu = Ng^2 / \Delta$ where g is the atom-cavity coupling, Δ is the detuning from the atomic resonance, and N is the number of atoms in the cavity mode. Figure 1 shows the frequency shift per atom scaling inversely with Δ , measured with our frequency-modulation scheme.

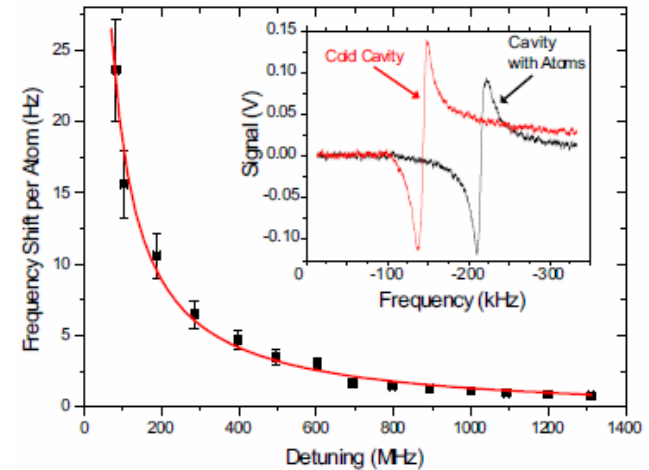


Figure 1. Frequency shift of the cavity resonance per atom vs. detuning between the probe sideband and the atomic resonance. Inset shows a frequency sweep of the probe sideband in the cold cavity case and when atoms are loaded into the cavity mode volume.

References

1. A. Kuzmich, N. Bigelow and L. Mandel, *Europhys. Lett.* **42**, 481 (1998).
2. D. Wineland, J. Bollinger, F. L. Moore and D. J. Heinzen, *Phys. Rev. A* **50**, 67 (1994).
3. J. E. Lye, J. J. Hope and J. D. Close, *Phys. Rev. A* **67**, 043609 (2003).
4. H. Mabuchi, J. Ye and H. J. Kimble, *Appl. Phys. B* **68**, 1095 (1999).
5. R. G. Devoe and R. G. Brewer, *Phys. Rev. A* **30**, 2827 (1984).
6. Jun Ye, Long-Sheng Ma and John L. Hall, *J. Opt. Soc. Am. B* **15**, 6 (1998).

MANIFESTATION OF CONTINUOUS QUANTUM ZENO EFFECT BASED ON COLD ATOM INTERFEROMETRY

P.WANG, R.B.LI, J.WANG, H.W.XIONG, AND M.S.ZHAN[†]

State Key Laboratory of Magnetic Resonance and Atomic and Molecular Physics, Wuhan Institute of Physics and Mathematics, and Center for Cold Atom Physics, Chinese Academy of Sciences, Wuhan 430071, P. R. China

[†]E-mail: mszhan@wipm.ac.cn

In the past forty years, there have been intensive studies on quantum Zeno effect (QZE). The QZE is the suppression of the decay of an unstable system or transition between different quantum states by frequent or continuous measurements. Although it is firstly proposed as a paradox or even a defect in quantum mechanics, many experiments^{1,2} have confirmed the observation of this counterintuitive effect, and there are ceaseless theoretical studies about the concept and understanding of QZE.

Oscillating system is an important physical system to study the quantum Zeno effect. Based on our cold atom interferometry system, recently we carried out an experiment to observe the unique property of QZE. For cold atomic cloud of ⁸⁵Rb, a coherent Raman transition between two hyperfine ground states $|1\rangle$ and $|2\rangle$ was induced by laser beams denoted by R_1 and R_2 , as shown in figure 1. The atoms are initially in the state $|1\rangle$. During the coherent transition between $|1\rangle$ and $|2\rangle$, there is a measurement on the state $|2\rangle$ using a continuous measurement laser M inducing the transition between $|2\rangle$ and unstable state $|3\rangle$. The population in the state $|1\rangle$ was measured to show QZE.

Different from the previous experiments such as [2], we used a 2π pulse in inducing the coherent transition between two states $|1\rangle$ and $|2\rangle$. Compared to the ordinary π pulse, an interesting merit of 2π pulse lies in that the manifestation of QZE can be shown as a peak in the relation between the strength, frequency detuning of the measurement laser and D, where $D=1-P$ with P being the probability of finding an atom in the state $|1\rangle$ at the final time of the 2π pulse.

2

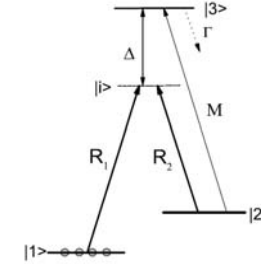


Figure 1: The scheme of the observation of quantum Zeno effect.

Figure 2 gives our main experimental data and theoretical simulation. For resonant measurement laser, we see a clear peak in D, and for the measurement laser intensity beyond the peak, there is a true QZE. It is interesting to note that the experimental results and theoretical simulation show that for large detuning shown in figure 2, we always do not find a peak. This means that too large detuning is not realistic to observe QZE when unavoidable experimental noise etc exist. In brief, our studies show that a 2π pulse can give us more objective criteria to judge whether or under what conditions there is a true QZE.

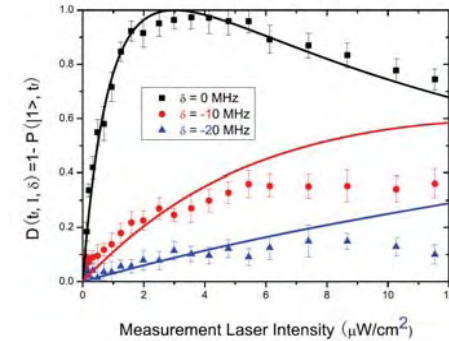


Figure 2: The experimental results of D for different frequency detuning δ and measurement laser intensity. The solid lines are theoretical simulation.

References

1. W. M. Itano et al, Phys. Rev. A 41, 2295 (1990).
2. E. W. Streed et al, Phys. Rev. Lett. 97, 260402 (2006).

1

Progress toward trapping and coupling neutral atoms with a magnetic cantilever

Y.-J. Wang, M. Eardley, S. Knappe, L. Hollberg, and J. Kitching

*Time and Frequency Division, National Institute of Standards and Technology,
Boulder, CO 80305, USA*

J. Moreland

*Electromagnetics Division, National Institute of Standards and Technology,
Boulder, CO 80305, USA*

Keywords: mechanical resonator; neutral atoms; trapping

1. Introduction

Resonant coupling of neutral atoms in atomic vapor to a mechanic resonator has been demonstrated through optical observation of magnetic Zeeman resonance excited by motion of a mechanic cantilever.¹ We analyze here the possibility of observing a sample of laser-cooled atoms magnetically trapped in the field gradient on the cantilever tip.²

2. Experimental setup and discussion

In our proposed experiment, a cloud with about 10^8 Rb atoms is collected in a magneto-optical trap (MOT) and laser-cooled down to $15 \mu\text{K}$ in a vacuum chamber at a pressure of 10^{-9} torr. The atoms will then be released, pulled by gravity, and stopped near a cantilever with a magnetic tip, which is located 20 cm below the MOT.

A magnetic gradient from a coil near the cantilever, in combination with a uniform magnetic field, creates a magnetic trapping potential to confine the atoms as shown in Fig. 1. Atoms will be transferred to and trapped by the magnetic field from the cantilever by ramping the uniform field and the current in the coil.

Once atoms are trapped by the cantilever tip, motion of the cantilever will be driven capacitively. An oscillating magnetic field produced by the

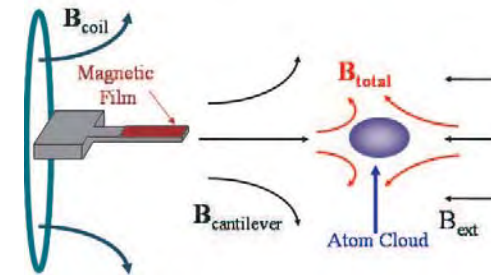


Fig. 1. Magnetic trap geometry. The coil and cantilever create a magnetic gradient. The uniform field cancels the field from the coil and the cantilever at one position and forms a magnetic trap for the atoms.

cantilever motion can induce spin-flips in trapped atoms.³ Discussions and simulations of such a trap and cantilever design will be shown in detail.

*This is a contribution of NIST, an agency of the US government, and is not subject to copyright.

References

1. Y.-J. Wang, M. Eardley, S. Knappe, J. Moreland, L. Hollberg and J. Kitching, *Phys. Rev. Lett.* **97**, p. 227602 (2006).
2. V. Vuletic, T. Fischer, M. Praeger, T. W. Hänsch, and C. Zimmermann, *Phys. Rev. Lett.* **80**, p. 1634 (1998).
3. P. Treutlein, D. Hunger, S. Camerer, T. W. Hänsch, and J. Reichel, e-print arxiv:quant-ph/0703199 (2007).

Single-Atom Single-Photon Quantum Interface

T. Wilk*, S. C. Webster¹, A. Kuhn¹ and G. Rempe

Max-Planck Institut für Quantenoptik,
Hans-Kopfermann-Str.1, 85748 Garching, Germany

*E-mail: tatjana.wilk@mpq.mpg.de

¹present address: Clarendon Laboratory, University of Oxford,
Parks Road, Oxford OX1 3PU, UK

We have realized an atom-photon quantum interface based on an optical high-finesse cavity. We demonstrate it by entangling a single atom with a single photon emitted into the cavity and by mapping the quantum state of the atom onto a second single photon. The latter step disentangles the atom from the light and produces an entangled photon pair.

Keywords: atom-cavity system, entanglement, state mapping;

Atom-cavity systems with the ability to generate single photons^{1–5} provide an ideal toolbox for quantum networks. Atoms stored in an intra cavity dipole trap for several seconds,⁶ act as quantum memories, whereas photons interconnect those distant nodes. The interface between stationary and flying qubits provided by the cavity boosts the overall efficiency of single photon generation compared to free-space and makes a state transfer from a single atom onto a single photon possible. This is demonstrated with the experimental realization of our intrinsically deterministic scheme (see Fig. 1) that creates an atom-photon entanglement followed by subsequent state mapping of the atomic state onto a second photon.

A single ⁸⁷Rb atom is coupled to an optical cavity and prepared in the $|F = 2, m_F = 0\rangle$ state of the $5S_{1/2}$ ground level by optical pumping. With the cavity axis as quantization direction, the cavity supports circularly polarized σ^+ and σ^- polarization modes. A π -polarized laser (resonant with the transition from $F=2$ to $F'=1$ of the excited $5P_{3/2}$ level) together with the cavity (resonant with the transition from $F=1$ to $F'=1$) drives a vacuum-stimulated Raman adiabatic passage to the $|F = 1\rangle$ state of the electronic ground level. Two different paths are possible, one to state $|+1\rangle \equiv |F = 1, m_F = +1\rangle$ resulting in the generation of a σ^- pho-

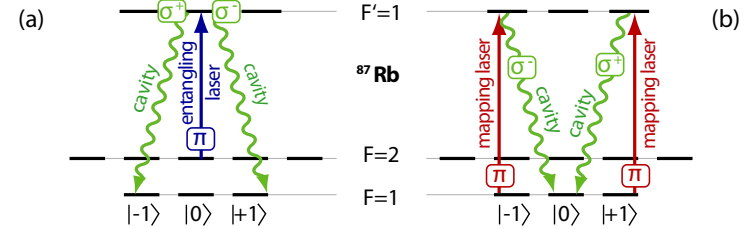


Fig. 1. Relevant levels and transitions to first, (a) entangle a single ⁸⁷Rb atom with a single photon emitted into the cavity mode, and, second, (b) map the atomic state onto a second photon emitted into the same mode. Details are explained in the text.

ton, and one to state $|-1\rangle \equiv |F = 1, m_F = -1\rangle$ resulting in the generation of a σ^+ photon. After photon emission the system is in the entangled state $|\Psi\rangle = \frac{1}{\sqrt{2}}(|+1, \sigma^- \rangle - |-1, \sigma^+ \rangle)$, where the phase of the superposition is defined by the transition amplitudes from the $|F = 2, m_F = 0\rangle$ state to the $|+1\rangle$ and $|-1\rangle$ states.

To map the atomic state onto a second photon a π -polarized laser resonant with the transition from $F=1$ to $F'=1$ together with the cavity drives a second Raman adiabatic passage. The population in state $|+1\rangle$ is transferred to $|0\rangle \equiv |F = 1, m_F = 0\rangle$ and a σ^+ photon is emitted, while the population in $|-1\rangle$ is also transferred to $|0\rangle$, but now a σ^- photon is emitted. The atom-photon entanglement is therefore converted into a polarization entanglement between two photons, $|\Psi\rangle = \frac{1}{\sqrt{2}}(|\sigma^+, \sigma^- \rangle - |\sigma^-, \sigma^+ \rangle)$, while the atom is disentangled from the light. The state of the two photons is analyzed by tomography of their polarization states, which also probes the prior entanglement between the atom and the first photon.

References

1. A. Kuhn, M. Hennrich and G. Rempe, *Phys. Rev. Lett.* **89**, p. 067901 (2002).
2. J. McKeever, A. Boca, A. D. Boozer, R. Miller, J. R. Buck, A. Kuzmich and H. J. Kimble, *Science* **303**, 1992 (2004).
3. M. Keller, B. Lange, K. Hayasaka, W. Lange and H. Walther, *Nature* **431**, 1075 (2004).
4. T. Wilk, S. C. Webster, H. P. Specht, G. Rempe and A. Kuhn, *Phys. Rev. Lett.* **98**, p. 063601 (2007).
5. M. Hijlkema, B. Weber, H. P. Specht, S. C. Webster, A. Kuhn and G. Rempe, *Nature Phys.* **3**, 253 (2007).
6. S. Nußmann, M. Hijlkema, B. Weber, F. Rohde, G. Rempe and A. Kuhn, *Phys. Rev. Lett.* **95**, p. 173602 (2005).

MICROFABRICATION PROCESS DEVELOPMENT FOR ION TRAP CHIPS BASED ON PLANAR SILICA-ON-SILICON TECHNOLOGY

G. WILPERS, M. BROWNNUTT, P. GILL, A.G. SINCLAIR
*National Physical Laboratory
 Teddington, Middlesex TW11 0LW, United Kingdom*

R.C. THOMPSON
*Blackett Laboratory, Imperial College London
 London SW7 2BZ, United Kingdom*

We have developed a design for a microfabricated ion trap based on SiO₂-on-Si technology. The trap potential and electrical operating characteristics have been modeled. The individual processing steps for fabricating these ion trap chips have been demonstrated. Work to combine these steps to a complete process is ongoing and will be described.

An ion trap containing an array of independent trapping segments is a possible architecture for an ion-trap quantum computer [1]. Linear segmented ion traps have been fabricated using Au-coated alumina [2,3] and doped GaAs [4]. Current developments include planar traps constructed on silicon [5,6], using metallic electrodes, and dielectrics of SiN and SiO₂. We proposed a trap with electrodes made of Au-coated SiO₂ that are spaced by highly doped silicon in a monolithic structure [7], and have been developing the processing techniques required for fabrication. Unit aspect-ratio traps can be fabricated resulting in deep trapping potentials, and complex arrays for trapping large numbers of ions are possible using this approach. Traps fabricated with this technology could be integrated with optical fibres and on-chip modulators.

With the trap electrodes in a unit aspect-ratio configuration, finite element modeling of the trap design shows that useful operating characteristics can be achieved. We have modeled the trapping potential for ion-electrode separations R in the range $90 \mu\text{m} \leq R \leq 350 \mu\text{m}$. For $R = 160 \mu\text{m}$, radial and axial motional frequencies of $\omega_r/(2\pi) = 4.5 \text{ MHz}$ and $\omega_z/(2\pi) = 2.0 \text{ MHz}$ are possible with realistic parameters (RF amplitude of 160 V and frequency of 21 MHz). The Si resistivity is chosen to be $10^{-3} \Omega\text{cm}$, to limit RF heating of the trap chip and to

avoid charge build up on the Si surface close to the ions. With these operating conditions, it is calculated that 0.4 mW of heat is generated, resulting in a 10 K temperature rise for a $9 \text{ mm} \times 9 \text{ mm}$ trap chip.

To create a 3D trap structure, a thermally oxidised Si wafer is processed using a combination of lithography, isotropic and anisotropic etching, and electroplating. A $15 \mu\text{m}$ thick layer of SiO₂ is grown on each side of the Si wafer; Au electrodes and tracks are then evaporated onto the SiO₂ surfaces. A SiO₂ etch removes the dielectric where the trap aperture is to exist, and between the electrodes (resulting in “fingers”). Following this, another etch process removes the Si to create the trap aperture; this etch also removes Si from under the SiO₂ electrode “fingers” to form cantilevers. The undersides and ends of the SiO₂ cantilever fingers are then coated with gold using a shadow evaporation technique. The electrodes are completed by electroplating out to $\sim 5 \mu\text{m}$ thickness with $\sim 10 \text{ nm}$ RMS roughness. All of these processing steps have been demonstrated individually. Difficulties currently exist in combining these steps together; latest progress will be reported. We have developed a compact design for UHV packaging of these ion trap chips, which includes a simple solution for the many electrical feedthrough connections required. Details of this will be presented.

Acknowledgments

This work is supported by NPL’s Strategic Research Programme and by EU contracts IST-2001-38875-QGATES, IST-2005-15714-SCALA and IST-517675-MICROTRAP.

References

1. D. Kielpinski, et al., *Nature* **417**, 709 (2002).
2. M. A. Rowe, et al., *Quant. Inf. Comp.* **2**, 257 (2002).
3. W. K. Hensinger, et al., *Appl. Phys. Lett.* **88**, 034101 (2006).
4. D. Stick, et al., *Nature Physics* **2**, 36 (2006).
5. R. Slusher, available at <http://tf.nist.gov/ion/workshop2006/workshoppapers.htm>
6. M. G. Blain, available at <http://tf.nist.gov/ion/workshop2006/workshoppapers.htm>
7. M. Brownnutt, G. Wilpers, P. Gill, R. C. Thompson and A. G. Sinclair, *N. J. Phys.* **8**, 232 (2006).

**INTERFERENCE FRINGES OF TWO INITIALLY
INDEPENDENT BOSE-EINSTEIN CONDENSATES BASED ON
INTERACTION-INDUCED INTERFERENCE THEORY***

HONGWEI XIONG[†], SHUJUAN LIU, MINGSHENG ZHAN

*State Key Laboratory of Magnetic Resonance and Atomic and Molecular Physics,
Wuhan Institute of Physics and Mathematics, Chinese Academy of Sciences,
Wuhan 430071, P. R. China*

The interference between two initially spatially-separated Bose-Einstein condensates (BECs) is a fundamental physical problem. The potential application of atom interferometry makes the theoretical and experimental researches on the interference mechanism become quite attractive.

In an exciting experiment by MIT's group [1], clear interference fringes were observed for two initially independent Bose condensates in dilute gas. In MIT's experiment, the cold atomic cloud was trapped in a double well potential. When the central barrier is sufficiently high, the tunneling between two wells can be omitted, and thus after evaporative cooling, two completely independent condensates can be created. After the double well was switched off, two condensates would expand freely and overlap after sufficient expansion time. A remarkable experimental result was found by MIT's group, where clear interference fringes were observed for two initially independent condensates.

The mystery in MIT's experiment [1] lies in that after simple and standard calculation, it seems that there are no interference fringes in the density expectation value (see for example [2]). Presently, the most popular viewpoint is the so-called measurement-induced interference theory [3]. Measurement-induced interference theory thinks that before the measurement of the density distribution, there is no interference term in the density expectation value even after the overlapping between two initially independent condensates. In measurement-induced interference interpretation, it is thought that the measurement process and the interference terms in the two-particle correlation would establish the coherence between two overlapping and initially

* This work is supported by NSFC under Grant Nos. 10634060, 10474117 and NBRPC under Grant Nos. 2006CB921406, 2005CB724508.

[†] Electronic address: xionghongwei@wipm.ac.cn

independent condensates. When the number of particles is much larger than one, with more and more particles being detected, the interference fringes would emerge with a random shift in a single-shot experiment.

Recently, we reconsider the physical mechanism of the interference phenomenon for two initially independent Bose condensates. In the ordinary calculation of the density expectation value before measurement, the ideal Bose gas model was adopted [2]. In MIT's experiment, however, there is interatomic interaction. We find that when interatomic interaction is considered, there would be already clear interference fringes in the density expectation value [4]. By using the experimental parameters of MIT's experiment, we find very good agreement between our theory and the experimental results of MIT's group.

Although our calculations are quite complex, the physical mechanism of our interaction-induced interference theory is simple. After the overlapping between two initially independent condensates, due to the interatomic interaction, there are coherent particle-number exchanges between two condensates [4,5]. The spatial coherence between two condensates would be established in this situation, and it is natural that there would be clear interference fringes.

Recently, we noticed that two different theoretical groups also found that interatomic interaction can induce interference fringes for two initially independent condensates [6-7]. Most recently, density-density correlation was proposed to test further the measurement-induced interference theory and interaction-induced interference theory [8].

References

- [1] Andrews et al, *Science* **275**, 637 (1997).
- [2] A. J. Leggett, *Rev. Mod. Phys.* **73**, 307 (2001).
- [3] J. Javanainen, S. M. Yoo, *Phys. Rev. Lett.* **76**, 161 (1996); M. Naraschewski et al, *Phys. Rev. A* **54**, 2185 (1996); J. I. Cirac et al, *Phys. Rev. A* **54**, R3714 (1996); Y. Castin, J. Dalibard, *Phys. Rev. A* **55**, 4330 (1997).
- [4] H. W. Xiong, S. J. Liu, M. S. Zhan, *cond-mat/0507354* (2005); H. W. Xiong, S. J. Liu, M. S. Zhan, *New J. Phys.* **8**, 245 (2006).
- [5] H. W. Xiong, S. J. Liu, M. S. Zhan, *Phys. Rev. B* **73**, 224505 (2006).
- [6] L. S. Cederbaum et al, *Phys. Rev. Lett.* **98**, 110405 (2007).
- [7] D. Masiello, W. P. Reinhardt, *cond-mat/0702067* (2007).
- [8] S. J. Liu, H. W. Xiong, *cond-mat/0612133* (2006).

High Resolution Stimulated Raman Spectroscopy for the $D_{3/2}$ and $D_{5/2}$ Metastable States Qubit in $^{40}\text{Ca}^+$

Rekishu Yamazaki², Hideyuki Sawamura¹, Kenji Toyoda^{1,2}, Utako Tanaka^{1,2} and Shinji Urabe^{1,2}

¹*Graduate School of Engineering Science, Osaka University,
1-3 Machikaneyama, Toyonaka, Osaka 560-8531, Japan*

²*JST, 4-1-8 Honcho, Kawaguchi-shi, Saitama 332-0012, Japan*

We are investigating a possibility of using two metastable states, $D_{3/2}$ and $D_{5/2}$, in $^{40}\text{Ca}^+$ as a qubit for the ion trap based quantum information processing. The use of two metastable states with a Raman coupling could ensure a large Rabi-frequency and therefore the gate speed, however, the large level separation of about 1.8 THz is an obstacle for the preparation of the phase-coherent Raman beams. We have developed a phase-locked laser system where the frequency difference of over a THz was bridged with a use of optical comb generator (OCG). Raman spectroscopy of the Zeeman sub-levels between the $D_{3/2}$ and $D_{5/2}$ metastable states was performed with the developed laser system. We report the results of the Raman spectroscopy as well as the direct measurement of the level separation between the $D_{3/2}$ and $D_{5/2}$ metastable states in $^{40}\text{Ca}^+$. In the best of our knowledge, the direct determination of the level separation between the two levels has not been performed previously. The effect of the AC Stark shift and the DC magnetic field was accounted for the determination of the level separation. We also discuss the current progress and the direction in the development of the quantum information processor using these two states.

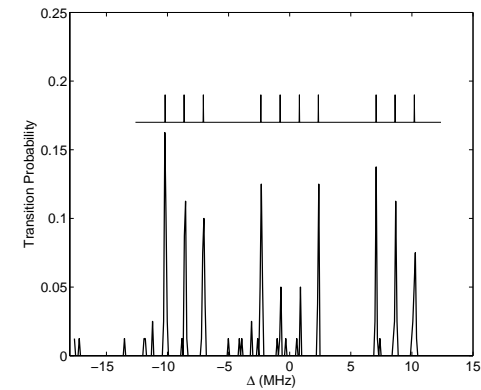


Fig. 1. Raman spectra observed in the experiment. 10 peaks observed in the figure are $\Delta m = 0$ transition (4 middle peaks) and $\Delta m = \pm 2$ transition (3 peaks on each side). The spectra above the data shows the calculated peak location for $B=2.81$ G for the corresponding transition.

GRAVITATIONAL SPLITTING OF A BEC IN A 10CM RING*

MATEUSZ ZAWADZKI, IAN NORRIS, AIDAN ARNOLD, AND ERLING RIIS

*SUPA, Department of Physics, University of Strathclyde
Glasgow, G4 0NG, Scotland*

Bose-Einstein condensates are stored in a 10 cm diameter vertically oriented magnetic ring trap and low loss propagation is observed over a total distance of ~ 2 m. After two revolutions in the ring the radial density distribution of the BEC is bimodal with the coolest (condensed) fraction having a fitted radial temperature of 10nK. If atoms are initially released from the exact top of the ring the atomic cloud splits into two counter-rotating clouds which can be recombined after one revolution.

A magnetic storage ring for atoms is formed by four current carrying loops creating a toroidal quadrupole magnetic field [1]. An azimuthal magnetic field from a single current carrying wire prevents Majorana losses. Additional coils near the top of the vertically oriented ring facilitate creation of a MOT and a magnetic trap. The IP trap typically contains $5 \cdot 10^8$ ^{87}Rb atoms with a lifetime of 50 s. Bose-Einstein condensates (BECs) with $\sim 2 \cdot 10^5$ atoms are formed.

Both laser cooled atoms and BECs have been released into the ring trap [1]. Figure 1 shows examples where the atoms are released ~ 60 mrad away from the top of the ring. Hence, they all disappear under the influence of gravity to one side but will not complete full circulation of the ring before coming to a halt outside our viewing window after about 700 ms. The atoms then reverse direction and reappear at the original position approximately 1.4 s after release. An azimuthal bias field of 10 G enables the low loss propagation in Fig. 1.

After two revolutions of the ring the returning atoms display a bimodal radial density distribution. The colder atomic distribution has a fitted radial ‘temperature’ of 10 nK, however this is an upper limit, as the condensate release energy is mainly due to mean-field repulsion.

By tailoring the azimuthal magnetic field gradient, the BEC can be released from the exact top of the ring: atoms are split under the influence of gravity into two counter-rotating parts. Figure 2 shows that after about 1 s both parts

reappear at the top of the ring, with tunable collision velocity. The present setup realises an ideal setup for Sagnac interferometry and interference fringes with a spatial period of $10 \mu\text{m}$ are expected when the relative velocity of the interfering wavepackets is 0.5 mm/s. No interference fringes have been observed to date, but the search now continues in the wake of recent experimental upgrades.

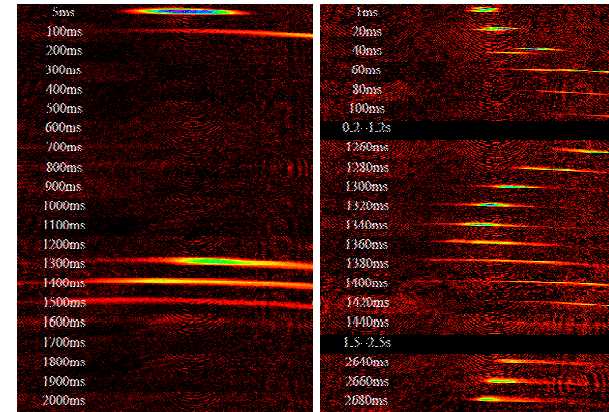


Figure 1. Experimental storage ring dynamics for $2\mu\text{K}$ atoms (left) and a BEC (right). Numbers denote time in ms after the release of the atoms into the ring and each frame is approximately $0.4 \times 5.4 \text{ mm}^2$. The atoms were initially ~ 60 mRad to the right of the top of the ring trap.

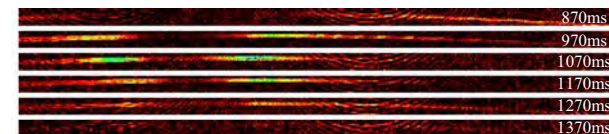


Figure 2. A BEC at the top of the ring was split into two counter-rotating clouds by the faster-than-harmonic circular potential. These split atomic clouds can be seen recombining here after one revolution in the ring. Times are in ms, each image is $0.15 \times 3.4 \text{ mm}^2$ and is taken after a 3 ms ballistic expansion. Fringes are, unfortunately, currently only due to our camera.

References

1. A. S. Arnold, C. S. Garvie and E. Riis, Phys. Rev. A **73** 041606(R) (2006).

* This work is supported by the Royal Society of Edinburgh, EPSRC and the Scottish Universities Physics Alliance (SUPA).

Transition from a Mott insulator to a two-dimensional superfluid in an optical lattice

MARTIN ZELÁN, EMIL LUNDH, MAGNUS REHN, ROBERT SAERS AND
ANDERS KASTBERG

*University of Umeå,
Department of Physics,
90187 Umeå,
Sweden.*

A dimensional crossover is predicted for a Bose gas in an anisotropic optical lattice. Upon changing the lattice depth in one direction, the gas undergoes a quantum phase transition from a one-dimensional Mott insulator to a two-dimensional superfluid. The transition is predicted to be in the Kosterlitz-Thouless universality class with a finite jump in the superfluid density.¹ Experimentally, this transition can be detected by a series of time of flight images, see figure 1.

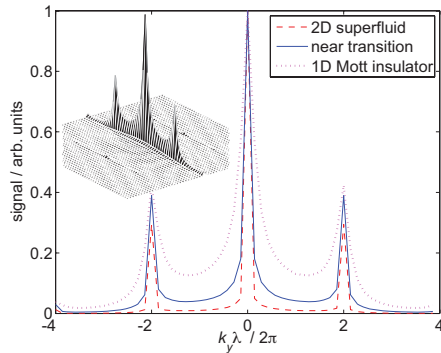


Fig. 1. Simulation of the experimental time of flight signal for the Mott insulator and superfluid phases

We will realize this experimentally in a setup for ^{87}Rb Bose-Einstein Condensates with good optical access. The system is well prepared for experiments with optical lattices with different geometry. Further more, our lasersystem for the optical lattices allow us to easily switch from near-resonance lattices to far detuned. There also exist plans to perform experimental studies of quasi-periodic lattices.

References

1. S. Bergkvist, R. Saers, E. Lundh, A. Rosengren, M. Rehn and A. Kastberg, *arXiv:cond-mat/0701616*.

EXTENDING THE FRONTIERS OF QUANTUM GASES TO MICROGRAVITY

T. C. ZOEST, E.M. RASEL, W. ERTMER FOR THE QUANTUS TEAM [†]
*Institut für Quantenoptik – Leibniz Universität Hannover, Welfengarten 1
 Hannover, 30167, Germany*

Quantum matter gives unique insights into a broad range of phenomena in fundamental physics as well as it offers prospects for novel quantum sensors. Reaching ever-new frontiers in low temperature physics and achieving full control of these elementary quantum systems are part of the central motivations for research on cooling and manipulation of atoms. The breaking of temperature records opened the way to many new scientific achievements, like atom interferometers and atomic clocks with highest accuracy, novel phase transitions or atom lasers.

Microgravity will extend the science of quantum gases towards inaccessible regimes of lowest temperatures below picokelvins, macroscopic dimensions, and unequalled durations of the unperturbed evolution of these distinguished quantum objects. These conditions set the stage for a study of the physics of ultra-dilute gases and giant matter-waves and the control of these macroscopic quantum objects quantum gas mixtures in an environment unbiased by gravity. Microgravity is also a decisive ingredient for the next leap in tests in fundamental physics of gravity, relativity and theories beyond the standard model.

In particular, microgravity is of high relevance for matter-wave interferometers and experiments with quantum matter (Bose-Einstein Condensates or degenerate Fermi gases) as it permits the extension the unperturbed free fall of these test particles in a low-noise environment. This is a prerequisite for fundamental tests in the quantum domain such as the equivalence principle or the realisation of ideal reference systems. The QUANTUS team, formed by a consortium of the Leibniz University of Hanover, the University of Hamburg, Berlin, Ulm and ZARM as well as the Max-Planck Institute, realised a compact facility to study a Rubidium Bose-Einstein Condensate in the extended free fall at the drop tower in Bremen and during parabolic flights. The facility will permit to study the generation and outcoupling of BEC in microgravity, the study of decoherence and atom interferometry. The remote controlled and

[†] Work supported by DLR 50 WM 0346, Germany.

miniaturised facility, which produces Bose-Einstein condensates of Rubidium, is presently under preparation for the first drops in early fall 2007. Precursor experiments demonstrating magneto-optical trapping during a sequence of drops of 4 seconds duration have been performed last December.

Ca⁺ IONS FOR FREQUENCY METROLOGY

C. ZUMSTEG, C. CHAMPENOIS, P. DUBÉ[†], G. HAGEL,
M. HOUSSIN, M. VEDEL, F. VEDEL, M. KNOOP*

*Université de Provence - CNRS , PIIM,
Centre de St Jérôme, Case C21, 13397 Marseille Cedex 20, France*

[†] *NRC, Institute for National Measurement Standards,
1200 Montreal Road, M-36, Rm 146 Ottawa, Ontario K1A 0R6, Canada*
**E-mail: Martina.Knoop@univ-provence.fr*

Rf trapped earth-alkaline ions are versatile candidates for frequency metrology. The electric quadrupole transition between the ground and the first metastable state is a first choice for a frequency standard in the optical domain, while a CPT interrogation protocol can combine three optical photons and serve as a reference for THz radiation.

1. Optical metrology

Among the candidates for an optical frequency standard, a single Ca⁺ ion is extremely attractive. The electric quadrupole transition at 729 nm proposed as frequency reference (clock transition) has a natural linewidth below 200 mHz corresponding to a quality factor of 2×10^{15} ; the wavelengths of the required lasers lie in the visible and near-infrared domain. A single Ca⁺ ion, cooled in a miniature radiofrequency trap and confined in the Lamb-Dicke regime, is an almost perfectly isolated atomic system suited for long interrogation times. The main contribution to the systematic uncertainty of this frequency standard, at the 9×10^{-16} level, is the Stark effect due to black body radiation at room temperature, provided the quadrupole shift is corrected. Frequency stability is limited by the quantum projection noise and is expected to reach $2.5 \times 10^{-15}/\sqrt{\tau}$. The Ca⁺ ion is expected to outperform the best microwave atomic frequency references, and to be competitive with other atomic optical frequency references.

Probing of the clock transition of a single ion is carried out using quantum jump statistics which requires interrogation times of several seconds to avoid power broadening. The line width of the probe laser (local oscillator)

should reach the hertz level for a duration at least as long as the interrogation time to take full advantage of the quality factor of the clock transition. Our local oscillator is a lab-built titanium-sapphire laser pumped with 5 W of laser radiation at 532 nm, stabilised onto an Invar reference cavity. Measurement by an auto-correlation technique yields a linewidth below the kHz with a resolution limited by the length of our optical fibre (10 km). Absolute stabilisation of the clock laser on an ultra-stable high-finesse ULE cavity is under way. To record the clock signal, the discrete Doppler frequency profile must be reduced to only few bands. To this purpose, the ion should be localized to better than 120 nm (Lamb-Dicke regime) by laser cooling and optimization of the trapping field.

2. THz metrology

The ultra-narrow quadrupole transition, combined with the two cooling lasers, can also be used to create three-photon coherent population trapping in a dark state. This provides a p method to create a coherent superposition of the two metastable states. The dark line can be employed for frequency metrology in the THz domain in a robust set-up with the interrogation of a (large) ion cloud thanks to the (first order) Doppler-free geometry of the laser beams.¹ The aimed frequency stability lies in the 10^{-14} range. The referenced THz signal can be propagated over long distances, the useful information being carried by the relative frequency of the three optical photons.

References

1. C. Champenois, G. Hagel, M. Houssin, M. Knoop, C. Zumsteg, and F. Vedel, to be published